Monochloramine dissipation mechanisms in storm sewer systems

by

Qianyi Zhang

A thesis submitted in partial fulfillment of the requirements for the degree of

Doctor of Philosophy

in

Environmental Engineering

Department of Civil and Environmental Engineering

University of Alberta

ABSTRACT

Many municipalities in Canada and all over the world use chloramination for drinking water secondary disinfection to avoid DBPs formation from conventional chlorination. However, the long-lasting monochloramine (NH_2Cl) disinfectant can pose a significant risk to aquatic life through its introduction into municipal storm sewer systems and thus fresh water sources by residential, commercial, and industrial water uses. To establish guidelines for total active chlorine (TAC) containing water discharge in storm sewers, the stormwater TAC concentration was monitored in Edmonton, Alberta, Canada, during the summers of 2015 and 2016. The results showed that TAC concentration varied from 0.02 to 0.77 mg/L in summer 2015, which exceeds the discharge effluent limit of 0.02 mg/L. As compared to 2015, the TAC concentrations were significantly lower during summer 2016 (0 to 0.24 mg/L), most likely because of the higher precipitation during summer 2016, which probably reduced outdoor tap water uses. Other physicochemical characteristics of stormwater and biological community distribution of sewer pipe biofilm were analyzed, and no significant difference was found during these two years. The statistical analysis of NH_2Cl decay laboratory experiments illustrated that natural organic matter (NOM) concentration is the dominant factor in determining the NH_2Cl decay rate in stormwater samples.

The NH_2Cl dissipation mechanisms were first studied in the presence of tap water, as it is the major source of TAC in storm sewers. A good model allowing prediction of NH_2Cl loss in tap water can assist in the understanding of NH_2Cl dissipation mechanisms in stormwater. In tap water, the NH_2Cl loss rate can be influenced by temperature, pH, Cl/N molar ratio, the initial NH_2Cl and NOM concentrations. In this research, a kinetic model was developed to predict the NH_2Cl loss under various conditions. A temperature-dependent model was also developed.

As NOM is the dominant factor that contributes to the NH_2Cl decay in stormwater, to study the NH_2Cl dissipation mechanisms, the reactions between NOM and active chlorine species were first studied. In this research, it is proposed that NOM reacts with both NH_2Cl and free chlorine released from NH_2Cl auto-decay. Based on this assumption, a kinetic model was developed and applied to estimate the NH_2Cl decay in stormwater samples, and the modeling results matched well with the experimental data under all the conditions. Further, the stormwater dissolved organic matter (SWDOM) collected from various neighborhoods were analyzed by FTIR and fluorescence EEM techniques. Humic substances were found to be dominant in SWDOM both before and after chloramination.

To study the NH_2Cl biological decay, stormwater biofilms were cultured in annular reactors on PCV and cement materials under operational conditions similar to the storm sewer environment. The results indicate that under the same operational condition, higher abundances of total bacteria, ammonia oxidizing bacteria (AOB) and nitrite oxidizing bacteria functional gene copies could be detected on cement slides as opposed to those on PVC materials. Further, batch experiments were conducted to study the NH_2Cl dissipation kinetics in the presence of stormwater biofilms. Three pathways that contribute to NH_2Cl decay were evaluated: (i) direct NH_2Cl reaction with biofilm, (ii) AOB cometabolism, and (iii) the NH_2Cl reaction with AOB utilized associated products, and a kinetic model was developed to predict these dissipation processes in storm sewers. The modeled results showed good matches with the experimental data, which is suggested that this model can be used to describe the NH_2Cl dissipation under various stormwater conditions.

Finally, the NH_2Cl auto-, chemical and biological dissipation pathways were summarized in this research. Field tests were conducted to study the NH_2Cl dissipation with continuous tap water discharge into storm sewers. The results showed a significant decrease of NH_2Cl

concentration from the discharge point to the sampling point at the beginning of discharge, while the decreases reduced with discharge time. To describe this continuous discharge process, a time coefficient *f* was introduced into the model. With the calibration by *f*, the modeled results can describe well the sampling data under various discharge times. The field sample analysis and model development in this research not only can be applied to the regulation of tap water outdoor discharge in Edmonton, but also can provide useful information for the stormwater chloramination studies in other regions.

PREFACE

All of the research in this thesis was designed and planned by myself under the supervision from Dr. Yang Liu at University of Alberta. All the published, submitted and to be submitted research works were compiled by myself, my supervisor Dr. Yang Liu and the following contributions from collaborators and co-authors.

Chapter 3 has been published as Zhang, Q., Gaafar, M., Yang, R. C., Davies, E. G. R., Bolton, J. R., & Liu, Y., "Field data analysis of active chlorine-containing stormwater samples". Journal of Environment Management 2018, 206: 51-59. In this chapter, Mr. Gaafar Mohamed contributed to the manuscript writing of the sampling location selection section. Dr. Chen Ding contributed to the statistical analysis. Dr. Evan Davies and Dr. James Bolton contributed to the experimental planning and manuscript edits. Dr. Rong-cai Yang contributed to the manuscript edits.

Chapter 4 has been published as Zhang, Q., Davies, E. G. R., Bolton, J. R., & Liu, Y., "Monochloramine loss mechanisms in tap water". Water Environment Research 2017, 89(11): 1999-2005. In this chapter, Dr. Bolton contributed to the experimental design in terms of pH control and temperature dependent equation development, as well as the manuscript edits. Dr. Evan Davies contributed to the manuscript edits.

Chapter 5 has been partially published as Zhang, Q., Davies, E. G., Bolton, J. R., & Liu, Y., "Monochloramine loss mechanisms and dissolved organic matter characterization in stormwater". Science of The Total Environment 2018, 631: 745-754. In this chapter, Dr. Evan Davies and Dr. James Bolton contributed to the manuscript edits. Dr. Chad (Qingxia) Liu provided the FT-IR instrument for sample analysis.

Chapter 6: Dr. Evan Davies, Dr. James Bolton contributed to the manuscript edits.

Chapter 7: Mr. Gaafar Mohamed and Dr. Evan Davies contributed to the location selection and field plan development.

DEDICATION

I dedicate my thesis work to:

My parents Mr. Bo Zhang and Mrs. Chaoyang Qian, who gave me unconditional supports for every decision I made and encouraged me to overcome the difficulties in my life.

ACKNOWLEDGEMENT

To begin I would like to express my sincere and deep gratitude to my supervisor Dr. Yang Liu. She brought me to scientific research field and gave me kind support and guidance during my research study. Her thoughtful insight and scientific enthusiasm guided me to complete my research ideas and increase my research ability.

I am greatly thankful to Dr. Evan Davies for introducing me the information about storm sewer systems and inspiring me to improve my English writing skills. Besides, I would like to express my appreciation to Dr. Jim Bolton for the knowledge he provided in terms of the chemical reactions and other suggestions for field monochloramine dissipation studies. Finally, I thank Dr. Chad (Qingxia) Liu for providing the FT-IR instrument to our stormwater sample analysis.

I would also like to sincerely thank Wendy Bertin, Brandy Mckay, Michelle Dzenkiw, Tanya Hunter, Helena Reynolds, Matt Brinkworth, Tim Nelson, Ryan Ledl and other colleagues from City of Edmonton (EPCOR now) and Mohamed Gaafar from University of Alberta for their contributions in the field sampling design and collection. Special appreciations go to summer students Yu Wei, Song Bo and Angus Derocher who helped to conduct field sampling and laboratory analyses during summer 2015 and 2016.

I would like to thank my colleagues and technicians in the department of Civil and Environmental Engineering: Huixin Zhang, Zhiya Sheng, Yanxi Shao, Sen Yang, Paul Cabling, David Zhao, Liang Chen, and all my other colleagues.

Moreover, I would like to thank the sponsors of this research: City of Edmonton and the Natural Sciences and Engineering Research Council of Canada (NSERC).

Finally, I would like to express my gratitude to my family and close friends for their support and encouragement.

TABLE OF CONTENTS

CHAPTER 6. THE ROLE OF BIOFILM ON MONOCHLORAMINE DISSIPATION IN STORM SEWER SYSTEMS: DIRECT REACTIONS OR AOB COMETABOLISM 122

ABBREVIATIONS

AMO	Monooxygenase
AOB	Ammonia oxidizing bacteria
BAPs	Biomass associated products
BOD_5	5 day biochemical oxygen demand
CCME	Canadian Council of Ministers of the Environment
Cl/N	Active chlorine to ammonia-nitrogen ratio
COD	Chemical oxygen demand
COM	Commercial
DBPs	Disinfection by-products
DO	Dissolved oxygen
DOC	Dissolved organic carbon
DOC_r	Reactive dissolved organic carbon
DOM	Dissolved organic matter
DPD	N, N-diethyl-*p*-phenylenediamine
EEM	Excitation−Emission Matrix
EPS	Extracellular polymeric substance
FTIR	Fourier transform infrared
HAAs	Haloacetic acids
HANs	Haloacetonitriles
IND	Industrial
NOB	Nitrite oxidizing bacteria
NOM	Natural organic matter

NRNOM	Nordic Reservoir dissolved organic matter
ORP	Oxidation/reduction potential
PAO	phenylarsine oxide
PRK	Park
PVC	Polyvinyl chloride
*q*PCR	Real-time quantitative polymerase chain reaction
RES	Residential
S_{total}	Total free chlorine and NH_2Cl reactive fractions
SWDOM	Stormwater dissolved organic matter
TAC	Total active chlorine
TDS	Total dissolved solids
THMs	Trihalomethanes
TOTNH3	Total free ammonia
TSS	Total suspended solids
UAPs	Utilization associated products

LIST OF TABLES

LIST OF FIGURES

CHAPTER 1. GENERAL INTRODUCTION AND RESEARCH OBJECTIVES

1. 1. Background

1.1.1. Chlorination and chloramination in drinking water disinfection

At the turn of twentieth century, chlorine as a disinfectant was widely used for drinking water disinfection as it is highly effective in microbial disinfection (Crittenden et al., 2012). In the chlorination process, chlorine gas is initially introduced into water, and rapidly reacts with water to form hydrochloric acid through the following reaction: Cl_2 (g) + $H_2O \rightarrow HCl + HOCl$. hypochlorous acid (HOCl), hypochlorite (OCl^-) and solved chlorine gas (Cl_2) are called free chlorine. Free chlorine species are highly reactive in water. They not only kill microorganisms, but also react with natural organic matter (NOM) in water and form disinfection by-products (DBPs). Chlorinated DBPs can cause harmful impacts to human health, and mainly consist of trihalomethanes (THMs), haloacetic acids (HAAs), haloacetonitriles (HANs), haloketone, etc. (Hrudey, 2009; Kim et al., 2003; Morris et al., 1980). Further, free chlorine is volatile, which causes a decrease of its disinfection efficiency after water flows into drinking water distribution systems, thus leading to the regrowth of bacteria.

To reduce the formation of DBPs and to keep a disinfection effect in the distribution system, chloramination is applied widely for drinking water secondary disinfection. In addition to chlorination, ammonia gas is added to react with free chlorine species and produce inorganic chloramines. Inorganic chloramines are also called combined chlorine, which include monochloramine (NH_2Cl), dichloramine ($NHCl_2$) and trichloramine (NCl_3). In drinking water chloramination, NH_2Cl is the dominant disinfectant. Because of its better oxidation ability and long-lasting property, NH_2Cl presents a better disinfection efficiency than do $NHCl_2$ and NCl_3. Compared with free chlorine, NH_2Cl is less reactive, and produces lower concentrations of DBPs.

In addition, the persistent residual of NH_2Cl can provide continuous disinfection effects after drinking water flows into distribution systems (Brodtmann and Russo, 1979; Mitcham et al., 1983; Norman et al., 1980). As a result of such advantages, chloramination is widely applied for secondary disinfection by water utilities.

1.1.2. The pathways of chloraminated water discharge into fresh water sources

Because NH_2Cl is comparably stable in water, it can lead to detrimental environmental influence by its introduction into storm sewers and fresh water sources. Tap water can be discharged into storm sewer systems through various outdoor tap water uses, such as car washing, garden and lawn irrigation, and driveway washing.

Residential outdoor tap water usage commonly happens from spring to fall, and reaches the peak during summer months (Lyman, 1992). The study from White et al. (2004) showed that during summer period, 40 to 60% of residential water consumption in Texas was outdoor water uses, and most of it was associated with lawn and plant irrigation activities. Further, the water usage data in Phoenix indicated that 60%-75% of residential water was used to maintain outdoor landscaping and swimming pools (Balling et al., 2008). In Canada, residential outdoor tap water uses also account for a large percentage, and mainly are allocated to landscaping irrigation and swimming pools. According to the study from Mayer et al., (1999), 58% of annual water use was for outdoor purposes in Waterloo and Cambridge, Ontario. Further, their research showed that the percentage of outdoor water usage was highly related to climate. With drier climates such as those Tempe and Scottsdale, the ratio of outdoor residential water usage was as twice as that for cities with wetter climates.

In addition to residential landscaping, the lawn watering from public parks, commercial golf courses also increase the outdoor tap water usage, especially during summer months. The irrigation frequency is highly related to precipitation. As such, NH_2Cl contamination is more likely to occur during dry weather periods.

Commercial car washing accounts for only approximately 1% of municipal water usage, and the dirty wash water is typically discharged into sanitary sewer systems (Brown, 2002, 2000; Sablayrolles et al., 2010; Zaneti et al., 2012), which does not impact the water quality in storm sewer systems. However, the situation is unclear for car dealerships and car rental companies. If the vehicle wash wastewater from dealerships and rental companies is discharged directly into storm sewers, it can lead to subsequent stormwater contamination.

Finally, the integrity of large-volume pressure-vessels from industrial production is tested by filling them with tap water. The size of these vessels, such as boilers and large storage tanks, varies from an inner diameter of 60 cm (PricewaterhouseCoopers LLP, 2008) to 10.7 m and 76 m in length (Cessco Fabrication and Engineering Ltd, 2014). After hydro-testing, the tap water is occasionally discharged to the stormwater system without dechloramination (Zhang et al., 2018), and causes active chlorine contamination of the stormwater.

1.1.3. The harmful impact of active chlorine species on the aquatic environment

Total active chlorine (TAC), which is the sum of free chlorine and combined chlorine, can cause great harm to the aquatic environment. Brungs (1973) showed that with continuous discharge, the TAC concentration of effluent discharge should not exceed 0.01 and 0.002 mg/L to protect aquatic biotas. His research also suggested that with intermittent discharge of TAC containing water for 2 hours/day, the TAC concentration should not exceed 0.04 mg/L. In 1984, Brooks and Bartos reported that with an exposure duration of 2 hours, the active chlorine has 1% lethal and 50% lethal concentrations of as low as 0.06 mg/L and 0.08 mg/L respectively to some fish (Brooks and Bartos, 1984). In 1985, EPA proposed that 0.0053 mg/L of TAC could cause

50% mortality to some invertebrate species (United States Environmental Protection Agency, 1985). Moreover, as compared with free chlorine species, long-lasting chloramines showed chronic risk to fish growth with a much lower concentration (Brungs, 1973). Therefore, to protect aquatic life, the Canadian Council of Ministers of the Environment guidelines listed a maximum TAC concentration in surface waters of only 0.5 μg/L (CCME, 1999), and reduced the permissible TAC concentration in discharged effluent from 0.2 to 0.02 mg/L in their Canada-wide strategy (CCME, 2009).

The NH_2Cl concentration in Edmonton tap water is commonly around 2 mg active Cl/L. As aquatic organisms are sensitive to TAC, the tap water discharge into storm sewer systems may pose mortal damage to them. To protect aquatic environment and to adhere to the CCME's guideline, the TAC concentrations in stormwater should be monitored, especially during the summer period. Further, although NH_2Cl is persistent in tap water, it can still dissipate through various pathways. Therefore, the study of NH_2Cl dissipation mechanisms in storm sewer systems is also urgently needed.

1.2. Research scope and objectives

1.2.1. Research needs

Although chloramination has long been used in drinking water distribution system, the contamination of stormwater and fresh water sources by NH_2Cl and other active chlorine species from tap water discharge has not received considerable attention. In addition, the NH_2Cl dissipation processes have been well studied in drinking water distribution systems. However, the stormwater qualities show significant difference from drinking water, the NH_2Cl dissipation mechanisms in drinking water cannot be directly applied for storm sewer systems. The understanding on the NH_2Cl decay mechanisms in storm sewers is still lacking.

1.2.2. Research objectives

The main objectives of this research are (1) to elucidate NH_2Cl dissipation mechanisms in stormwater, and (2) to developing models to simulate NH_2Cl dissipation processes in storm sewers.

1.2.3. Research approach

To achieve research objectives, this research was conducted through the following three interconnected phases: (i) field investigation; (ii) laboratory study; (iii) model development. The detailed contents were described below and shown in Fig. 1.1.

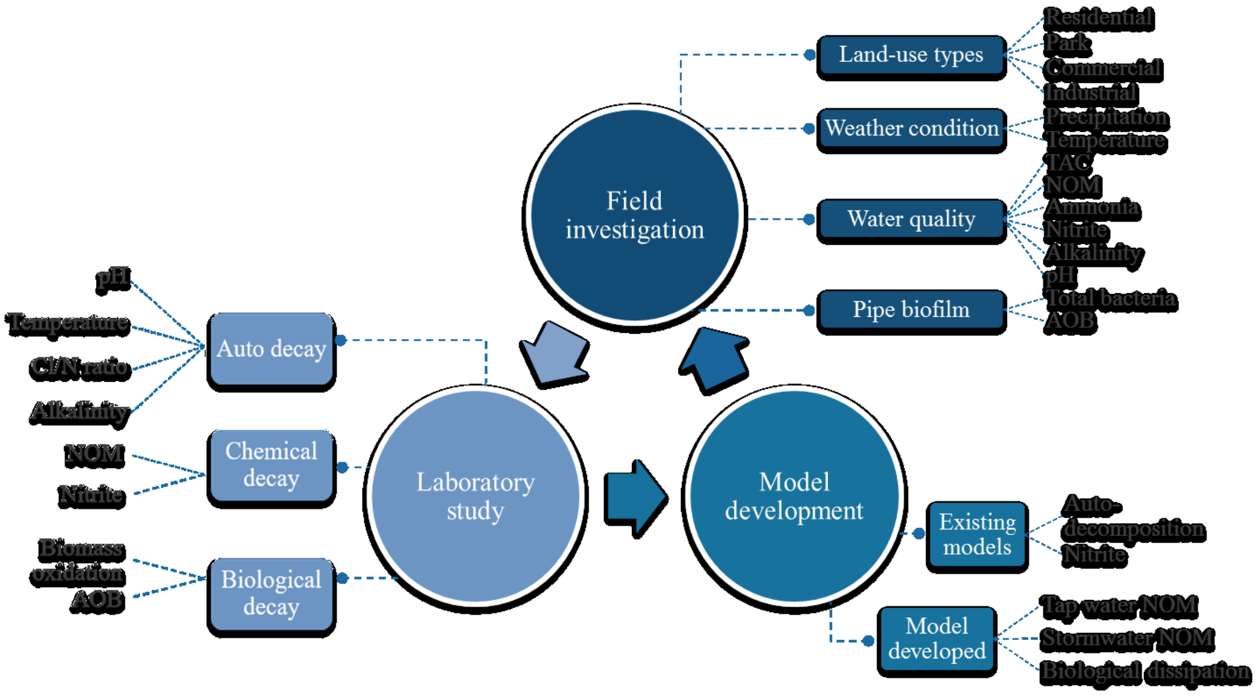

Fig. 1.1. Flow chart of research route

(i) Field investigation

Stormwater was collected twice per month from May to October in 2015 and April to October in 2016 under dry and wet weather conditions. Samples were collected from both upstream and downstream manholes in residential, park, commercial and industrial neighborhoods. Biofilm samples were collected on storm sewer pipes under the same neighborhoods. After samples were collected, the physiochemical characteristics of stormwater were measured. The bacterial community distribution in storm sewer pipes was also analyzed. In addition, the relationship between TAC concentration and perception was evaluated.

Moreover, the field NH_2Cl decay test was conducted in summer 2017, and the decay rate obtained in this field study was used for further model calibration.

The detailed methodology, results and discussions were presented in Chapters 3 and 7.

(ii) Laboratory study

The NH_2Cl dissipation pathways in storm sewer systems include (a) auto-decomposition; (b) chemical reactions with tap water and stormwater components; and (c) biological dissipation pathway. In laboratory studies, the NH_2Cl decay mechanisms through these three pathways were studied respectively.

NH_2Cl auto-decomposition The NH_2Cl auto-decomposition has been studied thoroughly in previous research. Based on the literature, the NH_2Cl auto-decomposition can be impacted by pH, temperature, the active chlorine to ammonium nitrogen ratio (Cl/N) and alkalinity concentrations. In this research, the reaction assumptions from the literature were directly applied in our study.

Chemical reactions with tap water and stormwater components NO_2^- and DOC are the two major components that react with NH_2Cl in stormwater. Since the reactions with NO_2^- have been studied in literature, our research mainly focused on the reactions between NH_2Cl and stormwater DOC. Further, under dry weather conditions, tap water was considered as the major TAC source in storm sewers with continuous discharge. Therefore, the NH_2Cl decay mechanism in tap water was also studied.

NH_2Cl biological dissipation pathway To study the NH_2Cl biological dissipation in storm sewer systems, biofilms were cultured under stormwater conditions in annular reactors, and the microbial community distribution in reactor biofilms was studied. Moreover, NH_2Cl biological dissipation experiments were conducted in reactors, and the NH_2Cl biological decay mechanisms were evaluated.

The detailed methodology, results and discussions were presented in Chapters 4, 5 and 6.

(iii) Model development

With the results from literatures and laboratory experiments, kinetic models were developed to describe the NH_2Cl dissipation processes through the three NH_2Cl decay pathways. Kinetic models are commonly used to describe the reaction rates of various reaction processes, with reaction rate coefficients provided to each reaction. The NH_2Cl auto-decomposition model and the reaction with NO_2^- were used from literatures. The NH_2Cl decay models in tap water and stormwater samples, and the NH_2Cl biological dissipation model were developed in this research based on laboratory experimental results. Finally, the auto-, chemical and biological NH_2Cl dissipation models were combined to simulate the NH_2Cl dissipation in real storm sewers. The feasibility of this comprehensive model was validated though field NH_2Cl dissipation tests.

The detailed methodology, results and discussions were presented in Chapters 4, 5, 6 and 7.

1.3. Thesis outline

The structure of this dissertation is presented below.

Chapter 1 introduces the general background and defines the scope and objectives of this research.

Chapter 2 compares different total and free chlorine analysis methods, and introduces the NH_2Cl auto-decomposition, chemical reaction with various components and the biological dissipation pathways.

Chapter 4 investigates the NH_2Cl loss mechanisms in tap water under various temperature, pH and Cl/N ratios and initial NH_2Cl and natural organic matter (NOM) concentrations. A model was developed to describe the NH_2Cl dissipation process in tap water

Chapter 3 presents the results from field data analysis of active chlorine-containing stormwater samples during summer 2015 and 2016. TAC concentration and other physicochemical and biological characteristics of stormwater and storm sewer biofilm samples collected from these two years were analyzed and compared. Moreover, laboratory experiments were conducted to find the dominant factor that contributes to NH_2Cl dissipation in stormwater

Chapter 5 evaluates the NH_2Cl loss mechanisms and dissolved organic matters characterization in stormwater. In this chapter, the reaction mechanisms between NOM and active chlorine species were studied, and stormwater NOM before and after chloramination were analyzed and compared. Further, a model was developed to simulate the NH_2Cl decay in various stormwater samples

Chapter 6 studies the NH_2Cl biological dissipation pathways. Storm sewer biofilms were cultured in annular reactors under various conditions. The biofilm microbial communities were identified and compared. Moreover, the NH_2Cl biological dissipation model was developed based on batch NH_2Cl decay experiments under various storm sewer conditions.

Chapter 7 combines the NH_2Cl dissipation pathways described in previous chapters and compares the NH_2Cl dissipation results from completed kinetic model with the results from field

NH_2Cl dissipation tests. Also, the NH_2Cl decay processes under various storm sewer conditions were simulated from the completed kinetic model.

Chapter 8 provides the general conclusions of this dissertation and the recommendations for future studies.

Appendix shows the additional data from stormwater field sampling and laboratory analysis

1.4. Reference

Al-Kofahi, S., Steele, C., VanLeeuwen, D., St. Hilaire, R., 2012. Mapping land cover in urban residential landscapes using very high spatial resolution aerial photographs. Urban For. Urban Green. 11, 291–301. doi:10.1016/j.ufug.2012.05.001

Bal Krishna, K.C., Sathasivan, A., Chandra Sarker, D., 2012. Evidence of soluble microbial products accelerating chloramine decay in nitrifying bulk water samples. Water Res. 46, 3977–3988. doi:10.1016/j.watres.2012.05.026

Balling, R.C., Gober, P., Jones, N., 2008. Sensitivity of residential water consumption to variations in climate: An intraurban analysis of Phoenix, Arizona. Water Resour. Res. 44. doi:10.1029/2007WR006722

Bernhardt, E.S., Band, L.E., Walsh, C.J., Berke, P.E., 2008. Understanding, managing, and minimizing urban impacts on surface water nitrogen loading. Ann. N. Y. Acad. Sci. doi:10.1196/annals.1439.014

Breiman, L., 2001. Random forests. Mach. Learn. 45, 5–32. doi:10.1023/A:1010933404324

Brodtmann, N. V., Russo, P.J., 1979. Use of chloramine for reduction of trihalomethanes and disinfection of drinking water. J. Am. Water Works Assoc. doi:10.2307/41269574

Brooks, A.S., Bartos, J.M., 1984. Effects of Free and Combined Chlorine and Exposure Duration on Rainbow Trout, Channel Catfish, and Emerald Shiners. Trans. Am. Fish. Soc. 113, 786–793. doi:10.1577/1548-8659(1984)113<786:EOFACC>2.0.CO;2

Brown, C., 2002. Water Use in the Professional Car Wash Industry, International Carwash Association, Inc.

Brown, C., 2000. Water Conservation in the Professional Car Wash Industry, A Report for the International Carwash Association.

Brungs, W. a, 1973. Effects of residual chlorine on aquatic life. J. Water Pollut. Control Fed. 45, 2180–2193. doi:10.2307/25038016

Canadian Council of Ministers of the Environment, 2009. Canada-wide Strategy for the Management of Municipal Wastewater Effluent. Winnipeg.

Canadian Council of Ministers of the Environment, 1999. Canadian Water Quality Guidelines for the Protection of Aquatic Life: Reactive Chlorine Species. Winnipeg.

Cessco Fabrication and Engineering Ltd, 2014. Products and services [WWW Document]. URL http://cessco.ca/fabrication/products-and-services (accessed 11.15.16).

Coomes, P. a, Rockaway, T.D., Rivard, J., Kornstein, B., 2010. North America Residential Water Usage Trends Since 1992, US EPA.

Crittenden, J.C., Trussell, R.R., Hand, D.W., Howe, K.J., Tchobanoglous, G., 2012. MWH's Water Treatment: Principles and Design: Third Edition, MWH's Water Treatment: Principles and Design: Third Edition. doi:10.1002/9781118131473

Duirk, S.E., Gombert, B., Croué, J.P., Valentine, R.L., 2005. Modeling monochloramine loss in the presence of natural organic matter. Water Res. 39, 3418–3431. doi:10.1016/j.watres.2005.06.003

Echeverry-Galvis, M.A., Peterson, J.K., Sulo-Caceres, R., 2014. The social nestwork: Tree structure determines nest placement in Kenyan weaverbird colonies. PLoS One 9. doi:10.1371/journal.pone.0088761

EPCOR Utilities Inc., 2015. Edmonton Waterworks Annual Report to Alberta Environment and Water 2015.

Fisher, R., 1925. Statistical methods for research workers, Biological monographs and manuals. doi:10.1056/NEJMc061160

Hrudey, S.E., 2009. Chlorination disinfection by-products, public health risk tradeoffs and me. Water Res. doi:10.1016/j.watres.2009.02.011

Kaushal, S.S., Groffman, P.M., Band, L.E., Elliott, E.M., Shields, C.A., Kendall, C., 2011. Tracking nonpoint source nitrogen pollution in human-impacted watersheds. Environ. Sci. Technol. 45, 8225–8232. doi:10.1021/es200779e

Kiéné, L., Lu, W., Lévi, Y., 1998. Relative importance of the phenomena responsible for chlorine decay in drinking water distribution systems. Water Sci. Technol. 38, 219–227. doi:10.1016/S0273-1223(98)00583-6

Kim, J., Chung, Y., Shin, D., Kim, M., Lee, Y., Lim, Y., Lee, D., 2003. Chlorination by-products in surface water treatment process. Desalination 151, 1–9. doi:10.1016/S0011-9164(02)00967-0

Kuang, X., Sansalone, J., 2011. Cementitious porous pavement in stormwater quality control: pH and alkalinity elevation. Water Sci. Technol. 63, 2992–2998. doi:10.2166/wst.2011.505

Liaw, a, Wiener, M., 2002. Classification and Regression by randomForest. R news 2, 18–22. doi:10.1177/154405910408300516

Liu, A., Egodawatta, P., Guan, Y., Goonetilleke, A., 2013. Influence of rainfall and catchment characteristics on urban stormwater quality. Sci. Total Environ. 444, 255–262. doi:10.1016/j.scitotenv.2012.11.053

Lyman, R.A., 1992. Peak and off-peak residential water demand. Water Resour. Res. 28, 2159–2167. doi:10.1029/92WR01082

Maestre, J.P., Wahman, D.G., Speitel, G.E., 2016. Monochloramine Cometabolism by Mixed-Culture Nitrifiers under Drinking Water Conditions. Environ. Sci. Technol. 50, 6240–6248. doi:10.1021/acs.est.5b05641

Maestre, J.P., Wahman, D.G., Speitel, G.E., 2013. Monochloramine cometabolism by Nitrosomonas europaea under drinking water conditions. Water Res. 47, 4701–4709. doi:10.1016/j.watres.2013.05.019

Makepeace, D.K., Smith, D.W., Stanley, S.J., 1995. Urban stormwater quality: Summary of contaminant data. Crit. Rev. Environ. Sci. Technol. 25, 93–139. doi:10.1080/10643389509388476

Mayer, P.W., Deoreo, W.B., Opitz, E.M., Kiefer, J.C., Davis, W.Y., Dziegielewski, B., Nelson, J.O., 1999. Residential End Uses of Water. Aquacraft, Inc. Water Eng. Manag. 310. doi:4309b

Mays, L.W., 2002. Water demand analysis, in: Urban Water Supply Handbook. McGRAW-HILL.

Mitcham, R.P., Shelley, M.W., Wheadon, C.M., 1983. Free chlorine versus ammonia-chlorine: disinfection, trihalomethane formation, and zooplankton removal. J. Am. Water Works Assoc. 75, 196–198.

Morris, J.C., Christman, R.F., Glaze, W.H., Helz, G.R., Hoehn, R.C., Jolley, R.L., 1980. The chemistry of disinfectants in water: reactions and products, Drinking Water and Health. National Academy of Sciences, Washington, DC. doi:10.1016/0160-4120(91)90308-D

Norman, T.S., Harms, L.L., Looyenga, R.W., 1980. The Use of Chloramines To Prevent Trihalomethane Formation. J. Am. Water Works Assoc. 72, 176–180.

Nouri, H., Beecham, S., Kazemi, F., Hassanli, A.M., 2013. A review of ET measurement techniques for estimating the water requirements of urban landscape vegetation. Urban Water J. 10, 247–259. doi:10.1080/1573062X.2012.726360

Pitt, R., Maestre, A., Morquecho, R., 2004. The national stormwater quality database (NSQD, version 1.1), 1st Annual Stormwater Management Research Symposium Proceedings.

PricewaterhouseCoopers LLP, 2008. Alberta Pressure Vessel Manufacturing Sector Benchmarking Report 2008 Provincial Trends : Global Currents, PricewaterhouseCoopers LLP.

R Development Core Team, R.F.F.S.C., 2008. R: A Language and Environment for Statistical Computing. Vienna Austria R Found. Stat. Comput. doi:10.1007/978-3-540-74686-7

Rittmann, B.E., Regan, J.M., Stahl, D.A., 1994. Nitrification as a source of soluble organic substrate in biological treatment. Water Sci. Technol. 30, 1–8.

Sablayrolles, C., Vialle, C., Vignoles, C., Montrejaud-Vignoles, M., 2010. Impact of carwash discharge on stormwater quality (Toulouse, France). Water Sci. Technol. 62, 2737–2746. doi:10.2166/wst.2010.929

Sathasivan, A., Fisher, J., Kastl, G., 2005. Simple method for quantifying microbiologically assisted chloramine decay in drinking water. Environ. Sci. Technol. 39, 5407–5413. doi:10.1021/es048300u

Shlens, J., 2014. A Tutorial on Principal Component Analysis. ArXiv 1–13. doi:10.1.1.115.3503

Siripong, S., Rittmann, B.E., 2007. Diversity study of nitrifying bacteria in full-scale municipal wastewater treatment plants. Water Res. 41, 1110–1120. doi:10.1016/j.watres.2006.11.050

Strassler, E., Pritts, J., Strellec, K., 1999. Preliminary data summary of urban storm water best management practices, US EPA.

United States Environmental Protection Agency, 1985. Ambient Aquatic Life Water Quality Creteria for Chlorine. Florida.

Vikesland, P.J., Ozekin, K., Valentine, R.L., 2001. Monochloramine decay in model and distribution system waters. Water Res. 35, 1766–1776. doi:10.1016/S0043-1354(00)00406-1

Wahman, A.D.G., Maestre, J.P., Jr, G.E.S., 2016. Title : Monochloramine cometabolism by drinking water relevant nitrifying biofilm 362–373. doi:10.5942/jawwa.2016.108.0092

Wahman, D.G., Speitel, G.E., 2012. Relative importance of nitrite oxidation by hypochlorous acid under chloramination conditions. Environ. Sci. Technol. 46, 6056–6064. doi:10.1021/es300934x

White, R., Havalak, R., Nations, J., Thomas, J., Chalmers, D., Dewey, D., 2004. How much water is enough? Using pet to develop water budgets for residential landscapes.

Zaneti, R., Etchepare, R., Rubio, J., 2012. More environmentally friendly vehicle washes: Water reclamation. J. Clean. Prod. 37, 115–124. doi:10.1016/j.jclepro.2012.06.017

Zhang, Q., Davies, E.G.R., Bolton, J., Liu, Y., 2017. Monochloramine loss mechanisms in tap water. Water Environ. Res. doi:10.2175/106143017X14902968254421

Zhang, Q., Gaafar, M., Yang, R.-C., Ding, C., Davies, E.G.R., Bolton, J., Liu, Y., 2018. Field data analysis of active chlorine-containing stormwater samples. Jounral Environ. Manag. 206, 51–59.

CHAPTER 2. LITERATURE REVIEW

2.1. Comparison of analysis methods for active chlorine species

Active chlorine species are commonly analyzed in water and wastewater by the following methods: iodometric titration, amperometric titration, and N, N-diethyl-p-phenylenediamine (DPD) titration and colorimetry. The reactions involved in these methods are shown in Table 2.1.

Iodometric titration is used only for a total chlorine analysis, as both free and combined chlorine species react with the iodine ion (I^-). Iodometric titration consists of forward and backward methods. The forward method is one of the oldest methods to determine active chlorine concentration. In this method, potassium iodide (KI) is added to samples to react with active chlorine species and produce the triiodide ion (I_3^-). After all the active chlorine species react with I^-, a starch solution is added and the color of the sample turns blue. The triiodide ion (I_3^-) is then titrated by 0.01 N or 0.025 N sodium thiosulfate ($Na_2S_2O_3$) to the colorless point (APHA/AWWA/WEF, 2012; Harp, 2002). In the backward iodometric titration method, a known volume of standard sodium thiosulfate ($Na_2S_2O_3$) or phenylarsine oxide (PAO) reagent is first added to samples to react with active chlorine species. As the sodium thiosulfate or phenylarsine oxide is in excess, the amount of unreacted reagent can be titrated by a standard iodine solution. The total chlorine is calculated by the volume of iodine solution used in the titration (APHA/AWWA/WEF, 2012). Note, the titration is recommended to be performed in a pH range of 3~4 and at a temperature below 20 ℃. (APHA/AWWA/WEF, 2012).

The amperometric titration method measures active chlorine concentrations by a change in current that arises from the chemical reactions of the titrant in water samples. In this method, the current change is measured by a special amperometric cell. To determine free chlorine concentrations, phenylarsine oxide (PAO) is added to the sample to react with free chlorine species. Combined chlorine species react more slowly with PAO than free chlorine species. To quantify the combined chlorine species, the standard KI reagent is first added to samples to react with NH_2Cl and $NHCl_2$, and produce I_3^-. Then, the concentration of I_3^- can be titrated by the standard PAO reagent and measured to quantify the chlorine present in the sample (APHA/AWWA/WEF, 2012; Harp, 2002).

The DPD method is the most widely used method to determine free and total active chlorine concentrations in water and wastewater (Gordon et al., 1991). At a near neutral pH, in the presence of free chlorine species, a red color (Würster dye) forms rapidly with the addition of DPD reagent to the sample (Harp, 2002). Free chlorine concentrations can then be measured based on the color of Würster dye produced in the solution. DPD methods include a colorimetric method and a ferrous titration method. In the colorimetric method, the absorption of the red color is measured at a wavelength of 515 nm (Moberg and Karlberg, 2000). In the titration method, the red color is titrated with a standard ferrous reducing reagent such as ferrous ammonium sulfate to a colorless end point (Harp, 2002). Similar to the amperometric titration method, NH_2Cl and $NHCl_2$ react with DPD slowly. To measure total chlorine concentrations, a standard KI reagent is added into samples first, as iodine ion can react with DPD faster than NH_2Cl and $NHCl_2$. However, as there is no evidence that NCl_3 reacts with I^-, the NCl_3 concentration cannot be quantitated in the methods (Gordon et al., 1991).

Table 2.1. Reactions involved in the active chlorine analysis methods (APHA/AWWA/WEF, 2012; Harp, 2002)

Analysis method		**Correlative reactions**
Iodometric titration method	Forward	$Cl_2 + 3I^- \rightarrow I_3^- + 2Cl^-$ $NH_2Cl + 3I^- + H_2O + H^+ \rightarrow NH_4OH + Cl^- + I_3^-$ $NHCl_2 + 3I^- + H_2O + 2H^+ \rightarrow NH_4OH + 2Cl^- + I_3^-$ $I_3^- + 2S_2O_3^{2-} \rightarrow 3I^- + S_4O_6^{2-}$
	Back	$Cl_2 + 2S_2O_3^{2-} \rightarrow 2Cl^- + S_4O_6^{2-}$ $NH_2Cl + 2S_2O_3^{2-} + H_2O + H^+ \rightarrow S_4O_6^{2} + NH_4OH + Cl^-$ $NHCl_2 + 2S_2O_3^{2-} + H_2O + 2H^+ \rightarrow S_4O_6^{2} + NH_4OH + 2Cl^-$ $I_3^- + 2S_2O_3^{2-}$ (excess) $\rightarrow 3I^- + S_4O_6^{2-}$
Amperometric titration method		(PAO) 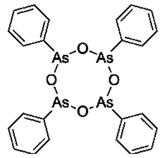 $Cl_2 + 2H_2O \rightarrow PhAsO(OH)_2 + 2Cl^- + 2H^+$ (Ph=phenyl) 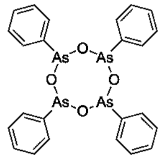 $I_3^- + H_2O \rightarrow 3I^- + PhAsO(OH)_2 + 2H^+$ (Ph=phenyl)
DPD methods	colorimetry	(DPD) 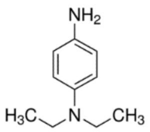 $+ Cl_2 \rightarrow$ Würster dye (red color) $+ 2Cl^- + H^+$ 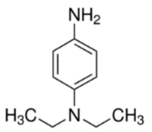 $+ I_3^- \rightarrow$ Würster dye (red color) $+ 3I^- + H^+$
	Titration	Würster dye (red color) $+ Fe^{2+} \rightarrow$ DPD $+ Fe^{3+}$

In iodometric titration methods, I_3^- as the product from the forward iodometric titration ($Cl_2 + 3I^- \rightarrow I_3^- + 2Cl^-$), is more easily oxidized than $S_4O_6^{2-}$ ($Cl_2 + 2S_2O_3^{2-} \rightarrow 2Cl^- + S_4O_6^{2-}$). Therefore, if a water sample contains high concentrations of interferences, inaccurate results are easily obtained using the forward method. However, the iodometric titration methods can only measure total active chlorine (TAC) concentrations higher than 1 mg/L. Since TAC concentrations in stormwater are significantly lower than 1 mg/L, these methods are not recommended to measure TAC concentrations in stormwater samples (Harp, 2002).

The amperometric titration method is generally considered to be the most accurate method to detect both free and combined chlorine species because it shows little effect of interferences. However, this method requires technical skill and a stable environment (APHA/AWWA/WEF, 2012), which cannot be achieved in the field, and it takes a longer time than colorimetric measurement methods.

The DPD titration method commonly shows inflated results compared to other methods (Derrigan et al., 1993), as DPD can react with the oxygen dissolved in the samples during the titration process, thus increasing the measurement results. Moreover, Fe^{2+} as the titrant reagent used in this method, is somewhat unstable and easily oxidized, which also increases the measurement results (Harp, 2002).

Reports in the literature have suggested that the DPD colorimetric method can provide measurement results as accurate as the amperometric titration method. In addition, the DPD colorimetric method is easy to operate in the field using a Hach Chlorine Test Kit, and colorimetric methods are faster than titration methods, which also benefits the field analysis (Wilde, 1991). Therefore, the DPD colorimetric method is considered to be the best method to measure active chlorine species in this research.

2.2. NH_2Cl auto-decomposition mechanisms and kinetic models

During chloramination, ammonia is used to convert residual chlorine to chloramines, which reduces the formation of disinfection by-products (DBPs). At near neutral pH, with an active chlorine to ammonia nitrogen (Cl/N) molar ratio < 1, monochloramine (NH_2Cl) is the predominant chlorine species in tap water (Bernhardt et al., 2008; Crittenden et al., 2012; Valentine et al., 1988; Woolschlager et al., 2001). NH_2Cl dissipation in storm sewers occurs in three pathways: (1) auto-decomposition, (2) the chemical reactions with chemicals such as NO_2^- and natural organic matter (NOM), and (3) biological dissipation.

Under near neutral pH, NH_2Cl can auto-decompose through a series of reactions, and the auto-decomposition rate depends markedly on pH, temperature, the Cl/N molar ratio, alkalinity, and the initial NH_2Cl concentration (Bal Krishna et al., 2012; Liu et al., 2011; Vikesland et al., 2001). At lower pH, higher temperature, a higher Cl/N molar ratio, and higher initial NH_2Cl and alkalinity concentrations, the NH_2Cl auto-decomposition rate is accelerated (Vikesland et al., 2001). A kinetic model that described the reaction constants of all the reactions involved in chloramination was proposed by Jafvert and Valentine (1992). To simulate NH_2Cl auto-decomposition under a more realistic condition, the model was modified by Vikesland and collegues in 2001. In tap water, NH_2Cl is the dominant active chlorine species and the concentration of trichloramine (NCl_3) can be ignored (Ma and Bibby, 2017). Therefore, reactions related to NCl_3 were removed from the model. As alkalinity is widely present in drinking water, the impact of alkalinity was considered in this model. This auto-decomposition model has been widely used in NH_2Cl dissipation studies, and has also been applied to describe the NH_2Cl auto-decay processes in our research. The detailed reactions in this model are listed in Table 2.2.

Table 2.2. NH_2Cl auto-decomposition model developed by Vikesland et al. (2001)

No.	Reaction Types	Reaction Equations	References
1	Auto-decomposition reactions	$HOCl + NH_3 \rightleftharpoons NH_2Cl + H_2O$	Morris and Isaac, 1981
2		$HOCl + NH_2Cl \rightleftharpoons NHCl_2 + H_2O$	
3		$2NH_2Cl \rightarrow NHCl_2 + NH_3$	Jafvert and Valentine, 1992
4		$NHCl_2 + NH_3 \rightarrow 2NH_2Cl$	Hand and Margerum, 1983
5		$NHCl_2 + H_2O \rightarrow I^a$	Jafvert and Valentine, 1987
6		$NHCl_2 + I \rightarrow HOCl + pd1^b$	Leao, 1981
7		$NH_2Cl + I \rightarrow pd2^b$	
8		$NH_2Cl + NHCl_2 \rightarrow pd3^b$	
9	Equilibrium reactions	$HOCl = H^+ + OCl^-$	Snoeyink and Jenkins, 1980
10		$NH_4^+ = NH_3 + H^+$	
11		$H_2CO_3 = HCO_3^- + H^+$	
12		$HCO_3^- = CO_3^{2-} + H^+$	

a. I represents an unidentified intermediate.

b. pd1–pd3 (pd means products) may include N_2, H_2O, Cl^-, H^+, NO_3^-, and other unidentified products (Jafvert and Valentine, 1992).

2.3. NH_2Cl reactions with chemical components

NOM and chemicals such as, nitrite (NO_2^-), ferrous ion (Fe^{2+}), and bromide (Br^-) existing in natural water bodies and drinking water distribution systems can react with NH_2Cl, thus accelerating NH_2Cl dissipation rates in storm sewer systems (Vikesland et al., 2001; Wahman and Speitel, 2012; Zhang et al., 2017).

With excess ammonia added during chloramination, ammonia oxidizing bacteria (AOB) are able to grow in drinking water distribution systems and generate biofilms in distribution systems. NO_2^-, an AOB metabolic product, can be produced through nitritation process and reacts with active chlorine species (AWWA, 2013, 2006; Sathasivan et al., 2009; Zhang et al., 2009). The reaction between hypochlorite (OCl^-) and NO_2^- was well studied by researchers in the late 1980s (Dlyamandoglu et al., 1990; Hao et al., 1994). Compared to studies of free chlorine, the study of reactions between NH_2Cl and NO_2^- began relativity late. Valentine and Selleck, 1981, proposed that NO_2^- was not oxidized by NH_2Cl in 1:1 stoichiometry. Following the reaction mechanisms of free chlorine and NO_2^-, Margerum et al. proposed the reaction expression and constants for NH_2Cl with NO_2^- in 1994. They assumed that NO_2^- reacts with NH_2Cl under acidic conditions, producing nitryl chloride (NO_2Cl) as an intermediate, which is different from the reactions between OCl^- and NO_2Cl (Margerum et al., 1994). In the same year, the kinetics of reactions between NH_2Cl and NO_2^- were evaluated by Hao et al. With the reaction rate constants developed in their research, the NH_2Cl dissipation rate can be simulated under various pH, temperature, and initial ammonium, NH_2Cl, and NO_2^- concentrations. These reactions were also used by Vikesland et al. (2001) in the development of the drinking water NH_2Cl dissipation model. In 2012, Wahman and Speitel proposed that the NH_2Cl and HOCl released from NH_2Cl auto-decomposition should be considered in the NH_2Cl dissipation model, which helped to increase the accuracy of the NH_2Cl decay model.

NOM widely exists in natural water bodies such us rivers (Hedges et al., 1994), lakes (Peuravuori et al., 1997), reservoirs (Qin et al., 2006), groundwater (Liu and Amy, 1993), and stormwater (McElmurry et al., 2014). NOM consists of a complex matrix of organic materials; its composition varies in different water bodies (Fabris et al., 2008; Matilainen et al., 2010) and in different seasons in the same water bodies (Matilainen et al., 2010; Sharp et al., 2006a, 2006b; Smith and Kamal, 2009). NOM is also found in drinking water, as it cannot be completely removed from source water through drinking water treatment (Jacangelo et al., 1995). The rate of NH_2Cl dissipation can be accelerated in the presence of NOM. The mechanisms of NH_2Cl dissipation in the presence of NOM was studied by Vikesland et al. in 1998. Their research proposed that rather than a catalyst, NOM plays as a reductant to react with NH_2Cl, thus leading to the NH_2Cl faster decay. However, the possible reactions between NOM and NH_2Cl were not studied. In 2002, Duirk et al. proposed that NH_2Cl reacts with NOM through two pathways: rapid reaction and long-term reaction. They assumed that NOM consists of sites that rapidly react with NH_2Cl at the beginning of the reaction and sites that react with NH_2Cl continuously during NH_2Cl dissipation. In this research a model was developed to describe the decay process. However, with an increase in NH_2Cl and total free ammonia (including NH_4^+ and NH_3) concentrations under the same active Cl/N molar ratio, the kinetic constants of the long-term reaction decreased, which means that some intermediate products, such as free chlorine and $NHCl_2$ formed during NH_2Cl auto-decomposition, may also react with NOM. Therefore, in 2005, Duirk and colleagues proposed that rather than NH_2Cl, free chlorine reacts with NOM in a long-term reaction. Under this assumption, the NOM long-term reaction rate constant does not change with pH, a theory that produces more realistic NH_2Cl decay kinetics than earlier theories. Based on the model developed by Duirk et al. (2005), Zhu and Zhang (2016) suggested that both NH_2Cl and free chlorine species participate in rapid and slow reactions with NOM in NH_2Cl dissipation, presenting a better simulation of NH_2Cl decay rates in drinking water distribution systems.

Bromide can enter water bodies through mineral erosion (Flury and Papritz, 1993), tracer usage (Gish et al., 1986; Jury et al., 1986), agricultural applications (Wegman et al., 1983), urban runoff (Sollars et al., 1982), and industrial discharges (Winid, 2015). Though surface waters usually contain low concentrations of bromide (Wang et al., 2017), a small amount of bromide can pose a threat to treated drinking water (Heeb et al., 2014; Westerhoff et al., 2004). Specifically, NH_2Cl can react with bromide (Br^-), which might lead to the formation of harmful disinfection by-products (DBPs). (Luh and Mariñas, 2014). The reaction kinetics were first studied by Trote et al. in 1980. Under their assumption, the reaction rate is a function of NH_2Cl, Br^-, and H^+ concentrations, and the reaction products included haloamine and bromochloramine (NHBrCl). Besides, the reaction rate constant was also estimated in this research. NHBrCl as an initial product in the NH_2Cl Br^- reaction, was confirmed by the research from Bousher et al. (1989). The authors suggested that rather than NH_2Cl, NH_3Cl^+ was formed to react with Br^- Moreover, the final products varied under different buffer capacities. In 2001, a kinetic model of NH_2Cl dissipation in the presence of Br^- was developed by Vikesland et al. In addition to NH_2Cl Br^- reactions, reactions between HOCl and Br^- cited in Valentine, 1986, were also included in this model. However, although the NH_2Cl dissipation rate is described well in this model, the production of NHBrCl cannot be simulated well. In 2010, additional possible reactions with NHBrCl were proposed (Alsulaili et al., 2010) and are widely used in present models.

The ferrous ion (Fe^{2+}) in drinking water is mainly derived from groundwater, which receives Fe^{2+} from rocks and minerals (Piché and Larachi, 2006; Postawa et al., 2013), and pipeline corrosion (El Azher et al., 2008). Dissolved carbon dioxide and other acids in tap water are also corrosive to metal pipe, and contribute to the release of Fe^{2+} (Sarin et al., 2004, 2001; Sontheimer et al., 1981). Fe^{2+} reacts with free chlorine with a 2:1 stoichiometry (Knocke, 1990), which follows the same reaction stoichiometry as the NH_2Cl Fe^{2+} reaction. Vikesland and Valentine (2000) suggested two mechanisms for reactions between NH_2Cl and Fe^{2+}: (i) a direct reaction of NH_2Cl with Fe^{2+}, which is a rate limiting reaction for NH_2Cl disappearance and (ii) an autocatalytic reaction by ferric oxide precipitate, which accelerates the NH_2Cl decay rate. Based on this hypothesis, they developed a kinetic model two years later (Vikesland and Valentine, 2002), and this model can be applied to predict NH_2Cl decay under various drinking water conditions.

2.4. NH_2Cl biological dissipation mechanisms

Biological dissipation of NH_2Cl takes three pathways: (i) direct reactions with biomass, extracellular polymeric substance (EPS), and other bacterial metabolic products; (ii) cometabolism by ammonia oxidizing bacteria (AOB); and (iii) reactions with AOB utilization associated products (UAPs) (Bal Krishna et al., 2012; Maestre et al., 2016, 2013).

As a widely used disinfectant in drinking water, NH_2Cl can react with bacteria and control the spread of pathogens (Kool et al., 1999). NH_2Cl is also consumed by the metabolic products produced by bacterial degradation (Maestre et al., 2013). In drinking water distribution systems and other water pipes, bacteria secrete EPS to form biofilm (Pedersen, 1990). EPS accounts for more than 90% of biofilm (Coburn et al., 2016; Xue et al., 2014), and it increases the resistance of bacteria to disinfectants (LeChevallier et al., 1988).

Furthermore, NH_2Cl can be consumed by the ammonia monooxygenase (AMO) enzyme in AOB through cometabolism (Maestre et al., 2013; Maestre et al., 2016; Wahman et al., 2016). Microbial cometabolism is the degradation of non-growth components by nonspecific enzymes in the presence of a growth substrate (Dalton and Stirling, 1982; Maestre et al., 2013). Hooper et al. (1997) proposed that in the presence of ammonia as the nitrogen source, AMO enzyme in *Nitrosomonas europaea* (an AOB species) cometabolizes more than 35 halogenated chemicals. In 2005 and 2016, Wahman and colleagues reported that AMO degraded low concentrations of four trihalomethanes in pure *Nitrosomonas europaea* and mixed culture nitrifying bacteria (Wahman et al., 2006, 2005). The cometabolism of NH_2Cl by *Nitrosomonas europaea* is firstly studied by Woolschlager in 2000. Based on his research, NH_2Cl can be converted to chlorohydroxylamine by

AMO. As nitrifying biofilm is commonly observed in drinking water distribution systems (Gomez-Alvarez et al., 2014; Zhang et al., 2009), to simulate the NH_2Cl dissipation in drinking water pipelines, a kinetic model was proposed in the presence of *Nitrosomonas europaea* by Maestre et al. in 2013. The authors proposed that three pathways should be considered in this model: (1) direct reactions between biomass and NH_2Cl, (2) AMO cometabolism, and (3) the reaction between NH_2Cl and UAP from *Nitrosomonas europaea* degradation. UAP is a class of soluble products produced during bacteria metabolism (Abrahamson et al., 1996; Laspidou and Rittmann, 2002; Ni et al., 2011), which are likely to react with NH_2Cl during its biological decay. However, since the composition of AOB is complex in natural environments, NH_2Cl dissipation in a pure culture may not represent the real situation. Therefore, in 2016, NH_2Cl biological decay in mixed-culture nitrifying were studied, and a new kinetic model was developed (Maestre et al., 2016).

Although NH_2Cl auto-, chemical, and biological decay pathways were well studied under drinking water conditions, no researches were found to predict the NH_2Cl loss mechanisms in storm sewer systems. As stormwater quality and storm sewer environments are significantly different from those of drinking water pipes, a new model was needed to predict NH_2Cl dissipation in storm sewers.

2.5. Reference

Abrahamson, M., Lewandowski, Z., Geesey, G., Skjåk-Bræk, G., Strand, W., Christensen, B.E., 1996. Development of an artificial biofilm to study the effects of a single microcolony on mass transport. J. Microbiol. Methods 26, 161–169. doi:10.1016/0167-7012(96)00908-6

Alsulaili, A., Speitel, G.E., Katz, L.E., 2010. Monochloramine and total haloamine decay after a short prechlorination time in the presence of bromide. Water Sci. Technol. Water Supply 10, 512–516. doi:10.2166/ws.2010.171

APHA/AWWA/WEF, 2012. Standard Methods for the Examination of Water and Wastewater. Stand. Methods 541. doi:ISBN 9780875532356

AWWA, 2013. Nitrification Prevention and Control in Drinking Water. Am. Water Work. Assoc. 320.

AWWA, 2006. Fundamentals and Control of Nitrification in Chloraminated Drinking Water Distribution Systems (AWWA Manual M56), 1st ed. American Water Works Association, Denver, CO.

Bal Krishna, K.C., Sathasivan, A., Chandra Sarker, D., 2012. Evidence of soluble microbial products accelerating chloramine decay in nitrifying bulk water samples. Water Res. 46, 3977–3988. doi:10.1016/j.watres.2012.05.026

Bernhardt, E.S., Band, L.E., Walsh, C.J., Berke, P.E., 2008. Understanding, managing, and minimizing urban impacts on surface water nitrogen loading. Ann. N. Y. Acad. Sci. doi:10.1196/annals.1439.014

Bousher, A., Brimblecombe, P., Midgley, D., 1989. Kinetics of reactions in solutions containing monochloramine and bromide. Water Res. 23, 1049–1058. doi:10.1016/0043-1354(89)90180-2

Coburn, K.M., Wang, Q., Rediske, D., Viola, R.E., Hanson, B.L., Xue, Z., Seo, Y., 2016. Effects of extracellular polymeric substance composition on bacteria disinfection by monochloramine: Application of MALDI-TOF/TOF-MS and multivariate analysis. Environ. Sci. Technol. 50, 9197–9205. doi:10.1021/acs.est.6b00927

Crittenden, J.C., Trussell, R.R., Hand, D.W., Howe, K.J., Tchobanoglous, G., 2012. MWH's Water Treatment: Principles and Design: Third Edition, MWH's Water Treatment: Principles and Design: Third Edition. doi:10.1002/9781118131473

Dalton, H., Stirling, D.I., 1982. Co-metabolism. Philos. Trans. R. Soc. London. Ser. B Biol. Sci. 297, 481–496.

Derrigan, J., Lin, L., Jensen, J., 1993. Comparison of free and total chlorine measurement methods in municipal wastewaters. Water Environ. Res. 65, 205–212. doi:doi:10.2175/WER.65.3.3

Dlyamandoglu, V., Mariñas, B.J., Selleck, R.E., 1990. Stoichiometry and Kinetics of the Reaction of Nitrite with Free Chlorine in Aqueous Solutions. Environ. Sci. Technol. 24, 1711–1716. doi:10.1021/es00081a014

Duirk, S.E., Gombert, B., Choi, J., Valentine, R.L., 2002. Monochloramine loss in the presence of humic acid. J. Environ. Monit. 4, 85–89. doi:10.1039/b106047n

Duirk, S.E., Gombert, B., Croué, J.P., Valentine, R.L., 2005. Modeling monochloramine loss in the presence of natural organic matter. Water Res. 39, 3418–3431. doi:10.1016/j.watres.2005.06.003

El Azher, N., Gourich, B., Vial, C., Soulami, M.B., Ziyad, M., 2008. Study of ferrous iron oxidation in Morocco drinking water in an airlift reactor. Chem. Eng. Process. Process Intensif. 47, 1877–1886. doi:10.1016/j.cep.2007.10.013

Fabris, R., Chow, C.W.K., Drikas, M., Eikebrokk, B., 2008. Comparison of NOM character in selected Australian and Norwegian drinking waters. Water Res. 42, 4188–4196. doi:10.1016/j.watres.2008.06.023

Flury, M., Papritz, A., 1993. Bromide in the natural environment: occurrence and toxicity. J. Environ. Qual. 22, 747–758. doi:10.2134/jeq1993.00472425002200040017x

Gish, T.J., Zhuang, W., Helling, C.S., Kearney, P.C., 1986. Chemical transport under no-till field conditions. Geoderma 38, 251–259. doi:10.1016/0016-7061(86)90019-4

Gomez-Alvarez, V., Schrantz, K.A., Pressman, J.G., Wahman, D.G., 2014. Biofilm community dynamics in bench-scale annular reactors simulating arrestment of chloraminated drinking water nitrification. Environ. Sci. Technol. 48, 5448–5457. doi:10.1021/es5005208

Gordon, G., Sweetin, D.L., Smith, K., Pacey, G.E., 1991. Improvements in the N,N-diethyl-p-phenylenediamine method for the determination of free and combined residual chlorine through the use of FIA. Talanta 38, 145–149. doi:10.1016/0039-9140(91)80122-G

Hand, V.C., Margerum, D.W., 1983. Kinetics and mechanisms of the decomposition of dichloramine in aqueous solution. Inorg. Chem. 22, 1449–1456. doi:10.1021/ic00152a007

Hao, O.J., Chien, C.M., Valentine, R.L., 1994. Kinetics of monochloramine reactions with nitrite. J. Environ. Eng.-asce. 120, 859–874. doi:10.1061/(ASCE)0733-9372(1994)120:4(859)

Harp, D.L., 2002. Current Technology of Chlorine Analysis for Water and Wastewater, Hach company.

Hedges, J.I., Cowie, G.L., Richey, J.E., Quay, P.D., Benner, R., Strom, M., Forsberg, B.R., 1994. Origins and Processing of Organic-Matter in the Amazon River as Indicated by Carbohydrates and Amino-Acids. Limnol. Oceanogr. 39, 743–761. doi:10.4319/lo.1994.39.4.0743

Heeb, M.B., Criquet, J., Zimmermann-Steffens, S.G., Von Gunten, U., 2014. Oxidative treatment of bromide-containing waters: Formation of bromine and its reactions with inorganic and organic compounds - A critical review. Water Res. 48, 15–42. doi:10.1016/j.watres.2013.08.030

Hooper, A.B., Vannelli, T., Bergmann, D.J., Arciero, D.M., 1997. Enzymology of the oxidation of ammonia to nitrite by bacteria, in: Antonie van Leeuwenhoek, International Journal of General and Molecular Microbiology. pp. 59–67. doi:10.1023/A:1000133919203

Jacangelo, J.G., DeMarco, J., Owen, D.M., Randtke, S.J., 1995. Selected processes for removing NOM: An overview. J. / Am. Water Work. Assoc. 87, 64–77. doi:10.2307/41295153

Jafvert, C.T., Valentine, R.L., 1992. Reaction scheme for the chlorination of ammoniacal water. Environ. Sci. Technol. 26, 577–586. doi:10.1021/es00027a022

Jafvert, C.T., Valentine, R.L., 1987. Dichloramine decomposition in the presence of excess ammonia. Water Res. 21, 967–973. doi:10.1016/S0043-1354(87)80015-5

Jury, W.A., Elabd, H., Resketo, M., 1986. Field Study of Napropamide Movement Through Unsaturated Soil. Water Resour. Res. 22, 749–755. doi:10.1029/WR022i005p00749

Knocke, W.R., 1990. Alternative oxidants for the removal of soluble iron and manganese. AWWA Research Foundation and American Water Works Association.

Kool, J.L., Carpenter, J.C., Fields, B.S., 1999. Effect of monochloramine disinfection of municipal drinking water on risk of nosocomial Legionnaires' disease. Lancet 353, 272–277. doi:10.1016/S0140-6736(98)06394-6

Laspidou, C.S., Rittmann, B.E., 2002. A unified theory for extracellular polymeric substances, soluble microbial products, and active and inert bi omass. Water Res. 36, 2711–2720. doi:10.1016/S0043-1354(01)00413-4

Leao, N.I., 1981. Dissertation. University of California.

LeChevallier, M.W., Cawthon, C.D., Lee, R.G., 1988. Factors promoting survival of bacteria in chlorinated water supplies. Appl. Environ. Microbiol. 54, 649–654.

Liu, H.M., Amy, G., 1993. Modeling Partitioning and Transport Interactions Between Natural Organic-Matter and Polynuclear Aromatic-Hydrocarbons in Groundwater. Environ. Sci. Technol. 27, 1553–1562.

Liu, S.G., Fan, C.F., Zhu, Z.L., 2011. Kinetics of Monochloramine Decay in Model and Distribution System Waters. Adv. Mater. Res. 183–185, 834–838. doi:10.4028/www.scientific.net/AMR.183-185.834

Luh, J., Mariñas, B.J., 2014. Kinetics of bromochloramine formation and decomposition. Environ. Sci. Technol. 48, 2843–2852. doi:10.1021/es4036754

Ma, X., Bibby, K., 2017. Free chlorine and monochloramine inactivation kinetics of Aspergillus and Penicillium in drinking water. Water Res. 120, 265–271. doi:10.1016/j.watres.2017.04.064

Maestre, J.P., Wahman, D.G., Speitel, G.E., 2016. Monochloramine Cometabolism by Mixed-Culture Nitrifiers under Drinking Water Conditions. Environ. Sci. Technol. 50, 6240–6248. doi:10.1021/acs.est.5b05641

Maestre, J.P., Wahman, D.G., Speitel, G.E., 2013. Monochloramine cometabolism by Nitrosomonas europaea under drinking water conditions. Water Res. 47, 4701–4709. doi:10.1016/j.watres.2013.05.019

Margerum, D.W., Schurter, L.M., Hobson, J., Moore, E.E., 1994. Water chlorination chemistry: Nonmetal redox kinetics of chloramine and nitrite ion. Environ. Sci. Technol. 28, 331–337. doi:10.1021/es00051a021

Matilainen, A., Vepsäläinen, M., Sillanpää, M., 2010. Natural organic matter removal by coagulation during drinking water treatment: A review. Adv. Colloid Interface Sci. 159, 189–197. doi:10.1016/j.cis.2010.06.007

McElmurry, S.P., Long, D.T., Voice, T.C., 2014. Stormwater Dissolved Organic Matter: Influence of Land Cover and Environmental Factors. Environ. Sci. Technol. 48, 45–53. doi:10.1021/es402664t

Moberg, L., Karlberg, B., 2000. An improved N,N'-diethyl-p-phenylenediamine (DPD) method for the determination of free chlorine based on multiple wavelength detection. Anal. Chim. Acta 407, 127–133. doi:10.1016/S0003-2670(99)00780-1

Morris, J. C. and Isaac, R.A., 1981. A critical review of kinetic and thermodynamic constants for the aqueous chlorine-ammonia system, in: R. L. Jolley, W. A. Brungs, J. A. Cotruvo, R. B. Cumming, J. S. Mattice, and V.A.J. (Ed.), Water Chlorination: Environmental Impact and Health Effects. Arbor Science, Ann Arbor, MI, pp. 49–62.

Ni, B.J., Ruscalleda, M., Pellicer-Nàcher, C., Smets, B.F., 2011. Modeling nitrous oxide production during biological nitrogen removal via nitrification and denitrification: Extensions to the general ASM models. Environ. Sci. Technol. 45, 7768–7776. doi:10.1021/es201489n

Pedersen, K., 1990. Biofilm development on stainless steel and pvc surfaces in drinking water. Water Res. 24, 239–243. doi:10.1016/0043-1354(90)90109-J

Peuravuori, J., Pihlaja, K., Välimäki, N., 1997. Isolation and characterization of natural organic matter from lake water: Two different adsorption chromatographic methods. Environ. Int. 23, 453–464. doi:10.1016/S0160-4120(97)00050-0

Piché, S., Larachi, F., 2006. Oxidation kinetics of Iron(II) complexes of trans-1,2-diaminocyclohexanetetraacetate (cdta) with dissolved oxygen: Reaction mechanism, parameters of activation and kinetic salt effects. Chem. Eng. Sci. 61, 3452–3462.

doi:10.1016/j.ces.2005.12.015

Postawa, A., Hayes, C., Criscuoli, A., Angelakis, F.M.A.N., Rose, J.B., Maier, A., McAvoy, D.C., 2013. Best practice guide on the control of iron and manganese in water supply. IWA publishing.

Qin, J.J., Oo, M.H., Kekre, K.A., Knops, F., Miller, P., 2006. Impact of coagulation pH on enhanced removal of natural organic matter in treatment of reservoir water. Sep. Purif. Technol. 49, 295–298. doi:10.1016/j.seppur.2005.09.016

Sarin, P., Snoeyink, V.L., Bebee, J., Jim, K.K., Beckett, M.A., Kriven, W.M., Clement, J.A., 2004. Iron release from corroded iron pipes in drinking water distribution systems: Effect of dissolved oxygen. Water Res. 38, 1259–1269. doi:10.1016/j.watres.2003.11.022

Sarin, P., Snoeyink, V.L., Bebee, J., Kriven, W.M., Clement, J.A., 2001. Physico-chemical characteristics of corrosion scales in old iron pipes. Water Res. 35, 2961–2969. doi:10.1016/S0043-1354(00)00591-1

Sathasivan, A., Chiang, J., Nolan, P., 2009. Temperature dependence of chemical and microbiological chloramine decay in bulk waters of distribution system. Water Sci. Technol. Water Supply 9, 493–499. doi:10.2166/ws.2009.387

Sharp, E.L., Parsons, S.A., Jefferson, B., 2006a. Seasonal variations in natural organic matter and its impact on coagulation in water treatment. Sci. Total Environ. 363, 183–194. doi:10.1016/j.scitotenv.2005.05.032

Sharp, E.L., Parsons, S.A., Jefferson, B., 2006b. The impact of seasonal variations in DOC arising from a moorland peat catchment on coagulation with iron and aluminium salts. Environ. Pollut. 140, 436–443. doi:10.1016/j.envpol.2005.08.001

Smith, E., Kamal, Y., 2009. Optimizing treatment for reduction of disinfection by-product (DBP) formation. Water Sci. Technol. Water Supply 9, 191–198. doi:10.2166/ws.2009.120

Snoeyink, V., Jenkins, D., 1980. Water chemistry. Wiley, New York.

Sollars, C.J., Peters, C.J., Perry, R., 1982. Bromide in urban runoff — water quality considerations, in: Efects of Waste Disposal on Groundwater and Surface Water (Proceedings of the Exeter Symposium). pp. 101–112.

Sontheimer, H., Kolle, W., Snoeyink, V.L., 1981. SIDERITE MODEL OF THE FORMATION OF CORROSION-RESISTANT SCALES. J. / Am. Water Work. Assoc.

Trote, T.W., Inman, G.W., Donald Johnson, J., 1980. Kinetics of Monochloramine Decomposition in the Presence of Bromide. Environ. Sci. Technol. 14, 544–549. doi:10.1021/es60165a008

Valentine, R.L., 1986. Bromochloramine Oxidation of N , N-Diethyl-p -phenylenediamine in the Presence of Monochloramine. Environ. Sci. Technol. 20, 166–170. doi:0013-936X/86/0920-0166

Valentine, R.L., Jafvert, C.T., Leung, S.W., 1988. Evaluation of a chloramine decomposition model incorporating general acid catalysis. Water Res. 22, 1147–1153. doi:10.1016/0043-1354(88)90010-3

Valentine, R.L., Selleck, R.E., 1981. Effect of bromide and nitrite on the degradation of monochloramine, in: 4. Conference on Water Chlorination: Environmental Impact and Health Effects. Pacific Grove.

Vikesland, P.J., Ozekin, K., Valentine, R.L., 2001. Monochloramine decay in model and distribution system waters. Water Res. 35, 1766–1776. doi:10.1016/S0043-1354(00)00406-1

Vikesland, P.J., Ozekin, K., Valentine, R.L., 1998. Effect of natural organic matter on monochloramine decomposition: Pathway elucidation through the use of mass and redox balances. Environ. Sci. Technol. 32, 1409–1416. doi:10.1021/es970589a

Vikesland, P.J., Valentine, R.L., 2002. Modeling the kinetics of ferrous iron oxidation by monochloramine. Environ. Sci. Technol. 36, 662–668. doi:10.1021/es002058j

Vikesland, P.J., Valentine, R.L., 2000. Reaction pathways involved in the reduction of monochloramine by ferrous iron. Environ. Sci. Technol. 34, 83–90. doi:10.1021/es990511p

Wahman, A.D.G., Maestre, J.P., Jr, G.E.S., 2016. Title : Monochloramine cometabolism by drinking water relevant nitrifying biofilm 362–373. doi:10.5942/jawwa.2016.108.0092

Wahman, D.G., Katz, L.E., Speitel, G.E., 2006. Trihalomethane cometabolism by a mixed-culture nitrifying biofilter. J. / Am. Water Work. Assoc. 98.

Wahman, D.G., Katz, L.E., Speitel, G.E., 2005. Cometabolism of trihalomethanes by Nitrosomonas europaea. Appl. Environ. Microbiol. 71, 7980–7986. doi:10.1128/AEM.71.12.7980-7986.2005

Wahman, D.G., Speitel, G.E., 2012. Relative importance of nitrite oxidation by hypochlorous acid under chloramination conditions. Environ. Sci. Technol. 46, 6056–6064. doi:10.1021/es300934x

Wang, Y., Small, M.J., VanBriesen, J.M., 2017. Assessing the Risk Associated with Increasing Bromide in Drinking Water Sources in the Monongahela River, Pennsylvania. J. Environ. Eng. 143, 4016089. doi:10.1061/(ASCE)

Wegman, R.C.C., Hamaker, P., de Heer, H., 1983. Bromide-ion balance of a polder district with large-scale use of methyl bromide for soil fumigation. Food Chem. Toxicol. 21, 361–367. doi:10.1016/0278-6915(83)90089-3

Westerhoff, P., Chao, P., Mash, H., 2004. Reactivity of natural organic matter with aqueous chlorine and bromine. Water Res. 38, 1502–1513. doi:10.1016/j.watres.2003.12.014

Wilde, E.W., 1991. Comparison of three methods for measuring residual chlorine. Water Res. 25, 1303–1305. doi:10.1016/0043-1354(91)90071-W

Winid, B., 2015. Bromine and water quality - Selected aspects and future perspectives. Appl. Geochemistry. doi:10.1016/j.apgeochem.2015.10.004

Woolschlager, J., Rittmann, B., Piriou, P., Kiene, L., Schwartz, B., 2001. Using a comprehensive model to identify the major mechanisms of chloramine decay in distribution systems, in: Water Science and Technology: Water Supply. pp. 103–110. doi:10.1002/yd.430

Woolschlager, J.E., 2000. A Comprehensive Disinfection and Water Quality Model for Drinking Water Distribution Systems. Northwestern University, Evanston.

Xue, Z., Lee, W.H., Coburn, K.M., Seo, Y., 2014. Selective reactivity of monochloramine with extracellular matrix components affects the disinfection of biofilm and detached clusters. Environ. Sci. Technol. 48, 3832–3839. doi:10.1021/es405353h

Zhang, Q., Davies, E.G.R., Bolton, J., Liu, Y., 2017. Monochloramine loss mechanisms in tap water. Water Environ. Res. doi:10.2175/106143017X14902968254421

Zhang, Y., Love, N., Edwards, M., 2009. Nitrification in drinking water systems. Crit. Rev. Environ. Sci. Technol. doi:10.1080/10643380701631739

Zhu, X., Zhang, X., 2016. Modeling the formation of TOCl, TOBr and TOI during chlor(am)ination of drinking water. Water Res. 96, 166–176. doi:10.1016/j.watres.2016.03.051

CHAPTER 3. FIELD DATA ANALYSIS OF ACTIVE CHLORINE-CONTAINING STORMWATER SAMPLES[1]

3.1. Introduction

Chlorine products have been used from the early 20th century to disinfect drinking water; however, this widely-used treatment has disadvantages, including the reactivity of chlorine with organic compounds in the water, which causes it to dissipate rapidly in distribution systems. This reactivity also results in the production of disinfection by-products (DBPs) (Hrudey, 2009). To limit the formation of chlorinated DBPs, an alternative water disinfection method, chloramination, has been developed and applied to drinking water systems throughout North America (Wahman and Speitel, 2012). After chlorination, ammonia is added to convert the residual chlorine to chloramines, of which monochloramine (NH_2Cl) is the dominant disinfection species. NH_2Cl has proven useful for water distribution systems, where it is desirable to have a longer-lasting residual and its corresponding disinfection effect (Brodtmann and Russo, 1979; Mitcham et al., 1983; Norman et al., 1980); however, it can also lead to detrimental environmental effects, as described below.

Drinking water chloramination may introduce chloramines into surface waters through various means, including distribution system leaks and breaks, lawn and garden watering, car and driveway washing, street cleaning, firefighting, and industrial or commercial wash-down and construction activities. Although residential outdoor water use is typically a relatively small percentage (6% in the United States, on average) of the total annual residential water use (Coomes et al., 2010), it may be considerable in summer months (Nouri et al., 2013): for example, 40 to

---

[1] A version of this chapter has been published: Zhang, Q., Gaafar, M., Yang, R. C., Davies, E. G. R., Bolton, J. R., & Liu, Y., 2018. Field data analysis of active chlorine-containing stormwater samples. Journal of Environment Management. 206, 51-59.

60% of residential water consumption in Texas (White et al., 2004) and almost 30% in California (Mays, 2002) were associated with lawn irrigation activities. In contrast, commercial car washing is responsible for only about 1% of municipal water use and its subsequent discharge to stormwater sewers can be negligible, since these companies typically remove some pollutants on-site (Sablayrolles et al., 2010; Zaneti et al., 2012) and discharge dirty wash water almost exclusively to sanitary sewer systems (Brown 2000, 2002). However, the situation is less clear for car dealerships and car rental locations, where cars may be washed outdoors. Finally, the production of large-volume industrial pressure-vessels – boilers and large storage tanks that have a minimum inner diameter of 60 cm (PricewaterhouseCoopers LLP, 2008), but that may be as large as 10.7 m in diameter, 76 m in length, and 680 tonnes in mass (Cessco Fabrication and Engineering Ltd, 2014) – require the use of municipal water for ‘hydro-testing’ of vessel integrity. After completion of the hydro-testing procedures, testing water is occasionally discharged to the stormwater system without dechloramination. These water uses are thought to be the major active chlorine sources in storm sewers under dry weather conditions, and consequently introduce chloramine-containing water into stormwater drainage systems.

At near-neutral pH, chloramines can release free chlorine through auto-decomposition processes (Vikesland et al., 2001). The chloramines and the free chlorine species released from chloramines are measured together as the total active chlorine (TAC) in stormwater. In 1973, Brungs's study showed that the TAC concentration of effluent discharge should not exceed 0.002-0.2 mg/L depending on the discharging period for the protection of aquatic organisms. Further, Brooks and Bartos reported that the active chlorine has a 1% lethal concentration of 0.08 mg/L to some fishes with an exposure duration of 120 minutes (Brooks and Bartos, 1984). In 1985, EPA proposed that the concentration causing 50% mortality can be as low as 0.0053 mg/L to some invertebrate species (United States Environmental Protection Agency, 1985). Elevated TAC in fresh water can be acutely lethal to fish, crayfish, snails and some fish-food organisms over exposures of 6 min to 48 hours. Also, long-lasting chloramine species can be toxic for fish growth with a much lower concentration, thus leading to a chronic environmental risk (Brungs, 1973). Moreover, the Canadian Council of Ministers of the Environment (CCME, 1999) guidelines for the protection of aquatic life list a maximum TAC concentration in surface waters of only 0.5 μg/L, and their recent Canada-wide strategy (CCME, 2009) reduced the permissible TAC concentration in discharged effluent from 0.2 to 0.02 mg/L. To adhere to these guidelines, it is clearly important to determine the TAC concentrations of sources that contribute to surface water flows, which include municipal stormwater discharges.

The objectives of the current study are to evaluate the TAC concentration and other water qualities in Edmonton storm sewers under dry and wet weather conditions in various neighborhoods during summer months, and to study the possible relevance of some stormwater characteristics to TAC dissipation rates. The TAC concentration as well as other physicochemical properties of stormwater, and the biological characteristics of storm sewer biofilm were analyzed in this research. Wet weather stormwater characteristics have been analyzed in a variety of studies (Liu et al., 2013; Makepeace et al., 1995; Pitt et al., 2004), but studies of dry weather stormwater qualities are relatively rare. Since many other cities also use chloramination for their drinking water disinfection, the TAC analysis results from this fieldwork in Edmonton can also be used as a reference case for other cities. This is believed to be the first research for TAC concentration analysis in storm sewers, and the results of this study should attract more attention to the issue of stormwater TAC contamination and its potentially harmful impacts on the aquatic environment.

3.2. Material and methods

3.2.1. Location selection

To study the impact of different outdoor water use types on the TAC concentration in stormwater, field samples were collected from storm sewers in four Edmonton neighborhoods selected to represent four major land-use types: (a) residential, as a reference for other land-uses, (b) parks and recreation, for their extensive green areas and correspondingly more uniform irrigation and fertilizer use than residential areas, (c) commercial, with a focus on automobile dealerships and rental business areas and (d) industrial, with a focus on areas with pressure vessel fabricators. Each neighborhood lies within one of two stormwater catchments, Kennedale in north Edmonton and 30th Avenue in south Edmonton. The Kennedale and 30th Avenue catchment maps are shown in Fig. 3.1 and the storm sewer network maps of the sampling locations are shown in Fig. 3.2.

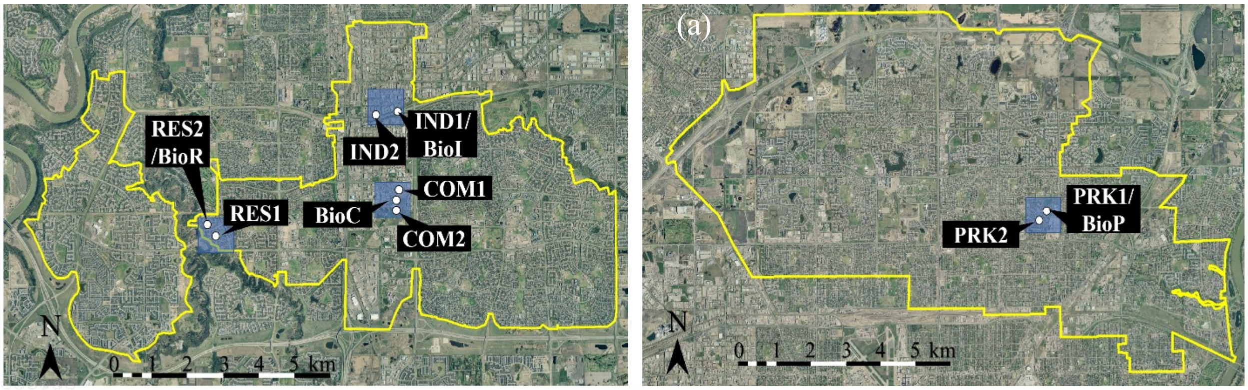

Fig. 3.1. (a) 30th Avenue and (b) Kennedale stormwater catchment maps

Within these two catchments, the four neighborhoods were then selected according to the following criteria. Stormwater drainage system characteristics played a key role, particularly the location of the neighborhood within the pipe network, the presence of stormwater ponds upstream and availability of access points for water sampling. In terms of location within the network, sampling near the sewer network's upstream-end would ensure that stormwater flows originated in the catchment under consideration, while sampling farther downstream would make it difficult to attribute pollutants to probable Sources. In addition, the selection of long, uninterrupted sections of pipe would permit attribution of changes in water quality to chemical and biological interactions occurring within the pipe section, and give more time for such interactions to occur. Potential locations with mixed land-uses within or upstream of the neighborhood were excluded. Finally, several potential neighborhoods were eliminated because of logistical hurdles, such as traffic conditions, site accessibility and sampling difficulty.

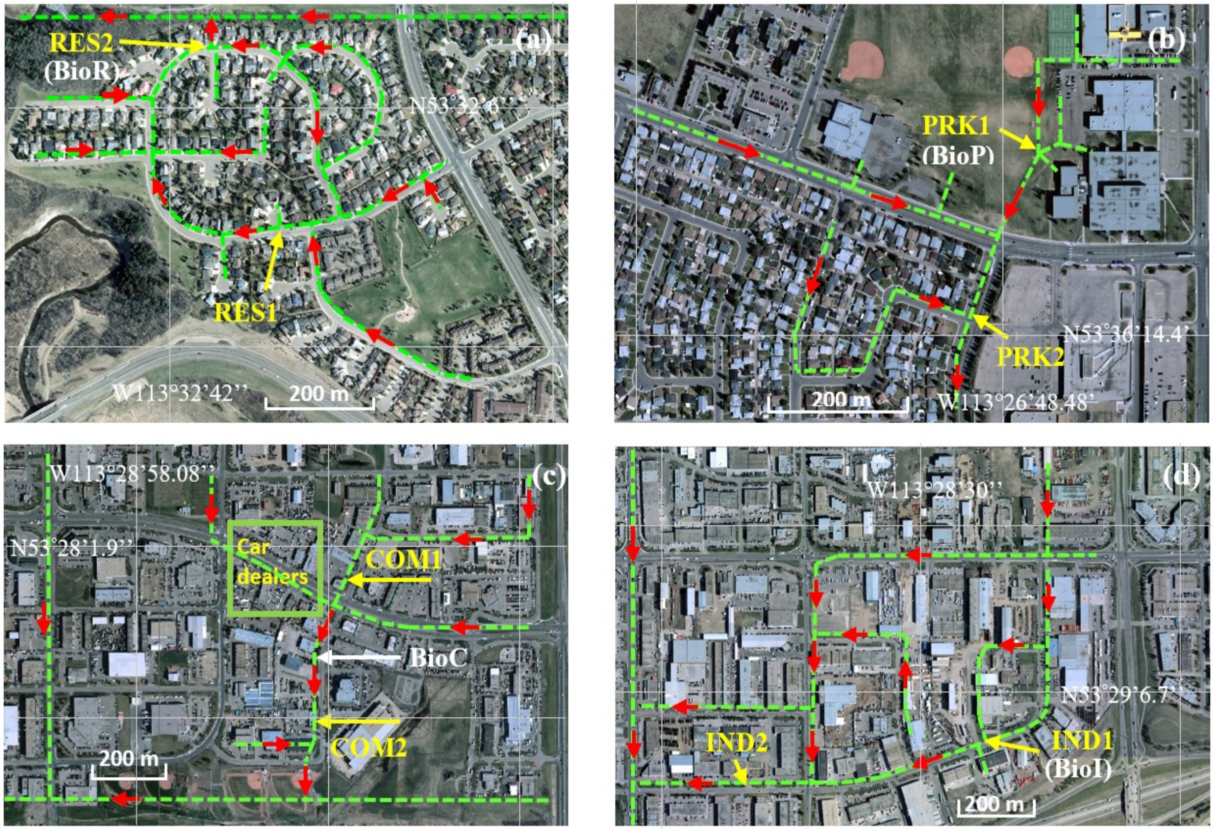

Fig. 3.2. Storm sewer network maps for (a) residential, (b) park, (c) commercial, (d) industrial sampling areas

In selecting the residential location, low-density neighborhoods with higher property values were prioritized for their relatively large lawn and garden areas (cf. the Albuquerque, New

Mexico, study conducted by Al-Kofahi et al., 2012). Application of the above criteria resulted in selection of the high property-value Blue Quill Estates neighborhood, shown in Fig. 3.2(a). The M. E. Lazerte Park in the Kennedale catchment was selected among the irrigated parks of the two catchments, based on data available for determining irrigation volumes, the type of water used for irrigation (potable), and the park location within the neighborhood and sewer pipe network. Its location is shown in Fig. 3.2(b). In the 30th Avenue basin, commercial car washes, dealerships and car rental agencies clustered in one location near 34th Avenue and 99th Street NW, which contained approximately two dozen automobile-related service providers. The location selected – at 93rd Street near 34th Avenue (see Fig. 3.2c) – had the largest number of automotive services businesses and met the pipe-network based criteria described above. For industrial sites, the pressure vessel industry is potentially a large point-source contributor of chloramine pollution. The production of large pressure vessels requires the use of municipal water for vessel-integrity testing; this testing water is occasionally discharged to stormwater rather than sanitary systems. Many pressure-vessel manufacturers were near the intersection of 97th Street and 45th Avenue in the 30th Avenue basin, as presented in Fig. 3.2(d).

3.2.2. Field investigations

Field sampling was conducted every two to three weeks from April to September, in both 2015 and 2016 for both dry weather and precipitation conditions. In the field, the sample TAC concentrations, temperatures, dissolved oxygen (DO), pH and conductivity were recorded during sampling. Microbial biofilms were sampled at the four locations: BioR, BioP, BioC and BioI (see Fig. 3.2) on storm sewer pipes.

3.2.3. Laboratory analyses

Samples were characterized according to their physical, chemical and biological properties. All analyses were performed within 24 hours of sample collection. The NH_4^+-N, NO_2^--N, NO_3^--N, total P, alkalinity, chemical oxygen demand (COD) and dissolved organic carbon (DOC) concentrations, as well as hardness, turbidity, total suspended solids (TSS) and total dissolved solids (TDS) were analyzed. The biofilm genomic DNA was extracted and *q*PCR was conducted. Primers for *q*PCR are listed in Table S3.6. Further, to study the TAC dissipation rate in stormwater, NH_2Cl stock solution was added into stormwater samples collected in the two years from each sampling location after filtration through 0.45 μm membrane filters to achieve an initial TAC concentration of 0.05 mM. The NH_2Cl concentration changes were recorded to compare the NH_2Cl decay rates in different stormwater samples. Additional information for stormwater quality analysis and NH_2Cl dissipation experiment design is provided in the supplementary information.

3.2.4. Statistic analysis methods

The student's *t* test was applied to test the significance level of two datasets, and the significance level can be represented by the *p*-value. A small *p*-value indicates that the datasets have statistical significance. 0.05 is commonly used as the threshold (Fisher, 1925). In this research, the student's *t* test was used to compare the significance level of stormwater physicochemical and biological characteristics between different sampling years and under different sampling locations. In addition, Random Forest (RF) was applied for the analysis of a variable's importance in stormwater NH_2Cl decay experiments. RF is an ensemble approach that grows a multitude of decision trees using randomly selected values from the original samples and votes the most popular class. The variable importance is represented by the percentage of Increased Mean Square Error (%IncMSE) and Increased Node Impurity Index (IncNodePurity). %IncMSE describes the prediction ability of mean square error with randomly permuted variables, and IncNodePurity measures the loss function when best splits are selected (Breiman, 2001; Echeverry-Galvis et al., 2014). The 'RandomForest' library (Liaw and Wiener, 2002) in R programing (R Development Core Team, 2008) was used for data analysis. With both high values of %IncMSE and Incnodepurity, the variable is considered to have high importance. Moreover, principal component analysis (PCA) is a statistical analysis method that uses an orthogonal transformation to lower the dimension of a dataset, thus revealing the possible correlation between variables (Shlens, 2014). In this research, PCA was conducted with XLSTAT software (Addinsoft SARL, France) to summarize the relationship of multiple chemical concentrations at the 8 different sampling locations.

3.3. Results and discussion

3.3.1. The TAC concentration changes in the stormwater sewers

Fig. 3.3 illustrates the TAC concentration changes in Edmonton storm sewers for each location during summer 2015 and 2016 from May 1 to September 23 in 2015 and April 22 to September 8 in 2016, as well as the precipitation data collected from nearby rainfall stations during the sampling periods (City of Edmonton, Canada).

From Fig. 3.3, it can be seen that the TAC concentrations varied from 0.02 to 0.77 mg/L during summer 2015, and were significantly higher than those of summer 2016 (0 to 0.24 mg/L) at all eight locations (p-value < 0.001). The values of TAC concentrations are shown in Tables S3.2 and S3.3. To be specific, as shown in Fig. 3.3 (a) (c) (e) (g), except the downstream residential location (RES 2), the TAC concentrations showed an increasing trend from May 01 to July 08, 2015 (from 0.14±0.05 mg/L to 0.47±0.18 mg/L, p-values > 0.05), which may have been caused by increasing water use activities (EPCOR Utilities Inc., 2015) associated with warmer temperatures and low rainfall during this period. For the residential neighborhood, increased lawn watering was likely to have introduced more potable water to the storm sewers and contributed to higher TAC values. A large lawn area (3.06 ha) at the park site required irrigation, which is likewise expected to have increased the TAC concentration over time. For the commercial neighborhood, an area with relatively large numbers of car dealerships and rental locations, the high TAC concentration detected suggests car-washing activities.

Further, high TAC concentrations were observed in the industrial area on July 08 (0.77 and 0.62 mg/L) arising from the discharge of tap water (1000 m^3) into a storm sewer by a local industry pressure vessel hydro-testing near the IND1 (upstream) location. As the NH_2Cl is comparably stable in stormwater, a high TAC chlorine concentration could still be detected in the downstream sampling location (IND2). In contrast to the dry weather results, high precipitation within three days (Table S3.4) before the subsequent sampling date (July 22, 2015) likely decreased the lawn and garden watering activities, as well as flushed the TAC out of the storm sewer system, which caused the lower TAC concentrations on the sampling day. Moreover, rainfall likely diluted the TAC concentrations at RES2, COM1-2, and IND1-2 on August 5, 2015. While the TAC concentrations increased again after storm conditions subsided. As colder temperatures in late September (average temperature: 9.4 °C during the 10 days before last sampling) decreased outdoor tap water uses, low TAC concentrations were detected on the last sampling date at most of the sampling locations.

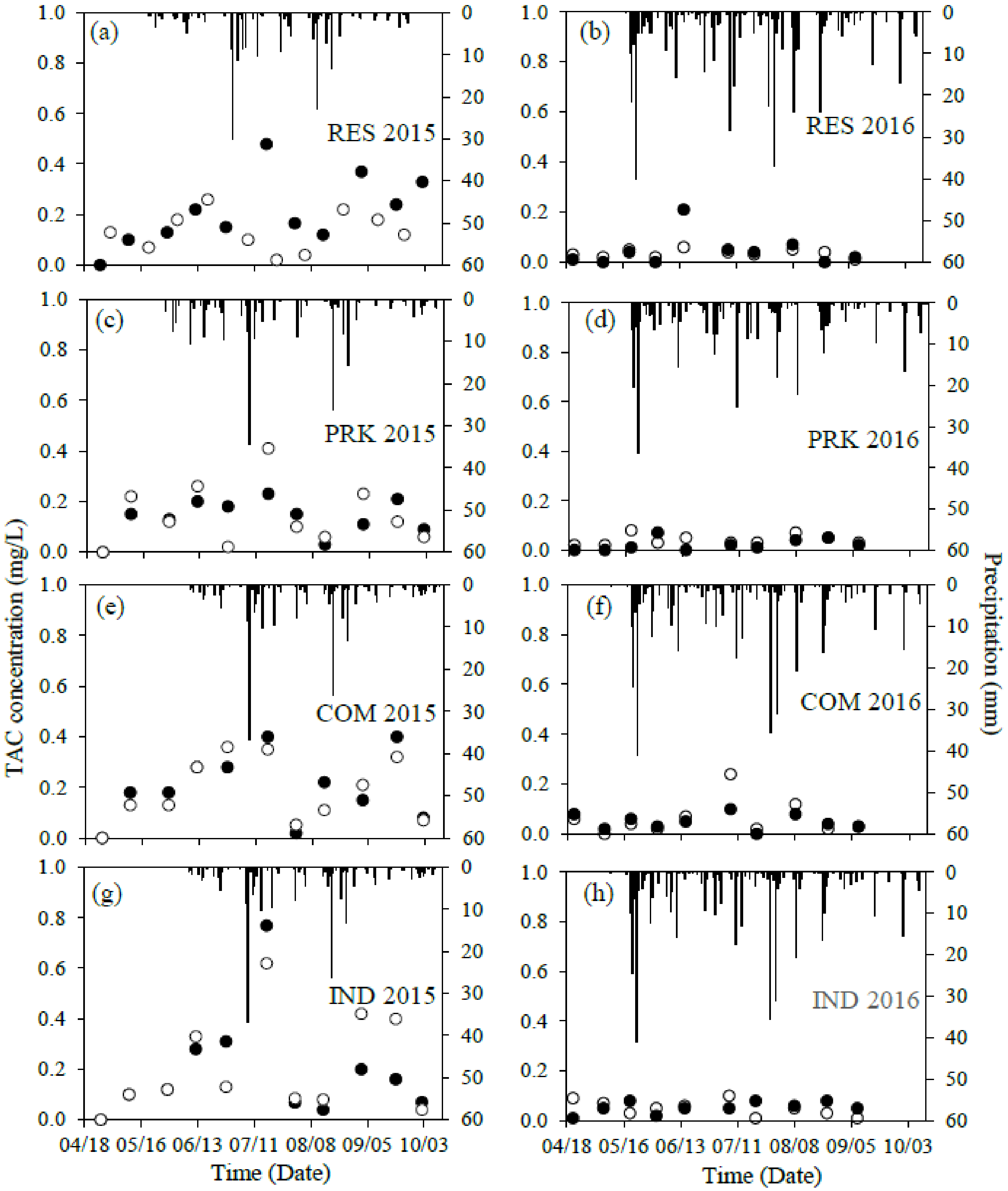

Fig. 3.3. Stormwater TAC concentrations and the corresponding precipitation data for each sampling area during summer 2015 and 2016 (TAC: total active chlorine; RES, PRK, COM, IND: residential, park, commercial and industrial areas; Black and white dots represent the TAC

concentration at upstream and downstream sampling locations respectively; Precipitation source: City of Edmonton Drainage Services)

In summer 2016, the stormwater shows lower TAC concentrations than summer 2015 on most of the sampling dates. As compared to summer 2015, which had an average precipitation of 201.4 mm in the sampling areas, more precipitation occurred during summer 2016 (420.9 mm). The parkland irrigation decreased from an average of 17.0 m^3/day in summer 2015 to 4.4 m^3/day in summer 2016. It is assumed that the higher precipitation has reduced outdoor tap water uses, such as lawn watering and car washing, thus decreasing the NH_2Cl discharge into the storm sewer system. Therefore, it can be concluded that during dry periods, the land uses rely more on potable water for irrigation, and the discharge of potable water leads to the TAC accumulation in storm sewers.

3.3.2. Other chemical characteristics of stormwater samples

Apart from the TAC concentrations, other physicochemical properties of Edmonton stormwater samples were analyzed. The concentrations of ammonium, nitrite, alkalinity, COD, DOC and pH values in dry weather stormwater samples are shown in Fig. 3.4. Other stormwater characteristics are provided in Tables S3.7 and S3.8. The physicochemical characteristics of stormwater samples collected during rainfall are shown in Table S3.9, and the changes of stormwater properties during a rainfall event are shown in Table S3.10.

Ammonium, nitrite, pH, alkalinity and natural organic matter (NOM) concentrations are known to affect the decay rate of NH_2Cl (Vikesland et al., 2001; Kiéné et al., 1998). Higher ammonium concentrations can contribute to the regeneration of NH_2Cl during NH_2Cl auto-decomposition process, thus reducing its decay rate (Vikesland et al., 2001). NH_2Cl can react with NO_2^-, leading to a decrease of the NH_2Cl concentration in stormwater. NH_2Cl decomposes more readily at lower pH and at higher alkalinity concentrations (Vikesland et al., 2001). Further, some of the organics in stormwater can react with NH_2Cl, which accelerates its decay rate (Duirk et al., 2005).

As shown in Fig. 3.4, the ammonium, nitrite, NOM concentrations and the pH show similar values during these two years, while alkalinity was slightly higher in summer 2015 than in summer 2016. The major sources of nitrogen in Edmonton urban stormwater are urban landscape runoff and atmospheric deposition (Bernhardt et al., 2008; Kaushal et al., 2011; Strassler et al., 1999). Rainfall itself commonly contains low concentrations of ammonium- and nitrite- nitrogen.

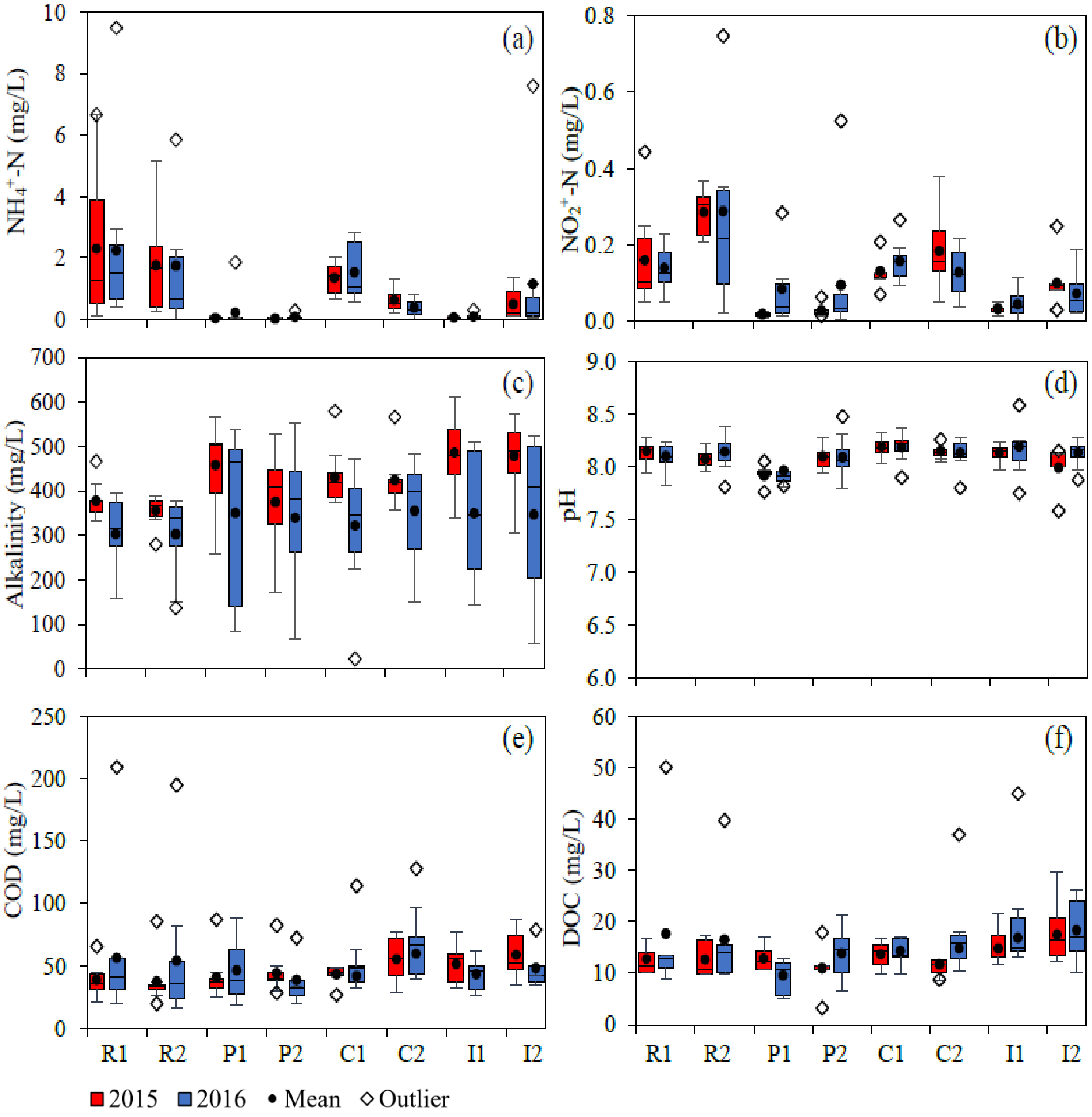

Fig. 3.4. The concentrations of ammonium (NH_4^+-N), nitrite (NO_2^--N), alkalinity, pH, chemical oxygen demand (COD) and dissolved organic carbon (DOC) changes in Edmonton stormwater samples during summer 2015 and 2016 under dry weather conditions. (Box plot: for each plot, the bottom, middle and top boxes represent the first quartile, median and third quartile of the dataset; R1, R2, P1, P2, C1, C2, I1, I2 represent upstream and downstream residential, park, commercial and industrial locations)

However, as urban runoff can bring ammonium- and nitrite- nitrogen into stormwater, the concentrations of these two chemicals are not diluted with high precipitation in storm sewers. Likewise, the insignificant change of NOM concentrations (represented by COD and DOC) during these two years may share the same cause. Further, the high alkalinity concentrations (over 100 mg/L) maintained the stable pH in these two years (Kuang and Sansalone, 2011). As compared to other parameters, the alkalinity concentration decreased most significantly with precipitation (Table S3.10). Therefore, it is assumed that the lower concentrations detected in 2016 were influenced by the frequently precipitation during that summer.

To compare the stormwater qualities among various locations, the ammonium- and nitrite-nitrogen concentrations are high in the residential area and low in the park area [Fig. 3.4(a) and (b)]. In terms of alkalinity and pH, they show similar mean values at different locations [Fig. 3.4(c) (d)]. In Fig. 3.4(e) and (f), except for occasionally quite high COD and DOC concentrations detected in some locations, the NOM concentrations were generally stable at each sampling location. These occasionally high concentrations were caused by the small precipitation on the sampling days, which introduced organic components from ground to storm sewers. Note that since only low precipitation occurred on these sampling days, they are not considered as wet weather conditions.

3.3.3. Bacterial communities in the storm sewer system

Research has long suggested that microorganisms play important roles in NH_2Cl dissipation (Rittmann et al., 1994; Siripong and Rittmann, 2007). Nitrification – a two-step microbiological process wherein NH_3 is initially oxidized to NO_2^- by ammonia oxidizing bacteria (AOB) and nitrite is then oxidized to NO_3^- by nitrite oxidizing bacteria (NOB) (Sathasivan et al., 2005; Bal Krishna et al., 2012) – can accelerate the NH_2Cl decay rate (Vikesland et al., 2001).

Most microbial cells present in stormwater tend to adhere to sewer pipe surfaces, where they secrete extracellular polymeric substances and develop into biofilms for the growth of microorganisms. Some organic components from biofilm can react with NH_2Cl, leading to the NH_2Cl dissipation. Further, NH_2Cl can be consumed by AOB cometabolism processes (Maestre et al., 2013).

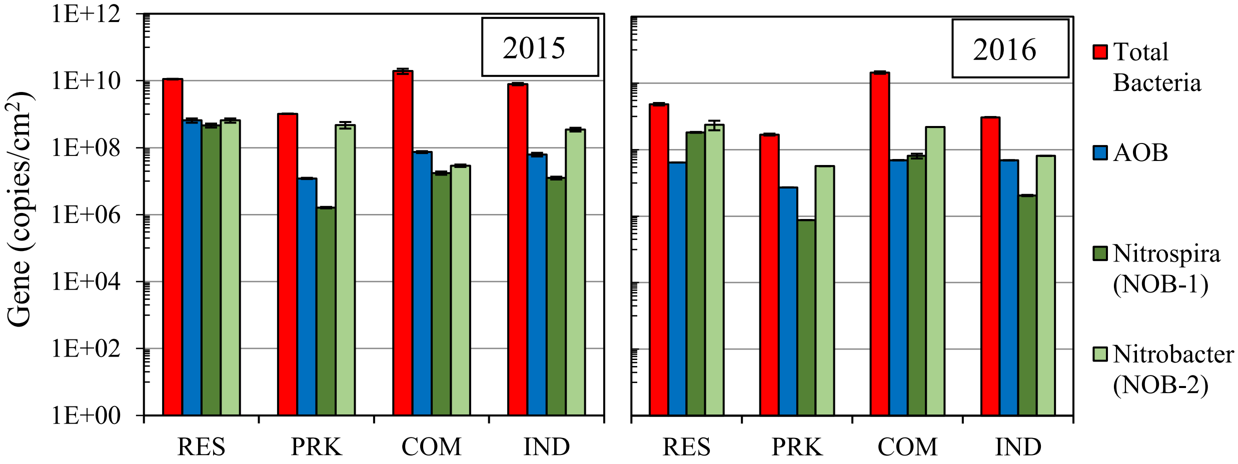

Fig. 3.5. Various bacterial gene copy numbers of biofilm on submerged pipe surface at different sampling locations collected on (a) August 22, 2015 and (b) August 19, 2016. (AOB for ammonia oxidizing bacteria; NOB for nitrite oxidizing bacteria)

Our *q*PCR results indicate no significant difference of the gene copy numbers of bacterial 16S rRNA gene (target total bacteria), amoA gene (target AOB), NSR and Nitro 16S rRNA gene (target two types of NOB: Nitrospira and Nitrobacteria) between the biofilm samples collected in the two years (p-value > 0.1); it is therefore assumed that the bacterial compositions are relatively stable in the storm sewers. Fig. 3.5 shows that the total bacterial gene copies were highest in the commercial area and lowest in the park area for both years. The AOB gene copies in the park area were clearly low (around 10^7 copies/cm^2) as compared to other locations, which corresponded to the low concentration of NH_4^+-N in the neighborhood stormwater. The gene copies of *Nitrobacteria* were higher than *Nitrospira* for all the locations in the two years (p-value < 0.05).

Compared to other areas, NOB and AOB were high in the residential area (*p*-value < 0.01), which matched the patterns of the high NH_4^+-N and NO_2^--N concentrations in this area. The high AOB and NOB concentrations in residential areas can enhance the NH_2Cl dissipation in stormwater. The commercial and industrial areas contained similar populations of AOB in the two years, while the two NOB species varied in these samples. Since the NH_4^+-N concentration is relatively stable in both years, but the NO_2^--N concentration varied during these two summers.

3.3.4. TAC decay test in stormwater samples

Fig. 3.6 illustrates the NH_2Cl dissipation rates in stormwater samples collected in summer 2015 and summer 2016 at different locations – the NH_2Cl decay rates clearly varied across stormwater samples. To estimate the TAC loss kinetics in stormwater, the dominant species in tap water, NH_2Cl, was added into stormwater samples to achieve a 0.05 mM of initial concentration. After 48 hours, approximately 40% to 60% of NH_2Cl still remained for most stormwater samples, which means that the NH_2Cl in stormwater from outdoor tap water discharge can still cause potential fresh water contamination after 48 hours. As mentioned, the concentrations of NOM, NO_2^--N, NH_4^+-N, and alkalinity, as well as the pH value are the most important factors contributing to the NH_2Cl decay. To study the importance of these factors, a second-order reaction was applied to describe the NH_2Cl decay processes ($r \geq 0.9$), and the decay rates were represented by a second-order reaction rate coefficient (k). The detailed chemical characteristics and the k values of stormwater sample are shown in Table S3.11.

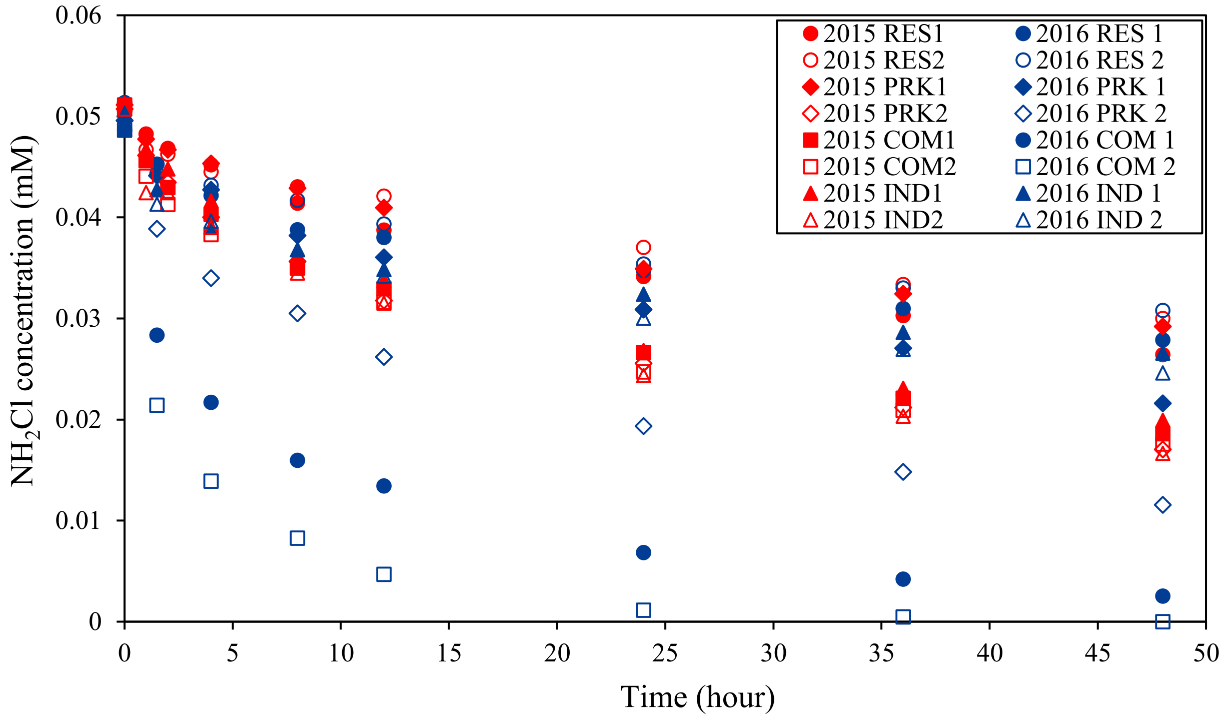

Fig. 3.6. Monochloramine (NH_2Cl) loss in stormwater samples collected in the summers of 2015 and 2016; Initial [NH_2Cl] = 0.049~0.051 mM (1.74~1.81 mg/L-Cl), temperature = 25 ºC

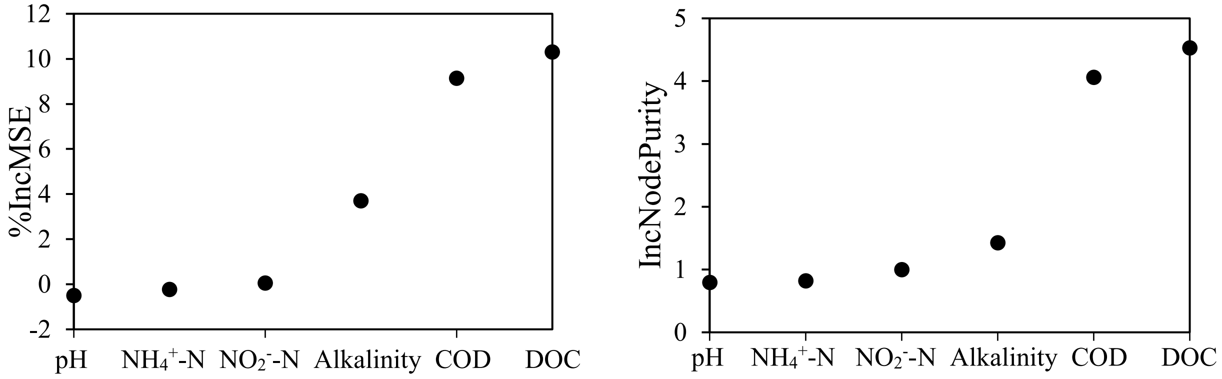

Fig. 3.7. Random Forest variable importance evaluation of pH, ammonium (NH_4^+-N), nitrite (NO_2^--N), alkalinity, chemical oxygen demand (COD) and dissolved organic carbon (DOC)

From Fig. 3.7, COD and DOC have both high %IncMSE and Incnodepurity values in RF analysis. Therefore, it can be assumed that they are the most important factors in determining the NH_2Cl decay rate. Recall that both COD and DOC represent the NOM concentrations in natural water samples, that is, NOM plays the dominant role in the stormwater NH_2Cl dissipation rate, and further, as compared to COD, DOC is the better index to describe the NOM concentration for NH_2Cl decay. The impact of pH, NH_4^+-N, NO_2^--N and alkalinity are not significant in stormwater.

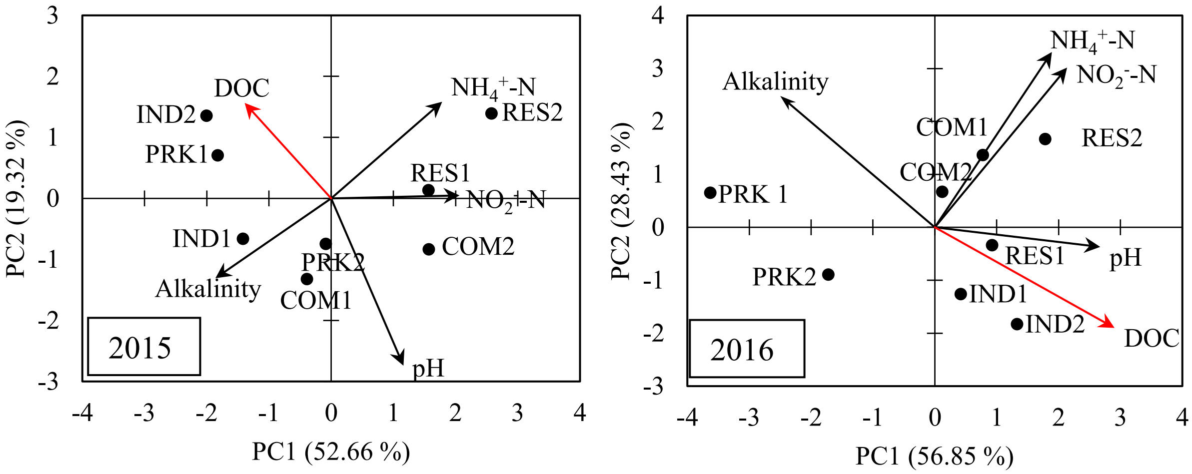

Fig. 3.8. Principal component analysis for pH, ammonium (NH_4^+-N), nitrite (NO_2^--N), alkalinity and dissolved organic carbon (DOC) in the summers of 2015 and 2016

As shown in Fig. 3.8, the dots and the vectors represent the sampling locations and the chemical concentrations, respectively. The angle of the vectors indicates the correlation of different chemicals. 0 and 180 degrees show highly positive and negative correlations, while 90 degree (orthogonal) means no association. The dots that are close to each other mean a similar stormwater quality at these locations. Specifically, the vectors of NO_2^--N and NH_4^+-N are comparably close in both years, from which it can be assumed that the concentrations of these two chemicals are correlative. This can also be verified by the high correlation coefficient in Pearson Correlation Analysis (Table S3.11 and S3.12). This phenomenon is considered to be caused by the impact of bacteria nitrification in storm sewer environment. In terms of the dots, for each neighborhood, since the two dots that represent upstream and downstream sampling locations that are distributed separately, their chemical properties are not suggested to be correlated. It is probable that the stormwater entering the pipes from branches between the two locations changed the stormwater quality. Further, with the dots further from the direction of a vector, the location is considered to have a higher corresponding chemical concentration. Therefore, the stormwater collected at the downstream industrial area (IND2) contained the highest DOC concentrations in both years, and it is possible caused by the introduction of organic matters from construction site through outdoor potable water and rainfall flushing in this area. Combining the results from Figs. 3.7 and 3.8 suggests that NH_2Cl has the highest dissipation rate in this area.

3.4. Conclusions

Active chlorine species have harmful environmental effects. Measured as TAC, they are introduced into stormwater sewers through various outdoor water uses, including lawn and landscape watering, car washing, and pressure-vessel testing, in the four neighborhoods of this study. The stormwater samples collected in Edmonton storm sewers show that TAC concentration varied from 0.02 to 0.77 mg/L during summer 2015 and exceeded the CCME (2009) Canada-wide Strategy standard of 0.02 mg/L for permissible TAC concentrations in the discharged effluent. The high TAC concentrations in study samples may therefore pose a risk to the aquatic environment. With higher precipitation during summer 2016, the TAC concentration decreased significantly in stormwater (0 to 0.24 mg/L). It is believed that the high precipitation decreased the frequency of outdoor tap water uses, thus reducing the TAC in stormwater. Other physicochemical and biological characteristics of stormwater and storm sewer biofilm samples show no significant difference between these two years. The NH_2Cl decay laboratory experiments indicate that the NOM concentration is the dominant factor that contributes to NH_2Cl dissipation in stormwater samples, and that DOC better represents the NOM concentration in stormwater than COD for the NH_2Cl dissipation study. PCA figures illustrate that the downstream industrial area had the highest DOC concentrations in both years, and these high DOC concentrations may lead to high TAC dissipation rates in this area. To further regulate the outdoor tap water discharge and protect aquatic environment, more research is required to improve the understanding of NH_2Cl dissipation mechanisms in real storm sewer systems.

3.5. Supplementary materials

3.5.1. Additional information of the drainage areas

Table S3.1. The total drainage area, percentage impervious and BMP features of sampling storm sewers

	Residential	**Park**	**Commercial**	**Industrial**
Drainage area (km^2)	0.34	0.27	1.04	1.48
Percentage impervious %	62%	51%	90%	65%
BMP	No	No	No	No

3.5.2. Additional information for field investigation

As mentioned in the manuscript, the field stormwater samples were collected in both dry and precipitation weathers. Either zero or low levels of precipitation occurred at least three days prior to a given sampling date – here defined as "dry weather" – which was likely to have resulted in greater outdoor water use and therefore more potable water runoff to storm sewers; stormwater samples were collected after precipitation occurred to provide control data. Note that cases of cumulative precipitation for two days preceding the sampling data as well as the sampling day itself are shown in Tables S4.4 and S4.5. For each neighborhood, two samples were collected from two storm sewer manholes, one in the upstream region of the neighborhood and one downstream.

To determine the physicochemical characteristics of stormwater on field, the TAC concentrations in the water samples were measured with a Hach Chlorine Test Kit (Free and Total, Model CN-70) using a DPD (diethyl-p-phenylenediamine) indicator with a detection limit of 0.02 mg/L. Conductivity and pH were analyzed by Extech EC500 Waterproof ExStikII pH/conductivity meter (Extech instruments, USA). Portable dissolved oxygen (DO) meter pen (Fisher Scientific, CA) was used to measure the DO concentration and temperature of stormwater samples. Additional measurements were later preformed in the laboratory. Stormwater samples were kept on ice during transportation from the sites and thereafter stored at 4 ºC in a temperature-controlled room at the University of Alberta.

For the biofilm sampling, triplicate samples were for each pipe collected by placing a 1.1 cm diameter template over a randomly-selected submerged pipe surface. Biofilms were scraped within the scribed area and stored in sterilized centrifuge tubes containing 5 mL of stormwater collected in the same sewer. Biofilm samples were kept on ice during transportation, and preserved at 4 °C until they were analyzed.

3.5.3. Additional information for laboratory analyses

The NH_4^+-N, NO_2^--N, NO_3^--N, and total P concentrations, chemical oxygen demand (COD) and alkalinity were analyzed using commercial test kits TNT832, TNT839, TNT835, TNT843, TNT821 and TNT870 (Hach, USA), respectively. Dissolved organic carbon (DOC) was measured by a Shimadzu TOC-L CPH E100 (detection limit is 4 μg-C/L). Hardness was analyzed by EDTA titration method (standard methods, 2340 B) and turbidity was determined by the 965 Turbidimeter (Orbeco-Hellige, USA). Total suspended solids (TSS) and total dissolved solids (TDS) were determined based on the protocol from standard methods 2540D and 2540E. Total genomic DNA from biofilms was extracted with the Power Soil Kit (MO-BIO, Carlsbad, CA, USA) according to the manufacturer's instructions. The extracted DNA was eluted to a final volume of 100 μL. *q*PCR assays were conducted using a CFX96TM Real-Time Detection System (Bio-RAD, California, USA).

NH_2Cl was used for TAC decay study in stormwater, as it is the dominant active chlorine species in tap water. Before NH_2Cl stock solution was added into stormwater samples, samples were filtered by 0.45 μm membrane filters and the TAC concentrations were measured to ensure no residual active chlorine in stormwater samples. All the NH_2Cl dissipation experiments were performed within 48 hours of sample delivery to the laboratory. NH_2Cl stock solutions were prepared with an active chlorine to nitrogen molar ratio of 1.0 by the addition of hypochlorous acid (HOCl) and ammonium chloride (NH_4Cl) into ultrapure water, and solutions were mixed for 30 min in the dark to ensure homogeneity before use. NH_2Cl stock solution was added into stormwater samples collected from four different neighborhoods to achieve 0.05 mM of initial NH_2Cl in stormwater samples. Then the stormwater samples were transferred into 128 mL flasks wrapped with aluminum foil, and stored at room temperature (25 °C). With an active Cl/N=1, the TAC molar concentration was assumed to be the same as NH_2Cl molar concentration. All the experiments were performed in triplicate.

3.5.4. Total active chlorine concentration changes in stormwater samples

Table S3.2. TAC concentrations in stormwater samples collected in summer 2015 at various locations

Sampling site		**01-May**	**20-May**	**03-Jun**	**18-Jun**	**08-Jul**	**22-Jul**	**05-Aug**	**26-Aug**	**10-Sep**	**23-Sep**
Residential Area	RES1	0.10	0.13	0.22	0.15	0.48	0.17	0.12	0.37	0.24	0.33
	RES2	0.13	0.07	0.18	0.26	0.10	0.02	0.04	0.22	0.18	0.12
Park Area	PRK1	0.15	0.13	0.2	0.18	0.23	0.15	0.03	0.11	0.21	0.09
	PRK2	0.22	0.12	0.26	0.02	0.41	0.10	0.06	0.23	0.12	0.06
Commercial Area	COM1	0.18	0.18	0.28	0.28	0.40	0.02	0.22	0.15	0.4	0.08
	COM2	0.13	0.13	0.28	0.36	0.35	0.05	0.11	0.21	0.32	0.07
Industrial Area	IND1	0.10	0.12	0.28	0.31	0.77	0.07	0.04	0.20	0.16	0.07
	IND2	0.10	0.12	0.33	0.13	0.62	0.08	0.08	0.42	0.4	0.04

3.5.5. Precipitation information

Table S3.3. TAC concentrations in stormwater samples collected in summer 2016 at various locations

Sampling site		21-April	06-May	19-May	01-June	15-June	07-July	20-July	08-Aug	24-Aug	08-Sep
Residential Area	RES1	0.01	0.00	0.04	0.00	0.21	0.05	0.04	0.07	0.00	0.02
	RES2	0.03	0.02	0.05	0.02	0.06	0.04	0.03	0.05	0.04	0.01
Park Area	PRK1	0.00	0.00	0.01	0.07	0.00	0.02	0.01	0.04	0.05	0.02
	PRK2	0.02	0.02	0.08	0.03	0.05	0.03	0.03	0.07	0.05	0.03
Commercial Area	COM1	0.08	0.02	0.06	0.03	0.05	0.10	0.00	0.08	0.04	0.03
	COM2	0.06	0.00	0.04	0.02	0.07	0.24	0.02	0.12	0.02	0.03
Industrial Area	IND1	0.01	0.05	0.08	0.02	0.05	0.05	0.08	0.06	0.08	0.05
	IND2	0.09	0.07	0.03	0.05	0.06	0.10	0.01	0.05	0.03	0.01

Tables S3.4 and S3.5 show the precipitation data on each sampling day and the total precipitation on three days near the sampling date (two days prior to sampling plus the sampling date) during summer 2015 and 2016.

Table S3.4. Precipitation data (mm) on the sampling date and over three days near the sampling date at different locations in summer 2015

Sampling No.	Sampling date	**I1 I2 C1 C2**		**P1 P2**		**R1 R2**	
		MillWoods Reservoir RG Site RG27		Ja Fife School RG Site RG38		Whitemud Creek RG57	
		Sampling day	3 days	Sampling day	3 days	Sampling day	3 days
1	01-May	0	0	0	0	0	0
2	20-May	0	0	0	0	0	0
3	03-Jun	0	0	0	5.5	0	0.8
4	18-Jun	0	1.6	0	1.5	0	2
5	08-Jul	0	0	0	0	0	0
6	22-Jul	2.1	13.1	0	12.0	1.2	10.2
7	05-Aug	1.5	1.8	0.5	1.2	0	0.9
8	26-Aug	0	0	0	0	0	0
9	10-Sep	0	0.7	0	2.1	0	0.8
10	23-Sep	0	0.3	0	1.2	0	0.3

Table S3.5. Precipitation data (mm) on the sampling date and over three days near the sampling date at different locations in summer 2016

Sampling No.	Sampling date	**I1 I2 C1 C2** MillWoods Reservoir RG Site RG27		**P1 P2** Ja Fife School RG Site RG38		**R1 R2** Whitemud Creek RG57	
		Sampling day	3 days	Sampling day	3 days	Sampling day	3 days
1	21-Apr	0	0	0	0	0	0
2	06-May	0	0	0	0	0	0
3	19-May	9.9	10.4	0	5.0	10	10.3
4	01-Jun	0	6.1	0	0.1	0	4.9
5	15-Jun	0	1.9	0	0.9	2.1	2.5
6	07-Jul	0.4	0.4	0	8.7	0.4	0.9
7	20-Jul	3.5	3.5	0	1.1	5.0	5.0
8	08-Aug	1.6	1.6	0.1	10.5	3.5	3.5
9	24-Aug	3.4	29.6	0	1.4	3.4	32.2
10	08-Sep	2.2	2.3	0	0	3.0	3.2

3.5.6. Quantitative polymerase chain reaction

Four independent *q*PCR assays were conducted to quantify the total bacterial 16S rRNA, AOB amoA gene, NOB-1 NSR and NOB-2 Nitro16S rRNA (Table S4.6). Reactions (20 μL) were performed in 96-well microplates. Each tube was separately loaded with 2 μL of genomic DNA (14-26ng/μL), plasmid standard or grade sterile water as negative control, followed by the forward and reverse primers (1 μL), together with 10 μL 1* iTap SYBR Green Supermix with ROX (Bio-RAD, Hercules, California) and 6 μL PCR grade sterile water. Triplicate composite samples were tested for all experiments. The efficiency of PCR amplification for each gene was between 80% and 110%. The primers used in qPCR analyzes are shown in Table S3.6.

Table S3.6. Primers used in *q*PCR

Bacteria types	Target	Primer	Sequence (5’-3’)	Reference
Total Bacteria	Bacterial 16S rRNA	*341f*	5’-CCTACGGGAGGCAGCAG-3’	Muyzer et al., 1993
		907r	5’-CCGTCAATTCCTTTRAGTTT-3’	Muyzer et al., 1995
AOB	amoA gene	*amoA-1F*	5’-GGGGTTTCTACTGGTGGT-3’	McTavish et al., 1993
		amoA-2R	5’-CCCCTCKGSAAAGCCTTCTTC-3’	McTavish et al., 1993
NOB-1	NSR 16S rRNA	*NSR 1113f*	5’-CCTGCTTTCAGTTGCTACCG-3’	Dionisi et al., 2002
		NSR 1264r	5’-GTTTGCAGCGCTTTGTACCG-3’	Dionisi et al., 2002
NOB-2	Nitro 16S rRNA	*Nitro 1198f*	5’-ACCCCTAGCAAATCTCAAAAAACCG-3’	Graham et al., 2007
		Nitro 1423r	5’-CTTCACCCCAGTCGCTGACC-3’	Graham et al., 2007

3.5.7. The physical and chemical characteristics of dry weather stormwater samples

Table S3.7. Edmonton stormwater sample characteristics in summer 2015

Sampling Location		Total P (mg/L)	Hardness (g/L as $CaCO_3$))	Temperature (ºC)	Conductivity (mS/cm)	DO (mg/L)	Turbidity (NTU)	TSS (mg/L)	TDS (g/L)
Residential Area	RES1	1.11 ± 0.37	1.0± 0.1	16.1 ± 0.8	3.0 ± 0.4	10.3 ± 0.4	57 ± 35	164 ± 82	2.1 ± 0.3
	RES2	0.78 ± 0.19	0.9 ± 0.1	15.9 ± 0.7	2.7 ± 0.4	9.9 ± 0.4	9 ± 1	19 ± 5	1.9 ± 0.2
Park Area	PRK1	0.59 ± 0.13	0.7 ± 0.2	15.8 ± 0.8	2.5 ± 0.5	10.4 ± 0.3	115 ± 50	283 ± 96	1.7 ± 0.3
	PRK2	0.24 ± 0.22	1.1 ± 0.1	13.7 ± 0.9	3.1 ± 0.5	10.6 ± 0.4	34 ± 40	193 ± 140	2.2 ± 0.4
Commercial Area	COM1	1.09 ± 0.30	0.8 ± 0.1	15.2 ± 1.0	2.9 ± 0.4	10.4 ± 0.2	21 ± 19	84 ± 52	2.4 ± 0.3
	COM2	0.51 ± 0.23	1.0 ± 0.1	16.2 ± 0.8	3.3 ± 0.5	10.1 ± 0.3	20 ± 5	45 ± 7	2.4 ± 0.3
Industrial Area	IND1	0.24 ± 0.13	1.0 ± 0.1	15.5 ± 0.9	4.0 ± 0.5	11.2 ± 0.5	39 ± 28	202 ± 110	2.8 ± 0.4
	IND2	0.17 ± 0.20	1.0 ± 0.1	15.2 ± 0.7	3.4 ± 0.6	11.0 ± 0.4	15 ± 18	165 ± 92	2.5 ± 0.4

Table S3.8. Edmonton stormwater sample characteristics in summer 2016

Sampling Location		Total P (mg/L)	Hardness (g/L as CaCO$_3$))	Temperature (ºC)	Conductivity (mS/cm)	DO (mg/L)	Turbidity (NTU)	TSS (mg/L)	TDS (g/L)
Residential Area	RES1	1.10 ± 0.29	4.4 ± 0.3	16.1 ± 2.3	4.4 ± 0.3	10.1 ± 1.3	12 ± 7	20 ± 17	2.6 ± 0.9
	RES2	1.22 ± 0.29	4.0 ± 0.3	15.1 ± 2.5	4.0 ± 0.3	10.4 ± 1.0	6 ± 3	6 ± 3	1.9 ± 0.6
Park Area	PRK1	1.02 ± 022	4.2 ± 0.6	15.1 ± 1.5	4.2 ± 0.6	10.3 ± 0.8	37 ± 27	37 ± 57	2.2 ± 0.2
	PRK2	0.86 ± 0.42	4.2 ± 1.3	13.4 ± 2.1	4.2 ± 1.3	11.5 ± 1.8	9 ± 4	5 ± 4	2.1 ± 0.4
Commercial Area	COM1	1.14 ± 0.31	4.7 ± 0.5	12.6 ± 3.3	4.7 ± 0.5	12.7 ± 1.5	17 ± 1	25 ± 17	2.1 ± 0.7
	COM2	1.05 ± 0.47	4.8 ± 0.6	13.9 ± 3.0	4.8 ± 0.6	11.0 ± 1.4	18 ± 7	19 ± 3	2.4 ± 0.9
Industrial Area	IND1	1.54 ± 0.60	5.9 ± 0.8	12.3 ± 3.0	5.9 ± 0.8	11.7 ± 1.2	47 ± 38	51 ± 17	3.5 ± 1.1
	IND2	1.18 ± 0.72	5.4 ± 0.7	13.3 ± 2.7	5.4 ± 0.7	11.0 ± 1.6	21 ± 16	43 ± 17	3.1 ± 0.8

3.5.8. The physical and chemical characteristics of wet weather stormwater samples

Table S3.9. The physiochemical properties of Edmonton stormwater samples collected on 22-July, 2015 during a rainfall event occurred in RES2, COM1, COM2, IND1 and IND2 locations

Sampling location	pH	NH_4^+-N (mg/L)	NO_2^--N (mg/L)	NO_3^--N (mg/L)	Alkalinity (mg/L)	COD (mg/L)
RES2	7.84	0.135	0.046	1.48	59.2	92.1
COM1	7.75	0.186	0.05	0.783	71.2	71.5
COM2	7.92	0.075	0.151	1.5	51.6	68.9
IND1	7.82	0.19	0.056	1.08	51.6	81.9
IND2	7.71	0.411	0.075	1.58	70.8	126

Table S3.10. The stormwater quality changes of Edmonton stormwater samples collected on IND1 locations during a rainfall event occurred on September 07, 2015 (samples were collected every 30 min)

Sample #	NH_4^+-N (mg/L)	NO_2^--N (mg/L)	NO_3^--N (mg/L)	Alkalinity (mg/L)	COD (mg/L)	Turbidity (NTU)
1	2.12	0.110	1.12	192	132	125.6
2	1.50	0.207	0.992	177	89.7	170.9
3	1.55	0.182	0.951	82.8	86.7	24.2
4	1.61	0.030	0.668	80.4	82.5	10.8
5	1.71	0.045	0.724	88.4	91.2	10.6
6	1.65	0.085	0.761	80.4	83.7	6.5
7	1.09	0.280	1.14	84.8	81.7	6.1
8	1.30	0.177	0.888	81.2	82.6	8.4

3.5.9. NH_2Cl dissipation data

Table S3.11. Stormwater quality and second-order NH_2Cl dissipation rate coefficients

Sampling Location		pH		NH_4^+-N (mg/L)		NO_2^--N (mg/L)		Alkalinity (mg/L)		COD (mg/L)		DOC (mg/L)		Second-order k ($mM^{-1}h^{-1}$)	
		2015	2016	2015	2016	2015	2016	2015	2016	2015	2016	2015	2016	2015	2016
Residential Area	RES 1	8.19	8.22	0.14	11.35	0.05	0.11	348	394	21.6	37.7	11.4	13.45	0.391	0.369
	RES 2	8.18	8.13	5.15	8.12	0.26	0.17	387	338	35.0	47.6	10.7	12.49	0.29	0.303
Park Area	PRK 1	8.01	8.06	0.01	0.005	0.02	0.07	544	495	40.0	39.8	11.9	12.67	0.32	0.524
	PRK 2	8.13	8.16	0.02	0.112	0.03	0.03	448	416	44.4	64.5	17.9	21.4	0.813	0.990
Commercial Area	COM 1	8.16	7.98	1.32	4.34	0.11	0.17	580	406	50.1	114.0	14.4	36.95	0.733	6.779
	COM 2	8.18	8.24	0.5	1.49	0.3	0.16	436	402	48.8	128.0	16.2	44.95	0.805	14.841
Industrial Area	IND 1	8.15	8.25	0.06	0.083	0.01	0.08	538	342	76.6	30.8	16.3	16.97	0.672	0.747
	IND 2	8.03	8.12	0.16	0.666	0.03	0.10	494	201	51.4	49.3	13.3	13.4	0.854	0.466

3.5.10. Stormwater chemistry correlation analysis by Pearson Correlation coefficients

Table S3.12. Pearson correlation coefficients of the stormwater chemistry in summer 2015

Correlation Coefficient	**NH_4^+-N (mg/L)**	**NO_2^--N (mg/L)**	**Alkalinity (mg/L)**	**pH**	**DOC (mg/L)**
NH_4^+-N (mg/L)	1.000	0.768	-0.512	0.443	-0.098
NO_2^--N (mg/L)	0.768	1.000	-0.235	0.343	-0.142
Alkalinity (mg/L)	-0.512	-0.235	1.000	-0.034	0.55
pH	0.443	0.343	-0.034	1.000	-0.273
DOC (mg/L)	-0.098	-0.142	0.55	-0.273	1.000

Table S3.13. Pearson correlation coefficients of the stormwater chemistry in summer 2016

Correlation Coefficient	**NH_4^+-N (mg/L)**	**NO_2^--N (mg/L)**	**Alkalinity (mg/L)**	**pH**	**DOC (mg/L)**
NH_4^+-N (mg/L)	1.000	0.621	0.424	0.257	0.509
NO_2^--N (mg/L)	0.621	1.000	0.420	0.161	0.131
Alkalinity (mg/L)	0.414	0.420	1.000	-0.015	0.299
pH	0.257	0.161	-0.015	1.000	0.719
DOC (mg/L)	0.509	0.131	0.299	0.719	1.000

3.6. References

Al-Kofahi, S., Steele, C., VanLeeuwen, D., St. Hilaire, R., 2012. Mapping land cover in urban residential landscapes using very high spatial resolution aerial photographs. Urban For. Urban Green. 11, 291–301. doi:10.1016/j.ufug.2012.05.001

Bal Krishna, K.C., Sathasivan, A., Chandra Sarker, D., 2012. Evidence of soluble microbial products accelerating chloramine decay in nitrifying bulk water samples. Water Res. 46, 3977–3988. doi:10.1016/j.watres.2012.05.026

Bernhardt, E.S., Band, L.E., Walsh, C.J., Berke, P.E., 2008. Understanding, managing, and minimizing urban impacts on surface water nitrogen loading. Ann. N. Y. Acad. Sci. doi:10.1196/annals.1439.014

Breiman, L., 2001. Random forests. Mach. Learn. 45, 5–32. doi:10.1023/A:1010933404324

Brodtmann, N. V., Russo, P.J., 1979. Use of chloramine for reduction of trihalomethanes and disinfection of drinking water. J. Am. Water Works Assoc. doi:10.2307/41269574

Brooks, A.S., Bartos, J.M., 1984. Effects of Free and Combined Chlorine and Exposure Duration on Rainbow Trout, Channel Catfish, and Emerald Shiners. Trans. Am. Fish. Soc. 113, 786–793. doi:10.1577/1548-8659(1984)113<786:EOFACC>2.0.CO;2

Brown, C., 2002. Water Use in the Professional Car Wash Industry, International Carwash Association, Inc.

Brown, C., 2000. Water Conservation in the Professional Car Wash Industry, A Report for the International Carwash Association.

Canadian Council of Ministers of the Environment, 2009. Canada-wide Strategy for the Management of Municipal Wastewater Effluent. Winnipeg.

Canadian Council of Ministers of the Environment, 1999. Canadian Water Quality Guidelines for the Protection of Aquatic Life: Reactive Chlorine Species. Winnipeg.

Cessco Fabrication and Engineering Ltd, 2014. Products and services [WWW Document]. URL http://cessco.ca/fabrication/products-and-services (accessed 11.15.16).

Coomes, P. a, Rockaway, T.D., Rivard, J., Kornstein, B., 2010. North America Residential Water Usage Trends Since 1992, US EPA.

Dionisi, H.M., Layton, A.C., Harms, G., Gregory, I.R., Robinson, K.G., Sayler, G.S., 2002. Quantification of Nitrosomonas oligotropha-like ammonia-oxidizing bacteria and nitrospira spp. from full-scale wastewater treatment plants by competitive PCR. Appl. Environ. Microbiol. 68, 245–253. doi:10.1128/AEM.68.1.245-253.2002

Duirk, S.E., Gombert, B., Croué, J.P., Valentine, R.L., 2005. Modeling monochloramine loss in the presence of natural organic matter. Water Res. 39, 3418–3431. doi:10.1016/j.watres.2005.06.003

Echeverry-Galvis, M.A., Peterson, J.K., Sulo-Caceres, R., 2014. The social nestwork: Tree structure determines nest placement in Kenyan weaverbird colonies. PLoS One 9. doi:10.1371/journal.pone.0088761

EPCOR Utilities Inc., 2015. Edmonton Waterworks Annual Report to Alberta Environment and Water 2015.

Fisher, R., 1925. Statistical methods for research workers, Biological monographs and manuals. doi:10.1056/NEJMc061160

Graham, D.W., Knapp, C.W., Van Vleck, E.S., Bloor, K., Lane, T.B., Graham, C.E., 2007. Experimental demonstration of chaotic instability in biological nitrification. ISME J. 1, 385–93. doi:10.1038/ismej.2007.45

Hrudey, S.E., 2009. Chlorination disinfection by-products, public health risk tradeoffs and me.

Water Res. doi:10.1016/j.watres.2009.02.011

Kaushal, S.S., Groffman, P.M., Band, L.E., Elliott, E.M., Shields, C.A., Kendall, C., 2011. Tracking nonpoint source nitrogen pollution in human-impacted watersheds. Environ. Sci. Technol. 45, 8225–8232. doi:10.1021/es200779e

Kiéné, L., Lu, W., Lévi, Y., 1998. Relative importance of the phenomena responsible for chlorine decay in drinking water distribution systems. Water Sci. Technol. 38, 219–227. doi:10.1016/S0273-1223(98)00583-6

Kuang, X., Sansalone, J., 2011. Cementitious porous pavement in stormwater quality control: pH and alkalinity elevation. Water Sci. Technol. 63, 2992–2998. doi:10.2166/wst.2011.505

Liaw, a, Wiener, M., 2002. Classification and Regression by randomForest. R news 2, 18–22. doi:10.1177/154405910408300516

Liu, A., Egodawatta, P., Guan, Y., Goonetilleke, A., 2013. Influence of rainfall and catchment characteristics on urban stormwater quality. Sci. Total Environ. 444, 255–262. doi:10.1016/j.scitotenv.2012.11.053

Maestre, J.P., Wahman, D.G., Speitel, G.E., 2013. Monochloramine cometabolism by Nitrosomonas europaea under drinking water conditions. Water Res. 47, 4701–4709. doi:10.1016/j.watres.2013.05.019

Makepeace, D.K., Smith, D.W., Stanley, S.J., 1995. Urban stormwater quality: Summary of contaminant data. Crit. Rev. Environ. Sci. Technol. 25, 93–139. doi:10.1080/10643389509388476

Mays, L.W., 2002. Water demand analysis, in: Urban Water Supply Handbook. McGRAW-HILL.

McTavish, H., Fuchs, J.A., Hooper, A.B., 1993. Sequence of the gene coding for ammonia monooxygenase in Nitrosomonas europaea. J. Bacteriol. 175, 2436–2444.

Mitcham, R.P., Shelley, M.W., Wheadon, C.M., 1983. Free chlorine versus ammonia-chlorine: disinfection, trihalomethane formation, and zooplankton removal. J. Am. Water Works Assoc. 75, 196–198.

Muyzer, G., De Waal, E.C., Uitterlinden, A.G., 1993. Profiling of complex microbial populations by denaturing gradient gel electrophoresis analysis of polymerase chain reaction-amplified genes coding for 16S rRNA. Appl. Environ. Microbiol. 59, 695–700. doi:0099-2240/93/030695-06$02.00/0

Muyzer, G., Teske, A., Wirsen, C.O., Jannasch, H.W., 1995. Phylogenetic relationships of Thiomicrospira species and their identification in deep-sea hydrothermal vent samples by denaturing gradient gel electrophoresis of 16S rDNA fragments. Arch. Microbiol. 164, 165–172. doi:10.1007/BF02529967

Norman, T.S., Harms, L.L., Looyenga, R.W., 1980. The Use of Chloramines To Prevent Trihalomethane Formation. J. Am. Water Works Assoc. 72, 176–180.

Nouri, H., Beecham, S., Kazemi, F., Hassanli, A.M., 2013. A review of ET measurement techniques for estimating the water requirements of urban landscape vegetation. Urban Water J. 10, 247–259. doi:10.1080/1573062X.2012.726360

Pitt, R., Maestre, A., Morquecho, R., 2004. The national stormwater quality database (NSQD, version 1.1), 1st Annual Stormwater Management Research Symposium Proceedings.

PricewaterhouseCoopers LLP, 2008. Alberta Pressure Vessel Manufacturing Sector Benchmarking Report 2008 Provincial Trends : Global Currents, PricewaterhouseCoopers LLP.

R Development Core Team, R.F.F.S.C., 2008. R: A Language and Environment for Statistical Computing. Vienna Austria R Found. Stat. Comput. doi:10.1007/978-3-540-74686-7

Rittmann, B.E., Regan, J.M., Stahl, D.A., 1994. Nitrification as a source of soluble organic substrate in biological treatment. Water Sci. Technol. 30, 1–8.

Sablayrolles, C., Vialle, C., Vignoles, C., Montrejaud-Vignoles, M., 2010. Impact of carwash discharge on stormwater quality (Toulouse, France). Water Sci. Technol. 62, 2737–2746. doi:10.2166/wst.2010.929

Sathasivan, A., Fisher, J., Kastl, G., 2005. Simple method for quantifying microbiologically assisted chloramine decay in drinking water. Environ. Sci. Technol. 39, 5407–5413. doi:10.1021/es048300u

Shlens, J., 2014. A Tutorial on Principal Component Analysis. ArXiv 1–13. doi:10.1.1.115.3503

Siripong, S., Rittmann, B.E., 2007. Diversity study of nitrifying bacteria in full-scale municipal wastewater treatment plants. Water Res. 41, 1110–1120. doi:10.1016/j.watres.2006.11.050

Strassler, E., Pritts, J., Strellec, K., 1999. Preliminary data summary of urban storm water best management practices, US EPA.

United States Environmental Protection Agency, 1985. Ambient Aquatic Life Water Quality Creteria for Chlorine. Florida.

Vikesland, P.J., Ozekin, K., Valentine, R.L., 2001. Monochloramine decay in model and distribution system waters. Water Res. 35, 1766–1776. doi:10.1016/S0043-1354(00)00406-1

Wahman, D.G., Speitel, G.E., 2012. Relative importance of nitrite oxidation by hypochlorous acid under chloramination conditions. Environ. Sci. Technol. 46, 6056–6064. doi:10.1021/es300934x

White, R., Havalak, R., Nations, J., Thomas, J., Chalmers, D., Dewey, D., 2004. How much water is enough? Using pet to develop water budgets for residential landscapes.

Zaneti, R., Etchepare, R., Rubio, J., 2012. More environmentally friendly vehicle washes: Water reclamation. J. Clean. Prod. 37, 115–124. doi:10.1016/j.jclepro.2012.06.017

CHAPTER 4. MONOCHLORAMINE LOSS MECHANISMS IN TAP WATER[2]

4.1. Introduction

Chlorine products have been used from early in the 20th century to disinfect drinking water. Unfortunately, this widely-used free-chlorine treatment has disadvantages, including the high reactivity of chlorine with natural organic compounds and the production of disinfection by-products (DBPs). To limit the formation of many chlorinated DBPs, chloramination, an alternative water disinfection technology, has been developed and applied in drinking water systems throughout North America (Zhou et al., 2013; USEPA, 2012b; Chowdhury et al., 2010; Hua and Reckhow, 2008; Minear and Amy, 1996; Wolfe et al., 1984). Chloramination has also proven useful for its long-lasting residual, with corresponding disinfection effect, in water distribution systems (Brodtmann and Russo, 1979; Mitcham et al., 1983; Norman et al., 1980).

During chloramination, ammonia is used to convert residual chlorine to chloramines (NH_2Cl, $NHCl_2$ and NCl_3), which reduces the formation of DBPs. At near neutral pH, with an active chlorine to ammonia-nitrogen (Cl/N) molar ratio < 1, monochloramine (NH_2Cl) is the predominant chlorine species in chloraminated water (Engineers, 2012). However, in a neutral or acid pH environment, NH_2Cl is relatively unstable. It can autodecompose through a series of reactions (Jafvert and Valentine, 1992; Vikesland et al., 2001), which results in a decreased disinfection efficiency. The NH_2Cl autodecomposition rate depends markedly on pH, temperature, Cl/N molar ratio and the initial NH_2Cl concentration (Vikesland et al., 2001). Further, chemical compounds existing in drinking water, including natural organic matter (NOM), nitrite, bromide and ferrous ions can also accelerate NH_2Cl decomposition (Vikesland et al., 2001; Zhou et al.,

---

[2] A version of this chapter has been published: Zhang, Q., Davies, E. G. R., Bolton, J. R., & Liu, Y., 2017. Monochloramine loss mechanisms in tap water. Water Environment Research. 89(11), 1999-2005.

2013). In this research, based on the Edmonton water quality report (EPCOR, 2015) and pre-chemical test results of this study, the concentrations of nitrite, bromide and ferrous ion in drinking water samples are very low (less than 0.01 mg/L for nitrite and ferrous ion, not detectable for bromide) and so their effects are not considered independently in this research. However, the non-negligible concentration of NOM in drinking water means that it should be considered. It should be noticed that for some utilities that may contain comparably high concentration of nitrite, bromide and ferrous ion, this model cannot be used to predict the NH_2Cl loss rates in these utilities.

After drinking water secondary disinfection (i.e., monochloramine disinfection before distribution), the NH_2Cl autodecomposition and the reaction between active chlorine and NOM are significant NH_2Cl loss pathways. River, lake and ground waters are usually used as drinking water sources, and previous studies have addressed the NH_2Cl loss rates in the presence of NOM in different rivers (Duirk et al., 2005). However, after secondary disinfection process, NH_2Cl can continuously dissipate in drinking water distribution systems. The modification of source waters through treatment processes before distribution may cause the NOM species in drinking water to differ from those in the source water, with a consequent difference in NH_2Cl loss processes. Under real drinking water conditions, the only reported work (Zhou et al., 2013) – according to web of science – built an NH_2Cl loss model under specific active chlorine to ammonia ratios, but did not study chemical reaction mechanisms.

The principal objective of this research is to develop a kinetic model to predict NH_2Cl loss in drinking water distribution systems under real drinking water conditions, thus providing a model for the management of drinking water disinfection and transportation. The model developed in this work predicts the NH_2Cl loss under a variety of conditions of temperature, pH and Cl/N ratios, and initial NH_2Cl and NOM concentrations. Further, the methodological approach applied here for model development should apply to alternative cases with different drinking water conditions and different water sources.

4.2. Materials and methods

4.2.1. Monochloramine decay experiments

Experimental setup Tap water from University of Alberta, Edmonton, Alberta, Canada constituted the water samples used in the experiments, with samples taken after the water faucet was left open for 30 min to ensure that the water samples used in this research can represent the water characteristics in drinking water distribution systems. River water (North Saskatchewan River) was used as the tap water source, and coagulation, flocculation, sedimentation, chlorination, UV disinfection, chloramination and filtration were adopted (EPCOR, Canada) for drinking water treatment in Edmonton. The experiments tested effects of different factors on the NH_2Cl loss rate: pH, active Cl/N ratio, NH_2Cl initial concentration, temperature and NOM. For each time the tap water sample was collected, the impact of one factor on NH_2Cl loss rate was studied. The value of NOM reactive site S was also determined at the same time.

Water samples in duplicates were tested, and all the glassware was pretreated to be chlorine demand-free. 300 mL samples of tap water were transferred into batch reactors wrapped with aluminum foil. The ammonium chloride standard solution (1 mg = 1 mL NH_4^+-N) was used to adjust the Cl/N molar ratio to 0.7. Then $NaHCO_3$ was used to buffer the system, and 20 mM (represent as TCO_3) was used as the final alkalinity concentration to achieve the stable pH. The pH of the solutions was adjusted to approximately 7.6 by the addition of NaOH or HCl. Finally, the reactors were stored in incubators set at 25 °C. In each experimental group, only one parameter at a time (including pH, Cl/N molar ratio, NH_2Cl initial concentration, temperature and NOM) was adjusted to different values to permit study of each specific condition.

A neutral pH is recommended for chloramination, while a slightly basic pH is usually used in drinking water treatment to protect pipes from corrosion. Thus, a pH range of 7.00 – 8.45 was studied in these experiments. To study the impact of pH on the NH_2Cl loss rate, NaOH and HCl solutions were used to adjust the pH to specific values (7.0, 7.6 and 8.45). The Cl/N molar ratio is commonly controlled to remain at-or-below 1 in drinking water treatment to reduce the formation of dichloramine and trichloramine, but the practical ratios vary from one treatment plant to another based on their operational conditions. To study the impact of the Cl/N molar ratio, more nitrogen standard solution was added to the reactors if a lower Cl/N ratio (0.5) was required. A monochloramine range of 0.056 mM to 0.2 mM was usually used for NH_2Cl dissipation study. To achieve higher initial NH_2Cl concentrations, the NH_2Cl stock solution was added to tap water when the impact of NH_2Cl concentrations (0.1 and 0.2 mM) on NH_2Cl decay was studied. This stock solution was prepared with a Cl/N molar ratio of 0.7 by adding free chlorine and ammonia standard solutions into ultrapure water, and solutions were mixed for 30 min in the dark before use to ensure homogeneity. Incubators were adjusted to different values (4, 25 and 35 ˚C) to study the effect of temperature. Note that because the experiments were designed to describe the NH_2Cl decay process in tap water, no additional NOM was added to the water samples; therefore, all NOM in water samples was from the tap water itself. To study the impact of NOM concentrations on NH_2Cl loss rate, the tap water was diluted with an equal amount of ultrapure water, and then extra NH_2Cl stock solution and nitrogen standard solution were added to achieve the required concentrations.

Water chemistry monitoring Since the Cl/N molar ratios in this research were less than 1, the total chlorine molar concentration was assumed to be the same as the NH_2Cl molar concentration. The NH_2Cl molar concentrations were measured by the HACH colorimetric method

8167 (with a detection limit of 0.02 mg-Cl/L), and this method was calibrated based on manufacturer's guidelines before NH_2Cl measurement. Total ammonia in water samples was determined by the HACH colorimetric method 10205 with a detection limit of 0.015 mg NH_3-N/L. The pH was measured by a calibrated VWR® sympHony™ B10P Benchtop pH Meter. The NOM concentration was analyzed based on the total dissolved organic carbon (total DOC) concentrations as measured by a Shimadzu TOC-L CPH E100 (detection limit is 4 μg-C/L).

<u>NOM reactive site determination</u> The method for NOM reactive site was determined from Duirk *et al.*'s (2005) study. 0.2 mM free chlorine was added to tap water samples to react with NOM. With the assumption that one molar of free chlorine can consume one molar of reactive DOC (DOC_r) in this study, the concentration of DOC_r in each sample can be determined based on the tap water total free chlorine demand when no more significant changes of free chlorine concentration could be observed in water samples for 5 days, which typically occurred approximately three weeks after the start of the experiment. The NOM reactive fraction S can then be solved by the ratio of DOC_r to total DOC concentrations. A control group that added 0.2 mM free chlorine into ultrapure water was set to eliminate the impact of free chlorine auto loss. Experiments were duplicates.

4.2.2. Reaction assumptions and model development

The monochloramine loss model used in this research was adapted from earlier models. Jafvert and Valentine (1992) developed an NH_2Cl loss model to describe NH_2Cl autodecomposition processes under various concentrations. Vikesland et al. (2001) then refined the model by adding other factors, including temperature, nitrite and bromide concentrations. In natural waters, the presence of NOM also significantly affects the NH_2Cl loss rate; therefore, Duirk et al. (2002) modeled the NH_2Cl loss in the presence of Aldrich humic acid under the assumption that only monochloramine reacted with NOM, and the reaction between NOM and NH_2Cl had two pathways: a rapid reaction within the first several hours and a consequent long-term reaction. In each pathway, only a specific fraction of NOM is involved in the reaction. However, with an increase of NH_2Cl and ammonia (including NH_4^+ and NH_3) concentrations at the same molar ratio, the kinetic constants of the long-term reaction decreased under this assumption, which means that some intermediate products, such as free chlorine and dichloramine, formed during the NH_2Cl autodecomposition processes. These intermediate products may be responsible for the NOM long-term reaction (Duirk et al. 2005). Duirk et al. (2005) first proposed that free chlorine, rather than NH_2Cl, reacts with NOM in the long-term reaction. Under this assumption – adopted also for this study – the NOM long-term reaction rate constant does not change with pH, which presents better NH_2Cl decay kinetics as compared with earlier theories. Therefore, this theory is also used in this research.

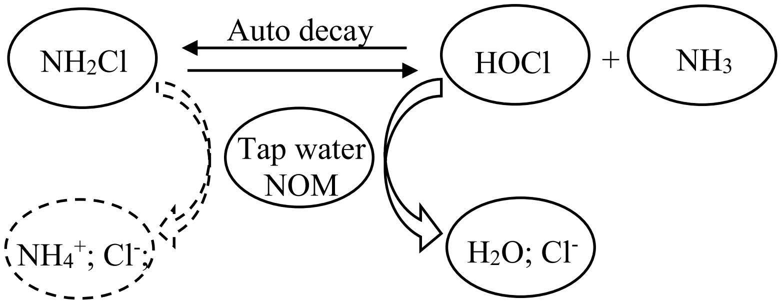

Fig. 4.1. The reaction assumptions for the reactions between active chlorine and tap water NOM

The reaction between different types of NOM and NH_2Cl solution in pre-experiments showed that the rapid reaction only happened in the first few hours of the reaction. In this research, since the model is built for the prediction of NH_2Cl decay in drinking water distribution systems, it is assumed that the NOM rapid reaction pathway was completed in on-site reservoirs before water flows into distribution systems. Therefore, only the long-term reaction was considered here

(Fig. 4.1). In the equations below, k_{docr} and S represent the kinetic constant and the NOM reactive site fraction included in the long-term reaction. $\mathrm{DOC_r}$ represents the reactive DOC. The reaction pathway is shown in eqn. 4.1.

$$\text{Pathway: } \mathrm{HOCl} + \mathrm{DOC_r} \xrightarrow{k_{\mathrm{docr}}} \text{Products.} \tag{4.1}$$

$$[\mathrm{DOC_r}] = \mathrm{S}\ [\text{total DOC}] \tag{4.2}$$

The mechanistic equation of this reaction is shown below (eqn. 4.3):

$$\frac{\mathrm{d[HOCl]}}{\mathrm{dt}} = -k_{\mathrm{docr}}[\mathrm{HOCl}][\mathrm{DOC_r}] \tag{4.3}$$

With this assumption, all the reactions of tap water $\mathrm{NH_2Cl}$ loss mechanisms are shown in Table 4.1.

Based on Duirk et al. (2005), k_{docr} and S were assumed to be constants under various pH values; further, to determine the value of S, a high HOCl concentration (0.2 mM HOCl) was used to oxidize the NOM reactive site S completely. The $\mathrm{NH_2Cl}$ autodecomposition model developed by Jafvert and Valentine (1992) and refined by Vikesland et al. (2001) was used to determine the $\mathrm{NH_2Cl}$ autodecomposition processes in tap water. k_{docr} was then estimated using the tap water NOM reaction (eqn. 4.3) to compensate for the experimental tap water $\mathrm{NH_2Cl}$ loss data, and COMSOL Multiphysics Chemical Reaction Engineering Module (COMSOL, Sweden) was applied to solve k_{docr}. The average value from each group of experiments was used as the final value of k_{docr}.

Table 4.1. Tap water NH_2Cl loss reactions developed by Jafvert and Valentine (1992), Vikesland et al. (2001), Duirk et al. (2005) and the present work

No.	Reaction Types	Reaction Equations	References
1	Autodecomposition reactions	$HOCl + NH_3 \rightarrow NH_2Cl + H_2O$	Morris and Isaac (1981)
2		$NH_2Cl + H_2O \rightarrow HOCl + NH_3$	
3		$HOCl + NH_2Cl \rightarrow NHCl_2 + H_2O$	
4		$NHCl_2 + H_2O \rightarrow HOCl + NH_2Cl$	
5		$2NH_2Cl \rightarrow NHCl_2 + NH_3$	Valentine and Jafvert (1988)
6		$NHCl_2 + NH_3 \rightarrow 2NH_2Cl$	Hand and Margerum (1983)
7		$NHCl_2 + H_2O \rightarrow I^a$	Jafvert and Valentine (1987)
8		$NHCl_2 + I \rightarrow HOCl + pd1^b$	Leao (1981)
9		$NH_2Cl + I \rightarrow pd2^b$	
10		$NH_2Cl + NHCl_2 \rightarrow pd3^b$	
11	Tap water NOM reaction	$HOCl + DOC_r \rightarrow pd4^c$	Present work
12	Equilibrium reactions	$HOCl = H^+ + OCl^-$	Snoeyink and Jenkins (1980)
13		$NH_4^+ = NH_3 + H^+$	
14		$H_2CO_3 = HCO_3^- + H^+$	
15		$HCO_3^- = CO_3^{2-} + H^+$	

[a] I represents an unidentified intermediate; [b] pd1-pd3 (pd means products) may include N_2, H_2O, Cl^-, H^+, NO_3^- and other unidentified products (Jafvert and Valentine, 1992); [c] pd4 may include H_2O, Cl^-, H^+ and NH_2Cl disinfection DBPs.

Temperature usually has a significant influence on reaction rates and equilibrium constants, and the tap-water temperature varies significantly among seasons. Therefore, the impact of temperature on kinetic or equilibrium constants for key rate-limiting reactions (Vikesland et al. 2001) should be considered in the model. The temperature-dependent reaction equations for NH_2Cl autodecomposition were studied by Vikesland et al. (2001), while the temperature-dependent reaction equations for NOM were not considered in previous research. Three different temperatures (4, 25 and 35 ˚C) were used here to estimate the temperature dependent equation for k_{docr}, with numerical values calculated also with COMSOL Multiphysics (COMSOL, Sweden).

The relationship between the temperature and k_{docr} was then solved using the Arrhenius equation (eqn. 4.4 and 4.5),

$$\ln(k_{\mathrm{TD}}) = \ln(\mathrm{A}) - \mathrm{E_a}/\mathrm{RT} \tag{4.4}$$

$$k_{\mathrm{TD}} = \mathrm{A}\exp(-\mathrm{E_a}/\mathrm{RT}) \tag{4.5}$$

Where $\mathrm{E_a}$ is activation energy, A is frequency factor, T is absolute temperature and R is ideal gas constant.

4.3. Results and discussion

4.3.1. Experimental results and discussion

Table 4.2. Tap water characteristics

DOC (mg/L)	NH_4^+-N (mg/L)	pH	SUVA$_{254}$ (L/mg×cm)	NH_2Cl (mM)
1.47 ± 0.15	0.466 ± 0.011	7.8 ± 0.1	0.0196	0.056 ± 0.001

The original tap water characteristics were determined (Table 4.2), and then the tap water was adjusted to the required conditions to study the NH_2Cl loss by varying the factors described above (Fig. 4.2).

Our experimental data did not show a significantly rapid NH_2Cl demand in tap water at the beginning of the experiment, which validated the assumption that almost no NOM rapid reactive sites appear in bulk tap water under our experimental conditions. In Fig. 4.2, points represent the experimental results and lines are the modeling results simulated by COMSOL Multiphysics software (COMSOL, Sweden).

Fig. 4.2(a) shows the acceleration of NH_2Cl decay rate under lower pH values in tap water. With a lower pH, more dichloramine ($NHCl_2$) can be produced due to the acid accelerating reaction $2NH_2Cl \rightarrow NHCl_2 + NH_3$, and since $NHCl_2$ is unstable and decomposes faster than NH_2Cl in a near-neutral pH (Valentine and Jafvert, 1988; Vikesland et al., 2001), the NH_2Cl decay rate increases.

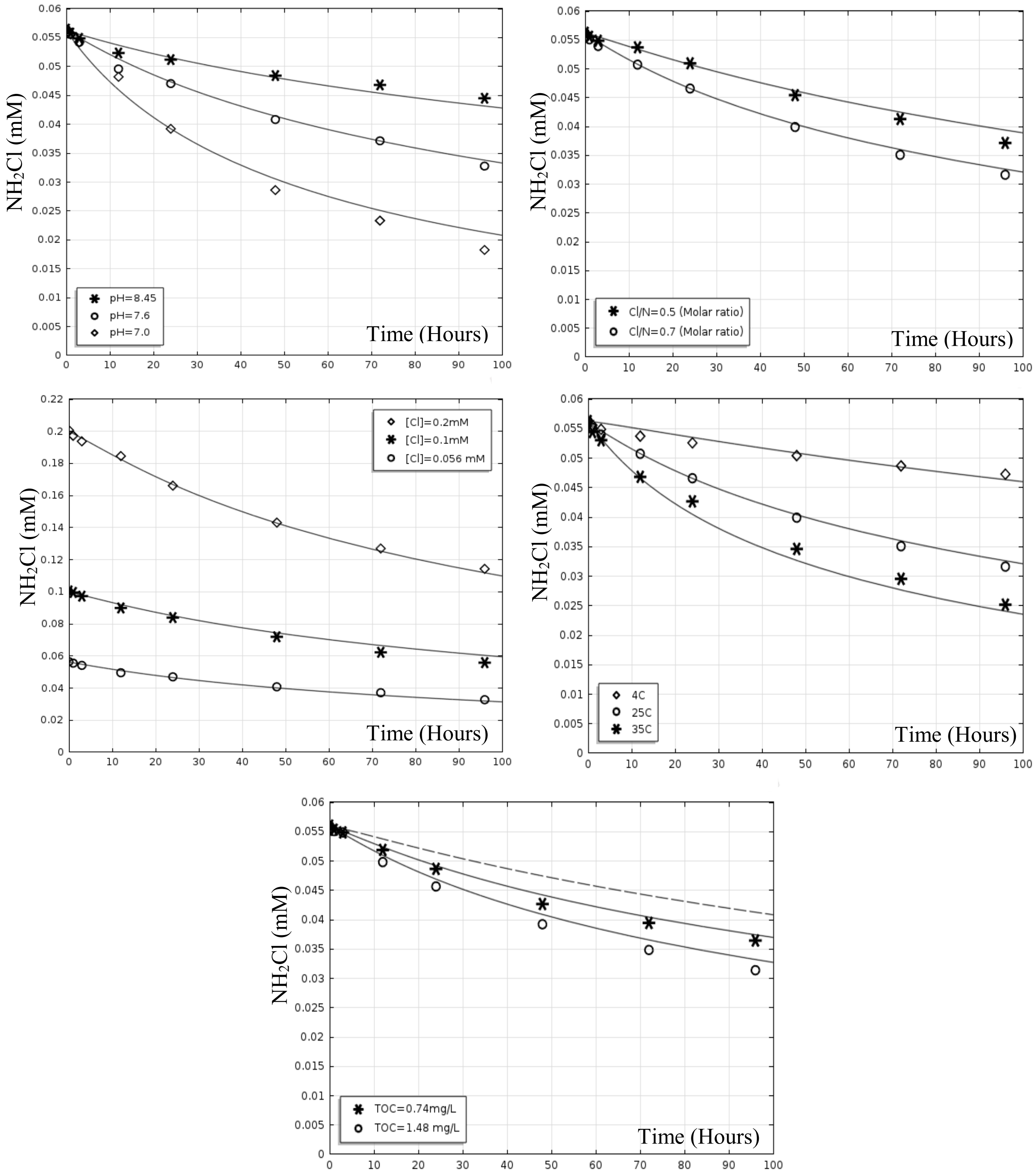

Fig. 4.2. NH_2Cl loss under various conditions (lines: modeling results), (a) $[NH_2Cl]_0$ = 0.056 mM, T = 25 °C. Cl/N = 0.7 mol/mol, [DOC] = 1.39 mg-C/L; (b) $[NH_2Cl]$ = 0.056 mM, pH = 7.6, T = 25 ºC, [DOC] = 1.63 mg-C/L; (c) Cl/N=0.7mol/mol, pH = 7.55, temperature=25 ºC, [DOC] =1.29mg-C/L; (d) $[NH_2Cl]$ = 0.056 mM, pH = 7.6, Cl/N = 0.7 mol/mol, [DOC] = 1.63 mg-C/L; (e) $[NH_2Cl]$ = 0.056 mM, pH = 7.6, Cl/N = 0.7 mol/mol, T=25 ºC. (Dashed line: NH_2Cl auto-decay curve)

As shown in Fig. 4.2(b), a lower Cl/N molar ratio will result in a decrease in the NH_2Cl loss rate. For a fixed NH_2Cl initial concentration, a lower Cl/N molar ratio will lead to more free ammonia (under the condition that the Cl/N molar ratio < 1), which can cause the regeneration of NH_2Cl by its reaction with HOCl (Table 4.1, reaction 1), and consequently decrease the NH_2Cl loss rate.

Fig. 4.2(c) shows that a higher initial NH_2Cl concentration will lead to an increased NH_2Cl loss rate. This observation may be explained by the fact that higher initial NH_2Cl concentrations lead to more free chlorine formation as an intermediate in the NH_2Cl autodecomposition process. Therefore, more NOM is oxidised by free chlorine, which increases the NH_2Cl loss rate. Further, with the same rate constant, a higher initial NH_2Cl concentration will increase the reaction rate of NH_2Cl autodecomposition reactions, which also contribute to the NH_2Cl decay.

As shown in Fig. 4.2(d), temperature produces a significant effect on NH_2Cl loss rate for both the NH_2Cl autodecomposition and the chemical reaction between free chlorine and NOM, and an increase in temperature leads to an increased NH_2Cl decomposition rate.

The impact on NH_2Cl decomposition under two different DOC concentrations in tap water was also studied, and the results are included in Fig. 4.2(e). To study the NH_2Cl dissipation rate under a lower DOC concentration, tap water samples were diluted with ultrapure water. Other factors such as pH, NH_2Cl and ammonium concentrations were then adjusted to the same as the original sample. From this figure, it appears that a higher initial DOC concentration does accelerate the NH_2Cl loss rate. Similar results have been reported previously (Duirk et al., 2002; Duirk et al., 2005). Additionally, the difference of the decay rates between

NH_2Cl autodecomposition shown in Fig 4.2(e) verifies the significant effect of NOM on the NH_2Cl loss rate in tap water. However, higher DOC concentrations were not studied in this research, since the NOM in tap water cannot be concentrated in the presence of NH_2Cl.

4.3.2. Model results and discussion

Table 4.3. Rate coefficient, temperature dependent equation and reactive fraction of NOM

Rate coefficient k_{docr} ($M^{-1}h^{-1}$)	**Temperature dependent equation ($M^{-1}h^{-1}$)**	**Reactive fraction S**
$\boldsymbol{k_{\mathrm{docr}} = (3.57 \pm 0.54) \times 10^{6}}$	$k_{\mathrm{docrTD}} = 1.54 \times 10^{22} \exp(-10733/\mathrm{T})$	0.43 ± 0.06

Experimentally-derived values for k_{docr} and *S* for tap water are shown in Table 4.3, as is the temperature dependent equation (eqn. 4.5). Specifically, a high HOCl concentration (0.2 mM HOCl) was used to completely react with reactive NOM, thus determining the DOC_r concentration in tap water and solving the value of S by eqn. 4.2. In terms of k_{docr}, it was assumed that NH_2Cl autodecomposition and the reaction between free chlorine and reactive NOM are the two dominant pathways that contribute to the NH_2Cl loss in tap water. The NH_2Cl autodecomposition model used in this study was developed by Jafvert and Valentine (1992) and refined by Vikesland et al. (2001). To solve the k_{docr} for the NOM free chlorine reaction, the NH_2Cl autodecomposition model was implemented into COMSOL Multiphysics Chemical Reaction Engineering Module (COMSOL, Sweden) along with the reaction 11 (Table 4.1). k_{docr} can be estimated by the software based on the experimental data. In terms of the temperature dependent equation for k_{docrTD}, the NH_2Cl loss experiments under 4, 25 and 35 ˚C were conducted to estimate the k_{docr}

values under different temperatures. The k_{docrTD} equation was then solved by Arrhenius equation (eqn. 4.4 and eqn. 4.5). To validate the modeling results, the loss rates calculated for the same conditions as the tap water samples were compared with the experimental data. These modeled NH_2Cl loss rates are presented by the curves in Fig. 4.2. As shown in Figs. 4.2(a) to 4.2(e), the experimental data show good matches with the modeling results. It appears that the NH_2Cl loss model built in this study can be used to describe the NH_2Cl loss under various conditions of temperature, pH and Cl/N molar ratios, as well as initial NH_2Cl and NOM concentrations. Further, the validation results show that the reaction assumptions proposed in this research permit prediction of NH_2Cl losses under different chloraminated tap water conditions. That is, although only tap water from one utility (University of Alberta, Edmonton, Canada) was used for model building in this study, to study the NH_2Cl loss rate in tap water with different NOM composition, the value of k_{docr} and S can be easily solved based on the method proposed in this study as well. Note, however, as mentioned in Duirk et al.'s study (2005), that the purpose of this model is to predict the NH_2Cl loss in tap water and not to represent the real chemical reactions occurring in tap water.

Table 4.4. NOM rate constant and reactive site fraction in tap water with 95% confidence intervals

Parameter	NOM reaction rate constant	S
Current study	$(3.57 \pm 0.54) \times 10^{6}\ M^{-1}h^{-1}$	0.43 ± 0.06
Duirk *et al.,* 2005	$7.72 \times 10^{5} \sim 4.95 \times 10^{5}\ M^{-1}h^{-1}$	0.68 ~ 0.42
Zhou *et al.*, 2013	$0.011722 \sim 0.014093\ h^{-1}$	Not determined

Table 4.4 compares rate constants and reactive site fractions from this research with the literature. The assumption for NOM kinetic constant studies used in this research was first proposed by Duirk et al. (2005). They compared the NOM from six rivers to study the impact of different NOM on the NH_2Cl loss rate. The rate constant solved in this work is significantly higher

than Duirk et al.'s study, most likely because the chemical species appearing in tap water are complex. Specifically, in addition to NOM, a variety of chemical species can accelerate the NH_2Cl loss, and since their concentrations are very low, their impact was omitted from the model. However, with higher concentrations of these species, the NH_2Cl loss rate could increase significantly and explain the higher value of k_{docr} found in this work.

In terms of the reactive site fraction, the value of S in this research is in the range of the literature results. It is therefore assumed that although the rapid reactive NOM was consumed during the disinfection process, most of the long-term reactive NOM still retained in tap water, which subsequently reacted with free chlorine after the treated water entered the drinking water network.

Zhou et al. (2013) also studied the NH_2Cl loss in tap water. However, their NOM reaction rate constant is significantly lower than that of this work, because the reaction rate between NH_2Cl and NOM in their study was assumed to be related only to the concentration of NH_2Cl itself (a first-order reaction), while it was assumed to be related to the concentrations of both DOC and active chlorine concentration (second-order reaction) in this study. Further, in their study, NH_2Cl was assumed to react with NOM over the longer-term and thus contributed to the NH_2Cl loss, rather than free chlorine. As an intermediate, free chlorine usually has a concentration approximately 1000 times lower than NH_2Cl in chloraminated water. Therefore, to achieve the same NH_2Cl decay rate, the rate constant of the reaction between NH_2Cl and NOM should be significantly lower than HOCl and NOM. Finally, the reactive site S was not considered in their research, that is, all the NOM in tap water was assumed to react with NH_2Cl, which also produces a lower k_{docr} value in their research.

4.4. Conclusions

Temperature, pH and Cl/N ratios and initial NH_2Cl and NOM concentrations are the dominant factors in determining NH_2Cl losses in tap water. In this research, a model was developed to predict such losses under various conditions; its results exhibit good matches with the experimental data, which validates the model for NH_2Cl loss prediction under various real water conditions. Although the NH_2Cl is the dominant disinfect species in tap water, rapid reaction between NH_2Cl and NOM should not be considered in the model after water flows into drinking water distribution systems. The NOM reactive site fraction S and rate constant k_{docr} were estimated under the assumption that only the long-term reaction between free chlorine and reactive NOM occurred in tap water. Although the values of S and k_{docr} may differ by tap water source, this research provides a useful general methodology for NH_2Cl loss studies in drinking water; further, the methods applied here can also be used to solve for values of k_{docr} in tap water from different water sources. Note that the model built here does not present the real reaction mechanisms in tap water, but it does meet the purpose of this research: prediction of NH_2Cl losses under real water conditions. Moreover, the value of k_{docr} solved in this model may not be directly used for tap water from other sources, and the model built in this study cannot be applied to tap water that contains high concentrations of nitrite, bromide and ferrous ion. Therefore, further studies need to be done to predict the NH_2Cl loss in tap water with the present of these chemicals.

4.5. References

Brodtmann Jr, N.V., and Russo, P.J. (1979) The Use of Chloramine for Reduction of Trihalomethanes and Disinfection of Drinking Water. J. Am. Chem. Soc., 71: 40-42.

Chowdhury, S., Champagne, P., and McLellan, P. J. (2010) Factorial Analysis of Trihalomethanes Formation in Drinking Water. Water Environ. Res., 82, 556–566.

Cowman, G. A., and Singer, P. C. (1995) Effect of Bromide Ion on Haloacetic Acid Speciation Resulting from Chlorination and Chloramination of Aquatic Humic Substances. Environ. Sci. and Technol., 30(1), 16-24.

Duirk, S. E., Gombert, B., Choi, J., and Valentine, R. L. (2002) Monochloramine Loss in the Presence of Humic Acid. J. Environ. Monit., 4(1), 85-89.

Duirk, S. E., Gombert, B., Croué, J. P., and Valentine, R. L. (2005) Modeling Monochloramine Loss in the Presence of Natural Organic Matter. Water Res., 39(14), 3418-3431.

Crittenden, J. C., and Montgomery, W. H. (2012) MWH's Water Treatment: Principles and Design. Hoboken, N.J.: Wiley.

EPCOR Utilities Inc. (2015) Waterworks Annual Quality Assurance Report – 2015. Retrieved from http://www.epcor.com/water/water-quality/reports-edmonton/Documents/wq-edmonton-quality-assurance-2015.pdf.

Granstrom M. L. (1954) Ph.D. Dissertation, Harvard University, Cambridge, MA.

Hand, V. C., and Margerum, D. W. (1983) Kinetics and Mechanisms of the Decomposition of Dichloramine in Aqueous Solution. Inorg. Chem., 22(10), 1449-1456.

Hua, G. H.; and Reckhow, D. A. (2008) DBP Formation during Chlorination and Chloramination: Effect of Reaction Time, pH, Dosage, and Temperature. J. Am. Water Works Assoc., 100, 82–92

Jafvert, C. T., and Valentine, R. L. (1987) Dichloramine Decomposition in the Presence of Excess Ammonia. Water Res., 21(8), 967-973.

Jafvert, C. T., and Valentine, R. L. (1992) Reaction Scheme for the Chlorination of Ammoniacal water. Environ. Sci. Technol., 26(3), 577-586.

Leao, S. F. (1981) Ph.D. Dissertation, University of California, Berkeley, CA.

Minear, R. A.; and Amy, G. L. (1996) Disinfection By-Products in Water Treatment The Chemistry of Their Formation and Control. CRC Press.

Mitcham, R. P., Shelley, M. W., and Wheadon, C. M. (1983) Free Chlorine versus Ammonia-Chlorine: Disinfection, Trihalomethane Formation, and Zooplankton Removal. J. Am. Water Works Assoc., 75: 196–198.

Morris, J. C., and Isaac, R. A. (1983) Critical Review of Kinetic and Thermodynamic Constants for the Aqueous Chlorine-Ammonia System. Water chlorination: environmental impact and health effects, 4.

Norman, T. S., Harms, L. L., and Looyenga, R. W. (1980) The Use of Chloramines to Prevent Trihalomethane Formation. J. Am. Chem. Soc., 72: 176–180.

Snoeyink, V. L. and Jenkins, D. (1980) Jenkins Water Chemistry. Wiley.

United States Environmental Protection Agency (USEPA). (2012b) Chloramines in Drinking Water. Available at: http://water.epa.gov/lawsregs/rulesregs/sdwa/mdbp/chloramines_index.cfm, last accessed January 16, 2015.

Valentine, R. L., and Jafvert, C. T. (1988) General Acid Catalysis of Monochloramine Disproportionation. Environ. Sci. Technol., 22(6), 691-696.

Vikesland, P. J., Ozekin, K., and Valentine, R. L. (1998) Effect of Natural Organic Matter on Monochloramine Decomposition: Pathway Elucidation through the Use of Mass and Redox Balances. Environ. Sci. Technol., 32(10), 1409-1416.

Vikesland, P. J., Ozekin, K., and Valentine, R. L. (2001) Monochloramine Decay in Model and Distribution System Waters. Water Res., 35(7), 1766-1776.

Wolfe, R. L., Ward, N. R., and Olson, B. H. (1984) Inorganic Chloramines as Drinking Water Disinfectants: a Review. J. Am. Water Works Assoc., 76(5), 74-88.

Zhou, L., Zhang, Y., and Zeng, G. (2013) Monochloramine Decay for Two Chlorine to Ammonia Ratios in Bulk Water. Water Environ. Res., 85(11), 2194-2200.

CHAPTER 5. MONOCHLORAMINE LOSS MECHANISMS AND DISSOLVED ORGANIC MATTER CHARACTERIZATION IN STORMWATER[3]

5.1. Introduction

Chloramination is widely used for drinking water secondary disinfection. Compared with free chlorine, monochloramine (NH_2Cl), the dominant species in chloramination, is less reactive and can provide a longer-lasting disinfection effect in drinking water distribution system (Brodtmann and Russo, 1979; Norman et al., 1980). However, the persistent NH_2Cl can lead to serious environmental problems through its introduction into storm sewers and thus fresh water sources. Outdoor tap water uses such as residential garden watering, lawn irrigation in parks, car washing at dealerships and industrial pressure vessel hydro-testing can all lead to the discharge of NH_2Cl into storm sewers. Our previous study showed that the total active chlorine (TAC) concentration in Edmonton municipal storm sewers varied from 0 to 0.77 mg/L under dry weather conditions during the summers of 2015 and 2016 (Zhang et al., 2018) which exceeded the Canadian Council of Ministers of the Environment guideline's recommended concentration of 0.02 mg/L in discharge effluent in most of times (Canadian Council of Ministers of the Environment, 2009). That is, once the chloraminated stormwater is discharged into fresh water sources, it may pose serious risks to the aquatic environment. To enhance the regulation of chloraminated tap water discharges, knowledge of NH_2Cl dissipation mechanisms in stormwater is important. However, although the NH_2Cl dissipation processes has been widely studied in drinking water distribution systems, little research has been undertaken to monitor NH_2Cl decay in storm sewer systems.

---

[3] A version of this chapter has been partially published: Zhang, Q., Davies, E. G., Bolton, J. R., & Liu, Y., 2018. Monochloramine loss mechanisms and dissolved organic matter characterization in stormwater. Science of The Total Environment. 631, 745-754.

In drinking water distribution systems, NH_2Cl autodecomposition as well as reactions with water chemical components are considered the major NH_2Cl dissipation pathways (Vikesland et al., 2001; Zhang et al., 2017). NH_2Cl can autodecompose by a complex set of reactions that ultimately result in the oxidation of ammonia and the reduction of active chlorine. The rates of these reactions depend on the solution pH, alkalinity and initial NH_2Cl concentrations, as well as on the ratio of chlorine to ammonia nitrogen. Further, chemical compounds existing in the water system, such as natural organic matter (NOM), nitrate (NO_2^-), ferrous ion (Fe^{2+}) and bromide (Br^-), can enhance the NH_2Cl decay rate (Duirk et al., 2005; Vikesland et al., 2001; Zhang et al., 2017). To study the NH_2Cl dissipation in a storm sewer system, these reactions should also be considered. However, since Fe^{2+} is unstable and can easily be oxidised to ferric ion (Fe^{3+}) because of the high dissolved oxygen concentration in stormwater (Zhang et al., 2018), and the concentration of Br^- is too low to be detected by Ion-exchange Chromatography, these two chemicals are not considered in our study.

The NH_2Cl autodecomposition model and the reactions with NO_2^- have been studied comprehensively by Vikesland et al. (2001) and Wahman and Speitel (2012). In terms of the reaction with DOM, the DOM from various water sources may have different compositions, and can show different characteristics when it reacts with NH_2Cl (Duirk et al., 2005). Therefore, to describe the NH_2Cl loss in stormwater, the principal objectives of this research are (i) to study the reactions between active chlorine species and stormwater DOM (SWDOM) during NH_2Cl dissipation processes and (ii) to develop a kinetic model to describe these processes under various stormwater conditions, such as pH, alkalinity, NH_4^+, NO_2^- and DOM concentrations. Also, temperature usually shows significant influence on reaction rates of chemical reactions. As stormwater commonly showed lower temperature than ground environment, the impact of temperature on stormwater NH_2Cl dissipation was also studied.[4] Further, our previous study showed that the NH_2Cl decay rate is largely governed by the DOM concentration in stormwater samples (Zhang et al., 2018). Therefore, the characteristics of DOM in stormwater samples collected under different neighborhoods (residential, parkland, commercial and industrial areas) were analyzed before and after chloramination.

The model developed in this research can be applied to simulate NH_2Cl dissipation rates under various stormwater conditions. The model results can be used as a reference to evaluate potential active chlorine contamination by outdoor tap water discharge, thus contributing to the regulation of outdoor chloraminated water uses, and ideally eliminating active chlorine contamination in stormwater. Since may other municipalities also use chloramines for drinking water disinfection, it is believed that the model built in this research can also benefit them. Although the SWDOM characteristics may vary among various areas, the methodology developed in this study should be widely applicable.

5.2. Material and methods

5.2.1. Experimental design

Stormwater samples collected under dry weather conditions were used for the NH_2Cl dissipation study, as relatively high TAC concentrations were detected under this weather condition during the summers of 2015 and 2016 (Zhang et al., 2018). However, because only limited stormwater volumes can be collected from storm sewers in dry weather, the SWDOM cannot be studied by directly extraction from stormwater samples. Therefore, a commercial NOM (Nordic Reservoir NOM, purchased from International Humic Substances Society), which has a similar Fourier transform infrared (FTIR) spectrum with Edmonton SWDOM (Fig. S5.1), was

---

[4] This sentence is not included in the published manuscript.

utilized both to study the impact of NOM on NH_2Cl dissipation, and to develop the dissipation model. A similar FTIR spectrum reflects a close chemical composition among these samples.

Laboratory DOM solutions were prepared by dissolving Nordic Reservoir NOM (NRNOM) into ultrapure water from a Barnstead™ Smart2Pure™ Water Purification System (Massachusetts, USA) to the required concentrations. NH_2Cl stock solutions were prepared with an active chlorine to nitrogen (Cl/N) molar ratio of 1.0 or 0.7 by the addition of hypochlorous acid (HOCl) and ammonium chloride (NH_4Cl) solutions into ultrapure water. HOCl and NH_4Cl standard solutions were purchased from Ricca Chemical Company (Texas, USA). 4 mM of sodium bicarbonate ($NaHCO_3$) was spiked into DOM solutions to stablize the pH. Hydrochloric acid (HCl) with a concentration of 6 M was added to adjust the pH to the required values. pH values from 7.0 to 8.5 were studied in this research since the stormwater pH was normally within this range (Zhang et al., 2018).

To conduct the NH_2Cl dissipation experiments in the presence of NRNOM, NH_2Cl stock solutions with an active Cl/N molar ratio of 0.7 were added into buffered DOM solutions to achieve certain initial NH_2Cl concentrations. Then, the solutions were transferred into 128 mL flasks wrapped with aluminum foil. NH_2Cl concentration changes were recorded at certain time intervals. The initial NH_2Cl concentrations were determined by adding the same amount of NH_2Cl stock solution into ultrapure water with the same volumes as the DOM solutions. Moreover, free chorine released from NH_2Cl autodecomposition can also react with DOM. The free chlorine and DOM reactions were studied with the same experimental procedure as for the NH_2Cl dissipation experiments by adding HOCl into buffered DOM solutions.

To study the impact of temperature on NH_2Cl dissipation, NRNOM was firstly dissolved into ultrapure water under two different DOC concentrations. After that, solutions were stored in cold rooms with temperatures of 5 °C, 10 °C and 15 °C for 30 min to achieve homogenous temperature of solutions with surrounding environment. NH_2Cl dissipation experiments were then conducted under the same procedures as described before.[5]

Field stormwater samples were collected from storm sewers in four neighborhoods to represent the major land-use types: (1) residential, for garden watering, (2) city parks, for lawn irrigation, (3) commercial, for car washing from dealerships and car rental businesses and (4) industrial, for pressure vessel hydro-testing. For each land use type, two stormwater samples from upstream and downstream manholes were collected. Detailed information on location selections is provided in the supporting information (Table S5.1). After samples were delivered to the laboratory, they were filtered through 0.45 μm filters to remove suspended particles. NH_2Cl stock solutions with an active Cl/N molar ratio of 1 were then added to achieve an initial total active chlorine (TAC) concentration of 0.05 mM (1.78 mg/L-active chlorine). After that, the pH of the stormwater samples was recorded. Since stormwater samples already had high alkalinity, no additional $NaHCO_3$ was added to buffer the samples.

The method for the determination of NRNOM and SWDOM reactive fractions was developed from Duirk et al.'s study (2005). The rapid free chlorine and NH_2Cl reactive fractions ($S_{HOClrapid}$ and $S_{NH2Clrapid}$) were determined by the rapid free chlorine and NH_2Cl demands in free chlorine and NH_2Cl decay experiments. The total free chlorine and NH_2Cl reactive fractions (S_{total}) which include rapid and long-term reactive DOM are considered to be same since NH_2Cl continuously releases HOCl by its autodecomposition, which can then react with DOM. S_{total} was determined by the reaction between excess concentrations of free chlorine and NRNOM solutions or stormwater samples. The DOM concentrations were quantified by dissolved organic carbon

---

[5] This paragraph is not included in the published manuscript.

(DOC) concentrations. With the assumption that one mole of free chlorine can consume one mole of reactive DOC (DOC_r) (Duirk et al., 2005), the concentration of DOC_r in each sample can be determined based on the total free chlorine demand when no significant changes of free chlorine were observed in the NRNOM solutions or stormwater samples. The S_{total} of NRNOM and SWDOM can be solved by determining the ratio of DOC_r to total DOC concentrations. A control group with the same initial free chlorine concentration in ultrapure water was set to eliminate the impact of free chlorine self-dissipation.

All experiments were carried out in triplicates, and all glassware was pretreated to be chlorine demand-free by soaking in concentrated HOCl solutions for 24 hours and rinsing thoroughly with ultrapure water. Except for temperature control experiments, all the other NH_2Cl and free chorine dissipation experiments were conducted in a 25℃ incubator. All HOCl and NH_2Cl dissipation experiments were completed within 48 hours to prevent a significant pH change in the solutions.

To characterize the Edmonton SWDOM before and after chloramination, fluorescence Excitation−Emission Matrix (EEM) and FTIR spectroscopy were applied. Chloraminated stormwater samples were prepared by adding 2 mM (excess) NH_2Cl into raw stormwater. Raw and chloraminated SWDOM samples were compared. The SWDOM samples were collected by freeze-drying 20 mL of 0.45 μm filtered stormwater samples. The FRI technique (Chen et al., 2003) was applied to analyze the EEM results. The $SUVA_{254}$ of stormwater samples and NRNOM solutions were also determined using Varian Cary 50 Bio UV-Visible Spectrophotometer (Palo Alto, USA).

5.2.2. Analysis methods

With Cl/N molar ratios less than 1, the total active chlorine and NH_2Cl molar concentrations were considered to be same (Crittenden et al., 2012). Therefore, the total active chlorine (TAC) concentration was measured as the NH_2Cl concentration by the HACH (Loveland, USA) colorimetric method 8167 (with a detection limit of 0.02 mg-Cl/L). The NH_4^+-N, NO_2^--N and alkalinity were analyzed using HACH commercial test kits TNT832, TNT839, and TNT870 with detection limits of 0.015 mg/L NH_3-N, 0.015 mg/L NO_2^--N and 25 mg/L $CaCO_3$, respectively. DOC was measured by a Shimadzu TOC-LCSN Standard Model (detection limit is 40 μg-C/L). Moreover, pH was analyzed by Extech EC500 Waterproof ExStikII pH/conductivity meter (Nashua, USA). FTIR spectra were obtained from the Thermo Scientific™ Nicolet™ iS™50 FT-IR Spectrometer (Waltham, UK). Freeze-drying was conducted using FreeZone 4.5 Liter -50C Benchtop Freeze Dryers (Kansas City, USA). Fluorescence EEM was tested by Cary Eclipse Fluorescence Spectrophotometer (Santa Clara, USA) and then plotted using the R program EEM package (R Development Core Team, 2008). The EEMs were recorded between excitation wavelengths (λ_{exc}) of 200 and 500 nm at a 10 nm step increment. For each excitation wavelength, the emission was collected at longer wavelengths at 0.5 steps. The photomultiplier tube voltage was 600V. The UV_{254} absorbance was analyzed by Varian Cary® 50 Bio UV-Visible Spectrophotometer (Palo Alto, USA).

5.3. Model development

5.3.1. Reaction assumptions

To describe the NH_2Cl loss processes in stormwater samples, the NH_2Cl dissipation model in the presence of NRNOM was first studied. This model consists of two parts: the NH_2Cl autodecomposition processes, and reactions with DOM. The NH_2Cl auto-decay model used in this research was proposed by Jafvert and Valentine (1992) and refined by Vikesland et al. (2001). The DOM component was developed from previous models as follows. The impact of organic components in the NH_2Cl decay processes was first modeled by Duirk et al. (2002). However, they considered only the rapid and long-term reactions between DOM and NH_2Cl, and the kinetic constants of the long-term reaction decreased with increases of NH_2Cl and ammonia concentrations. In 2005, Duirk et al. (2005) proposed that rather than NH_2Cl, free chlorine released from NH_2Cl autodecomposition is involved in the long-term DOM reaction. Based on the model developed by Duirk et al. (2005), Zhu and Zhang (2016) suggested that both NH_2Cl and free chlorine species should be considered to have rapid and slow reactions with DOM in NH_2Cl dissipation. This assumption is also used and verified in this study. Therefore, four pathways were applied in our model: (I) the DOM rapid reaction with free chlorine; (II) the DOM long-term reaction with free chlorine; (III) the DOM rapid reaction with NH_2Cl; and (IV) the DOM long-term reaction with NH_2Cl. For each pathway, the reaction equation and the reaction rate mechanistic equation are shown below:

Pathway (I): $\mathrm{HOCl} + \mathrm{DOC}_{\mathrm{HOClrapid}} \xrightarrow{k_{\mathrm{doc1}}} \mathrm{Products.}$ (5.1)

$$[\mathrm{DOC}_{\mathrm{HOClrapid}}] = \mathrm{S}_{\mathrm{HOClrapid}}\,[\mathrm{total\ DOC}] \tag{5.2}$$

$$\frac{\mathrm{d[HOCl]}}{\mathrm{dt}} = -k_{\mathrm{doc1}}[\mathrm{HOCl}][\mathrm{DOC}_{\mathrm{HOClrapid}}] \tag{5.3}$$

Pathway (II): $\mathrm{HOCl} + \mathrm{DOC}_{\mathrm{HOCllongterm}} \xrightarrow{k_{\mathrm{doc2}}} \mathrm{Products.}$ (5.4)

$$[\mathrm{DOC}_{\mathrm{HOCllongterm}}] = (\mathrm{S}_{\mathrm{total}} - \mathrm{S}_{\mathrm{HOClrapid}})\,[\mathrm{total\ DOC}] \tag{5.5}$$

$$\frac{\mathrm{d[HOCl]}}{\mathrm{dt}} = -k_{\mathrm{doc2}}[\mathrm{HOCl}][\mathrm{DOC}_{\mathrm{HOCllongterm}}] \tag{5.6}$$

Pathway (III): $\mathrm{NH_2Cl} + \mathrm{DOC}_{\mathrm{NH2Clrapid}} \xrightarrow{k_{\mathrm{doc3}}} \mathrm{Products.}$ (5.7)

$$[\mathrm{DOC}_{\mathrm{NH2Clrapid}}] = \mathrm{S}_{\mathrm{NH2Clrapid}}\,[\mathrm{total\ DOC}] \tag{5.8}$$

$$\frac{d[NH_2Cl]}{dt} = -k_{doc3}[NH_2Cl][DOC_{NH2Clrapid}] \quad (5.9)$$

Pathway (IV): $NH_2Cl + DOC_{NH2Cllongterm} \xrightarrow{k_{doc4}} Products.$ (5.10)

$$[DOC_{NH2Cllongterm}] = (S_{total} - S_{NH2Clrapid}) [total\ DOC] \quad (5.11)$$

$$\frac{d[NH_2Cl]}{dt} = -k_{doc2}[NH_2Cl][DOC_{NH2Cllongterm}] \quad (5.12)$$

Further, our previous study showed that the NO_2^--N concentration varied from 0.015 to 0.745 mg/L in Edmonton stormwater during the summers of 2015 and 2016 (Zhang et al., 2018). Since NO_2^- can consume NH_2Cl, the reactions between NO_2^- and NH_2Cl should also be considered to predict the NH_2Cl loss rate in real stormwater. The NO_2^- – NH_2Cl reaction equations, which were studied by Margerum et al. (1994) and developed by Vikesland et al. (2001) and Wahman and Speitel (2012), were applied in this research. All the reactions involved in the stormwater NH_2Cl dissipation in are shown in Fig. 5.1 and Table 5.1.

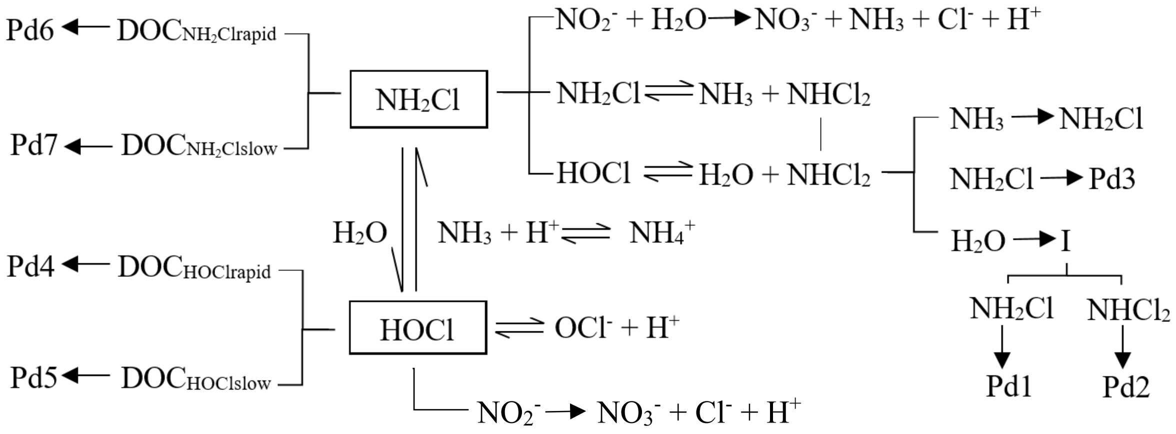

Fig. 5.1. The reactions involving in NH_2Cl dissipation in stormwater (Pd: products)

Table 5.1. NH_2Cl loss reactions in stormwater developed by Jafvert and Valentine (1992), Margerum et al. (1994), Vikesland et al. (2001), Duirk et al. (2005), Wahman and Speitel (2012), Zhu and Zhang (2016) and the present work

	Reaction	Rate Coefficient or Equilibrium Constant	References
1	$HOCl + NH_3 \rightarrow NH_2Cl + H_2O$	$k_1 = 1.5 \times 10^{10} \mathrm{M^{-1}h^{-1}}$	Morris and Isaac, 1981
2	$NH_2Cl + H_2O \rightarrow HOCl + NH_3$	$k_2 = 7.6 \times 10^{-2} \mathrm{h^{-1}}$	Morris and Isaac, 1981
3	$HOCl + NH_2Cl \rightarrow NHCl_2 + H_2O$	$k_3 = 1.3 \times 10^{6} \mathrm{M^{-1}h^{-1}}$	Morris and Isaac, 1981
4	$NH_2Cl + H_2O \rightarrow HOCl + NH_2Cl$	$k_4 = 2.7 \times 10^{-3} \mathrm{h^{-1}}$	Morris and Isaac, 1981
5	$2NH_2Cl \rightarrow NHCl_2 + NH_3$	$k_5{}^{a}$	Jafvert and Valentine, 1992
6	$NHCl_2 + NH_3 \rightarrow 2NH_2Cl$	$k_6 = 2.2 \times 10^{8} \mathrm{M^{-2}h^{-1}}$	Hand and Margerum, 1983
7	$NHCl_2 + H_2O \rightarrow I$	$k_7 = 4.0 \times 10^{5} \mathrm{M^{-1}h^{-1}}$	Jafvert and Valentine, 1987
8	$NHCl_2 + I^{b} \rightarrow HOCl + pd1^{c}$	$k_8 = 1.0 \times 10^{8} \mathrm{M^{-1}h^{-1}}$	Leao, 1981
9	$NH_2Cl + I \rightarrow pd2^{c}$	$k_9 = 3.0 \times 10^{7} \mathrm{M^{-1}h^{-1}}$	Leao, 1981
10	$NH_2Cl + NHCl_2 \rightarrow pd3^{c}$	$k_{10} = 5.5 \mathrm{M^{-1}h^{-1}}$	Leao, 1981
11	$HOCl + NO_2^{-} \rightarrow H^{+} + NO_3^{-} + Cl^{-}$	$k_{11}{}^{d}$	Margerum et al., 1994
12	$NH_2Cl + NO_2^{-} + H_2O \rightarrow NH_4^{+} + NO_3^{-} + Cl^{-} + H^{+}$	$k_{12}{}^{e}$	Wahman and Speitel, 2012
13	$HOCl + DOC_{HOClrapid} \rightarrow pd4^{f}$	$k_{13} = 2.3 \times 10^{6} \mathrm{M^{-1}h^{-1}}$	Present work
14	$HOCl + DOC_{HOClslow} \rightarrow pd5^{f}$	$k_{14} = 3.9 \times 10^{2} \mathrm{M^{-1}h^{-1}}$	Present work
15	$NH_2Cl + DOC_{NH2Clrapid} \rightarrow pd6^{g}$	$k_{15} = 3.4 \times 10^{4} \mathrm{M^{-1}h^{-1}}$	Present work
16	$NH_2Cl + DOC_{NH2Clslow} \rightarrow pd7^{g}$	$k_{16} = 15.9 \mathrm{M^{-1}h^{-1}}$	Present work
17	$HOCl = H^{+} + OCl^{-}$	$\mathrm{pK}_a = 7.5$	Snoeyink and Jenkins, 1980
18	$NH_4^{+} = NH_3 + H^{+}$	$\mathrm{pK}_a = 9.3$	Snoeyink and Jenkins, 1980
19	$H_2CO_3 = HCO_3^{-} + H^{+}$	$\mathrm{pK}_a = 6.4$	Snoeyink and Jenkins, 1980
20	$HCO_3^{-} = CO_3^{2-} + H^{+}$	$\mathrm{pK}_a = 10.3$	Snoeyink and Jenkins, 1980

a $k_5 = k_{\mathrm{H}}[\mathrm{H^+}] + k_{\mathrm{HCO_3}}[\mathrm{HCO_3}^-] + k_{\mathrm{H_2CO3}}[\mathrm{H_2CO_3}]$, where $k_{\mathrm{H^+}} = 2.5 \times 10^7 M^{-2}h^{-1}$,$k_{\mathrm{HCO_3}} = 800 M^{-2}h^{-1}$, $k_{\mathrm{H_2CO3}} = 4 \times 10^4 M^{-2}h^{-1}$.

b I represents an unidentified intermediate in NH_2Cl auto-decomposition.

c pd1-pd3 (pd means product) may include N_2, H_2O,Cl^-,H^+, NO_3^- and other unidentified products (Jafvert and Valentine, 1992).

d $k_{11} = \frac{k_{1\mathrm{n}}[\mathrm{H^+}](1+\frac{k_{2\mathrm{n}}}{K_{4\mathrm{n}}}[\mathrm{NO_2}^-])}{\frac{k_{-1\mathrm{n}}}{k_{4\mathrm{n}}}[\mathrm{NH_3}]+(1+\frac{k_{2\mathrm{n}}}{K_{4\mathrm{n}}}[\mathrm{NO_2}^-])}$, where $k_{1\mathrm{n}} = 1.6 \times 10^8 M^{-2}h^{-1}$,$\frac{k_{-1\mathrm{n}}}{k_{4\mathrm{n}}} = 1.9 \times 10^6 M^{-1}$,$\frac{k_{2\mathrm{n}}}{K_{4\mathrm{n}}} = 217 M^{-1}$.

e $k_{12} = \frac{k_{1\mathrm{n}'}[\mathrm{H}^+](1+\frac{k_{2\mathrm{n}}}{K_{4\mathrm{n}}}[\mathrm{NO_2}^-])}{\frac{k_{-1\mathrm{n}'}}{K_{4\mathrm{n}}}[\mathrm{NH_3}]+(1+\frac{k_{2\mathrm{n}}}{K_{4\mathrm{n}}}[\mathrm{NO_2}^-])}$, where $k_{1\mathrm{n}'} = k_{\mathrm{Hn}}[\mathrm{H}^+] + k_{\mathrm{HCO_3}n}[\mathrm{HCO_3}^-] + k_{\mathrm{H_2CO3n}}[\mathrm{H_2CO_3}],\ k_{\mathrm{Hn}} =$

$4.3 \times 10^{10} M^{-2} h^{-1}, k_{\mathrm{HCO_3}n} = 4.3 \times 10^{3} M^{-2} h^{-1},\ k_{\mathrm{H_2CO_3}n} = 3.4 \times 10^{6} M^{-2} h^{-1},\ k_{-1\mathrm{n}'}/k_{4\mathrm{n}} =$

$2.1 \times 10^{-5} Mh \times k_{1n'}$.

f pd4-5, pd8 may include H_2O, Cl^-, H^+ and chlorine disinfection by-products (DPBs).

g pd6-7, pd 9-10 may include NH_4^+, H_2O, Cl^-, H^+ and NH_2Cl DPBs.

Lower temperature was commonly detected in Edmonton stormwater (Zhang et al., 2018). As lower temperature can lead to the decrease of NH_2Cl dissipation, to describe the NH_2Cl dissipation under different temperatures, the temperature coefficient α was introduced in to the model. Under each temperature, a specific α can be solved based on by adding temperature controlled experimental data to the model developed under 25 °C (Table 5.1). And then, the relationship between α and temperature can be solved.[6]

5.3.2. Parameter estimation

All the DOM reaction rate constants were solved with the NH_2Cl dissipation model (Table 5.1) to compensate for the experimental NH_2Cl loss data in NRNOM solution under various initial conditions. These values were estimated by COMSOL Multiphysics (Stockholm, Sweden) with the Levenberg–Marquardt algorithm, which is commonly applied to solve non-linear least squares problems in computer programs (Gavin, 2017). The average rate constants solved under various conditions were used in the model to estimate the modeling NH_2Cl dissipation rates and to compare with experimental results. Specifically, the rapid and long-term reaction rate constants between HOCl and DOC (k_{doc1} and k_{doc2}) were first estimated by free chlorine decay experiments for various pH values. The k_{doc3} and k_{doc4} were then solved by the NH_2Cl decay experiments.

---

[6] This paragraph is not included in the published paper.

5.4. Results and discussion

5.4.1. Impacts of NRNOM on NH_2Cl decay in stormwater

In laboratory experiments, the NH_2Cl decay rates with the presence of NRNOM were studied under various pH, initial NH_2Cl and DOC concentrations, and the results are shown in Fig. 5.2. The free chlorine decay process in the presence of NRNOM was studied first (Figure 5.2(a)).

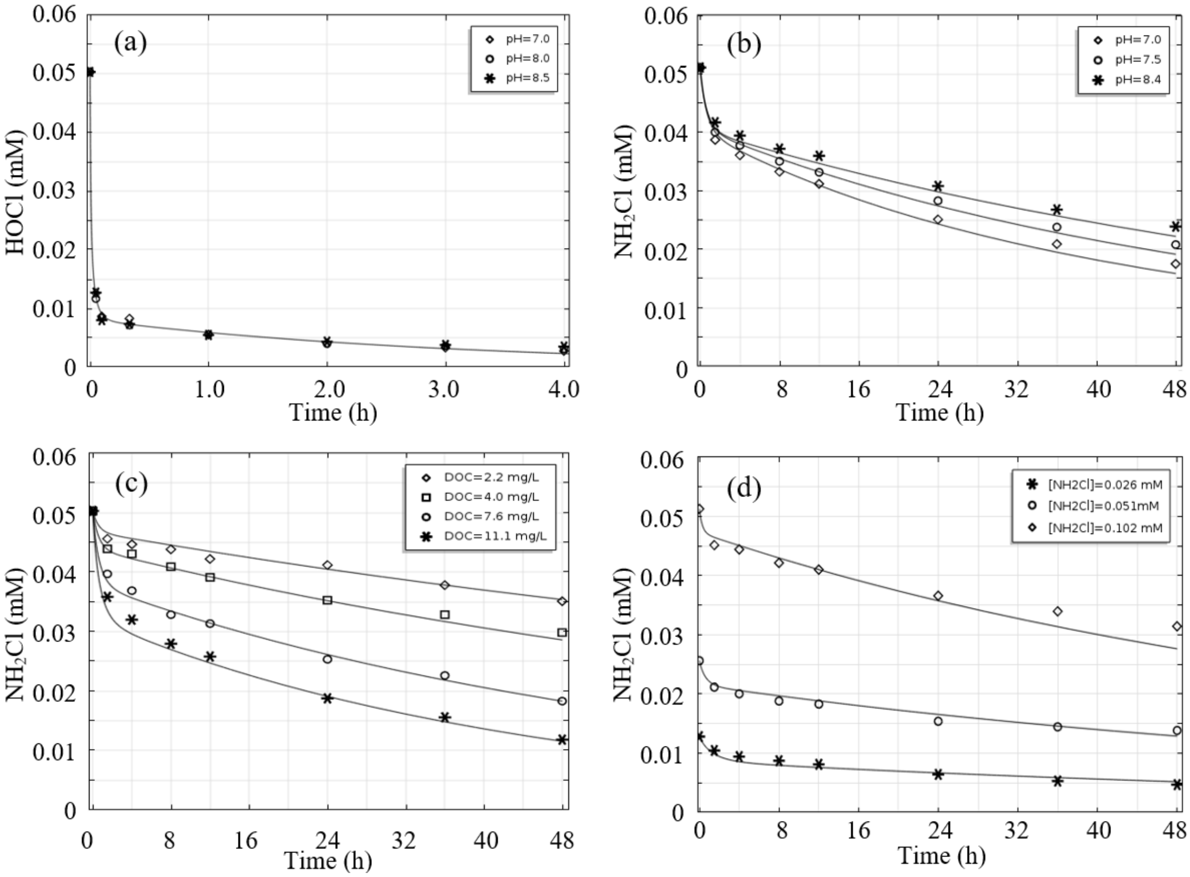

Fig. 5.2. The HOCl and NH_2Cl loss under various conditions (lines: model results), $NaHCO_3$ = 4 mM, T = 25 ºC, (a) [DOC] = 7.4 mg-C/L; (b) [DOC] = 6.4 mg-C/L, Cl/N = 0.7 mol/mol; (c) pH = 8.0, Cl/N = 0.7 mol/mol; (d) [DOC] =5.1 mg-C/L, pH = 8.0, Cl/N = 0.7 mol/mol

As can be seen, with the same initial free chlorine concentration, no significant difference in the dissipation rates can be observed under various pH values. Therefore, it is believed that the impact of pH on free chlorine dissipation can be omitted. The NH_2Cl decay rate increased with a lower pH, higher DOC and initial NH_2Cl concentrations. Specifically, reaction 5 in Table 5.1 (2 $NH_2Cl \rightarrow NHCl_2 + NH_3$) is the dominant reaction in NH_2Cl autodecomposition. This reaction rate can be accelerated with lower pH, which results in the increase of NH_2Cl decay rate in Fig. 5.2(b) (Jafvert and Valentine, 1987; Vikesland et al., 2001; Zhang et al., 2017). Further, according to equations (5.3), (5.6), (5.9) and (5.12), the reaction rates between active chlorine (free chorine and NH_2Cl) and DOM can be increased by higher initial free chlorine, NH_2Cl and DOM concentrations, thus the consequence of higher NH_2Cl dissipation rates (Fig. 5.2 (c), (d)). Further, with a higher initial NH_2Cl concentration, more HOCl was released from NH_2Cl autodecomposition, which also enhanced the NH_2Cl dissipate rates as shown in Fig. 5.2 (d).

The values of NRNOM reactive fractions $S_{HOClrapid}$, $S_{NH2Clrapid}$ and S_{total} were solved based on the measured free chlorine and NH_2Cl rapid and total demands in laboratory experiments, and are shown in Table S5.2. Further, the rate constants ($k_{\mathrm{doc1}}, k_{\mathrm{doc2}}, k_{\mathrm{doc3}}, k_{\mathrm{doc4}}$) were solved based on the laboratory free chlorine and NH_2Cl loss experiments, and the resulting values are shown in Table 5.1. To validate the model, the modeled free chlorine and NH_2Cl loss rates were predicted by COMSOL Multiphysics under the same initial conditions as laboratory experiments, and the results were compared (Fig. 5.2).

Fig. 5.2 shows that the simulated curves correspond closely to the experimental results, which means this model can be applied for NH_2Cl dissipation rates estimation in the presence of NRNOM under various pH values, initial DOC and NH_2Cl concentrations. Fig. 5.2 (a) shows the free chlorine decay process in the presence of NRNOM, and it reflects the two stage reactions between free chlorine and NRNOM. Specifically, the free chlorine showed a rapid decay during the first few minutes, and the decay rate then decreased significantly thereafter. This phenomenon validates the assumptions that both rapid and long-term reactions should be applied between free chlorine and DOM. The NH_2Cl also showed a two-step decay process, which consists of the rapid NH_2Cl demand in the first few hours and the slow decay thereafter (Fig. 5.2 (b) (c) (d)). These two-step processes also match our modeling assumptions.

5.4.2. Impact of temperature on NH_2Cl dissipation[7]

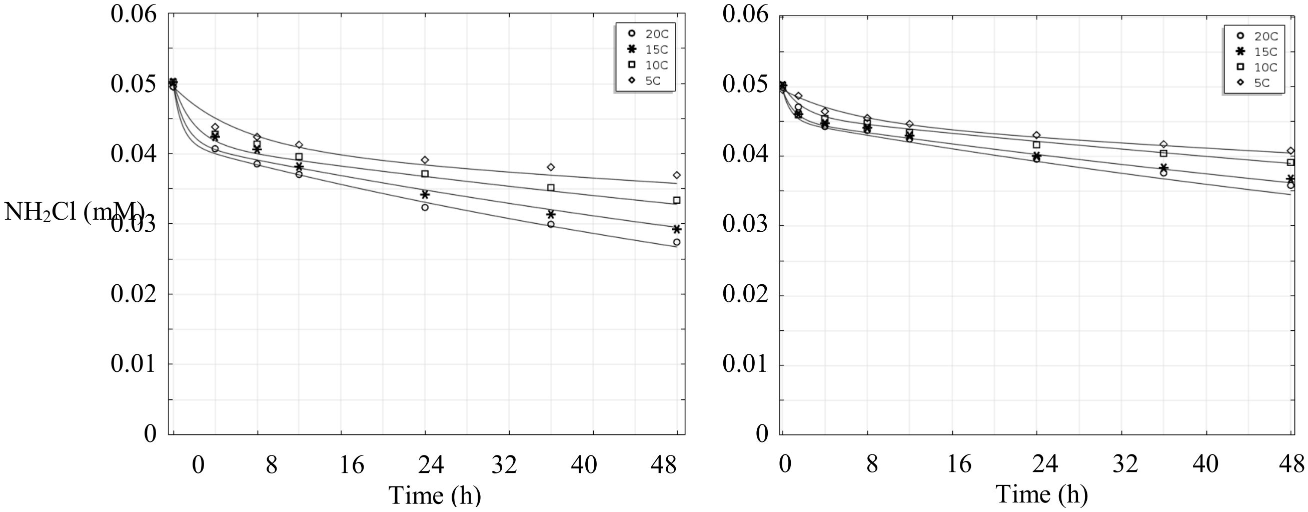

Fig. 5.3. The NH_2Cl loss under various temperatures (lines: model results), $NaHCO_3$ = 4 mM, T = 25 ºC, Cl/N = 0.7 mol/mol, pH = 8.0, (a) [DOC] = 5.4 mg-C/L; (b) [DOC] = 2.9 mg-C/L

Fig. 5.3 shows the impact of temperature on NH_2Cl dissipation with the present of NRDOM. As can be seen, under the same DOC concentrations, with the decrease of temperature, the NH_2Cl dissipation rate decreased. To model the NH_2Cl dissipation under lower temperatures, the relationship between temperature and the temperature coefficient α were solved and represented by the following equation ($R^2 > 0.99$):

$$\alpha_T = 22 \times T + 2.99 \tag{5.13}$$

Where T is temperature (°C).

---

[7] This section is not included in the published manuscript.

Under this equation, for each temperature, a specific α can be solved. The NH_2Cl dissipation rate under various temperature can be then modeled by using α to calibrate the NH_2Cl dissipation curves simulated 25 °C. From Fig. 5.3, good matches between model and experimental results are shown under all the temperatures. Therefore, it is believed that with the calibration by the temperature coefficient equation, the model can be applied for the simulation of NH_2Cl decay with the present of NOM under various temperatures. Note that the temperature coefficient equation introduced here does not present the real reaction mechanisms of temperature impact on NH_2Cl dissipation, but it does meet the purpose of this research to predict the NH_2Cl loss with the present of NOM under different temperatures.

5.4.3. Impact of stormwater SWDOM on NH_2Cl dissipation

To simulate the NH_2Cl dissipation in real stormwater, stormwater samples were collected in both the upstream and downstream of residential, park, commercial and industrial neighborhoods in Edmonton. Before experiments were conducted, the pH, alkalinity, initial concentrations of NH_4^+-N, DOC, NO_2^--N, and the UV254 absorbance were recorded (Table S3). As described above, similar FTIR spectra of the 8 SWDOM samples and NRNOM indicate the similar chemical components that may present in these samples. That is, the SWDOM and NRNOM may show similar chemical properties in the reactions with NH_2Cl. Therefore, the model built for NH_2Cl dissipation in the presence of NRNOM may also work for the stormwater samples. Under this assumption, the model built in Table 5.1 was also applied for stormwater NH_2Cl loss study. The S_{total}, $S_{HOClrapid}$ and $S_{NH2Clrapid}$ of SWDOM were determined using the same method as with NRNOM, and the values are shown in Table S5.2. The modeled and experimental NH_2Cl dissipation results in stormwater samples are shown in Fig. 5.4.

Although the modeled curves in Fig. 5.4 do not fit the experimental values as closely as was observed in NRNOM solutions, the model still gave comparably reliable results to estimate the NH_2Cl loss rate in real stormwater, especially for residential and industrial areas. However, since the SWDOM consists of various natural sources, the chemical characteristics of SWDOM from different locations also varied, which lead to the slight difference between the modeled and experimental results in the different samples. Therefore, for a better understanding of the reaction mechanisms between SWDOM and NH_2Cl, the SWDOM compositions in different neighborhoods were studied.

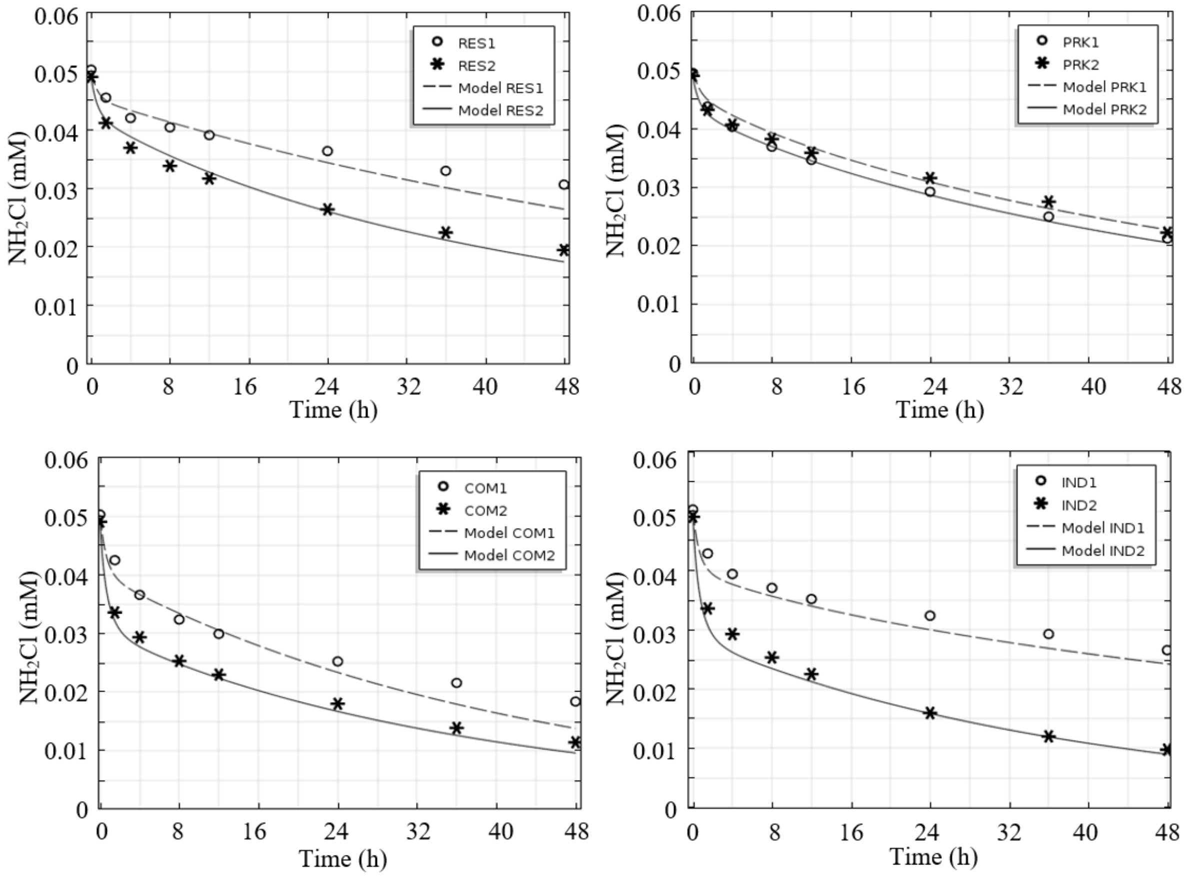

Fig. 5.4. The NH_2Cl dissipation in stormwater samples collected from (a) residential, (b) park, (c) commercial, and (d) industrial upstream and downstream locations

5.4.4. Stormwater DOM analysis

The FTIR spectra of SWDOM collected from the downstream sampling location in each neighborhood before and after chloramination are presented in Fig. 5.5, and the values of the major peaks are labeled on each figure. Each peak represents a set of functional groups. The potential functional groups of these peaks are shown in Table 5.2.

Table 5.2. The summary of potential functional groups in SWDOM

Peak No.	Peak position (cm^{-1})	Potential functional groups	Reference
1	997	C-O (ether); C-H (alkene)	Nakanishi and Solomon, 1977
2	1097-1101	C-O (aliphatic and ring ether; alcohol); C_6H_5- (phenyl); C-N (amine); C=O (carbonyl)	Nakanishi and Solomon, 1977
3	1413-1424	COO^-; O-H (carboxylic acid); C-O (phenolic group)	Chen et al., 2002
4	1532	COO^-	Guan et al., 2006
5	1620-1640	C=C (aromatic); C=O (conjugated carbonyl); H_2O (water of crystallization)	Chen et al., 2002; Nakanishi and Solomon, 1977
6	3374-3407	N-H (amine, amide); O-H (alcohol; phenol)	Nakanishi and Solomon, 1977
7	3544	O-H (alcohol; phenol)	Nakanishi and Solomon, 1977

Based on Figure 5.5, it is assumed that the stormwater from various neighborhoods consists of similar functional groups because of the similar peaks present. Specifically, peak 1 (wavenumber: 997 cm^{-1}) represents the potential presence of a carbon oxygen bond (C-O) in an ether and the carbon hydrogen bond (C-H) in an alkene. The etheric C-O can be produced during chlorination (Morris et al., 1980), and the olefinic C-H can be consumed by the oxidation of carbon-carbon double bond (C=C) and the substitution of –H by –Cl during chloramination, which leads to the variation of peak 1 after chloramination. Peak 2 (wavenumber: 1097-1101 cm^{-1}) indicates the potential existence of etheric and alcoholic C-O, phenyl and amic carbon-nitrogen

(C-N) bounds and carbonyl carbon oxygen double bond (C=O) in SWDOM. As compared to other bonds, the C-N polarity can result in a high intensity in FTIR spectra (Nakanishi and Solomon, 1977), which suggests a cause for the strong peak 2. After chloramination, peak 2 slightly increased in residential, park and industrial samples; this may be caused by the generation of C-N bonds from NH_2Cl reactions. However, this peak decreased in commercial area samples after chloramination, a result that suggests that a relatively higher percentage of phenyl and carbonylic C=O existed in this sample, as they can be finally consumed in the presence of active chlorine species (Bond et al., 2012; Morris et al., 1980; Yang et al., 2008). Peak 3 (wavenumber: 1413-1424 cm^{-1}) showed the most significant changes after chloramination in all four locations. This peak represents three functional groups: the carboxylate group (COO^{-}) and oxygen-hydrogen bond (O-H) from carboxylic acid, and the C-O from phenolic group. Since this peak almost disappeared after the NH_2Cl reaction, these functional groups are suggested to be consumed by active chlorine species during chloramination (Bond et al., 2012). However, because of the weak oxidizing ability of NH_2Cl, these functional groups do not directly react with NH_2Cl, which means they are more likely to be oxidized by free chlorine species released from NH_2Cl self-decomposition (Larson and Weber, 1994; Morris et al., 1980). This also verifies the assumption that both NH_2Cl and free chlorine are involved in the reactions with DOM in stormwater. Likewise, the peak 4 (wavenumber: 1532 cm^{-1}) in the park area disappeared for the same reason. The next peak (peak 5, wavenumber: 1620-1640 cm^{-1}) is considered to contain aromatic C=C, carbonylic C=O and water of crystallization. Both aromatic C=C and carbonylic C=O are relatively reactive with active chlorine species (Bond et al., 2012; Larson and Weber, 1994; Morris et al., 1980). Since peak 5 does not show significant decrease after chloramination in these samples, it can be concluded that the water of crystallization is more likely contributors to this peak. Peaks 6 (wavenumber: 3374-3407 cm^{-1}) and 7 (wavenumber: 3544 cm^{-1}) increased after chloramination, which means that N-H from amine, amide and O-H from alcohol and/or phenol may have been generated. The O-H and N-H can be produced by the free chlorine reactions with C=O and NH_2Cl reactions with some NOM respectively (Yang et al., 2008). In conclusion, COO^-, carboxylic O-H, phenyl and phenolic C-O are considered to be the functional groups consumed by active chlorine species in SWDOM, and both NH_2Cl and free chlorine released from NH_2Cl are involved in the reactions with SWDOM.

Florescence EEM is another technique that can contribute to an understanding of DOM composition. Fig. 5.6 shows the EEM spectra of the SWDOM samples before and after chloramination. The EEM spectra are commonly divided into five regions (Region I to V), which were defined based on Sen-Kavurmaci et al. (2016) and Chen et al. (2003). The fluorophore group represented by each region and the relevant boundaries are shown in Table 5.3.

Table 5.3. Fluorophore groups and the regional boundaries of EEM fluorescence

	Region I	**Region II**	**Region III**	**Region IV**	**Region V**
fluorophore group	Aromatic proteins I	Aromatic proteins II	Fulvic-like	Microbial byproducts	Humic-like
Boundary (nm)	λ_{exc} 200~250 λ_{emis} 200~330	λ_{exc} 200~250 λ_{emis} 330~380	λ_{exc} 200~250 λ_{emis} 380~600	λ_{exc} 250~500 λ_{emis} 200~380	λ_{exc} 250~500 λ_{emis} 380~600

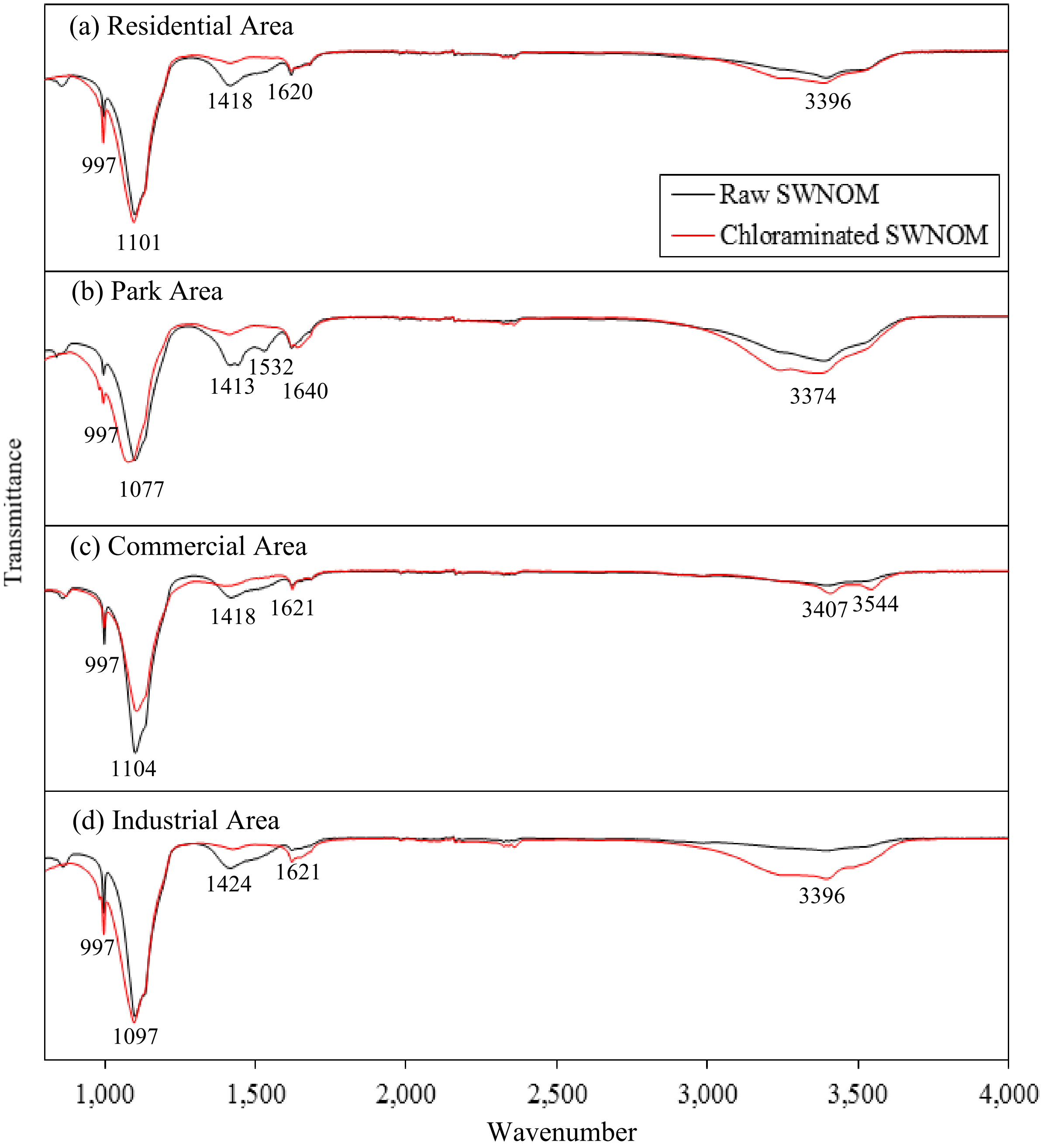

Fig. 5.5. The FTIR spectra and the peak values of downstream stormwater samples collected from (a) residential; (b) park; (c) commercial; (d) industrial areas

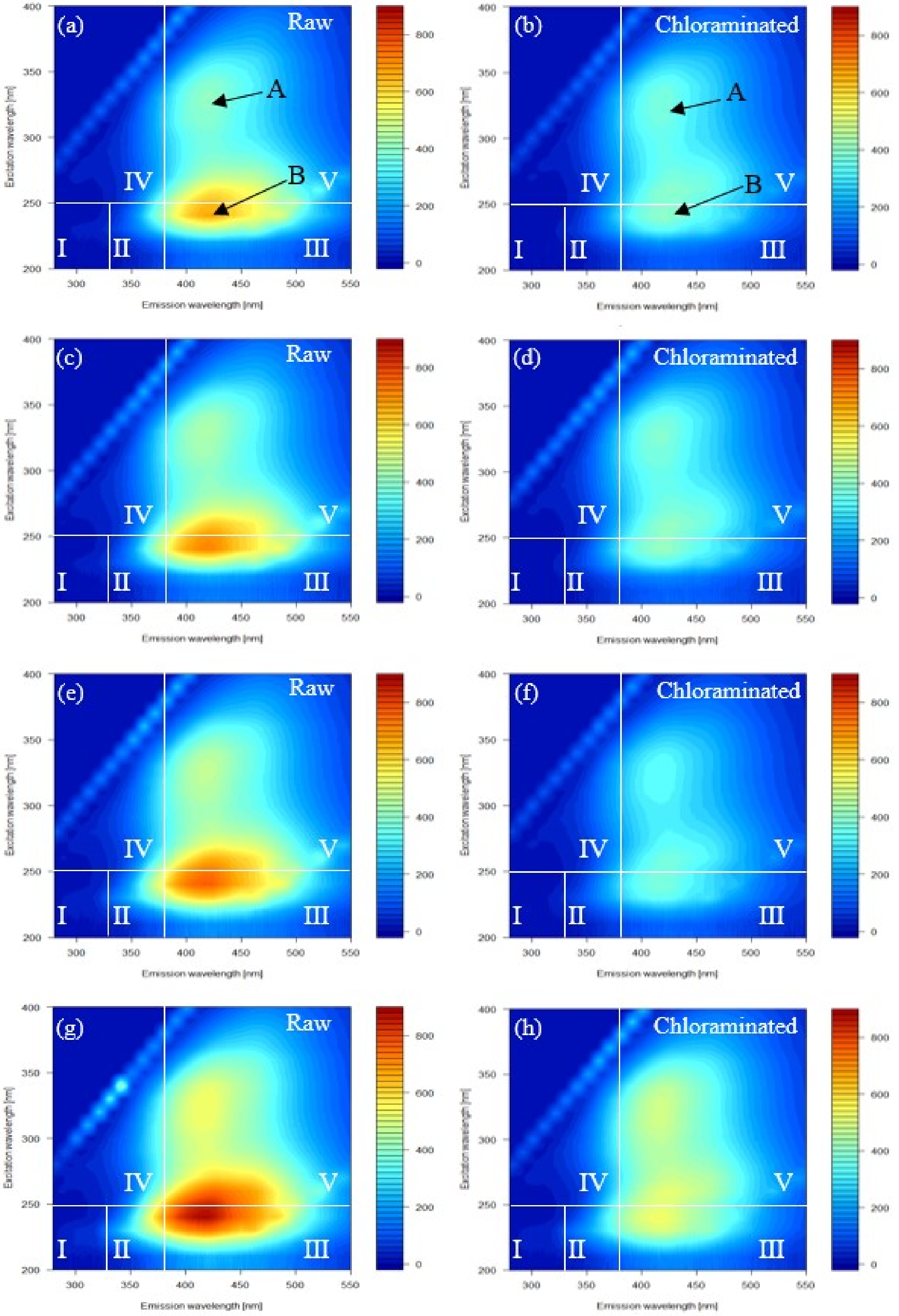
(a)
Raw
A
B
I
II
III
IV
V
(b)
Chloraminated
(c)
(d)
(e)
(f)
(g)
(h)
Excitation wavelength [nm]
Emission wavelength [nm]
200
250
300
350
400
450
500
550
0
200
400
600
800

Fig. 5.6. EEMs for SWDOM collected from (a) (b) residential, (c) (d) park, (e) (f) commercial, and (g) (h) industrial downstream locations before and after chloramination

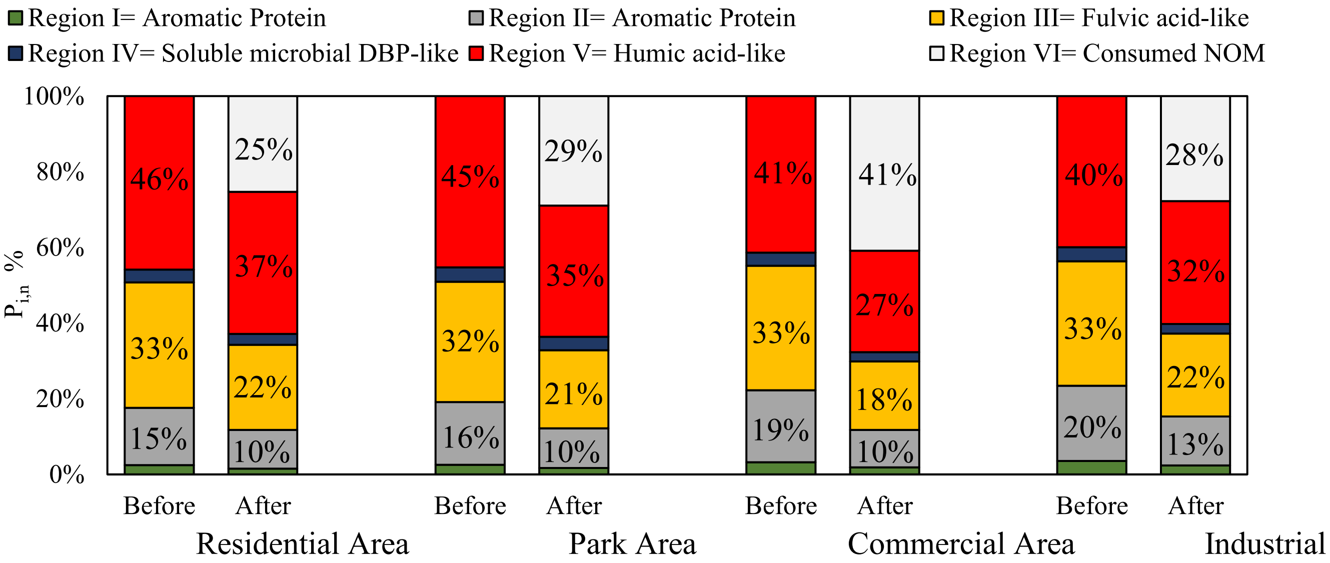

Fig. 5.7. Distribution of FRI in SWDOM samples before and after chloramination

Fig. 5.6 shows that the raw stormwater samples collected from various locations have similar EEMs, which corresponds to the FTIR results. Region III and V account for the largest ratio of SWDOM. Also, the two peaks (labelled as A and B in Fig. 5.6) are located in these two regions in all the figures, from which one can deduce that humic- and fulvic-like materials are the dominant species in SWDOM. Besides, the weak intensities of regions I, II and IV indicates low bacterial activity in the stormwater. After excess NH_2Cl was added, the EEM intensities of the four stormwater samples decreased significantly, especially in regions III and V. That is, the NH_2Cl as the major reactant with the humic substances in SWDOM, was able to convert a part of DOM to inorganic components.

Fig. 5.7 shows similar results to those observed in Fig. 5.6, which indicates that humic and fulvic acid-like substances are the dominant components of SWDOM fluorophore. Further, region II consists of comparably large percentages (15% to 20%) in raw SWDOM samples. However, as shown in Fig. 5.6, rather than aromatic protein, it is more likely to be caused by the impact of a shoulder from peak B. Moreover, after chloramination, 25% to 41% of SWDOM fluorophores were consumed, which means that instead of organic disinfection by-products, some organics in the raw stormwater samples were able to convert to inorganics during chloramination processes. More fulvic acid-like substances (region III) were transformed to inorganic components than humic acid-like substances (region V), which suggests that fulvic acid-like substances are more reactive with active chlorine species in stormwater samples. As fulvic acids (FAs) commonly contain more acidic functional groups, especially COOH, combined the results from FTIR spectra, the higher assumption of fulvic acid-like substances in SWDOM may be caused by the additional COOH from FAs. Further, more organic fluorophores were consumed in the commercial area samples as compared to other locations. With the FTIR results in Fig. 5.5, a significant decrease of peak 2, shown only in commercial stormwater samples, indicates the possible consumption of C=O bonds. Therefore, it is assumed that the higher organic consumption in the park area samples may arise from the additional C=O bonds existing in this area's stormwater humic substances. Although the FTIR and EEM results illustrate that commercial SWDOM may be slightly different from other locations, this difference does not impact the simulation of NH_2Cl dissipation in various stormwater samples.

Moreover, humic substances are the dominant precursors of disinfection DBPs during chloramination (Chen and Valentine, 2007; Wu et al., 2003), and based on EEM results, SWDOM mainly consists of humic substances. Also, the FTIR spectra show that nitrogen can be substituted into organics after SWDOM reacted with NH_2Cl. Therefore, in addition to NH_2Cl contamination, with the discharge of NH_2Cl containing tap water into storm sewers, the disinfection DBPs produced during chloramination in stormwater should also raise attention and the need for further studies.

5.5. Conclusions

NH_2Cl as the dominant active chlorine species in tap water can be introduced into storm sewers through outdoor potable water uses and can cause further contamination of fresh water sources. To enhance the regulation of chloraminated tap water discharge into storm sewers, the NH_2Cl loss mechanisms in stormwater were studied, and a kinetic model was developed to predict this decay process under various stormwater conditions, including pH, alkalinity, NH_4^+, NO_2^- and DOM concentrations. In this model, the fast and long-term reactions between SWDOM and active chlorine species were incorporated, and the reaction rate constants were solved. To simulate the NH_2Cl decay under different temperatures, a temperature coefficient α was introduced into the model. Based on experimental data, a linear functional equation between temperature and α was solved.[8] Our modeled NH_2Cl decay rates can correspond closely to experimental results under all the experimental conditions.

Further, to have a better understanding of the SWDOM and active chlorine reactions, the SWDOM collected from residential, parkland, commercial and industrial neighborhood sites were characterised by FTIR and fluorescence EEM techniques. The results showed that the SWDOM from different locations had similar compositions, and humic substances were the dominant component in all the SWDOM. After reaction with NH_2Cl, 25% to 41% of SWDOM fluorophores converted to inorganic components, while most of organics remained as organic forms. It should be noted that humic substances, as the major precursors of disinfection DBPs, may cause an increase in DBP concentration in stormwater and then lead to contamination of fresh water sources.

---

[8] These two sentences are not included in the published manuscript.

Finally, although SWDOM characteristics may vary among various cities, the methodology developed for stormwater NH_2Cl dissipation prediction and the SWDOM characteristic analysis in this research can all be applied for other areas. This research contributes to an understanding of NH_2Cl loss mechanisms in storm sewers, thus aiding the regulation of outdoor tap water discharge and the evaluation of NH_2Cl contamination in stormwater.

5.6. Supplementary Material

5.6.1. FTIR spectra for different SWDOMs and NRNOM

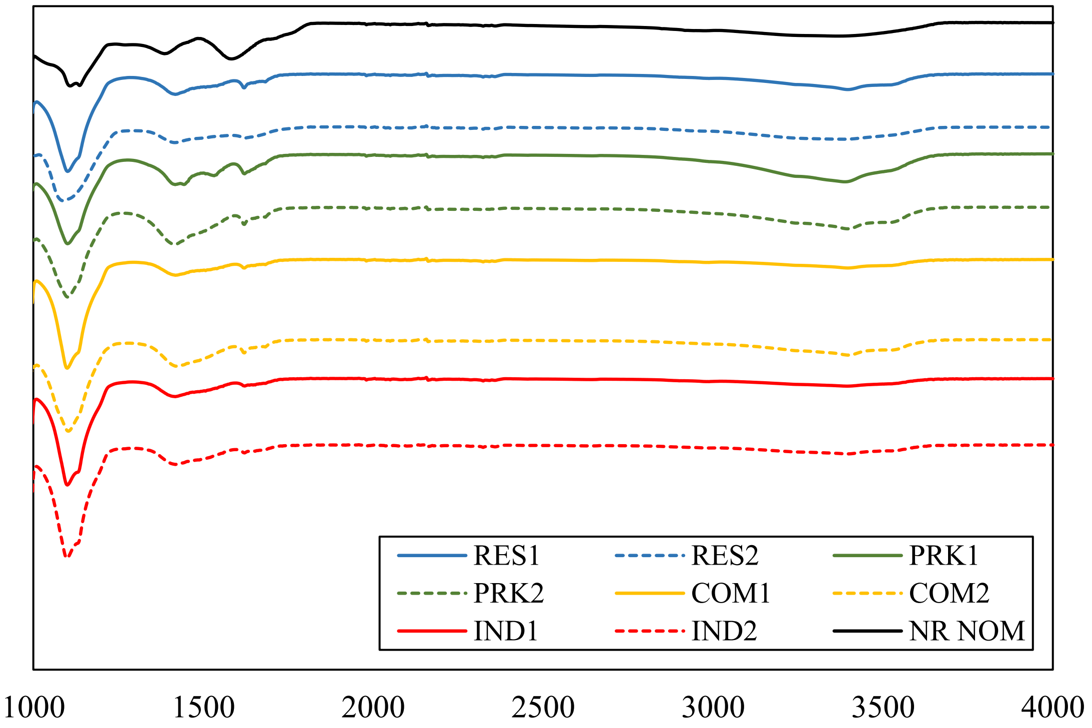

Fig. S5.1. FTIR spectra collected from NRNOM, upstream and downstream residential (RES1, RES2), park (PRK1, PRK2), commercial (COM1, COM2), and industrial (IND1, IND2) neighborhoods

5.6.2. Sampling location selection

Table S5.1. Description of sampling locations

Sampling location	Description
Residential area	Low-density neighborhoods with higher property values for their relatively large lawn and garden areas;
Park area	Tap water irrigated park with irrigation data available;
Commercial area	commercial car washes, dealerships and car rental agencies clustered;
Industrial area	The production of large pressure vessels.

For each neighborhood, stormwater samples were collected from two stormsewer manholes, one in the upstream region of the neighborhood and one downstream.

5.6.3. Reactive sites of different SWDOMs and NRNOM

Table S5.2. Fractions of monochloramine and free chlorine rapid reactive sites and total reactive sites in various samples

Sampling location	**NR NOM**	**RES1**	**RES2**	**PRK1**	**PRK2**	**COM1**	**COM2**	**IND1**	**IND2**
$S_{NH2Cl\ rapid}$	0.0193	0.0046	0.0111	0.0045	0.0065	0.0060	0.0122	0.0057	0.0147
$S_{HOCl\ rapid}$	0.0663	0.0016	0.0235	0.0258	0.0298	0.0026	0.0249	0.0197	0.0298
S_{total}	1.40	0.67	0.74	0.57	0.82	1.03	1.01	0.42	1.10

5.6.4. The physical and chemical characteristics of stormwater

Table S5.3. Edmonton stormwater sample characteristics in residential, park, commercial and industrial upstream and downstream locations

Sampling location		**pH**	**NH_4-N (mg/L)**	**DOC (mg/L)**	**NO_2-N (mg/L)**	**Alkalinity (mg $CaCO_3$/L)**	**$SUVA_{254}$**
Residential Area	RES1	8.32	2.58	12.43	0.209	302	1.98
	RES2	8.24	0.621	9.66	0.745	343	2.55
Park Area	PRK1	8.14	0.011	10.73	0.015	487	1.30
	PRK2	8.31	0.053	11.47	0.041	455	2.44
Commercial Area	COM1	8.38	0.925	15.6	0.151	252	1.88
	COM2	8.3	0.264	14.05	0.216	420	2.09
Industrial Area	IND1	8.43	0.061	16.48	0.05	192	2.20
	IND2	8.41	0.441	14.96	0.129	510	2.42

5.6.5. The equations for FTR technique (Chen et al., 2003)

$$\Phi_{i,n} = MF_i \int_{ex} \int_{em} I(\lambda_{ex}\lambda_{em})\, d\lambda_{ex} d\lambda_{em} \tag{S5.1}$$

where $\Phi_{i,n}$ is the normalized EEM volume of region "i"; $I(\lambda_{ex}\lambda_{em})$ is the fluorescence intensity at certain excitation-emission pair; MF_i is the multiplication factor for each region, which equals to the inverse of the fraction projected excitation-emission area.

$$\Phi_{T,n} = \sum_{i=1}^{5} \Phi_{i,n} \tag{S5.2}$$

where $\Phi_{T,n}$ is the total normalized EEM volume of the five regions.

$$P_{i,n} = (\Phi_{i,n}/\Phi_{T,n}) \times 100\% \tag{S5.2}$$

where $P_{i,n}$ is the percent fluorescence response.

5.7. References

Brodtmann, N. V., Russo, P.J., 1979. Use of chloramine for reduction of trihalomethanes and disinfection of drinking water. J. Am. Water Works Assoc. doi:10.2307/41269574

Canadian Council of Ministers of the Environment, 2009. Canada-wide Strategy for the Management of Municipal Wastewater Effluent. Winnipeg.

Chen, J., Gu, B., LeBoeuf, E.J., Pan, H., Dai, S., 2002. Spectroscopic characterization of the structural and functional properties of natural organic matter fractions. Chemosphere 48, 59–68. doi:10.1016/S0045-6535(02)00041-3

Chen, W., Westerhoff, P., Leenheer, J.A., Booksh, K., 2003. Fluorescence Excitation-Emission Matrix Regional Integration to Quantify Spectra for Dissolved Organic Matter. Environ. Sci. Technol. 37, 5701–5710. doi:10.1021/es034354c

Chen, Z., Valentine, R.L., 2007. Formation of N-nitrosodimethylamine (NDMA) from humic substances in natural water. Environ. Sci. Technol. 41, 6059–6065. doi:10.1021/es0705386

Crittenden, J.C., Trussell, R.R., Hand, D.W., Howe, K.J., Tchobanoglous, G., 2012. MWH's Water Treatment: Principles and Design: Third Edition, MWH's Water Treatment: Principles and Design: Third Edition. doi:10.1002/9781118131473

Duirk, S.E., Gombert, B., Choi, J., Valentine, R.L., 2002. Monochloramine loss in the presence of humic acid. J. Environ. Monit. 4, 85–89. doi:10.1039/b106047n

Duirk, S.E., Gombert, B., Croué, J.P., Valentine, R.L., 2005. Modeling monochloramine loss in the presence of natural organic matter. Water Res. 39, 3418–3431. doi:10.1016/j.watres.2005.06.003

Gavin, H.P., 2017. The Levenberg-Marquardt method for nonlinear least squares curve-fitting problems. Dep. Civ. Environ. Eng. Duke Univ. 1–17. doi:10.1080/10426914.2014.941480

Guan, X.H., Shang, C., Chen, G.H., 2006. ATR-FTIR investigation of the role of phenolic groups in the interaction of some NOM model compounds with aluminum hydroxide. Chemosphere 65, 2074–2081. doi:10.1016/j.chemosphere.2006.06.048

Hand, V.C., Margerum, D.W., 1983. Kinetics and mechanisms of the decomposition of dichloramine in aqueous solution. Inorg. Chem. 22, 1449–1456. doi:10.1021/ic00152a007

Jafvert, C.T., Valentine, R.L., 1992. Reaction scheme for the chlorination of ammoniacal water. Environ. Sci. Technol. 26, 577–586. doi:10.1021/es00027a022

Jafvert, C.T., Valentine, R.L., 1987. Dichloramine decomposition in the presence of excess ammonia. Water Res. 21, 967–973. doi:10.1016/S0043-1354(87)80015-5

Larson, R.A., Weber, E.J., 1994. Reaction mechanisms in environmental organic chemistry. CRC press.

Leao, N.I., 1981. Dissertation. University of California.

Margerum, D.W., Schurter, L.M., Hobson, J., Moore, E.E., 1994. Water chlorination chemistry: Nonmetal redox kinetics of chloramine and nitrite ion. Environ. Sci. Technol. 28, 331–337. doi:10.1021/es00051a021

Morris, J. C. and Isaac, R.A., 1981. A critical review of kinetic and thermodynamic constants for the aqueous chlorine-ammonia system, in: R. L. Jolley, W. A. Brungs, J. A. Cotruvo, R. B. Cumming, J. S. Mattice, and V.A.J. (Ed.), Water Chlorination: Environmental Impact and Health Effects. Arbor Science, Ann Arbor, MI, pp. 49–62.

Morris, J.C., Christman, R.F., Glaze, W.H., Helz, G.R., Hoehn, R.C., Jolley, R.L., 1980. The chemistry of disinfectants in water: reactions and products, Drinking Water and Health. National Academy of Sciences, Washington, DC. doi:10.1016/0160-4120(91)90308-D

Nakanishi, K., Solomon, P.H., 1977. Infrared Absorption Spectroscopy, Book section Analytical

Techniques for Atmospheric Measurement.

Norman, T.S., Harms, L.L., Looyenga, R.W., 1980. The Use of Chloramines To Prevent Trihalomethane Formation. J. Am. Water Works Assoc. 72, 176–180.

R Development Core Team, R.F.F.S.C., 2008. R: A Language and Environment for Statistical Computing. Vienna Austria R Found. Stat. Comput. doi:10.1007/978-3-540-74686-7

Sen-Kavurmaci, S., Birben, N.C., Tomruk, A., Bekbolet, M., 2016. Characterization of organic matter in natural waters by EEM fluorescence properties. Desalin. Water Treat. 57. doi:10.1080/19443994.2015.1022804

Snoeyink, V., Jenkins, D., 1980. Water chemistry. Wiley, New York.

Vikesland, P.J., Ozekin, K., Valentine, R.L., 2001. Monochloramine decay in model and distribution system waters. Water Res. 35, 1766–1776. doi:10.1016/S0043-1354(00)00406-1

Wahman, D.G., Speitel, G.E., 2012. Relative importance of nitrite oxidation by hypochlorous acid under chloramination conditions. Environ. Sci. Technol. 46, 6056–6064. doi:10.1021/es300934x

Wu, W.W., Chadik, P. a, Delfino, J.J., 2003. The relationship between disinfection by-product formation and structural characteristics of humic substances in chloramination. Environ. Toxicol. Chem. 22, 2845–2852. doi:10.1897/02-542

Yang, X., Shang, C., Lee, W., Westerhoff, P., Fan, C., 2008. Correlations between organic matter properties and DBP formation during chloramination. Water Res. 42, 2329–2339. doi:10.1016/j.watres.2007.12.021

Zhang, Q., Davies, E.G.R., Bolton, J., Liu, Y., 2017. Monochloramine loss mechanisms in tap water. Water Environ. Res. doi:10.2175/106143017X14902968254421

Zhang, Q., Gaafar, M., Yang, R.-C., Ding, C., Davies, E.G.R., Bolton, J., Liu, Y., 2018. Field data analysis of active chlorine-containing stormwater samples. J. Environ. Manage. 206, 51–59.

Zhu, X., Zhang, X., 2016. Modeling the formation of TOCl, TOBr and TOI during chlor(am)ination of drinking water. Water Res. 96, 166–176. doi:10.1016/j.watres.2016.03.051

CHAPTER 6. THE ROLE OF BIOFILM ON MONOCHLORAMINE DISSIPATION IN STORM SEWER SYSTEMS: DIRECT REACTIONS OR AOB COMETABOLISM[9]

6.1. Introduction

Chloramination has been widely used for drinking water secondary disinfection. Monochloramine (NH_2Cl), as the dominant disinfectant, can provide long-lasting disinfection effect in drinking water distribution systems (Brodtmann and Russo, 1979; Mitcham et al., 1983; Norman et al., 1980). However, NH_2Cl can enter storm sewers, and thus fresh water sources (e.g., rivers or lakes) through outdoor tap water uses such as lawn irrigation, garden watering, car washing and driveway wash-down. Our previous research showed that in the Edmonton area, the total active chlorine (TAC) concentration varied from 0.02-0.77 mg/L in stormwater during summer 2015 (Zhang et al., 2018), which exceeded the Canadian Council of Ministers of the Environment guideline of 0.02 mg/L in discharge effluent (Canadian Council of Ministers of the Environment, 2009). TAC can cause 50% mortality to fishes at a concentration as low as 0.0053 mg/L (United States Environmental Protection Agency, 1985), and chloramine species pose chronic risks to the aquatic environment because of its persistent property (Brungs, 1973). However, the TAC contamination in stormwater has not yet received much-needed attention.

Although NH_2Cl is comparably stable in tap water, it can dissipate in storm sewers through three different pathways: auto-decomposition; biological decay; and chemical-decomposition through reactions with chemicals such as natural organic matter (NOM), nitrate (NO_2^-), ferrous ion (Fe^{2+}) and bromide (Br^-) (Duirk et al., 2005; Vikesland et al., 2001; Zhang et al., 2018, 2017). Our previous study evaluated the mechanisms of NH_2Cl auto- and chemical dissipation in bulk

---

[9] A version of this chapter has been submitted: Zhang, Q., Davies, E.G.R., Bolton, J., & Liu, Y., 2018. The role of biofilm on monochloramine dissipation in storm sewer systems: direct reactions or AOB cometabolism. Water research, February, 2018.

stormwater samples, and we developed a model to describe NH_2Cl dissipation in various stormwater conditions. However, NH_2Cl biological-dissipation mechanism in storm sewer systems was not studied. Three reactions that attribute to the NH_2Cl biological-dissipation in the presence of suspended AOB were proposed in literature: (i) the direct reaction with AOB; (ii) the cometabolism by ammonia oxidizing bacteria (AOB); and (iii) the reaction with AOB utilization associated products (UAP) (Maestre et al., 2016). However, in storm sewer biofilm, rather than AOB, the direct reactions with other biomass should also be considered in pathway (i). All the pathways that involved in the NH_2Cl biological-dissipation in stormwater systems are shown in Fig. 6.1. To be more specific, NH_2Cl can react with various organic components, which include bacterial cells, extracellular polymeric substances (EPS) secreted by biomass for formation of biofilm and the metabolic products produced from bacteria degradation. Further, NH_2Cl can be consumed by the nonspecific enzyme ammonia monooxygenase (AMO) in AOB (Maestre et al., 2016, 2013; Wahman et al., 2016). Although more than 99% of bacteria present as the formation of biofilm in natural and engineering systems, previous research mainly focused on the NH_2Cl dissipation due to suspended biomass (Maestre et al., 2016, 2013), and AOB were assumed to be dominant in the biomass cultured under drinking water conditions (Maestre et al., 2016). The only reported study on the impact of biofilms on NH_2Cl decay in drinking water conditions (Wahman et al., 2016) utilized reaction kinetics parameters obtained from suspended biomass studies, and inconstant cometabolism rate coefficients were observed for different experimental groups. No studies have been performed on the mechanisms of NH_2Cl decay with biofilm. In this research, a kinetics model that is more relevant to stormwater conditions is yet to be developed.

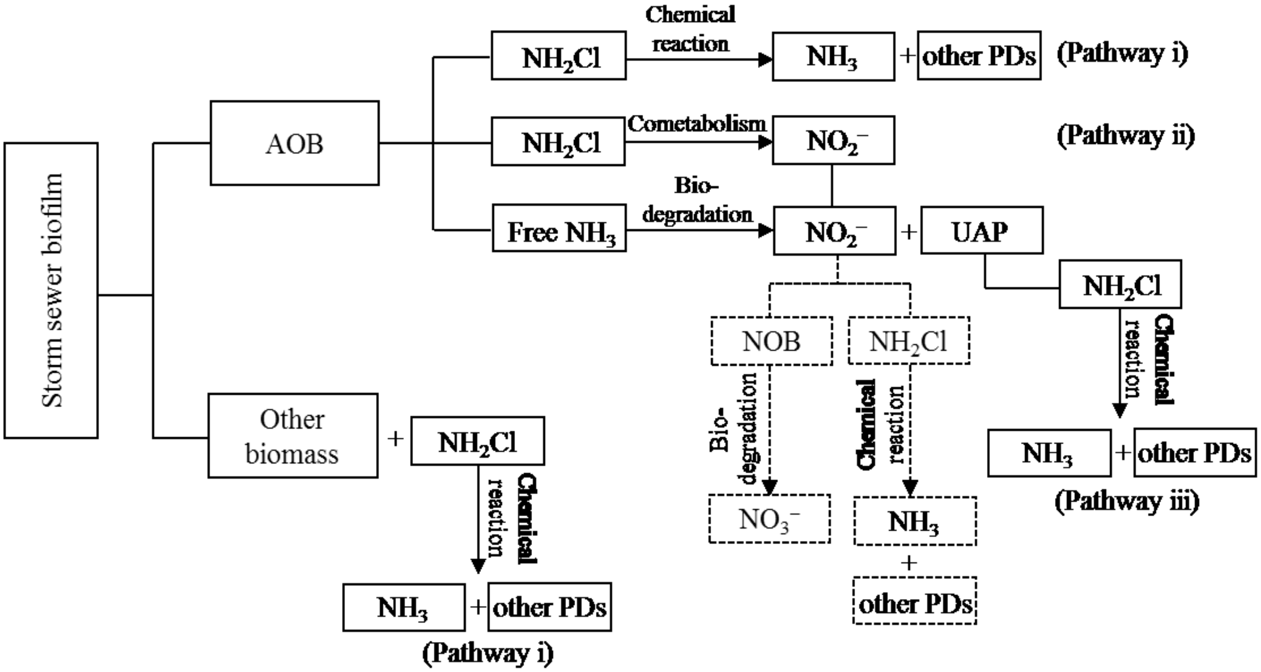

* Pathways with dashed lines are not considered in this research due to their limited contribution to NH_2Cl biological-dissipation; PDs: Products.

Fig. 6.1. Monochloramine biological-dissipation pathways in storm sewer systems.

Therefore, the objectives of this research are to evaluate microbial community compositions in simulated storm sewer systems, and to develop models to describe the NH_2Cl decay process with the presence of storm sewer biofilm under various initial NH_2Cl, total free ammonia nitrogen ($TOTNH_3$-N), AOB and total biomass concentrations. This is the first research to evaluate the NH_2Cl dissipation processes for mixed culture biofilms in a storm sewer environment. Further, in drinking water distribution systems, bacteria are mainly present as the formation of biofilm, and rather than AOB cultures, drinking water biofilm showed diversity of bacteria communities (Gomez-Alvarez et al., 2014). Therefore, the methodology and model developed in this study can benefit studies of NH_2Cl dissipation in both storm sewer and drinking water distribution systems.

6.2. Material and methods

6.2.1. Stormwater biofilm cultivation in annular reactors

To study the NH_2Cl decay mechanisms in the presence of storm sewer biofilm, the bacterial community distribution in biofilms was firstly studied. Storm sewer biofilms were cultured in two annular bioreactors with operating conditions that mimic different storm sewer environments, such as pipe materials (PVC and concrete), $TOTNH_3$-N (0.4 and 2 mg/L) and NH_2Cl (0 and 1 mg/L) concentrations. To be specific, each reactor had a volume of 960 mL, and contained 7 cement coated and 8 polyvinyl chloride (PVC) slides. Cement and PVC materials were selected because they are commonly used for storm sewer pipes. Reactors were inoculated for 3 days by fresh stormwater that was replaced every 24 h. Stormwater was collected from Edmonton stormwater manholes in dry weather conditions. After 3 days, synthetic stormwater was fed continuously into reactors with a hydraulic retention time (HRT) of 6 h. The synthetic stormwater contained 344 mg/L Na^+, 150 mg/L Mg^{2+}, 150 mg/L Ca^{2+}, 10 mg/L K^+, 1085 mg/L SO_4^{2-}, 163 mg/L Cl^-, 0.019 mg/L Zn^{2+}, 0.0019 mg/L Cu^{2+}, 0.175 mg/L B^{3+}, 0.0011 mg/L Mo^{6+} and 0.0015 mg/L Ni^{2+} to achieve the typical water quality characteristics of dry weather stormwater. Further, 13.7 mg/L sodium acetate (total organic carbon concentration = 4 mg/L) was added as an organic carbon source – at this concentration, sodium acetate caused the synthetic stormwater to achieve the same 5-day biochemical oxygen demand (BOD_5) as typical stormwater. $TOTNH_3$-N and NH_2Cl were fed separately into the reactors. $TOTNH_3$-N is defined as the sum of ammonia nitrogen (NH_4^+-N) and free ammonia (NH_3-N) in solution. For the first stage, reactor 1 (R1) and reactor 2 (R2) were fed with 0.4 mg/L and 2 mg/L $TOTNH_3$-N concentrations respectively. No NH_2Cl was fed during this period. 2 mg/L and 0.4 mg/L were selected since 2 mg/L was close to the highest average $TOTNH_3$-N concentration detected in Edmonton dry weather stormwater (Zhang et al., 2018), and

0.4 mg/L is the minimum concertation to trigger nitrification under our operating conditions. Completely nitrification was established as 95% of TOTNH$_3$-N was converted to NO$_3^-$-N. To achieve the shear stress in typical storm sewers, rotation speed was maintained at 80 rpm for both reactors. This rotation speed was also able to provide sufficient dissolved oxygen (DO) (over 5 mg/L in effluent) as field stormwater for bacteria growth. Reactors were wrapped by aluminum foil to create dark environment as in storm sewers.

The second stage studied the impact of NH$_2$Cl on bacterial community compositions, and was conducted after the reactors had been in operation for 8 months. NH$_2$Cl was pumped into reactors with a concentration of 1 mg-Cl/L in the influent, which is a value close to the highest TAC value detected in Edmonton stormwater (Zhang et al., 2018). Biofilms were collected after reactors were in operation for 2, 7, 9 and 11 months to observe the bacterial community diversities with different cultivation times and the presence of NH$_2$Cl. Bacterial communities of biofilms grown on cement and PVC slides were investigated through DNA extraction and quantitative polymerase chain reaction (*q*PCR) analysis. Total bacteria, AOB, and two NOB species (*Nitrospira* and *Nitrobacter*) were identified with *rpoB*, *amoA*, *NSR* and *Nitro* 16S rDNA genes respectively, and the primers used for *q*PCR analysis are shown in Table S6.1. Half the biofilm from each slide was collected for DNA extraction, and samples were collected in duplicate for each material under each condition. After this DNA collection, the reactors were operated under the same conditions for an additional 1 month or longer for biofilm regrowth. Influent and effluent water qualities were monitored 2-3 times per week. TOTNH$_3$-N, nitrite (NO$_2^-$) and nitrate (NO$_3^-$), dissolved organic carbon (DOC), pH and DO were assayed. During the operating period, pH was maintained within a "real stormwater range" of 8.0-8.3 (Zhang et al., 2018). Samples were filtered by 0.45 μm membrane filters before chemical analysis.

During the biofilm cultivation period, the feeding NH_2Cl solution was prepared with an active chlorine to nitrogen (Cl/N) molar ratio of 1. The detailed preparation process was described by Zhang et al. (2018). Ultrapure water used for solution preparation was obtained from a Barnstead™ Smart2Pure™ Water Purification System (Massachusetts, USA).

6.2.2. Batch kinetic studies

Batch kinetic experiments were designed for the study of NH_2Cl biological dissipation model and conducted after biofilm cultivation. PVC and cement slides were not studied separately since they showed similar bacteria community compositions in terms of total bacteria, AOB and NOB (Fig. 6.2). Four experimental groups were applied for kinetic model development: (I) positive control (to study the AOB activity in two reactors); (II) negative control with AOB inhibitor (to study the direct reaction of biofilm and some microbial metabolic products with NH_2Cl); (III) cometabolism experiments (to study the impact of AOB cometabolism by NH_2Cl decay rates); and (IV) low temperature control (10°C) (to study the impact of low temperature on NH_2Cl decay). The first three groups were conducted at room temperature (22°C), while 10°C was selected for low temperature control because it was close to the lowest stormwater temperature measured during summer months (Zhang et al., 2018). After each experiment, the reactors were fed synthetic stormwater for 4 days to recover biofilm and avoid significant biofilm growth during the batch study period. To study the direct reactions between biomass and NH_2Cl (negative control), AOB was inactivated by 50 mg/L of chlorobenzene (99+% pure) to eliminate the impact of cometabolism on NH_2Cl decay. Chlorobenzene was used as the inhibitor since it does not react with active chlorine species in solution. This group was conducted at the end of the experiment, since AOB activity cannot be recovery after inactivation. The direct reactions happened in negative control group include the reactions with biomass, biofilm EPS, bacteria associated products

(BAPs) from AOB activity (Maestre et al., 2013; Wahman et al., 2016) and metabolic products from other bacteria. As proposed by Abrahamson et al. (1996), Laspidou and Rittmann (2002) and Ni et al. (2011), bacteria metabolic products can be divided into two classes: biomass associated products (BAPs) formed from hydrolysis of bound EPS, and UAPs produced by bacteria metabolism. With the inhibition of AOB activity in the negative control, UAPs was not produced. Therefore, the reaction between NH_2Cl and AOB produced UAPs needs to be considered separately. However, with biofilm cultured in annular reactors, this reaction cannot be studied separately. Therefore, the reaction rate constant of UAPs (NH_2Cl biological-dissipation pathway iii) was directly used from previous research (Maestre et al., 2016).

In each experimental group, the NH_2Cl decay rates were tested under different initial NH_2Cl and TOTNH_3-N concentrations in both reactors to provide various conditions for the model. Before batch experiments started, reactors were rinsed with ultrapure water 3 times to remove the suspended biomass and chemicals. For each batch study, the initial TOTNH_3-N and NH_2Cl concentrations were analyzed before the experiment started. 4 mM of sodium bicarbonate was spiked into solutions to stabilize the pH, and additional hydrochloric acid (HCl) was added to adjust the pH to around 8. Table 6.1 provides details of the experimental conditions. For the temperature control group, reactors and solutions were stored in 10°C cold room for 30 min prior to the start of the experiment to equilibrate the reactor temperatures with the surrounding environment. During batch kinetic experiments, reactors were covered with aluminum foil to ensure a darkened environment and then maintained at the same rotation speed as in the previous reactor operating period to guarantee sufficient DO in solution and to provide similar water shear to storm sewer conditions. The batch experiments were conducted within 50 min to avoid significant changes of biomass states. No replicates of chemical analysis were conducted in the batch experiments due to time and sample volume limitations.

Table 6.1. Experimental conditions for batch kinetic studies

Exp. No.	**Reactor No.**	**Monochloramine (mg active Cl/L)**	**Total free ammonia nitrogen (mg N/L)**	**Chlorine to ammonia ration (Cl_2/N)**	**Total biomass (mg TSS/L)**	**Calculated ammonia oxidising bacteria (AOB) (mg TSS/L)**	**pH**
			Positive control				
A	1	N/A	2.63	N/A	189	1.06	8.02
B	1	N/A	0.78	N/A	189	1.06	8.04
C	2	N/A	2.64	N/A	203	4.43	8.05
D	2	N/A	0.79	N/A	203	4.43	8.07
			Negative control (with AOB inhibitor)				
A	1	1.97	1.75	1.12	189	1.06	8.07
B	1	1.00	0.43	2.32	189	1.06	8.03
C	2	1.99	1.75	1.14	203	4.43	8.07
D	2	1.00	0.46	2.17	203	4.43	8.04
			Cometabolism experiments				
A	1	1.97	1.85	1.06	189	1.06	8.09
B	1	0.94	0.42	2.24	189	1.06	8.05
C	2	1.97	2.04	0.96	203	4.43	8.07
D	2	0.94	0.42	2.24	203	4.43	8.05
			Low temperature control (10 °C)				
A	1	1.93	1.76	1.10	189	1.06	8.02
B	1	1.01	0.78	1.29	189	1.06	8.04
C	2	1.93	1.76	1.10	203	4.43	8.02
D	2	1.01	0.78	1.29	203	4.43	8.04

After completion of the kinetic studies, biofilm thicknesses on cement-coated and PVC slides were measured. The detailed measurement procedure and results are shown in the supporting information (Fig. S6.2). The biofilm in each reactor was quantified as total suspended solids (TSS) concentration and determined by collecting biofilm from slides as well as reactor inner surfaces in certain areas. Moreover, a standard curve for TSS and absorbance at 600 nm (A_{600}) wavelength was built by mixing biofilm with certain volumes of ultrapure water and diluting progressively. Under each TSS concentration, triplicate A_{600} readings were obtained. To determine how many milligrams of biofilm were consumed by each milligram of active chlorine (Yr), biofilm samples were reacted with 7 mg-Cl/L NH_2Cl solution. The biofilm that was consumed by NH_2Cl was measured by A_{600}. This experiment was conducted in triplicate, and the average value was applied as a final value in the model.

6.2.3. Modeling assumptions

To describe the NH_2Cl loss processes in the presence of stormwater biofilm, the reaction assumptions proposed by Maestre et al. (2016) for an AOB mixed culture were modified and applied. As described above, four reactions related to the NH_2Cl biological decay rates were considered for model development in this research: (1) AOB metabolism; (2) reaction with inactive biofilm; (3) AOB cometabolism; and (4) reaction with UAP produced by AOB. Note that the AOB inactivation rate was not considered here, since our initial experiments showed that in the presence of 2 mg-Cl/L NH_2Cl, no significant bacteria inactivation occurred from AOB-abundant biofilm within 1 hour (Fig. S6.1).

For reaction (1) in Table 6.2, AOB metabolism activity was described by the ammonia Monod equation, and the reaction rate expression was solved based on the experimental results from the positive control group. The ammonia Monod equation was developed by Maestre et al. (2016), who used only AOB in their study. However, in this research, as mixed culture grew in stormwater biofilm (Fig. 6.2), a ratio of AOB to total biomass was applied to estimate the AOB concentration in the reactor. In *q*PCR results (Fig. 6.2), *rpoB* as a single copy fuctional gene is commonly used to represent the total bacteria numbers in biofilm (Case et al., 2007). The AOB concentration (X_a) was identified by *amoA* gene with the assuption that each AOB cell contained an average of 2.5 *amoA* gene (He et al., 2007; Okano et al., 2004). Accroding to the *q*PCR analysis, AOB accounted for 0.56% and 2.18% of total bacterial cells in R1 and R2.

Table 6.2. NH_2Cl biological dissipation reaction assumptions developed from Maestre et al., 2016, 2013

	Reaction	Ammonia Monod	Reaction with biofilm	First-order cometabolism	UAP reactivity
	Pathway No.	(1)	(2)	(3)	(4)
	Kinetic rate expression	$\frac{k_{TOTNH_3}X_aS_{TOTNH_3}\alpha_1}{K_{S_{NH3}}+S_{TOTNH_3}\alpha_1}$	$k_{Biomass}X_rS_{NH_2Cl}{}^*$	$k_{come}S_{NH_2Cl}{}^*$	$k_{UAP}S_{UAP}S_{NH_2Cl}{}^*$
Reaction stoichiometry	$S_{TOTNH3-N}{}^*$ (mole $TOTNH_3$-N/L)	-1	1	\	1
	$S_{NH_2Cl}{}^*$ (moles active Cl/L)	\	-1	-1	-1
	$S_{NO_2^-}{}^*$ (moles NO_2^-/L)	\	\	1	\
	$S_{NO_3^-}{}^*$ (moles NO_3^-/L)	1	\	\	\
	$S_{UAP}{}^*$ (moles UAP/L)	f_{UAP}	\	\	-1
	$X_a{}^*$ (mg TSS/L)	\	\	\	\
	$X_r{}^*$ (mg TSS/L)	\	$-Y_r$	\	\

${}^*k_{TOTNH_3}$: ammonia maximum specific rate of degradation;

$K_{S_{NH3}}$: ammonia half-saturation constant;

α_1: free ammonia nitrogen to $TOTNH_3$-N ratio, in this research, $\alpha_1 = 0.05$;

$k_{Biomass}$, k_{come}, k_{UAP}: reaction rate constants of each reaction;

$S_{TOTNH3-N}$, S_{NH_2Cl}, $S_{NO_2^-}$, , $S_{NO_3^-}$, S_{UAP}: molar concentrations of $TOTNH_3$-N, NH_2Cl, NO_2^-, NO_3^-, UAP;

X_a and X_r: initial AOB and total biofilm concentrations;

Y_r: stoichiometric relationship of Xr consumed per active chlorine reacted.

The reaction rate of reaction (2) was affected by the total biofilm concentration (X_r) and the NH_2Cl concentration: each milligram of active chlorine can consume Y_r milligram of biofilm.

The cometabolism pathway (reaction (3)) was considered to be affected by both NH_2Cl concentration and initial X_a in previous research that used only AOB (Maestre et al., 2016, 2013; Wahman et al., 2016). However, in the presence of storm sewer biofilm, with different AOB concentrations in the two reactors, similar NH_2Cl cometabolism rates were observed in our experiments. Therefore, we have assumed that the NH_2Cl cometabolism rate was not related to X_a in the presence of storm sewer biofilm. Reaction (4) described the UAP reaction with NH_2Cl, and the value of the rate constant (k_{UAP}) from Maestre et al. (2016)'s research was used.

In Table 6.2, all the unknown kinetic constants were solved by compensating reaction rate expressions for the experimental NH_2Cl decay results under various conditions. Based on our experimental results, these unknown values were estimated using COMSOL Multiphysics (Stockholm, Sweden) with the Levenberg–Marquardt algorithm solver, which is commonly used to solve non-linear least squares problems in computer programs (Gavin, 2017). The average value for each constant was used in the final model, and the accuracy of the model was evaluated by Normalized Mean Square Error (NMSE). NMSE is a statistical method that commonly uses to describe the difference between observed and modeled values. In this research, the expression of NMSE is defined below (Kusiak and Wei, 2014):

$$\mathrm{NMSE} = \frac{\sum_{i=1}^{N}(y_{ob}-y_{mod})^2}{\sum_{i=1}^{N}(y_{mod})^2} \tag{1}$$

Where y_{ob} is the observed value from the laboratory experiment, y_{mod} is the predicted value from the model, and N is the number of analysis points in each laboratory experiment.

The NMSE value for each experiment is shown in Table S6.2. In this research, with NMSE values no more than 0.015, the modeled and experimental data are considered to show good matches (Kusiak and Wei, 2014). The NH_2Cl auto-decomposition and the reaction with NO_2^- developed in previous research (Vikesland et al., 2001; Wahman and Speitel, 2012; Zhang et al.,

2017) were first included in the model . However, the results showed consumption of less than 1% of NH_2Cl through these two pathways. Therefore, to simplify the model, they were removed from our NH_2Cl biological dissipation studies. Also, as the reaction between NO_2^- and NH_2Cl can be omitted, the competition of NH_2Cl and nitrite-oxidizing bacteria (NOB) for NO_2^- was also excluded.

6.2.4. Analysis methods

With Cl/N molar ratios equal to or less than 1, the NH_2Cl-Cl concentration was assumed to be the same as the total active chlorine (TAC) concentration (Crittenden et al., 2012). Therefore, the NH_2Cl concentrations (unit: mg-Cl/L) were measured as TAC concentrations using the HACH (Loveland, USA) colorimetric method 8167 (with a detection limit of 0.02 mg-Cl/L). The $TOTNH_3$-N, NO_2^--N, NO_3^--N and alkalinity concentrations were analysed with HACH commercial test kits TNT832, TNT839, TNT835, and TNT870 with detection limits of 0.015 mg/L NH_3-N, 0.015 mg/L NO_2^--N, 0.2 mg/L NO_3^--N and 25 mg/L $CaCO_3$, respectively. A portable dissolved oxygen (DO) meter pen (Fisher Scientific, CA) was used to measure DO concentrations and temperatures of stormwater samples. Extech EC500 Waterproof ExStikII pH/conductivity meter was used to analyze pH (Nashua, USA). The TSS was determined following the standard methods 2540D protocol. The A_{600} absorbance was obtained with a HACH DR 3900™ Laboratory VIS Spectrophotometer. The sodium acetate concentration was analyzed with a Shimadzu TOC-L CPH E100 (detection limit is 4 μg-C/L).

6.3. Result and discussion

6.3.1. Bioreactor performance

In the first stage, when no NH_2Cl was introduced to the reactors, completed nitrification was observed after the reactors ran for three weeks. With 0.4 mg/L and 2 mg/L $TOTNH_3$-N fed to reactors R1 and R2, respectively, the average effluent concentrations were as low as 0.02 and 0.03 mg/L, and almost all the TOTNH$_3$-N was converted to NO$_3^-$-N. After 1 mg-Cl/L of NH$_2$Cl was fed into the reactors (Stage II), the TOTNH$_3$-N removal was same as in stage I. Further, measurements indicated that NH$_2$Cl was completely removed from both reactors, and no NH$_2$Cl was detected in their effluents. In both operational stages, with an influent pH of 7.9-8.0, effluent pH in R1 increased to approximately 8.3 and showed no significant change in R2, perhaps because the stronger nitrification in R2 reduced the potential pH increment. Effluent DOC concentrations were stable at around 1.3 mg/L. With sufficient DO in the influents (over 7 mg/L), the effluent DO concentrations were maintained above 5 mg/L.

6.3.2. Bacterial distribution on reactor biofilms

Fig. 6.2 shows the *q*PCR results for the total bacteria *rpoB* gene, AOB *amoA* gene, and NOB *NSR* and *Nitro* genes in PVC and cement biofilms under different reactor operating periods. In both reactors, a higher statistical abundance of four functional genes was found on cement slides than on PVC slides (P values < 0.05), results that correspond to the biofilm thickness results in Fig. S6.2. Specifically, in both reactors, the copy numbers of all the four functional genes showed increasing trends from September 2016 to March 2017, which demonstrates the slow growth rates of bacteria in stormwater conditions.

To study the effect of NH$_2$Cl on microbial communities, 1 mg-Cl/L NH$_2$Cl was fed into reactors, as explained above. The total bacteria gene copies consequently increased continually (p value < 0.01), which showed no significant effect by 1 mg-Cl/L of NH$_2$Cl. Also, the *amoA* gene showed a stable abundance before and after chloramination in R1 (10^6 gene copies/cm^2, p value $>$ 0.1), but a slight increase was observed in R2 after chloramination (2.5×10^7 gene copies/cm^2, p value < 0.05); this result suggested that AOB was not sensitive to 1 mg-Cl/L NH$_2$Cl. In contrast, the higher sensitivity of *Nitrospira* to NH_2Cl was made apparent by continuously decreasing *NSR* gene copy numbers after chloramination. *Nitrobacter* functional genes showed no remarkable changes after chloramination in R1 (p value > 0.1), but they declined in R2 (p value < 0.05). As compared with *Nitrospira,* high concentrations of *Nitrobacter* were observed in both reactors, perhaps because of their high salinity tolerance (Cébron and Garnier, 2005), as dry-weather stormwater contains high dissolved salts concentrations of approximately 2 g/L. This observation corresponds to the field results obtained from Edmonton storm sewer biofilms (Zhang et al., 2018).

In a comparison of bacterial abundances in R1 and R2, copy numbers of total bacteria functional genes showed no significant differences in these two reactors (p value > 0.05). In terms of AOB, *amoA* functional gene abundance was one log higher in R2 than R1 (p value < 0.01), which corresponds to the different TOTNH_3-N fed in reactors. Likewise, the *Nitrospira* functional gene (*NSR*) showed the same trend as *amoA* (p value < 0.01). However, no significant difference of *Nitro* gene copy numbers was observed between the two reactors (p value > 0.05). It can be explained that *Nitrobacter* was not sensitive with the nitrogen source (TOTNH_3-N) elevated from 0.4 to 2 mg/L.

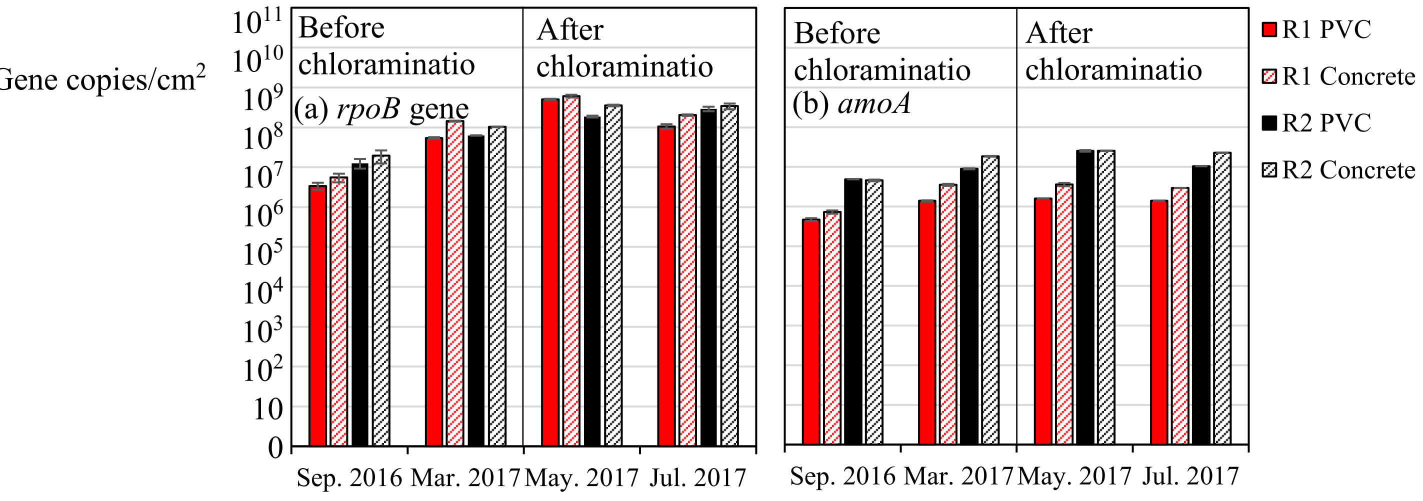

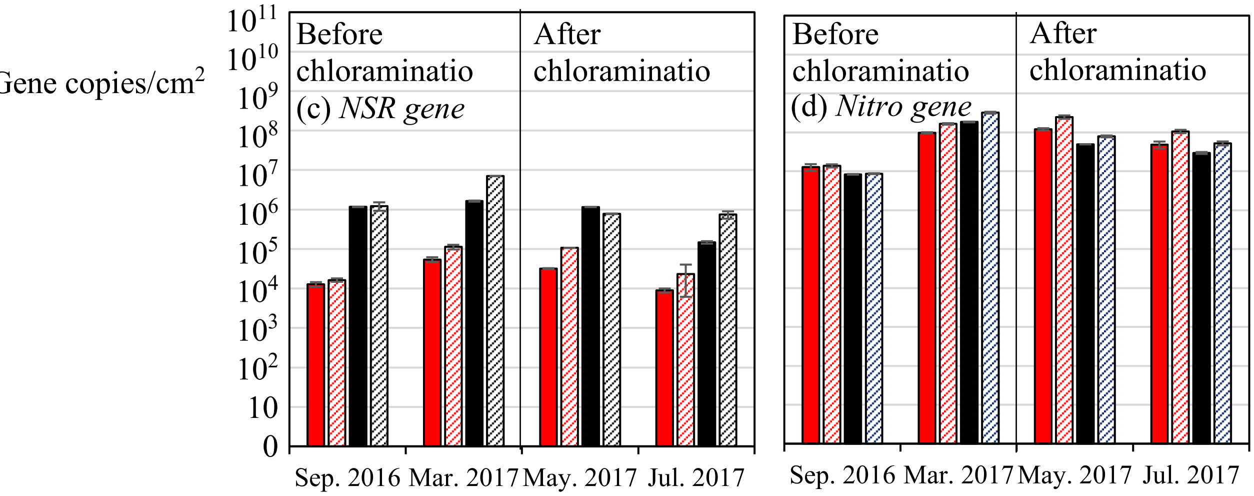

Fig. 6.2. Biofilm gene abundance changes of (a) total bacteria rpoB gene, (b) AOB amoA gene, (c) NOB NSR and (d) NOB Nitro genes in R1 and R2 at different operation periods

6.3.3. NH_2Cl biological decay processes

The AOB activities were studied by monitoring TOTNH_3-N degradation rates in batch reactors. As shown in Fig. 6.3, with the same initial TOTNH_3-N concentrations, R2 showed a higher TOTNH_3-N degradation rate than R1, and therefore more AOB activity. This result corresponds to the higher *amoA* gene copies in R2 biofilm. Moreover, almost no NO_2^- accumulation was detected during TOTNH_3-N kinetic studies, which indicated that the TOTNH_3-N was converted to NO_3^--N immediately through a complete-nitrification process.

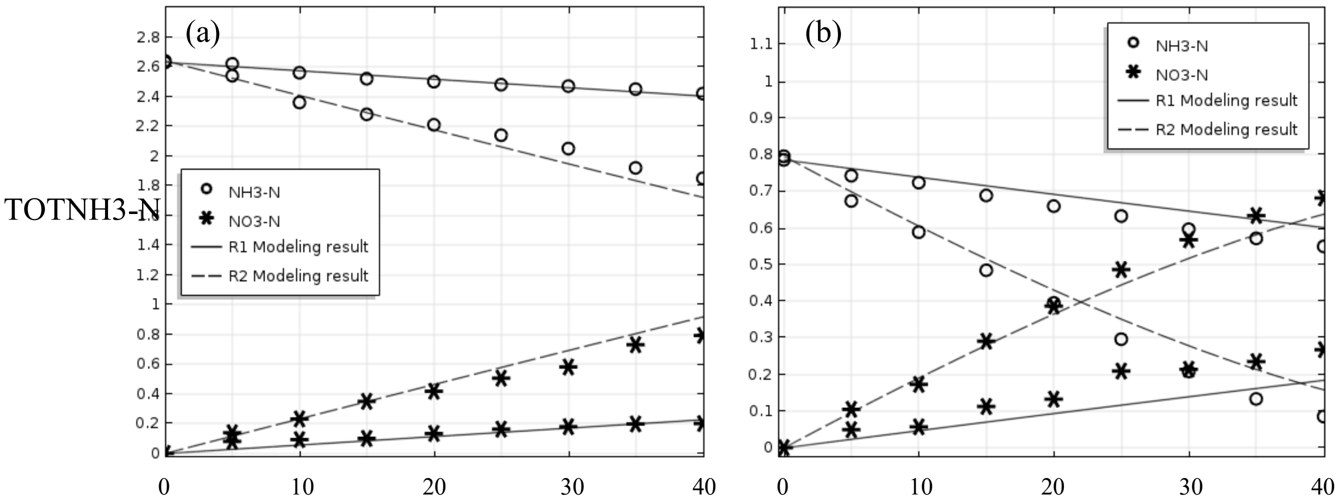

Fig. 6.3. TOTNH3-N degradation in annular reactors under (a) high and (b) low initial TOTNH3-N concentrations

To simulate the TOTNH$_3$-N degradation in various stormwater conditions, the ammonia Monod equation was solved based on the experimental results from the positive control group (no NH$_2$Cl added) (Table 6.2, equation (1)). The TOTNH$_3$-N degradation and NO$_3^-$-N production curves under the same conditions as laboratory experiments were then modeled, with the results shown in Fig. 6.3 (solid and dashed lines). Clearly, the modeled curves closely approximate experimental results in terms of TOTNH$_3$-N degradation under different initial conditions (NMSE values ≤ 0.010, Table S6.2), and therefore the ammonia Monod equation developed in this research can be used to describe AOB activity in storm sewer biofilm.

Fig. 6.4 shows the NH$_2$Cl dissipation with inactivated AOB (50 mg/L of chlorobenzene added to eliminate microbial activity). In this group, NH$_2$Cl reacted with biofilm-containing biomass, EPS, BAPs from AOB and metabolic products from other bacteria. With higher initial NH$_2$Cl concentrations, both reactors showed higher NH$_2$Cl decay rates. Based on experimental data, the reaction rate constant, $k_{Biomass}$ (Table 6.2), was solved. As shown in Fig. 6.4, although the modeled curves showed slightly over/under estimation with experimental data, they are still in an acceptable range (NMSE values ≤ 0.015, Table S6.2), which means the direct reaction between NH_2Cl and biofilm can be predicted by this model.

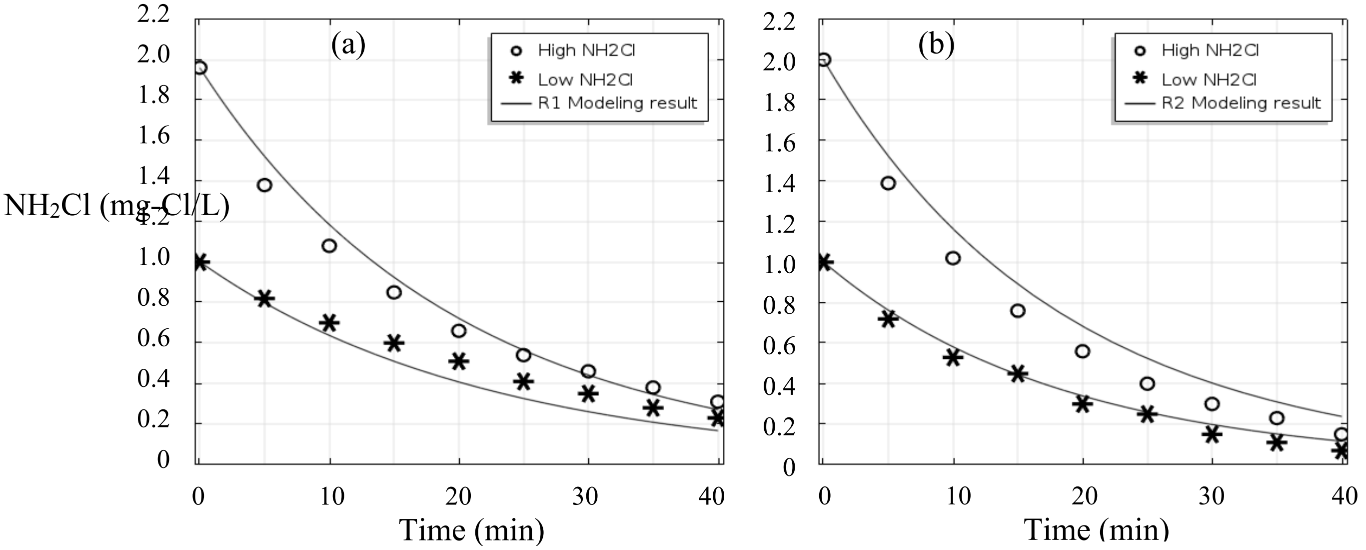

Fig. 6.4. NH_2Cl dissipation with biofilm only in (a) R1 and (b) R2

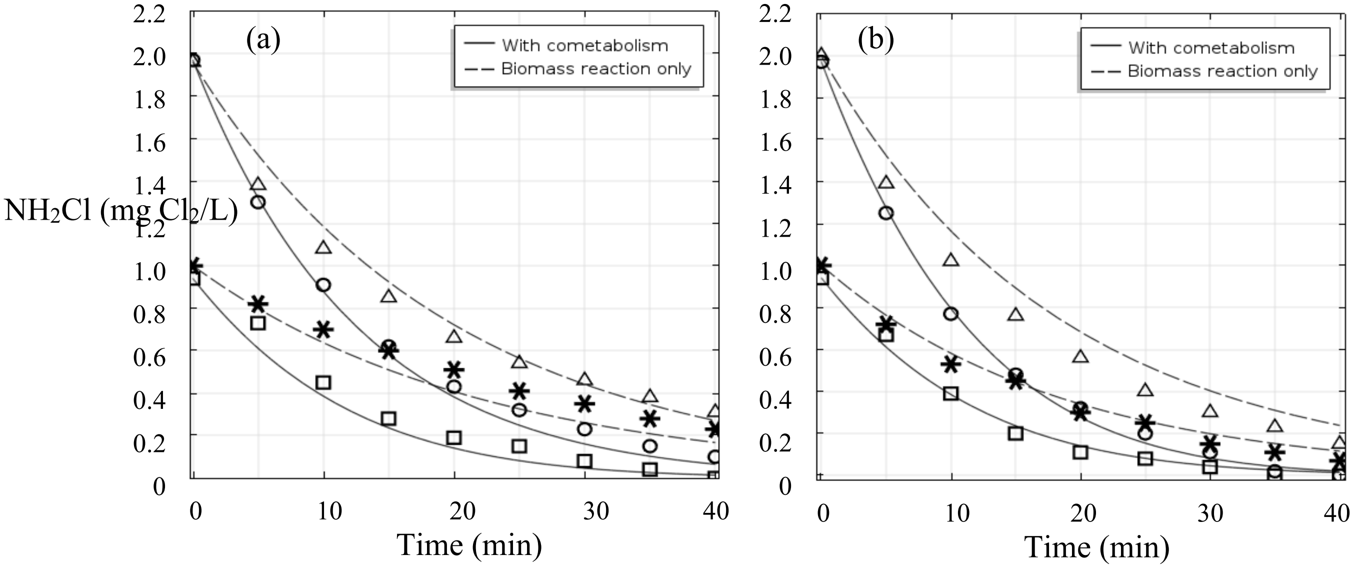

Fig. 6.5. The overall NH_2Cl dissipation and with biofilm only in (a) R1 and (b) R2 (Points: experimental results from negative control and cometabolism experiments)

Fig. 6.5 compares two cases of NH_2Cl dissipation: 1) dissipation with inactivated biofilm (Fig. 6.4 conditions, dashed lines), and 2) dissipation with active biofilm (cometabolism experiments, solid lines) under different TOTNH$_3$-N and NH$_2$Cl conditions. Although AOB were not dominant in reactor biofilms in these experiments, the difference between solid and dashed lined indicates that the impact of AOB activity on NH$_2$Cl biological dissipation cannot be ignored. Two pathways contributed to the NH$_2$Cl decay rates through AOB activity – 1) AOB cometabolism, and 2) UAP reactivity. Research suggested that to compare with these two pathways, cometabolism accounted for a significantly higher percentage than UAP reactivity in NH$_2$Cl biological-dissipation. The cometabolism rate was affected in turn by both the NH$_2$Cl concentration and initial AOB concentration (Maestre et al., 2016, 2013). Interestingly, in our study, although different AOB activities were observed in R1 and R2 biofilms, similar NH$_2$Cl decay rates were observed; therefore, cometabolism seems to be affected by factors other than initial AOB concentrations in a mixed cultured biofilm. For instance, diffusion limitations in intact biofilms may limit contact between AOB and NH$_2$Cl. Since AOB only accounted for a small percentage of the storm sewer biofilms (0.56% and 2.18% in R1 and R2 respectivety), before NH$_2$Cl contacted AOB, most of the NH$_2$Cl had been consumed by the direct reaction between biofilm and NH$_2$Cl (more than 80% in both reactors). Therefore, only a limited amount of NH$_2$Cl could be cometabolized by AOB (Fig. 6.5). As similar cometabolism rates were observed under different AOB activities, the AMO enzyme was sufficient in both reactors to reach maximum cometabolism rates.

Fig. 6.5 shows good agreement between the modeled NH$_2$Cl dissipation results and experimental data (NMSE values ≤ 0.015, Table S6.2), which validates our NH$_2$Cl cometabolism assumption. Moreover, the good correspondence between modeled and experimental results also indicates that the overall NH$_2$Cl biological dissipation model developed here can be used to simulate NH$_2$Cl decay with stormwater biofilms under various initial NH$_2$Cl, TOTNH$_3$-N, AOB and total biomass concentrations. Note that all the experiments were conducted with NH_2Cl concentrations of no more than 2 mg-Cl/L; therefore, the cometabolism assumption should be applied for similar or lower NH_2Cl concentrations, and may not apply for higher NH_2Cl concentrations.

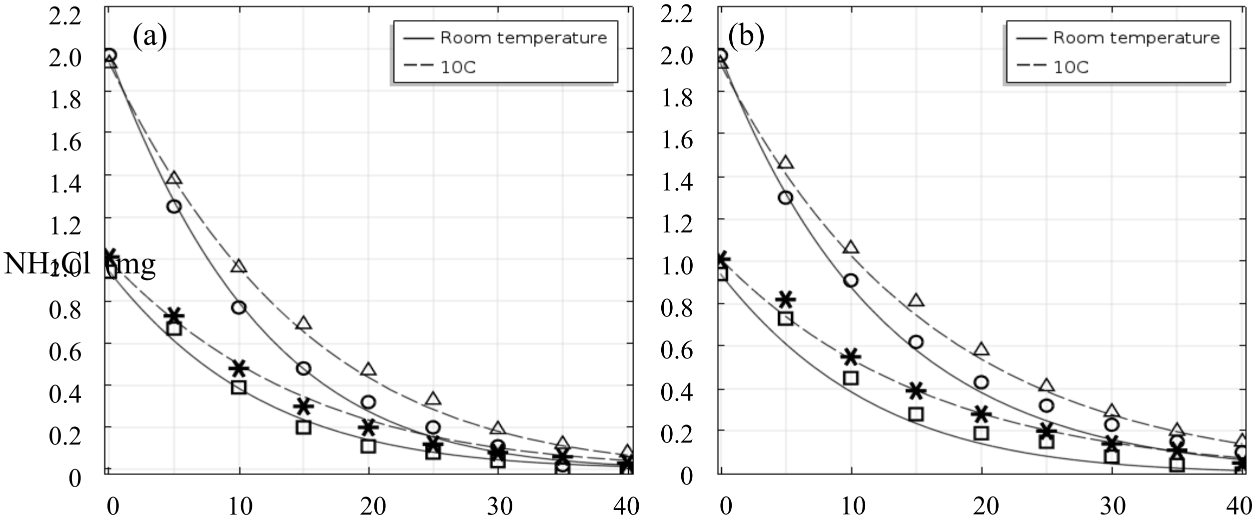

Fig. 6.6. The overall NH_2Cl dissipation under 10 °C and room temperature in (a) R1 and (b) R2 (Points: experimental results from cometabolism experiments and low temperature control group)

Fig. 6.6 shows the impact of temperature on NH_2Cl dissipation. Lower NH_2Cl dissipation rates occurred under 10 °C conditions, since less energy was provided for the NH_2Cl reactions from the surrounding environment. Further, AOB showed lower activity at 10 °C, which could also lead to reduced NH_2Cl consumption from cometabolism processes. To simulate the NH_2Cl dissipation at 10 °C, the NH_2Cl dissipation model was calibrated with an additional coefficient, $\beta_{10°C}$, whose value is provided in Table 6.3. As the simulated curves corresponded closely to the experimental results (NMSE values ≤ 0.03, Table S6.2), we conclude that the calibrated model can simulate NH_2Cl biological decay in stormwater biofilms at 10 °C conditions. Note that the temperature coefficient introduced here does not represent the true reaction mechanisms that determine temperature effects on NH_2Cl biological dissipation, but it does accurately predict NH_2Cl dissipation by stormwater biofilm at real storm sewer temperatures.

6.3.3. Kinetic parameter comparison

The modeling parameters solved in this study are summarized in Table 6.3, along with a comparison with the previous literature on NH_2Cl cometabolism processes.

Table 6.3. The kinetic parameters in this research and the comparison with previous studies using drinking water biofilm in annular reactor (Wahman et al., 2016) and Lake Austin mixed AOB culture (Maestre et al., 2016)

Parameter	This research	Drinking water annular reactor	Lake Austin mixed AOB culture
k_{TOTNH_3} (mg $TOTNH_3$/mg TSS–day)	8.5	Set at Lake Austin value	1.7
$K_{S_{NH3}}$ (mg NH_3-N/L)	0.012	0.057	0.083
$k_{Biomass}$ (L/mg TSS–day)	0.39	Set at Lake Austin value	1.5
k_{come} (Units are different)	41.2 (1/ day)	0.94-1.2 (L/mg TSS–day)	0.8 (L/mg TSS–day)
Y_{Xr} (mg TSS/mg active Cl)	4.4 ± 1.0	6.2	57
k_{UAP} (L/mol UAP–day)	Set at Lake Austin value	Set at Lake Austin value	2.3×10^7
f_{UAP} (mole UAP/mole TOTNH3)	Set at Lake Austin value	Set at Lake Austin value	0.062
$\beta_{10\,°C}$ (\ )	0.78	N/A	N/A

As compared to the literature, the higher k_{TOTNH_3} and lower $K_{S_{NH3}}$ values indicate higher AOB activity in the storm sewer biofilm. The lower AOB activity in Maestre et al. (2016) and Wahman et al. (2016) probably resulted from overestimation of AOB populations, since the authors assumed the mixed-culture suspended biomass and biofilms consisted only of AOB; however, a bacteria diversity analysis by Gomez-Alvarez et al. (2014) for drinking water biofilm determined that no more than 15% of cumulative bacteria distribution consisted of *Betaproteobacteria* and *Gammaproteobacteria* (includes AOB) in biofilms from annular reactor, which indicates the significant overestimation of AOB concentrations in these studies. Further, ammonia oxidizing populations may be underestimated in our experiments, because populations of ammonia-oxidizing archaea (AOA) in the reactors were not quantified in our model. However, research has long suggested that with TOTNH_3-N concentrations higher than 0.14 mg/L, AOB is more prevalent than AOA (French et al., 2012; Gomez-Alvarez et al., 2014), and therefore the impact of AOA is probably insignificant in this study.

In terms of the direct reaction between NH_2Cl and biofilm, a lower reaction rate constant ($k_{Biomass}$) was found than in previous research. This result may be attributed to the fact that biofilm has higher diffusion resistance than suspended microbes (as reported in other studies in Table 6.3), which lead to a slower NH_2Cl reaction with the inner layers of the biofilm (Arcangeli and Arvin, 1998). No studies to-date have reported on the impact of stormwater biofilms on NH_2Cl dissipation kinetics. Further, as compared to the suspended flocs, biofilms generate higher EPS which can be involved in the reaction between biofilm and NH_2Cl (Coburn et al., 2016), and can also result in a different reaction rate constant. Y_{Xr} represents the stoichiometric ratio of biomass consumed per active chlorine; Table 6.3 shows the Y_{Xr} determined from biofilm studies (4.4 mg TSS/mg Cl_2 in this study and 6.2 mg TSS/mg Cl_2 in drinking water annular reactor) to be approximately 10 times lower than the suspended biomass (57 mg TSS/mg Cl_2), which may also indicate the additional EPS involved in the reaction between NH_2Cl and biofilm.

The cometabolism reaction rate constants are not comparable between this research and the literature due to the different assumptions applied to this reaction. In this research, as AOB presented in the formation of biofilm, their concentration did not show a significant impact on NH_2Cl cometabolism rate. Therefore, the initial AOB concentration was not included in this reaction expression; in contrast, it was included by Maestre et al. (2016) in their NH_2Cl cometabolism rate, as suspended biomass was used in their cometabolism experiments. Further, although Wahman et al. (2016) included biofilm from drinking water system, the AOB populations (X_a) were assumed to be the same in different reactors. According to this assumption, the impact of AOB concentration on NH_2Cl cometabolism rates cannot be determined. Further, previously reported values of k_{come} are probably underestimates, because of the overestimated AOB concentrations in their studies.

6.4. Conclusion

This research investigated bacterial community structures and compositions in annular reactors in typical dry-weather storm sewer conditions. PVC and cement materials, as the common materials for storm sewer pipes, were selected for biofilm cultivation in the reactors. Low and high $TOTNH_3$-N concentrations were fed to two reactors respectively. Biofilms were collected regularly throughout the reactor operation period, and total, AOB and NOB functional genes were analysed with qPCR. The results illustrated a higher abundance of all the identified functional genes for the cement material than for PVC in all operating periods; the biofilm thickness was also greater for the cement surface. In addition, with different $TOTNH_3$-N (0.4 and 2 mg/L) in the reactors, more AOB and *Nitrospira* functional genes were detected in the biofilm from the high $TOTNH_3$-N reactor, while the *Nitrobacter* functional genes showed no significant effect from this $TOTNH_3$-N concentration difference.

Moreover, NH_2Cl biological dissipation mechanisms in the presence of stormwater biofilm were studied. In batch kinetic studies, NH_2Cl decreased to almost zero within 40 min of its introduction in both reactors. Three pathways contributed to this NH_2Cl biological dissipation: the reaction with biofilm only, the consumption by AOB cometabolism and the reaction with UAP produced by AOB activity. As compared with the previous research that mainly used suspended AOB for cometabolism studies, this study included the cometabolism reactions in the presence of mixed culture biofilm. Compared with values in the literature, the smaller Y_{Xr} and $k_{Biomass}$ values for the biofilm and NH_2Cl reaction indicate the additional EPS involved in the reaction with NH_2Cl. Further, NH_2Cl biological dissipation rates at 10 °C were studied to aid the simulation of NH_2Cl dissipation in a real storm sewer environment. The experimental and modeled results showed good matches under various conditions. Although storm sewer biofilm has a different bacterial distribution than drinking water biofilm, the methodology and assumptions used here may also apply to NH_2Cl dissipation by drinking water biofilm.

6.5. Supplementary materials

6.5.1. Fluorescence microscope analysis of AOB abundant biofilm before and after chloramination

The resistance of AOB to monochloramine was studied by comparing the AOB abundant biofilms before and after chloramination. To chloraminated the biofilm, biofilms were soaked into monochloramine solution with a concentration of 2 mg active Cl/L. 4 mM sodium bicarbonate was added to maintain the solution pH. After 1 hour, biofilm samples were directly stained by LIVE/DEAD ® BacLightTM Bacterial Viability Kits. The procedure for biofilm staining was described in Huang et al. (2015)'s research. Biofilm samples were observed by green and red fluorescence using 20x objective of ZEISS Axio Imager 2 Fluorescence Microscope (New York, USA). With the present of fluorescence, bacteria with undamaged membranes were stained as green, otherwise, bacteria were stained as red.

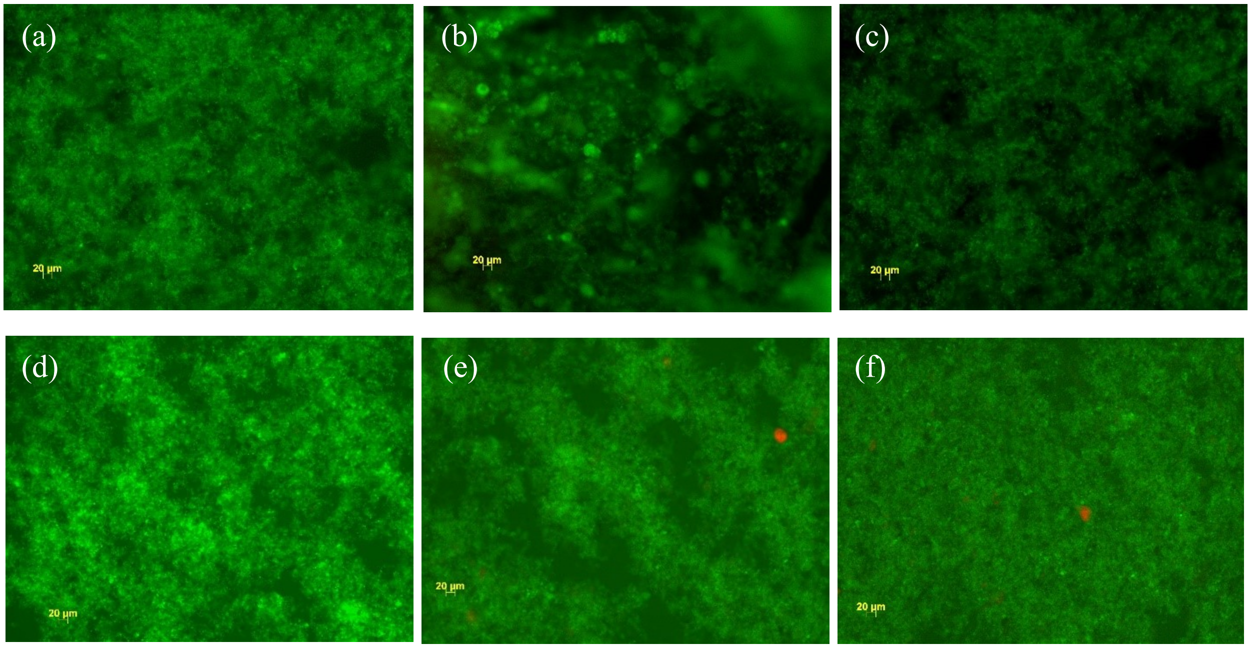

Fig. S6.1. The comparison of AOB abundant biofilm before (a) (b) (c) and after (d) (e) (f) chloramination with 2 mg active Cl/L of monochloramine

6.5.2. Stormwater biofilm thickness on different materials

Biofilm thickness in concrete and PVC slides were measured by random selection of 12 view fields in each slide using fluorescence microscope. Triplicate slides were tested for each material in each reactor. Before measurement, stormwater biofilms were stained with LIVE/DEAD ® BacLightTM Bacterial Viability Kits following the same procedure as descripted in Supporting Information Section 1. Fluorescence was used to observe the biofilms after staining. For each measurement, the top layer of the biofilm in a microscope field was first focused and record as depth zero. And then, the base layer was focused to obtain the depth of the biofilm in this microscope field.

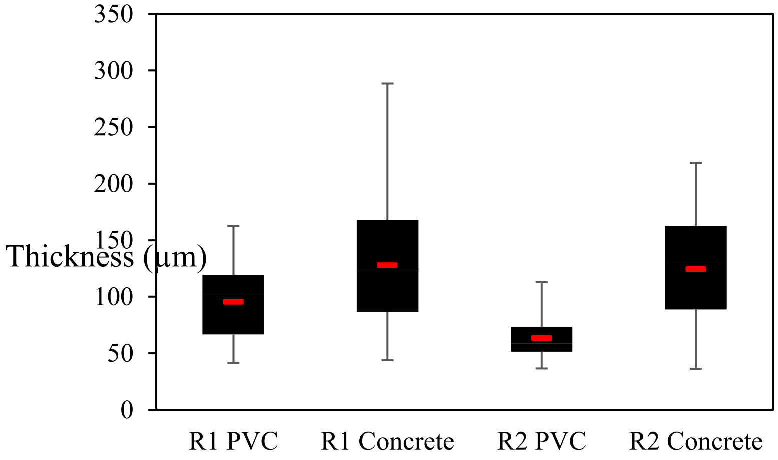

Fig. S6. 2. Biofilm thickness on different materials in different reactors

6.5.3. Quantitative polymerase chain reaction

Four independent *q*PCR assays were conducted to quantify the function gene copy numbers of total bacterial , ammonia-oxidizing bacteria (AOB), two nitrite-oxidizing bacteria species – *Nitrospira* and *Nitrobacter* by targeting rpoB, amoA, NSR and Nitro genes respectively (Table S6.1). Reactions (20 μL) were performed in 96-well microplates. Each tube was separately loaded with 2 μL of genomic DNA (14-26ng/μL), followed by the forward and reverse primers (1 μL), together with 10 μL 1* iTap SYBR Green Supermix with ROX (Bio-RAD, Hercules, California) and 6 μL PCR grade sterile water. Grade sterile water was also used as negative control. Triplicate composite samples were tested for all experiments. The efficiency of PCR amplification for each gene was between 80% and 110%. The primers used in qPCR analyzes are shown in Table S6.1.

Table S6.1. Primers used in qPCR

Bacteria types	**Target**	**Primer**	**Sequence (5'-3')**	**Reference**
Total Bacteria	rpoB gene	*1698f*	5'-AAC ATC GGT TTG ATC AAC-3'	Dahllof et al., 2000
		2041r	5'-CGT TGC ATG TTG GTA CCC AT-3'	Dahllof et al., 2000
AOB	amoA gene	*amoA-1F*	5'-GGGGTTTCTACTGGTGGT-3'	McTavish et al., 1993
		amoA-2R	5'-CCCCTCKGSAAAGCCTTCTTC-3'	McTavish et al., 1993
Nitrospira	NSR 16S rDNA	*NSR 1113f*	5'-CCTGCTTTCAGTTGCTACCG-3'	Dionisi et al., 2002
		NSR 1264r	5'-GTTTGCAGCGCTTTGTACCG-3'	Dionisi et al., 2002
Nitrobacter	Nitro 16S rDNA	*Nitro 1198f*	5'-ACCCCTAGCAAATCTCAAAAAACCG-3'	Graham et al., 2007
		Nitro 1423r	5'-CTTCACCCCAGTCGCTGACC-3'	Graham et al., 2007

6.4. Normalized Mean Square Error (NMSE) analysis

Table S6.2. The value of NMSE for each experiment

Experimental No.	**(I) Positive control**		**(II) Negative control (with AOB inhibitor)**	**(III) Cometabolism experiments**	**(IV) Low temperature control (10°C)**
Modeled parameter	TOTNH$_3$-N	NO$_3$-N	NH$_2$Cl-Cl	NH$_2$Cl-Cl	NH$_2$Cl-Cl
A	0.000	0.038	0.008	0.003	0.001
B	0.003	0.280	0.015	0.015	0.003
C	0.001	0.015	0.015	0.001	0.001
D	0.010	0.007	0.007	0.004	0.003

6.6. References

Abrahamson, M., Lewandowski, Z., Geesey, G., Skjåk-Bræk, G., Strand, W., Christensen, B.E., 1996. Development of an artificial biofilm to study the effects of a single microcolony on mass transport. J. Microbiol. Methods 26, 161–169. doi:10.1016/0167-7012(96)00908-6

Altmann, D., Stief, P., Amann, R., De Beer, D., Schramm, A., 2003. In situ distribution and activity of nitrifying bacteria in freshwater sediment. Environ. Microbiol. 5, 798–803. doi:10.1046/j.1469-2920.2003.00469.x

Arcangeli, J.P., Arvin, E., 1998. Modeling of the cometabolic biodegradation of trichloroethylene by toluene-oxidizing bacteria in a biofilm system. Environ. Sci. Technol. 31, 3044–3052. doi:10.1021/es9609112

Black, R., Sartaj, M., Mohammadian, A., Qiblawey, H.A.M., 2014. Biosorption of Pb and Cu using fixed and suspended bacteria. J. Environ. Chem. Eng. 2, 1663–1671. doi:10.1016/j.jece.2014.05.023

Brodtmann, N. V., Russo, P.J., 1979. Use of chloramine for reduction of trihalomethanes and disinfection of drinking water. J. Am. Water Works Assoc. doi:10.2307/41269574

Brungs, W. a, 1973. Effects of residual chlorine on aquatic life. J. Water Pollut. Control Fed. 45, 2180–2193. doi:10.2307/25038016

Canadian Council of Ministers of the Environment, 2009. Canada-wide Strategy for the Management of Municipal Wastewater Effluent. Winnipeg.

Case, R.J., Boucher, Y., Dahllöf, I., Holmström, C., Doolittle, W.F., Kjelleberg, S., 2007. Use of 16S rRNA and rpoB genes as molecular markers for microbial ecology studies. Appl. Environ. Microbiol. 73, 278–288. doi:10.1128/AEM.01177-06

Cébron, A., Coci, M., Garnier, J., Laanbroek, H.J., 2004. Denaturing gradient gel electrophoretic analysis of ammonia-oxidizing bacterial community structure in the lower seine river: Impact of paris wastewater effluents. Appl. Environ. Microbiol. 70, 6726–6737. doi:10.1128/AEM.70.11.6726-6737.2004

Cébron, A., Garnier, J., 2005. Nitrobacter and Nitrospira genera as representatives of nitrite-oxidizing bacteria: Detection, quantification and growth along the lower Seine River (France). Water Res. 39, 4979–4992. doi:10.1016/j.watres.2005.10.006

Coburn, K.M., Wang, Q., Rediske, D., Viola, R.E., Hanson, B.L., Xue, Z., Seo, Y., 2016. Effects of extracellular polymeric substance composition on bacteria disinfection by monochloramine: Application of MALDI-TOF/TOF-MS and multivariate analysis. Environ. Sci. Technol. 50, 9197–9205. doi:10.1021/acs.est.6b00927

Crittenden, J.C., Trussell, R.R., Hand, D.W., Howe, K.J., Tchobanoglous, G., 2012. MWH's Water Treatment: Principles and Design: Third Edition, MWH's Water Treatment: Principles and Design: Third Edition. doi:10.1002/9781118131473

Dahllof, I., Baillie, H., Kjelleberg, S., 2000. rpoB-based microbial community analysis avoids limitations inherent in 16S rRNA gene intraspecies heterogeneity. Appl. Environ. Microbiol. 66, 3376–3380. doi:10.1128/AEM.66.8.3376-3380.2000

Dionisi, H.M., Layton, A.C., Harms, G., Gregory, I.R., Robinson, K.G., Sayler, G.S., 2002. Quantification of Nitrosomonas oligotropha-like ammonia-oxidizing bacteria and nitrospira spp. from full-scale wastewater treatment plants by competitive PCR. Appl. Environ. Microbiol. 68, 245–253. doi:10.1128/AEM.68.1.245-253.2002

Duirk, S.E., Gombert, B., Croué, J.P., Valentine, R.L., 2005. Modeling monochloramine loss in the presence of natural organic matter. Water Res. 39, 3418–3431. doi:10.1016/j.watres.2005.06.003

French, E., Kozlowski, J.A., Mukherjee, M., Bullerjahn, G., Bollmann, A., 2012. Ecophysiological characterization of ammonia-oxidizing archaea and bacteria from freshwater. Appl. Environ. Microbiol. 78, 5773–5780. doi:10.1128/AEM.00432-12

Gavin, H.P., 2017. The Levenberg-Marquardt method for nonlinear least squares curve-fitting problems. Dep. Civ. Environ. Eng. Duke Univ. 1–17. doi:10.1080/10426914.2014.941480

Gieseke, A., Purkhold, U., Wagner, M., Amann, R., Schramm, A., 2001. Community Structure and Activity Dynamics of Nitrifying Bacteria in a Phosphate-Removing Biofilm. Appl. Environ. Microbiol. 67, 1351–1362. doi:10.1128/AEM.67.3.1351-1362.2001

Gomez-Alvarez, V., Schrantz, K.A., Pressman, J.G., Wahman, D.G., 2014. Biofilm community dynamics in bench-scale annular reactors simulating arrestment of chloraminated drinking water nitrification. Environ. Sci. Technol. 48, 5448–5457. doi:10.1021/es5005208

Graham, D.W., Knapp, C.W., Van Vleck, E.S., Bloor, K., Lane, T.B., Graham, C.E., 2007. Experimental demonstration of chaotic instability in biological nitrification. ISME J. 1, 385–93. doi:10.1038/ismej.2007.45

He, J.Z., Shen, J.P., Zhang, L.M., Zhu, Y.G., Zheng, Y.M., Xu, M.G., Di, H., 2007. Quantitative analyses of the abundance and composition of ammonia-oxidizing bacteria and ammonia-oxidizing archaea of a Chinese upland red soil under long-term fertilization practices. Environ. Microbiol. 9, 2364–2374. doi:10.1111/j.1462-2920.2007.01358.x

Huang, C.K., Shi, Y.J., El-Din, M.G., Liu, Y., 2015. Treatment of oil sands process-affected water (OSPW) using ozonation combined with integrated fixed-film activated sludge (IFAS). Water Res. 85, 167–176. doi:10.1016/j.watres.2015.08.019

Laspidou, C.S., Rittmann, B.E., 2002. A unified theory for extracellular polymeric substances, soluble microbial products, and active and inert bi omass. Water Res. 36, 2711–2720.

doi:10.1016/S0043-1354(01)00413-4

Maestre, J.P., Wahman, D.G., Speitel, G.E., 2016. Monochloramine Cometabolism by Mixed-Culture Nitrifiers under Drinking Water Conditions. Environ. Sci. Technol. 50, 6240–6248. doi:10.1021/acs.est.5b05641

Maestre, J.P., Wahman, D.G., Speitel, G.E., 2013. Monochloramine cometabolism by Nitrosomonas europaea under drinking water conditions. Water Res. 47, 4701–4709. doi:10.1016/j.watres.2013.05.019

McTavish, H., Fuchs, J.A., Hooper, A.B., 1993. Sequence of the gene coding for ammonia monooxygenase in Nitrosomonas europaea. J. Bacteriol. 175, 2436–2444.

Mitcham, R.P., Shelley, M.W., Wheadon, C.M., 1983. Free chlorine versus ammonia-chlorine: disinfection, trihalomethane formation, and zooplankton removal. J. Am. Water Works Assoc. 75, 196–198.

Ni, B.J., Ruscalleda, M., Pellicer-Nàcher, C., Smets, B.F., 2011. Modeling nitrous oxide production during biological nitrogen removal via nitrification and denitrification: Extensions to the general ASM models. Environ. Sci. Technol. 45, 7768–7776. doi:10.1021/es201489n

Norman, T.S., Harms, L.L., Looyenga, R.W., 1980. The Use of Chloramines To Prevent Trihalomethane Formation. J. Am. Water Works Assoc. 72, 176–180.

Okano, Y., Hristova, K.R., Leutenegger, C.M., Jackson, L.E., Denison, R.F., Gebreyesus, B., Lebauer, D., Scow, K.M., 2004. Application of Real-Time PCR to Study Effects of Ammonium on Population Size of Ammonia-Oxidizing Bacteria in Soil. Appl. Environ. Microbiol. 70, 1008–1016. doi:10.1128/AEM.70.2.1008-1016.2004

United States Environmental Protection Agency, 1985. Ambient Aquatic Life Water Quality Creteria for Chlorine. Florida.

Vikesland, P.J., Ozekin, K., Valentine, R.L., 2001. Monochloramine decay in model and distribution system waters. Water Res. 35, 1766–1776. doi:10.1016/S0043-1354(00)00406-1

Wahman, A.D.G., Maestre, J.P., Jr, G.E.S., 2016. Title : Monochloramine cometabolism by drinking water relevant nitrifying biofilm 362–373. doi:10.5942/jawwa.2016.108.0092

Wahman, D.G., Speitel, G.E., 2012. Relative importance of nitrite oxidation by hypochlorous acid under chloramination conditions. Environ. Sci. Technol. 46, 6056–6064. doi:10.1021/es300934x

Xue, Z., Lee, W.H., Coburn, K.M., Seo, Y., 2014. Selective reactivity of monochloramine with extracellular matrix components affects the disinfection of biofilm and detached clusters. Environ. Sci. Technol. 48, 3832–3839. doi:10.1021/es405353h

Zhang, Q., Davies, E.G.R., Bolton, J., Liu, Y., 2017. Monochloramine loss mechanisms in tap water. Water Environ. Res. doi:10.2175/106143017X14902968254421

Zhang, Q., Gaafar, M., Yang, R.-C., Ding, C., Davies, E.G.R., Bolton, J., Liu, Y., 2018. Field data analysis of active chlorine-containing stormwater samples. J. Environ. Manage. 206, 51–59.

CHAPTER 7. MONOCHLORAMINE DISSIPATION IN STORM SEWER SYSTEMS: FIELD TESTING AND MODEL DEVELOPMENT

7.1. Introduction

Monochloramine (NH_2Cl) has been widely used as a drinking water secondary disinfectant due to its long-lasting disinfection ability (US EPA et al., 2005; Wahman et al., 2009; Wahman and Speitel, 2012). However, NH_2Cl can contaminate the aquatic environment when tap water is discharged into storm sewer systems. Several outdoor tap water use activities can introduce NH_2Cl into storm sewers, such as lawn irrigation, garden watering, individual car washing, driveway cleaning and industrial pressure vessel testing (Balling et al., 2008; Mayer et al., 1999). To evaluate NH_2Cl concentrations in stormwater sewers, our previous studies collected and analyzed stormwater samples at different neighborhoods in Edmonton, Alberta, including residential and park locations with large garden and lawn areas, commercial locations such as car dealerships and rentals, and industrial areas with large pressure vessel boilers. These field sampling results showed that during the summers of 2015 and 2016, the total active chlorine (TAC) concentration in stormwater was as high as 0.77 mg/L (Zhang et al., 2018a), which exceeds the effluent discharge limit of 0.02 mg/L according to the Canada-wide strategy of the Canadian Council of Ministers of the Environment (CCME, 2009). Compared with concentrated precipitation periods, TAC concentrations were significantly higher under dry weather conditions (defined as low or no precipitation occurred during the sampling period).

Tap water is the main source of TAC in storm sewers during dry weather, and NH_2Cl is the dominant active chlorine species in tap water. To protect water sources from TAC contamination, NH_2Cl dissipation mechanisms in storm sewer systems were studied. Three pathways that contribute to NH_2Cl decay are (i) auto-decomposition, (ii) chemical reactions with natural organic matter (NOM) and nitrate (NO_2^-) in stormwater (Zhang et al., 2018a), and (iii) biological dissipation in the presence of storm sewer biofilm (Zhang et al., 2018b). The three pathways have been studied in previous research.

In the present study, a field NH_2Cl dissipation test with continuous tap water discharge into storm sewer pipes in Edmonton. A kinetics model was also developed to summarize three NH_2Cl decay pathways. The field test results were used to calibrate model parameters of NH_2Cl decay. The final model described the NH_2Cl decay process in storm sewers under various conditions, and can be applied to estimate NH_2Cl consumption between discharge points and outfalls. It is believed that this model can contribute to government regulation of outdoor tap water uses, thus decreasing fresh water contamination by TAC species. The model can be used to regulate the tap water discharge in other cities that have this issue in their storm sewers.

7.2. Material and methods

7.2.1. Site selection

The field NH_2Cl dissipation test was conducted in an uninterrupted storm sewer pipe (~ 200 m length) in a residential area in Edmonton. An uninterrupted pipe system was selected to prevent the impact of water flowing into branch pipelines (Fig. 7.1). The residential area was selected because of its low traffic density and its potential NH_2Cl contamination from grader irrigation and private car washing. The selected pipelines consisted of two pipe sections and were characterized in Fig. 7.1.

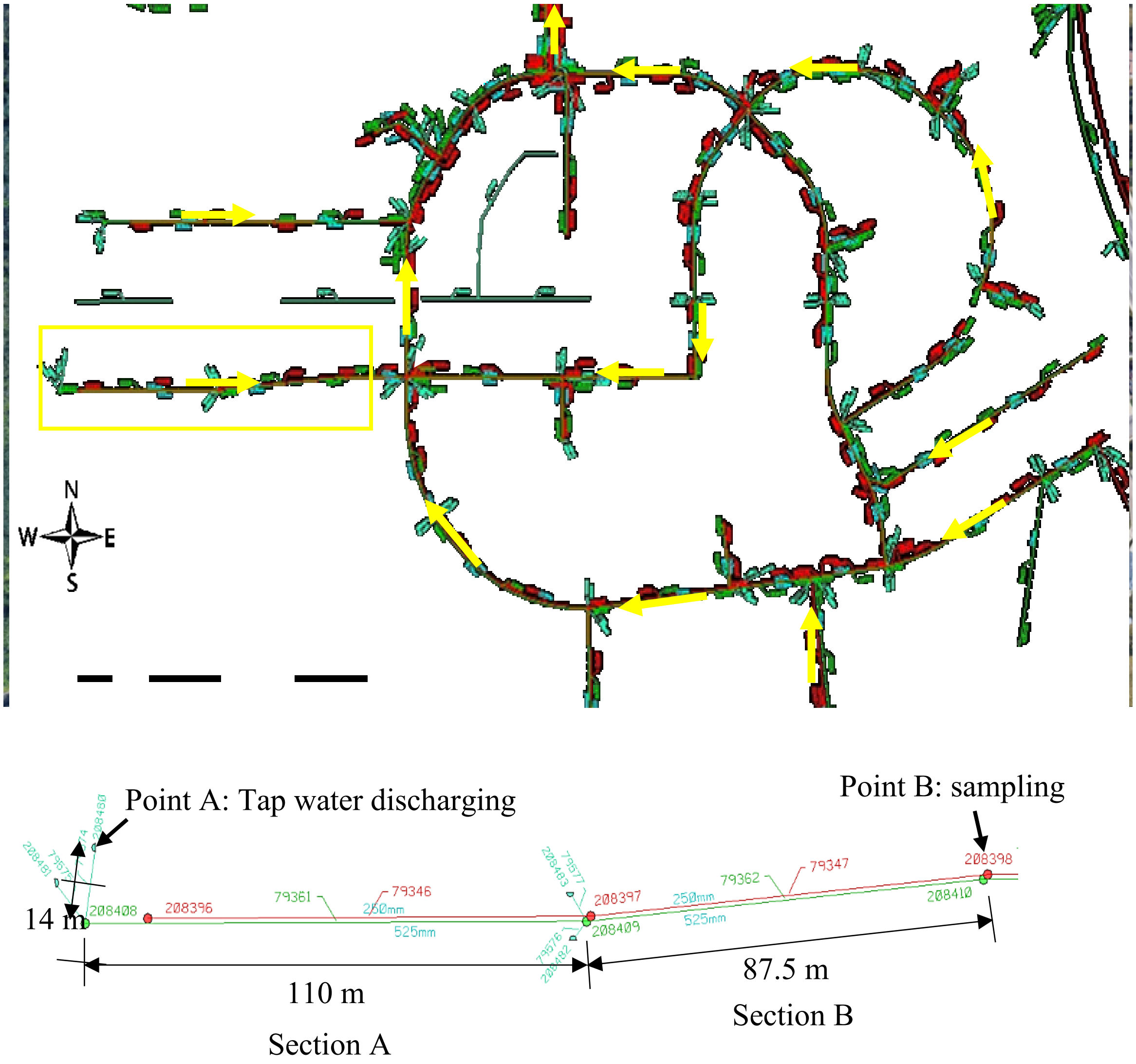

Pipe section	Material	Diameter (mm)	Slope (%)	Length (m)
A	Concrete	525	0.23%	110
B			0.27%	87.5

Fig. 7.1. Storm sewer network at field NH_2Cl dissipation test location (yellow arrow: flow direction; green lines: storm sewer pipelines; red lines: sewage pipelines).

7.2.2. Storm sewer sediment and biofilm characterization

Biofilm samples were collected on storm sewer pipes by scraping biofilms within a 1.1 cm diameter template over a randomly-selected submerged pipe surface. Samples were stored in sterilized centrifuge tubes containing 5 mL of stormwater collected in the same sewer. Biofilm samples were kept on ice during transportation, and preserved at 4 °C until they were analyzed. After samples were delivered in laboratory, genomic DNA was extracted and *q*PCR was conducted to analyze the populations of total bacterial and AOB following methods reported previously (Zhang et al., 2018c). The total bacteria and AOB were analyzed by *rpoB* and *amoA* functional genes. The primers used in *q*PCR analyzes are shown in Table S7.3. In addition, volatile suspended solids (VSS) were determined by following the protocol from Standard Methods 2540E (Wilder et al., 1997).

7.2.3 Tap water quality analysis

The initial NH_2Cl concentrations were analyzed as soon as the samples were taken, to prevent any changes of NH_2Cl concentrations through the NH_2Cl self-decomposition process. Other tap water characteristics such as pH, ammonium nitrogen (NH_4^+-N), nitrate nitrogen (NO_2^--N), alkalinity, and natural organic matter (NOM) concentrations were determined after samples were delivered to the laboratory for further NH_2Cl dissipation model development.

Since NH_2Cl is dominant in tap water, the NH_2Cl concentration was measured as the TAC concentration with the HACH (Loveland, USA) colorimetric method 8167 (detection limit 0.02 mg-Cl/L). The NH_4^+-N and alkalinity concentrations were analysed by HACH commercial test kits TNT832 and TNT870, respectively, with detection limits of 0.015 mg/L NH_3-N and 25 mg/L $CaCO_3$, respectively. The dissolved organic carbon (DOC) of tap water samples was measured with a Shimadzu TOC-L CPH E100 (detection limit 4 μg-C/L). The pH was analyzed by an Extech EC500 Waterproof ExStikII pH/conductivity meter (Extech instruments, USA).

7.2.4 Field NH_2Cl dissipation test

During the field NH_2Cl dissipation study, tap water was released from point A (a curb inlet) through a fire hydrant for approximately 40 min. The tap water flowrate was adjusted to 10 L/s before discharging. Once tap water was introduced into the storm sewer, time zero was recorded at point A. Tap water samples were collected every 5 min from time zero using 250 mL chlorine free glass bottles, and the NH_2Cl concentrations in these tap water samples were analyzed. At point B, time zero was recorded when the first flow was observed at this point, and the first sample was collected at time 1 min. After that, samples were collected every 5 to 10 min from the same manhole. NH_2Cl concentrations were analysed immediately after samples were collected to avoid the continuous reaction of NH_2Cl with storm sewer components in the samples. Moreover, dechloramination was conducted at point C and point D to prevent possible NH_2Cl contamination during the field test using commercial VITA-D-CHLOR tablets (Kent, USA).

7.3. Model development

7.3.1. Reaction assumptions

Fig. 7.2 describes the kinetic reactions involved in the NH_2Cl dissipation mechanisms in storm sewer systems. The reaction coefficients and equilibrium constants of these reactions were summarized in Table 7.1. The reactions involved in Fig. 7.2 and Table 7.1 were developed from literatures and our previous research (Duirk et al., 2005; Jafvert and Valentine, 1992; Maestre et al., 2016; Vikesland et al., 2001; Wahman and Speitel, 2012; Zhang et al., 2018a, 2018b, 2017).

To be specific, the NH_2Cl auto-decomposition kinetic model applied in this research was developed by Jafvert and Valentine (1992) and refined by Vikesland et al. (2001). In addition, Vikesland et al. (2001) also developed the reaction kinetics between NH_2Cl and NO_2^- in their research. Wahman and Speitel (2012) proposed that the reactions between NO_2^- and free chlorine that releases from NH_2Cl should also be considered in NH_2Cl dissipation models, and this assumption was also used in our current study. Moreover, NOM is a dominant factor that impact the NH_2Cl decay in bulk tap water and stormwater samples (Duirk et al., 2005, 2002, Zhang et al., 2018a, 2018c, 2017). The NH_2Cl reactions with stormwater and tap water NOM have been developed in a previous study (Zhang et al., 2017), which were included in the present model. The impacts of Fe^{2+} and Br^- were not considered in this model, since low concentrations were detected stormwater samples studied. Further, the storm sewers biofilm plays an important role in NH_2Cl dissipation, as it can directly react with NH_2Cl and consume NH_2Cl through AOB cometabolism (Maestre et al., 2016, 2013; Sathasivan et al., 2009). The NH_2Cl biological dissipation mechanisms in the presence of storm sewer biofilm have also been studied previously (Zhang et al. 2018c), and were included in the present model.

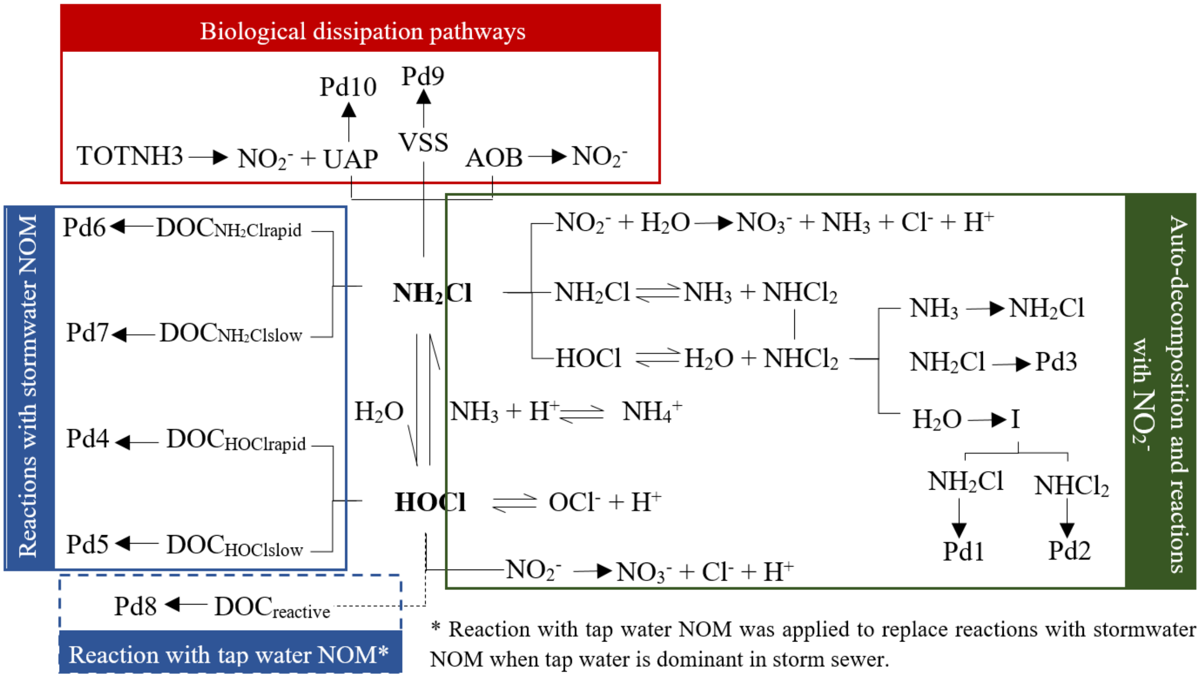

* Reaction with tap water NOM was applied to replace reactions with stormwater NOM when tap water is dominant in storm sewer.

Fig. 7.2. Reactions involving NH_2Cl dissipation in a storm sewer system (Pd: products).

Table 7.1. NH_2Cl dissipation reactions expected in storm sewers (Duirk et al., 2005; Jafvert and Valentine, 1992; Maestre et al., 2016; Vikesland et al., 2001; Wahman and Speitel, 2012; Zhang et al., 2018a, 2018b, 2017)

	Reaction	Rate Coefficient or Equilibrium Constant	References
NH_2Cl autodecomposition			
1	$HOCl + NH_3 \rightarrow NH_2Cl + H_2O$	$k_1 = 1.5 \times 10^{10} M^{-1}h^{-1}$	Morris and Isaac (1981)
2	$NH_2Cl + H_2O \rightarrow HOCl + NH_3$	$k_2 = 7.6 \times 10^{-2} h^{-1}$	
3	$HOCl + NH_2Cl \rightarrow NHCl_2 + H_2O$	$k_3 = 1.3 \times 10^{6} M^{-1}h^{-1}$	
4	$NH_2Cl + H_2O \rightarrow HOCl + NH_2Cl$	$k_4 = 2.7 \times 10^{-3} h^{-1}$	
5	$2\ NH_2Cl \rightarrow NHCl_2 + NH_3$	k_5[a]	Jafvert and Valentine (1992)
6	$NHCl_2 + NH_3 \rightarrow 2NH_2Cl$	$k_6 = 2.2 \times 10^{8} M^{-2}h^{-1}$	Hand and Margerum (1983)
7	$NHCl_2 + OH^- \rightarrow I$	$k_7 = 4.0 \times 10^{5} M^{-1}h^{-1}$	Jafvert and Valentine (1987)
8	$NHCl_2 + I$[b] $\rightarrow HOCl + pd1$[c]	$k_8 = 1.0 \times 10^{8} M^{-1}h^{-1}$	Leao (1981)
9	$NH_2Cl + I \rightarrow pd2$[c]	$k_9 = 3.0 \times 10^{7} M^{-1}h^{-1}$	
10	$NH_2Cl + NHCl_2 \rightarrow pd3$[c]	$k_{10} = 5.5\ M^{-1}h^{-1}$	
11	$HOCl = H^+ + OCl^-$	$pK_a = 7.5$	Snoeyink and Jenkins (1980)
12	$NH_4^+ = NH_3 + H^+$	$pK_a = 9.3$	
13	$H_2CO_3 = HCO_3^- + H^+$	$pK_a = 6.4$	
14	$HCO_3^- = CO_3^{2-} + H^+$	$pK_a = 10.3$	
Reactions with NO_2^-			
15	$HOCl + NO_2^- \rightarrow H^+ + NO_3^- + Cl^-$	k_{11}[d]	Margerum et al. (1994)
16	$NH_2Cl + NO_2^- + H_2O \rightarrow NH_4^+ + NO_3^- + Cl^- + H^+$	k_{12}[e]	Wahman and Speitel (2012)
Reactions with stormwater NOM			
17	$HOCl + DOC_{HOClrapid} \rightarrow pd4$[f]	$k_{13} = 2.3 \times 10^{6}\ M^{-1}h^{-1}$	Zhang et al. (2018a)
18	$HOCl + DOC_{HOClslow} \rightarrow pd5$[f]	$k_{14} = 3.9 \times 10^{2}\ M^{-1}h^{-1}$	
19	$NH_2Cl + DOC_{NH2Clrapid} \rightarrow pd6$[g]	$k_{15} = 3.4 \times 10^{4}\ M^{-1}h^{-1}$	
20	$NH_2Cl + DOC_{NH2Clslow} \rightarrow pd7$[g]	$k_{16} = 15.9\ M^{-1}h^{-1}$	
Reaction with tap water NOM			
21	$HOCl + DOC_{reactive} \rightarrow pd8$[f]	$k_{17} = 3.6 \times 10^{6}\ M^{-1}h^{-1}$	Zhang et al. (2017)
NH_2Cl biological dissipation			
22	NH_3 Monod: $TOTNH_3 \rightarrow NO_2^- + 0.062UAP$	k_{18}[h]	Zhang et al. (2018b)
23	Reaction with biofilm: $NH_2Cl + VSS$[i] $\rightarrow$ pd9[g]	$k_{19} = 2.5 \times 10^{3} M^{-1}h^{-1}$	
24	Cometabolism reaction: $NH_2Cl \rightarrow NO_2^-$	$k_{20} = 1.7 h^{-1}$	
25	UPA reaction: $NH_2Cl + UAP \rightarrow$ pd10[g]	$k_{21} = 9.6 \times 10^{5} M^{-1}h^{-1}$	

a. $k_5 = k_{\mathrm{H}}[\mathrm{H}^+] + k_{\mathrm{HCO_3}}[\mathrm{HCO_3}^-] + k_{\mathrm{H_2CO3}}[\mathrm{H_2CO_3}]$, where $k_{\mathrm{H^+}} = 2.5 \times 10^7 M^{-2}h^{-1}$, $k_{\mathrm{HCO_3}} = 800 M^{-2}h^{-1}$, $k_{\mathrm{H_2CO3}} = 4 \times 10^4 M^{-2}h^{-1}$;

b. I represents an unidentified intermediate in NH_2Cl auto-decomposition;

c. pd1-pd3 (pd means product) may include N_2, H_2O, Cl^-, H^+, NO_3^- and other unidentified products (Jafvert and Valentine, 1992);

d. $k_{11} = \frac{k_{1\mathrm{n}}[\mathrm{H}^+](1+\frac{k_{2\mathrm{n}}}{K_{4\mathrm{n}}}[\mathrm{NO_2}^-])}{\frac{k_{-1\mathrm{n}}}{k_{4\mathrm{n}}}[\mathrm{NH_3}]+(1+\frac{k_{2\mathrm{n}}}{K_{4\mathrm{n}}}[\mathrm{NO_2}^-])}$, where $k_{1\mathrm{n}} = 1.6 \times 10^8 M^{-2}h^{-1}$, $\frac{k_{-1\mathrm{n}}}{k_{4\mathrm{n}}} = 1.9 \times 10^6 M^{-1}$, $\frac{k_{2\mathrm{n}}}{K_{4\mathrm{n}}} = 217 M^{-1}$;

e. $k_{12} = \frac{k_{1\mathrm{n}'}[\mathrm{H}^+](1+\frac{k_{2\mathrm{n}}}{K_{4\mathrm{n}}}[\mathrm{NO_2}^-])}{\frac{k_{-1\mathrm{n}'}}{K_{4\mathrm{n}}}[\mathrm{NH_3}]+(1+\frac{k_{2\mathrm{n}}}{K_{4\mathrm{n}}}[\mathrm{NO_2}^-])}$, where $k_{1\mathrm{n}'} = k_{\mathrm{Hn}}[\mathrm{H}^+] + k_{\mathrm{HCO_3}n}[\mathrm{HCO_3}^-] + k_{\mathrm{H_2CO3n}}[\mathrm{H_2CO_3}]$, $k_{\mathrm{Hn}} = 4.3 \times 10^{10} M^{-2}h^{-1}$, $k_{\mathrm{HCO_3}n} = 4.3 \times 10^3 M^{-2}h^{-1}$, $k_{\mathrm{H_2CO_3}n} = 3.4 \times 10^6 M^{-2}h^{-1}$, $k_{-1\mathrm{n}'}/k_{4\mathrm{n}} = 2.1 \times 10^{-5} Mh \times k_{1n'}$;

f. pd4-5, pd8 may include H_2O, Cl^-, H^+, and chlorine disinfection by-products (DPBs);

g. pd6-7, pd 9-10 may include NH_4^+, H_2O, Cl^-, H^+, and NH_2Cl DPBs;

h. $k_{18} = \frac{1.8\times10^{-2}\times[\mathrm{AOB}]}{6.1\times10^{-5}+\alpha[\mathrm{TOTNH3}]}$ mg-TSSh^{-1}L^{-1}, [AOB] is considered to be constant, α is free ammonia to the TOTNH3 molar ratio;

i. The value of VSS used in this model is the VSS concentration (mg/L) divided by 156.9 based on the VSS consumption for each mole of NH_2Cl.

7.4. Results and discussion

7.4.1 Storm sewer and tap water characterization

To simulate NH_2Cl dissipation in storm sewer systems, the total biofilm concentration and the AOB concentration in storm sewer pipes were determined (Table 7.2). The VSS concentrations (Table 7.2) presented the total biomass concentration in the biofilms. Since the water temperature was 10 °C during the field test period, the modeled NH_2Cl decay rate was calibrated using a temperature coefficient developed in our previous studies (Zhang et al., 2017; Zhang et al. 2018b). Further, a time dependent coefficient *f* was introduced to calibrate the modeled NH_2Cl dissipation rates under various discharge times. The values of *f* under different sampling times (T) were solved based on field NH_2Cl dissipation tests. Before the field test, no flow was observed in the storm sewer pipes. Therefore, the impact of stormwater on NH_2Cl decay was not considered in this research.

Table 7.2. Average values of model parameters for field NH_2Cl decay tests in storm sewers

	Model parameter	**Measuring results**
Pipe biofilm	Biomass per pipe surface area (mg/cm^2)	8.06
	Water biofilm contact ratio (cm^2/L-water)	208
	Total bacterial functional gene (copies/cm^2)[a]	1.33E+10
	Total biomass concentration (mg/ L-water)	1676
	AOB functional gene (copies/cm^2)[b]	5.31E+08
	AOB concentration (mg/ L-water)	27
Tap water flow	DOC (mg/L)	1.39
	NH_4^+-N (mg/L)	0.390
	Alkalinity (mg CaCO3/L)	107
	pH	7.99
	Flow traveling time (points A to B, s)	420
	Flowrate (L/s)	10

a. Each bacterium is assumed to contain only one total bacterial functional gene (*rpoB* gene);

b. Each AOB cell is assumed to containe an average of 2.5 *amoA* gene (He et al., 2007; Okano et al., 2004).

7.4.2. Chloramine dissipation in storm water sewers

Fig. 7.3 shows the NH_2Cl concentration changes from the discharge point (point A) to the sampling point (point B) in the filed NH_2Cl decay test, as well as the comparison of modeled and field results at point B. As shown in Fig. 7.3(a), the initial NH_2Cl concentration at point A was slightly lower than the following values, and increased to a stable level at approximately 1.77 mg active Cl/L. The NH_2Cl concentration in the first sample showed a significant decrease at point B; and the extent of NH_2Cl decay reduced with the increase of discharge times. This observation indicates a decrease of NH_2Cl dissipation rate with tap water discharge time. With tap water continuously flowing into the storm sewer, the biofilm and other reactive components in the sewer pipes were consumed by NH_2Cl. In addition, under a flowrate of 10 L/s, some biofilm may be sloughed from the pipes. As fewer reactive components remained in the storm sewer, the NH_2Cl decay rate decreased. The modeled results from point B was simulated through the NH_2Cl dissipation model under the same condition of our field test. The detailed discussion of modeled results were described in the following sections.

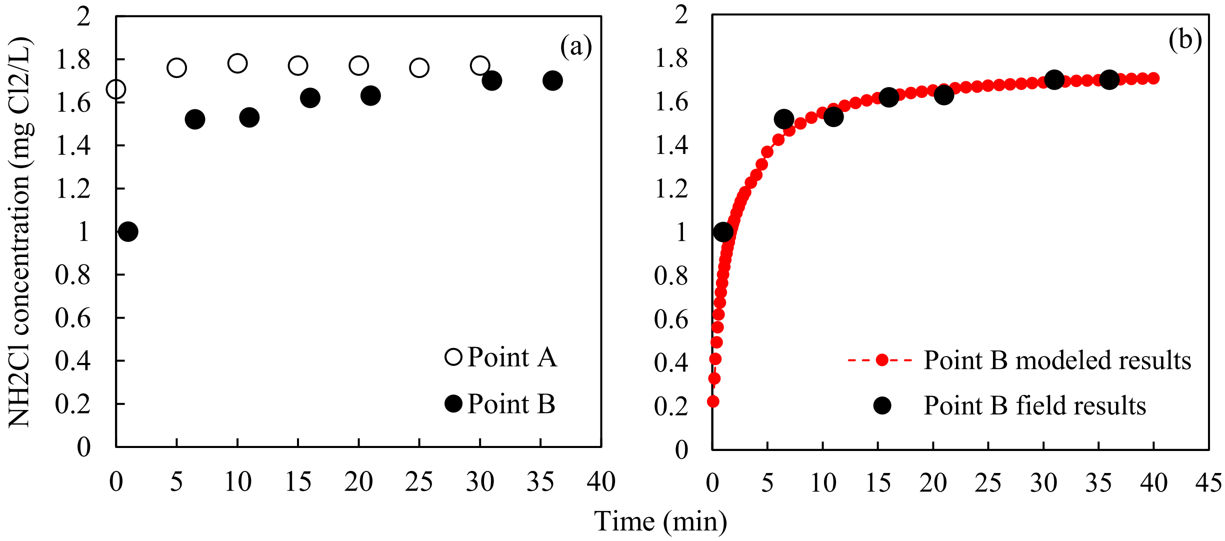

Fig. 7.3. NH_2Cl concentration changes in storm sewer pipes with continuous tap water discharge (a) field NH_2Cl concentration changes in point A and B; (b) the comparison of modeled and field results at point B.

7.4.3 Modeled monochloramine dissipation in storm water sewers

After tap water was discharged at point A, it took 420 seconds (s) to arrive at point B. That is, for each flow, the modeled NH_2Cl concentration at 420 s represents the residual NH_2Cl concentration at point B. As the first flush was not captured in our field testing, the NH_2Cl decay rate of first flush was solved by the model (Fig. 7.4, black line). After that, reactive components in the storm sewers continuously reacted with NH_2Cl and were flushed out by the tap water discharge causing the NH_2Cl decay rate to decrease. To describe this NH_2Cl decay rate variation under continuous discharge, f was introduced to calibrate the modeled results. The values of f under certain discharge times (T, min) were solved based on the field NH_2Cl dissipation rates from point A to point B, and the relationship between *f* and T can be described by the equation below (r^2=0.97):

$$f_T = \frac{1}{1.73T+1.90} \tag{1}$$

NH_2Cl dissipation curves under different discharge times were then solved by the model and are shown in Fig. 7.4. Fig. 7.3(b) shows the comparison of field testing and modeled NH_2Cl concentration changes with different discharge times at point B

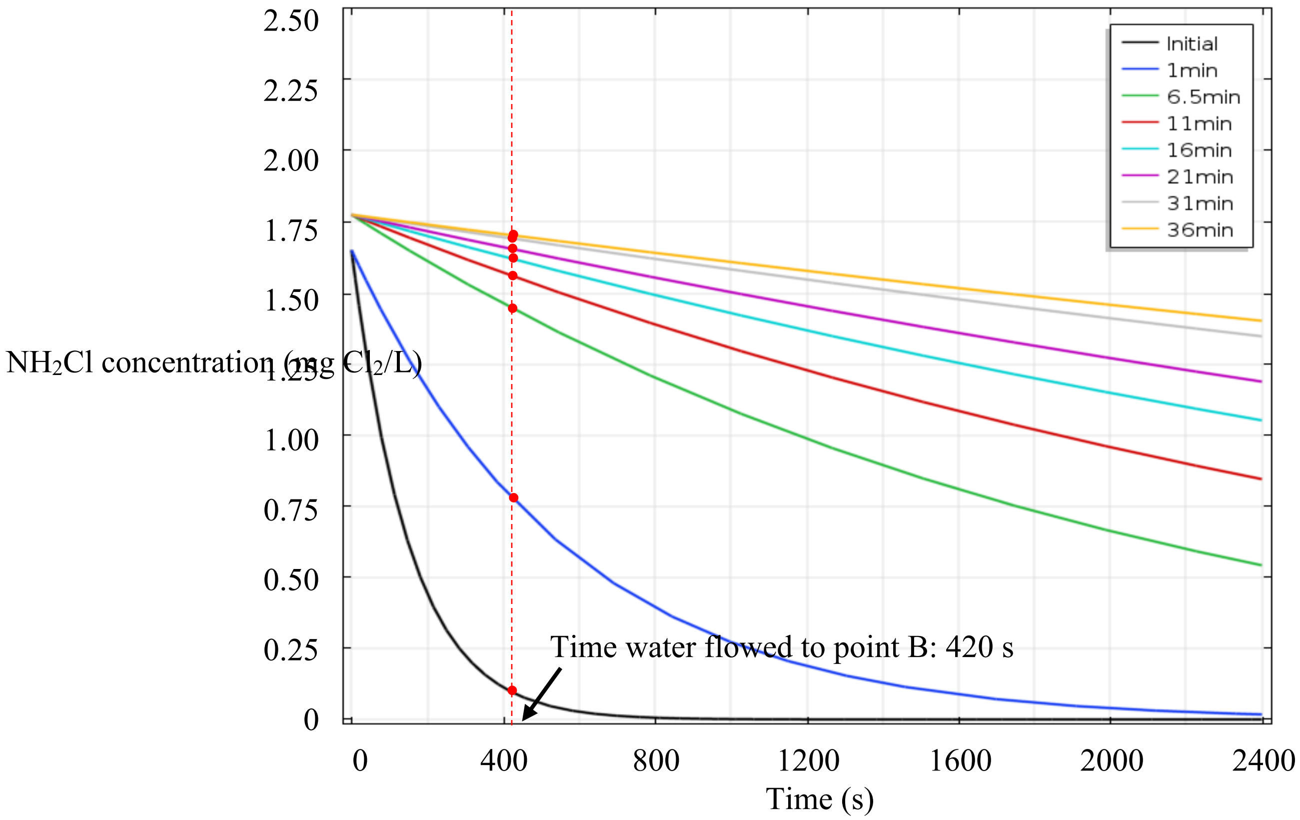

Fig. 7.4. Modeled NH_2Cl dissipation with continuous tap water discharge at different discharge times (Tap water discharge times are shown in the box at the top of the figure).

Fig. 7.4 describes the tap water NH_2Cl dissipations in storm sewers under certain discharge times. The initial NH_2Cl concentrations in the model were set at the values of the field test, and the discharge times correspond to the sample collection times at point B. The vertical dashed line indicates the modeled NH_2Cl concentrations of each flow traveled to point B. Fig. 7.4 shows that with longer discharge time, the NH_2Cl concentrations increased at point B, and the increment gradually reduced, which coincides with the field analysis results. To compare the modeled NH_2Cl concentrations at 420 s (point B) with field testing results under the same discharge periods (Fig. 7.3(b)), the simulated NH_2Cl concentrations correspond closely to the field data analyzed. Therefore, it can be proposed that the model developed in this study can be used to describe the NH_2Cl dissipation processes in Edmonton storm sewer systems under a continuous discharge condition.

Under dry weather conditions, some storm sewer pipes may still contain stormwater flow. With chloraminated water discharge, NH_2Cl dissipation rate can be accelerated by reacting with stormwater characteristics such as NOM, alkalinity, NO_2^- concentrations, pH, and water temperature (Duirk et al., 2005; Jafvert and Valentine, 1992; Maestre et al., 2016; Vikesland et al., 2001; Wahman and Speitel, 2012; Zhang et al., 2018b, 2018c, 2017). The impact of such stormwater characteristics should be considered in the NH_2Cl dissipation model. As biofilm and stormwater characteristics vary under different land use, NH_2Cl dissipation rates at residential, park, commercial, and industrial areas need to be simulated separately. In this research, the NH_2Cl dissipation rate boundaries were solved based on the maximum and minimum values of NH_4^+-N, NO_2^--N, alkalinity, NOM concentrations, pH, and temperature monitored in Edmonton stormwater during the summers of 2016 and 2015. The average biofilm concentration under each land use was applied in this model. The modeled results are shown in Fig. 7.6. The detailed pipe biofilm and stormwater characteristics can be found in Tables S7.1 and S7.2.

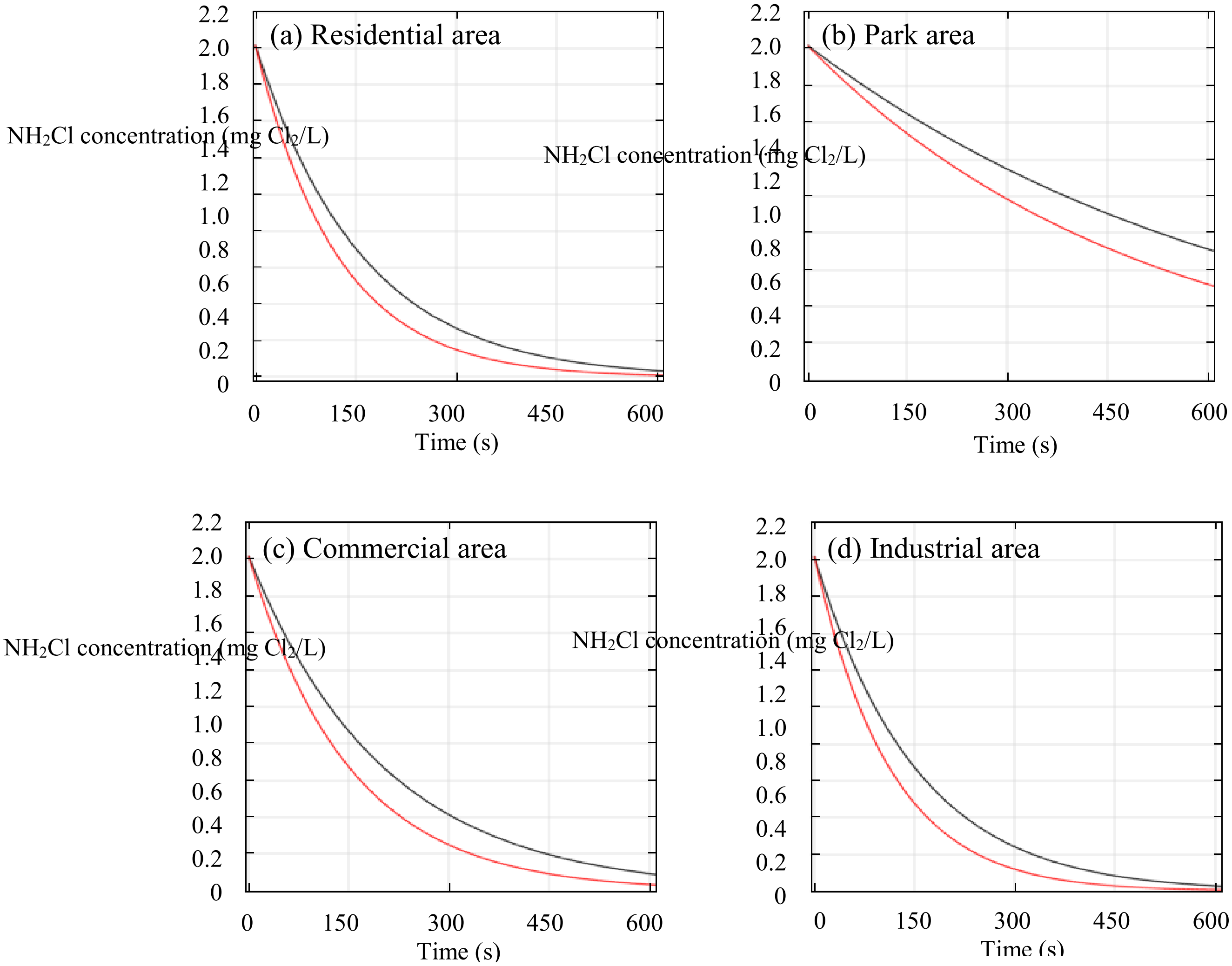

Fig. 7.6. Minimum (black curves) and maximum (red curves) NH_2Cl dissipation rates in storm sewers under (a) residential, (b) park, (c) commercial, and (d) industrial areas.

From Fig. 7.6, the minimum and maximum NH_2Cl dissipation rates do not show a great difference in each sampling area, which means the impact of stormwater characteristics on NH_2Cl decay rates are not significant. To avoid overestimating NH_2Cl dissipation rates, it is recommended that the minimum NH_2Cl decay rates be applied to regulate tap water outdoor discharges. Further, NH_2Cl dissipation shows similar rates in residential, commercial, and industrial areas, and can decay to almost 0 within 600 seconds. However, the NH_2Cl dissipation rates were significantly lower in park area. That is because less biofilm was detected under park area compared with other neighborhoods. Therefore, it can be deduced that rather than stormwater characteristics, biofilm plays a more important role in NH_2Cl dissipation in storm sewer systems.

7.5. Conclusion

The NH_2Cl dissipation rate in storm sewer systems depends on pH, temperature, natural organic matter and initial NH_2Cl concentrations, biofilm population and storm sewer characteristics. In addition, from the field test, a significant decay of the NH_2Cl concentration was observed in first discharge, but not much following that, which indicates the decrease of the NH_2Cl dissipation rate with extended NH_2Cl discharge periods. Therefore, to protect aquatic environment, the continuous tap water introduction to stormsewer should be carried out with cautious.

The NH_2Cl concentrations solved by the calibrated model corresponded closely to the field results, which indicates that the model used in this research can be applied to simulate NH_2Cl dissipation rates in real storm sewers with continuous discharge.

In addition, with stormwater in storm sewer systems, the NH_2Cl decay rate can be accelerated by reactions with stormwater components. To describe NH_2Cl dissipation in the presence of stormwater, the minimum and maximum NH_2Cl decay rates were solved based on the stormwater and sewer pipe characteristics. The results show that 2 mg active Cl/L in the initial NH_2Cl concentration can decay to 0 in residential, commercial, and industrial areas within nearly 600s, whereas decay is significantly slower in park area. As compared with stormwater characteristics, the NH_2Cl decay rate is impacted more by the biofilm concentration in storm sewers. With the model developed in this research, NH_2Cl dissipation rates under various stormwater and biofilm conditions can be simulated. This model can inform government regulations regarding tap water outdoor discharge, thus contributing to the protection of the aquatic environment.

7.6. Supplementary materials

7.6.1. Time coefficient *f* estimation

The relationship between *f* and discharge time (T) was assumed to follow the second order reaction, as a high regression coefficient can be obtained under this hypothesis. The values of *f* under different discharge times were solved based on the monochloramine decay rates in field test. Following this assumption, the linear relationship between 1/ *f* and T is shown in Fig. S7.1.

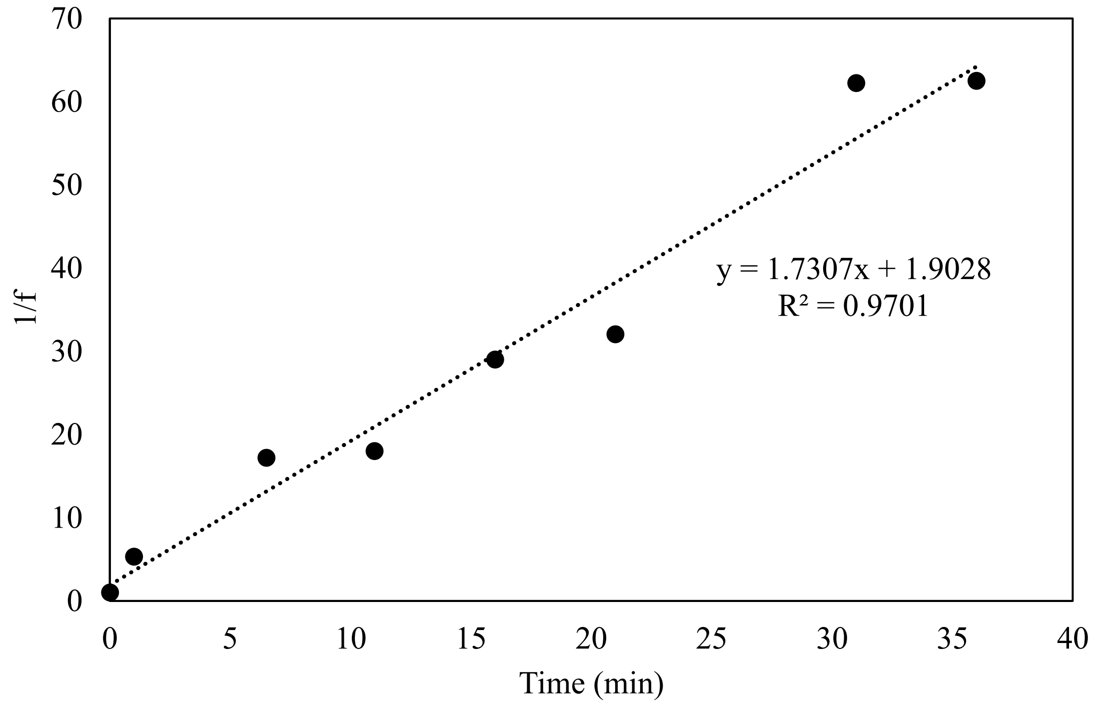

Fig. S7.1. The linear relationship between 1/f and discharge time (T)

7.6.2. Stormwater characteristics applied for monochloramine dissipation model

Table S7.1. The rapid and total reactive fractions in stormwater NOM under different locations

Sampling locations	Residential area	Park area	Commercial area	Industrial area
$S_{\mathrm{NH2Cl\ rapid}}$	0.00785	0.0055	0.0091	0.0102
$S_{\mathrm{HOCl\ rapid}}$	0.01255	0.0278	0.01375	0.02475
S_{Total}	0.705	0.695	1.02	0.76

Table S7.2. The maximum and minimum values of Edmonton stormwater characteristics during summer 2015 and summer 2016

	DOC (mg/L)		NH_4^+-N (mg/L)		Alkalinity (mg $CaCO_3$/L)		NO_2^--N (mg/L)		pH		Temperature (°C)		Bacteria concentration (mg VSS/L)	
	Min	Max	Min	Max	Min	Max	Min	Max	Min	Max	Min	Max	Total	AOB
RES*	10.0	16.8	0.00	6.65	157	415	0.02	0.75	7.81	8.39	10	22	1680	10.8
PRK*	5.1	21.4	0.00	0.12	66	566	0.01	0.52	7.76	8.48	10	22	323	2.2
COM*	8.7	37.0	0.00	2.85	151	482	0.04	0.38	7.8	8.37	10	22	1299	0.5
IND*	10.1	45.0	0.03	1.35	57	612	0.00	0.25	7.58	8.59	10	22	1749	18.0

*RES, PRK, COM and IND represent the residential, park, commercial and industrial sampling areas.

7.6.3. Quantitative polymerase chain reaction

Two independent *q*PCR assays were conducted to quantify the functional gene copy numbers of total bacterial and ammonia-oxidizing bacteria (AOB) by targeting *rpoB* and *amoA* genes respectively (Table S1). Reactions (20 μL) were performed in 96-well microplates. Each tube was separately loaded with 2 μL of genomic DNA (14-26ng/μL), followed by forward and reverse primers (1 μL), together with 10 μL 1* iTap SYBR Green Supermix with ROX (Bio-RAD, Hercules, California) and 6 μL PCR grade sterile water. Grade sterile water was also used as negative control. Triplicate composite samples were tested for all experiments. The efficiency of PCR amplification for each gene was between 80% and 110%. The primers used in qPCR analyzes are shown in Table S7.3.

Table S7.3. Primers used in *q*PCR

Bacteria types	**Target**	**Primer**	**Sequence (5'-3')**	**Reference**
Total Bacteria	rpoB gene	*rpoB 698f*	5'-AAC ATC GGT TTG ATC AAC-3'	Dahllof et al., 2000
		rpoB 2041r	5'-CGT TGC ATG TTG GTA CCC AT-3'	Dahllof et al., 2000
AOB	amoA gene	*amoA-1F*	5'-GGGGTTTCTACTGGTGGT-3'	McTavish et al., 1993
		amoA-2R	5'-CCCCTCKGSAAAGCCTTCTTC-3'	McTavish et al., 1993

7.7. References

Balling, R.C., Gober, P., Jones, N., 2008. Sensitivity of residential water consumption to variations in climate: An intraurban analysis of Phoenix, Arizona. Water Resour. Res. 44. doi:10.1029/2007WR006722

Dahllof, I., Baillie, H., Kjelleberg, S., 2000. rpoB-based microbial community analysis avoids limitations inherent in 16S rRNA gene intraspecies heterogeneity. Appl. Environ. Microbiol. 66, 3376–3380. doi:10.1128/AEM.66.8.3376-3380.2000

Duirk, S.E., Gombert, B., Choi, J., Valentine, R.L., 2002. Monochloramine loss in the presence of humic acid. J. Environ. Monit. 4, 85–89. doi:10.1039/b106047n

Duirk, S.E., Gombert, B., Croué, J.P., Valentine, R.L., 2005. Modeling monochloramine loss in the presence of natural organic matter. Water Res. 39, 3418–3431. doi:10.1016/j.watres.2005.06.003

Hand, V.C., Margerum, D.W., 1983. Kinetics and mechanisms of the decomposition of dichloramine in aqueous solution. Inorg. Chem. 22, 1449–1456. doi:10.1021/ic00152a007

He, J.Z., Shen, J.P., Zhang, L.M., Zhu, Y.G., Zheng, Y.M., Xu, M.G., Di, H., 2007. Quantitative analyses of the abundance and composition of ammonia-oxidizing bacteria and ammonia-oxidizing archaea of a Chinese upland red soil under long-term fertilization practices. Environ. Microbiol. 9, 2364–2374. doi:10.1111/j.1462-2920.2007.01358.x

Jafvert, C.T., Valentine, R.L., 1992. Reaction scheme for the chlorination of ammoniacal water. Environ. Sci. Technol. 26, 577–586. doi:10.1021/es00027a022

Jafvert, C.T., Valentine, R.L., 1987. Dichloramine decomposition in the presence of excess ammonia. Water Res. 21, 967–973. doi:10.1016/S0043-1354(87)80015-5

Leao, N.I., 1981. Dissertation. University of California.

Maestre, J.P., Wahman, D.G., Speitel, G.E., 2016. Monochloramine Cometabolism by Mixed-Culture Nitrifiers under Drinking Water Conditions. Environ. Sci. Technol. 50, 6240–6248. doi:10.1021/acs.est.5b05641

Maestre, J.P., Wahman, D.G., Speitel, G.E., 2013. Monochloramine cometabolism by Nitrosomonas europaea under drinking water conditions. Water Res. 47, 4701–4709. doi:10.1016/j.watres.2013.05.019

Margerum, D.W., Schurter, L.M., Hobson, J., Moore, E.E., 1994. Water chlorination chemistry: Nonmetal redox kinetics of chloramine and nitrite ion. Environ. Sci. Technol. 28, 331–337. doi:10.1021/es00051a021

Mayer, P.W., Deoreo, W.B., Opitz, E.M., Kiefer, J.C., Davis, W.Y., Dziegielewski, B., Nelson, J.O., 1999. Residential End Uses of Water. Aquacraft, Inc. Water Eng. Manag. 310. doi:4309b

McTavish, H., Fuchs, J.A., Hooper, A.B., 1993. Sequence of the gene coding for ammonia monooxygenase in Nitrosomonas europaea. J. Bacteriol. 175, 2436–2444.

Morris, J. C. and Isaac, R.A., 1981. A critical review of kinetic and thermodynamic constants for the aqueous chlorine-ammonia system, in: R. L. Jolley, W. A. Brungs, J. A. Cotruvo, R. B. Cumming, J. S. Mattice, and V.A.J. (Ed.), Water Chlorination: Environmental Impact and Health Effects. Arbor Science, Ann Arbor, MI, pp. 49–62.

Okano, Y., Hristova, K.R., Leutenegger, C.M., Jackson, L.E., Denison, R.F., Gebreyesus, B., Lebauer, D., Scow, K.M., 2004. Application of Real-Time PCR to Study Effects of Ammonium on Population Size of Ammonia-Oxidizing Bacteria in Soil. Appl. Environ. Microbiol. 70, 1008–1016. doi:10.1128/AEM.70.2.1008-1016.2004

Sathasivan, A., Chiang, J., Nolan, P., 2009. Temperature dependence of chemical and microbiological chloramine decay in bulk waters of distribution system. Water Sci. Technol. Water Supply 9, 493–499. doi:10.2166/ws.2009.387

Snoeyink, V., Jenkins, D., 1980. Water chemistry. Wiley, New York.

US EPA, OW, OGWDW, DWPD, 2005. Economic Analysis for the Final Stage 2 Disinfectants and Disinfection Byproducts Rule, Economic Analysis.

Vikesland, P.J., Ozekin, K., Valentine, R.L., 2001. Monochloramine decay in model and distribution system waters. Water Res. 35, 1766–1776. doi:10.1016/S0043-1354(00)00406-1

Wahman, D.G., Speitel, G.E., 2012. Relative importance of nitrite oxidation by hypochlorous acid under chloramination conditions. Environ. Sci. Technol. 46, 6056–6064. doi:10.1021/es300934x

Wahman, D.G., Wulfeck-Kleier, K. a, Pressman, J.G., 2009. Monochloramine disinfection kinetics of Nitrosomonas europaea using propidium monoazide quantitative PCR (PMA-qPCR) and LIVE/DEAD(R) BacLightTM. Appl Env. Microbiol 75, 5555–5562. doi:10.1128/AEM.00407-09

Wilder, B.H., Costa, H.S., Kosmowski, C.M., Purcell, W.E., 1997. 2540 Solids, in: Standard Methods for the Examination of Water and Wastewater. pp. 55–61.

Zhang, Q., Davies, E.G.R., Bolton, J., Liu, Y., 2017. Monochloramine loss mechanisms in tap water. Water Environ. Res. doi:10.2175/106143017X14902968254421

Zhang, Q., Davies, E.G.R., Bolton, J.R., Liu, Y., 2018a. Monochloramine loss mechanisms and dissolved organic matter characterization in stormwater. Sci. Total Environ. 631–632, 745–754. doi:10.1016/j.scitotenv.2018.02.335

Zhang, Q., Gaafar, M., Yang, R.C., Ding, C., Davies, E.G.R., Bolton, J.R., Liu, Y., 2018b. Field data analysis of active chlorine-containing stormwater samples. J. Environ. Manage. 206, 51–

59. doi:10.1016/j.jenvman.2017.10.009

Zhang, Q., Gaafar, M., Yang, R.C., Ding, C., Davies, E.G.R., Bolton, J.R., Liu, Y., 2018c. Field data analysis of active chlorine-containing stormwater samples. J. Environ. Manage. 206, 51–59. doi:10.1016/j.jenvman.2017.10.009

CHAPTER 8 GENERAL CONCLUIONS AND RECOMMENDATIONS

8.1. Thesis overview

Chloramination has been widely used for drinking water secondary disinfection because it maintains long-lasting disinfection and produces less disinfection by-products (DBPs). However, NH_2Cl, as the dominant disinfectant species in chloramination, can be discharged into municipal stormwater systems through outdoor tap water use, and ultimately fresh water sources. Tap water typically produces total active chlorine (TAC) concentrations of 2 mg/L. However, research has long suggested that the TAC is harmful to aquatic organisms at concentrations as low as 0.0053 mg/L (United States Environmental Protection Agency, 1985). Therefore, to protect the natural environment, it is important to study NH_2Cl dissipation mechanisms in storm sewer systems, and to assess the risks of tap water discharges. Although NH_2Cl contamination threatens surface waters, little research has monitored the NH_2Cl concentration variations and dissipation mechanisms in storm sewers.

Three pathways contribute to NH_2Cl dissipation in storm sewers – auto-decomposition, chemical reactions with components existing in stormwater such as natural organic matters (NOM) and NO_2^-, and biological dissipation. As tap water is the main source of TAC in stormwater, NH_2Cl dissipation in tap water was studied in this research. Stormwater samples were collected from upstream and downstream storm sewer manholes of residential, park, commercial, and industrial neighborhoods in Edmonton, Alberta, during the summers of 2015 and 2016. Samples were collected under both dry and wet weather conditions to compare the impact of precipitation on TAC concentrations in stormwater. TAC, temperature, DO concentration, oxidation/reduction potential (ORP), and pH were measured in stormwater samples. Other stormwater characteristics such as NH_4^+-N were analyzed in the laboratory. In addition, the biofilms on storm sewer pipelines were collected and bacterial communities were identified to study the impact of biofilm on the NH_2Cl decay rate. In lab experiments, the NH_2Cl dissipation through auto- and chemical pathways were studied first, and kinetic models were developed to simulate the NH_2Cl dissipation processes under various conditions. In terms of the NH_2Cl biological decomposition, storm sewer biofilms were cultured in annular reactors under two different pipe materials, PVC and concrete. The effect of pipe materials on microbial decay were then evaluated. Moreover, total bacteria, AOB and NOB in biofilms were identified. Batch experiments were conducted to evaluate the NH_2Cl biological decomposition mechanisms and develop kinetic model to predict these decay processes. The effect of NH_2Cl auto-, chemical-, and microbiological decay rates were finally combined and compared with data obtained from field NH_2Cl decay test to develop the NH_2Cl dissipation kinetic model for real storm sewers.

8.2. Conclusions

Conclusions derived from research described in chapters 3–7 are reported below.

1. In chapter 3, total active chlorine (TAC) concentrations in Edmonton stormwater samples were measured. The results show that the TAC concentrations varied from 0.02 to 0.77 mg/L during the summer of 2015 and from 0 to 0.24 mg/L during the summer of 2016, exceeding the CCME (2009) Canada-wide Strategy standard of 0.02 mg/L for permissible TAC concentrations at most of the sampling times. The high TAC concentrations in study samples may therefore pose a risk to the aquatic environment. As compared to summer 2015, more precipitation occurred during summer 2016. Therefore, it is believed that the high precipitation decreased the frequency of outdoor tap water uses, thus reducing the TAC in the stormwater. Other physicochemical and biological characteristics of stormwater and storm sewer biofilm samples showed no significant difference between 2015 and 2016. Statistical analysis method

‘RandomForest’ indicated that the NOM concentration was the dominant influence on NH_2Cl dissipation in stormwater samples. The NOM concentration was more accurately represented by the dissolved organic carbon (DOC) than by the chemical oxygen demand (COD) in the stormwater NH_2Cl dissipation study. In addition, the downstream industrial area had the highest DOC concentrations in both years, and these high DOC concentrations may lead to high TAC dissipation rates in this area.

2. In chapter 4, a chemical kinetic model was developed to predict NH_2Cl dissipation under different tap water conditions, and the results matched the experimental data, validating the model of NH_2Cl loss under various real water conditions. The dominant factors that impact the NH_2Cl loss rate in tap water are temperature, pH, the Cl/N ratio, and initial NH_2Cl and NOM concentrations. In this model, a rapid reaction between NH_2Cl and NOM was not considered, only the long-term reaction of HOCl released from NH_2Cl auto-decomposition with NOM was assumed to be present in this decay process. Under this assumption, the NOM reactive site fraction S and rate constant k_{docr} were calculated. Although these values may differ by tap water source, this research provides a useful general methodology for studies of NH_2Cl loss in drinking water. As low concentrations of Br^-, Fe^{2+}, and NO_2^- were detected in Edmonton tap water, the impact of these two species on NH_2Cl decay was not studied. Therefore, the model built in this study cannot be applied to predict the NH_2Cl loss rates in tap water containing high concentrations of these chemicals.
3. In chapter 5, NH_2Cl dissipation mechanisms in bulk stormwater were studied, and a kinetic model was developed to simulate NH_2Cl decay under various stormwater conditions, including pH, alkalinity, NH_4^+, NO_2^-, and dissolved organic matter (DOM) concentrations. Four pathways were assumed to involve reactions between DOM and active chlorine species in

NH_2Cl decay, including rapid and long-term reactions between DOM and NH_2Cl, and rapid and long-term reactions between DOM and HOCl released from NH_2Cl auto-decomposition. To simulate the NH_2Cl decay under different temperatures, a temperature coefficient α was introduced. Based on experimental data, a linear functional equation between temperature and α was solved. Our modeled NH_2Cl decay rates showed good matches with experimental results under various conditions. Further, the stormwater dissolved organic matter (SWDOM) characteristics were analyzed by Fourier transfer infrared (FTIR) spectroscopy and fluorescence excitation-emission matrix (EEM) spectroscopy. From the results, the SWDOM from different neighborhoods showed similar compositions, and humic substances were the dominant SWDOM. After reaction with NH_2Cl, although SWDOM was partially converted to inorganics, most of the organics remained as organic forms. It should be noted that humic substances, as the major precursors of disinfection by-products (DBPs), may cause an increase in DBP concentration in stormwater and then lead to contamination of fresh water sources.

4. In chapter 6, the stormwater biofilms were cultured in annular reactors under different initial TOTNH_3-N (the sum of NH_3-N and NH_4^+-N) concentrations. PVC and cement materials were selected for biofilm cultivation as these are common materials used in storm sewer pipes. Biofilms were collected along operation time and before and after chloramination with 1 mg active Cl/L of NH_2Cl, and total AOB and NOB functional genes were analyzed by *q*PCR. After biofilms were collected, the bacteria community structures and compositions were analyzed. Cement biofilms contained a higher abundance than PVC biofilms of all the identified functional genes under all the operation periods. More AOB and *Nitrospira* functional genes were observed in the high TOTNH_3-N reactor, while *Nitrobacter* functional genes showed no significant impact from this TOTNH3-N concentration elevation. Moreover, batch kinetic

experiments were conducted to study the NH_2Cl biological dissipation mechanisms. Three pathways contribute to NH_2Cl biological dissipation – reaction with biofilm only, consumption by AOB cometabolism, and reaction with utilization associated products (UAPs) produced by AOB activity. The experimental results indicated that rather than biomass and AOB cometabolism, NH_2Cl was mainly consumed by extracellular polymeric substance (EPS). As low temperature was detected in the real storm sewer during the summer experimental period, the impact of low temperature (10 °C) on NH_2Cl biological dissipation rates was studied,. Under different stormwater conditions, the experimental and modeled results showed good matches. Although the storm sewer environment varied at different locations, the methodology and assumptions developed in this research can be applied to NH_2Cl dissipation in other regions.

5. In chapter 7, NH_2Cl dissipation pathways were summarized and a comprehensive model was developed to study NH_2Cl decay processes in real storm sewers systems. In addition, a field test was conducted by continuously discharging tap water into a storm sewer for 40 min. NH_2Cl concentrations were analyzed every 5 to 10 min at the discharge point and at a downstream location. The results showed decreased NH_2Cl dissipation rates over the time of tap water discharge. To simulate the NH_2Cl decay with continuous discharge, a time coefficient f was introduced to calibrate the modeled results. After calibration, the NH_2Cl concentrations solved by the model can correspond closely to the field results. Therefore, it is believed that this model developed can simulate NH_2Cl dissipation in real storm sewers with continuous tap water discharge.

8.3. Recommendations for further work

8.3.1. Practical recommendations

To regulate the discharge of tap water to storm sewer systems, the comprehensive model developed in this research can be applied. With the detailed discharge information provided (flowrate, discharge volume, time and location), the model can then estimate the NH_2Cl concentration at outfall point. Therefore, before outdoor tap water discharge, it is recommended to simulate the NH_2Cl dissipation processes using this model, thus estimating the risk of tap water discharge. In this way, the potential contamination of NH_2Cl to aquatic environment can be significantly reduced.

8.3.2. Follow-on studies

After tap water was discharged into fresh water sources, the NH_2Cl concentration can be diluted significantly. Therefore, with a small tap water discharge, the NH_2Cl concentration may decrease to zero in a short period and show no harmful to aquatic biota. To determine the impact of tap water discharge to aquatic environment, it is suggested that the NH_2Cl dilution and dissipation processes in river water and other fresh water sources should be studied, and the NH_2Cl toxic zone in these water sources should be determined in the future studies.

Moreover, EPS is an important factor to react with NH_2Cl in biological dissipation processes. However, the constitution of EPS from different neighbourhoods may vary in storm sewers, leading to variations in NH_2Cl biological dissipation rates at these locations. Also, reaction mechanisms between NH_2Cl and EPS are not well understood and require additional investigation.

8.3.3. Large scientific questions

Florescence EEM analysis illustrates the high percentage of humic acid (HA) in SWDOM, which indicates the potential production of disinfection by-products (DBPs) in stormwater after tap water discharge, since HA is the dominant precursor of DBPs in chlorination and chloramination. Through the reactions between SWDOM and active chlorine species, the DBPs may accumulate in rivers. With these DBPs existing in rivers, they may come into drinking water as river water is the main source of drinking water. Therefore, to protect the drinking water safety, additional studies are required to detect the concentrations of DBPs in stormwater. However, although the DBPs in drinking water were well studied, the understanding of DBPs in stormwater is still lacking. Therefore, experiments should test for DBPs produced during the reaction between SWDOM and active chlorine species.

REFERENCES

Abrahamson, M., Lewandowski, Z., Geesey, G., Skjåk-Bræk, G., Strand, W., Christensen, B.E., 1996. Development of an artificial biofilm to study the effects of a single microcolony on mass transport. J. Microbiol. Methods 26, 161–169. doi:10.1016/0167-7012(96)00908-6

Al-Kofahi, S., Steele, C., VanLeeuwen, D., St. Hilaire, R., 2012. Mapping land cover in urban residential landscapes using very high spatial resolution aerial photographs. Urban For. Urban Green. 11, 291–301. doi:10.1016/j.ufug.2012.05.001

Alsulaili, A., Speitel, G.E., Katz, L.E., 2010. Monochloramine and total haloamine decay after a short prechlorination time in the presence of bromide. Water Sci. Technol. Water Supply 10, 512–516. doi:10.2166/ws.2010.171

Altmann, D., Stief, P., Amann, R., De Beer, D., Schramm, A., 2003. In situ distribution and activity of nitrifying bacteria in freshwater sediment. Environ. Microbiol. 5, 798–803. doi:10.1046/j.1469-2920.2003.00469.x

APHA/AWWA/WEF, 2012. Standard Methods for the Examination of Water and Wastewater. Stand. Methods 541. doi:ISBN 9780875532356

Arcangeli, J.P., Arvin, E., 1998. Modeling of the cometabolic biodegradation of trichloroethylene by toluene-oxidizing bacteria in a biofilm system. Environ. Sci. Technol. 31, 3044–3052. doi:10.1021/es9609112

AWWA, 2013. Nitrification Prevention and Control in Drinking Water. Am. Water Work. Assoc. 320.

AWWA, 2006. Fundamentals and Control of Nitrification in Chloraminated Drinking Water Distribution Systems (AWWA Manual M56), 1st ed. American Water Works Association, Denver, CO.

Bal Krishna, K.C., Sathasivan, A., Chandra Sarker, D., 2012. Evidence of soluble microbial products accelerating chloramine decay in nitrifying bulk water samples. Water Res. 46, 3977–3988. doi:10.1016/j.watres.2012.05.026

Balling, R.C., Gober, P., Jones, N., 2008. Sensitivity of residential water consumption to variations in climate: An intraurban analysis of Phoenix, Arizona. Water Resour. Res. 44. doi:10.1029/2007WR006722

Bernhardt, E.S., Band, L.E., Walsh, C.J., Berke, P.E., 2008. Understanding, managing, and minimizing urban impacts on surface water nitrogen loading. Ann. N. Y. Acad. Sci. doi:10.1196/annals.1439.014

Black, R., Sartaj, M., Mohammadian, A., Qiblawey, H.A.M., 2014. Biosorption of Pb and Cu using fixed and suspended bacteria. J. Environ. Chem. Eng. 2, 1663–1671. doi:10.1016/j.jece.2014.05.023

Bousher, A., Brimblecombe, P., Midgley, D., 1989. Kinetics of reactions in solutions containing monochloramine and bromide. Water Res. 23, 1049–1058. doi:10.1016/0043-1354(89)90180-2

Breiman, L., 2001. Random forests. Mach. Learn. 45, 5–32. doi:10.1023/A:1010933404324

Brodtmann, N. V., Russo, P.J., 1979. Use of chloramine for reduction of trihalomethanes and disinfection of drinking water. J. Am. Water Works Assoc. doi:10.2307/41269574

Brooks, A.S., Bartos, J.M., 1984. Effects of Free and Combined Chlorine and Exposure Duration on Rainbow Trout, Channel Catfish, and Emerald Shiners. Trans. Am. Fish. Soc. 113, 786–793. doi:10.1577/1548-8659(1984)113<786:EOFACC>2.0.CO;2

Brown, C., 2002. Water Use in the Professional Car Wash Industry, International Carwash Association, Inc.

Brown, C., 2000. Water Conservation in the Professional Car Wash Industry, A Report for the International Carwash Association.

Brungs, W. a, 1973. Effects of residual chlorine on aquatic life. J. Water Pollut. Control Fed. 45, 2180–2193. doi:10.2307/25038016

Canadian Council of Ministers of the Environment, 2009. Canada-wide Strategy for the Management of Municipal Wastewater Effluent. Winnipeg.

Canadian Council of Ministers of the Environment, 1999. Canadian Water Quality Guidelines for the Protection of Aquatic Life: Reactive Chlorine Species. Winnipeg.

Case, R.J., Boucher, Y., Dahllöf, I., Holmström, C., Doolittle, W.F., Kjelleberg, S., 2007. Use of 16S rRNA and rpoB genes as molecular markers for microbial ecology studies. Appl. Environ. Microbiol. 73, 278–288. doi:10.1128/AEM.01177-06

Cébron, A., Coci, M., Garnier, J., Laanbroek, H.J., 2004. Denaturing gradient gel electrophoretic analysis of ammonia-oxidizing bacterial community structure in the lower seine river: Impact of paris wastewater effluents. Appl. Environ. Microbiol. 70, 6726–6737. doi:10.1128/AEM.70.11.6726-6737.2004

Cébron, A., Garnier, J., 2005. Nitrobacter and Nitrospira genera as representatives of nitrite-oxidizing bacteria: Detection, quantification and growth along the lower Seine River (France). Water Res. 39, 4979–4992. doi:10.1016/j.watres.2005.10.006

Cessco Fabrication and Engineering Ltd, 2014. Products and services [WWW Document]. URL http://cessco.ca/fabrication/products-and-services (accessed 11.15.16).

Chen, J., Gu, B., LeBoeuf, E.J., Pan, H., Dai, S., 2002. Spectroscopic characterization of the structural and functional properties of natural organic matter fractions. Chemosphere 48, 59–68. doi:10.1016/S0045-6535(02)00041-3

Chen, W., Westerhoff, P., Leenheer, J.A., Booksh, K., 2003. Fluorescence Excitation-Emission Matrix Regional Integration to Quantify Spectra for Dissolved Organic Matter. Environ. Sci. Technol. 37, 5701–5710. doi:10.1021/es034354c

Chen, Z., Valentine, R.L., 2007. Formation of N-nitrosodimethylamine (NDMA) from humic substances in natural water. Environ. Sci. Technol. 41, 6059–6065. doi:10.1021/es0705386

Coburn, K.M., Wang, Q., Rediske, D., Viola, R.E., Hanson, B.L., Xue, Z., Seo, Y., 2016. Effects of extracellular polymeric substance composition on bacteria disinfection by monochloramine: Application of MALDI-TOF/TOF-MS and multivariate analysis. Environ. Sci. Technol. 50, 9197–9205. doi:10.1021/acs.est.6b00927

Coomes, P. a, Rockaway, T.D., Rivard, J., Kornstein, B., 2010. North America Residential Water Usage Trends Since 1992, US EPA.

Crittenden, J.C., Trussell, R.R., Hand, D.W., Howe, K.J., Tchobanoglous, G., 2012. MWH's Water Treatment: Principles and Design: Third Edition, MWH's Water Treatment: Principles and Design: Third Edition. doi:10.1002/9781118131473

Dahllof, I., Baillie, H., Kjelleberg, S., 2000. rpoB-based microbial community analysis avoids limitations inherent in 16S rRNA gene intraspecies heterogeneity. Appl. Environ. Microbiol. 66, 3376–3380. doi:10.1128/AEM.66.8.3376-3380.2000

Dalton, H., Stirling, D.I., 1982. Co-metabolism. Philos. Trans. R. Soc. London. Ser. B Biol. Sci. 297, 481–496.

Derrigan, J., Lin, L., Jensen, J., 1993. Comparison of free and total chlorine measurement methods in municipal wastewaters. Water Environ. Res. 65, 205–212. doi:doi:10.2175/WER.65.3.3

Dionisi, H.M., Layton, A.C., Harms, G., Gregory, I.R., Robinson, K.G., Sayler, G.S., 2002. Quantification of Nitrosomonas oligotropha-like ammonia-oxidizing bacteria and nitrospira spp. from full-scale wastewater treatment plants by competitive PCR. Appl. Environ. Microbiol. 68, 245–253. doi:10.1128/AEM.68.1.245-253.2002

Dlyamandoglu, V., Mariñas, B.J., Selleck, R.E., 1990. Stoichiometry and Kinetics of the Reaction of Nitrite with Free Chlorine in Aqueous Solutions. Environ. Sci. Technol. 24, 1711–1716. doi:10.1021/es00081a014

Duirk, S.E., Gombert, B., Choi, J., Valentine, R.L., 2002. Monochloramine loss in the presence of humic acid. J. Environ. Monit. 4, 85–89. doi:10.1039/b106047n

Duirk, S.E., Gombert, B., Croué, J.P., Valentine, R.L., 2005. Modeling monochloramine loss in the presence of natural organic matter. Water Res. 39, 3418–3431. doi:10.1016/j.watres.2005.06.003

Echeverry-Galvis, M.A., Peterson, J.K., Sulo-Caceres, R., 2014. The social nestwork: Tree structure determines nest placement in Kenyan weaverbird colonies. PLoS One 9. doi:10.1371/journal.pone.0088761

El Azher, N., Gourich, B., Vial, C., Soulami, M.B., Ziyad, M., 2008. Study of ferrous iron oxidation in Morocco drinking water in an airlift reactor. Chem. Eng. Process. Process Intensif. 47, 1877–1886. doi:10.1016/j.cep.2007.10.013

EPCOR Utilities Inc., 2015. Edmonton Waterworks Annual Report to Alberta Environment and Water 2015.

Fabris, R., Chow, C.W.K., Drikas, M., Eikebrokk, B., 2008. Comparison of NOM character in selected Australian and Norwegian drinking waters. Water Res. 42, 4188–4196. doi:10.1016/j.watres.2008.06.023

Fisher, R., 1925. Statistical methods for research workers, Biological monographs and manuals. doi:10.1056/NEJMc061160

Flury, M., Papritz, A., 1993. Bromide in the natural environment: occurrence and toxicity. J. Environ. Qual. 22, 747–758. doi:10.2134/jeq1993.00472425002200040017x

French, E., Kozlowski, J.A., Mukherjee, M., Bullerjahn, G., Bollmann, A., 2012. Ecophysiological characterization of ammonia-oxidizing archaea and bacteria from freshwater. Appl. Environ. Microbiol. 78, 5773–5780. doi:10.1128/AEM.00432-12

Gavin, H.P., 2017. The Levenberg-Marquardt method for nonlinear least squares curve-fitting problems. Dep. Civ. Environ. Eng. Duke Univ. 1–17. doi:10.1080/10426914.2014.941480

Gieseke, A., Purkhold, U., Wagner, M., Amann, R., Schramm, A., 2001. Community Structure and Activity Dynamics of Nitrifying Bacteria in a Phosphate-Removing Biofilm. Appl. Environ. Microbiol. 67, 1351–1362. doi:10.1128/AEM.67.3.1351-1362.2001

Gish, T.J., Zhuang, W., Helling, C.S., Kearney, P.C., 1986. Chemical transport under no-till field conditions. Geoderma 38, 251–259. doi:10.1016/0016-7061(86)90019-4

Gomez-Alvarez, V., Schrantz, K.A., Pressman, J.G., Wahman, D.G., 2014. Biofilm community dynamics in bench-scale annular reactors simulating arrestment of chloraminated drinking water nitrification. Environ. Sci. Technol. 48, 5448–5457. doi:10.1021/es5005208

Gordon, G., Sweetin, D.L., Smith, K., Pacey, G.E., 1991. Improvements in the N,N-diethyl-p-phenylenediamine method for the determination of free and combined residual chlorine through the use of FIA. Talanta 38, 145–149. doi:10.1016/0039-9140(91)80122-G

Graham, D.W., Knapp, C.W., Van Vleck, E.S., Bloor, K., Lane, T.B., Graham, C.E., 2007. Experimental demonstration of chaotic instability in biological nitrification. ISME J. 1, 385–93. doi:10.1038/ismej.2007.45

Guan, X.H., Shang, C., Chen, G.H., 2006. ATR-FTIR investigation of the role of phenolic groups in the interaction of some NOM model compounds with aluminum hydroxide. Chemosphere

65, 2074–2081. doi:10.1016/j.chemosphere.2006.06.048

Hand, V.C., Margerum, D.W., 1983. Kinetics and mechanisms of the decomposition of dichloramine in aqueous solution. Inorg. Chem. 22, 1449–1456. doi:10.1021/ic00152a007

Hao, O.J., Chien, C.M., Valentine, R.L., 1994. Kinetics of monochloramine reactions with nitrite. J. Environ. Eng.-asce. 120, 859–874. doi:10.1061/(ASCE)0733-9372(1994)120:4(859)

Harp, D.L., 2002. Current Technology of Chlorine Analysis for Water and Wastewater, Hach company.

He, J.Z., Shen, J.P., Zhang, L.M., Zhu, Y.G., Zheng, Y.M., Xu, M.G., Di, H., 2007. Quantitative analyses of the abundance and composition of ammonia-oxidizing bacteria and ammonia-oxidizing archaea of a Chinese upland red soil under long-term fertilization practices. Environ. Microbiol. 9, 2364–2374. doi:10.1111/j.1462-2920.2007.01358.x

Hedges, J.I., Cowie, G.L., Richey, J.E., Quay, P.D., Benner, R., Strom, M., Forsberg, B.R., 1994. Origins and Processing of Organic-Matter in the Amazon River as Indicated by Carbohydrates and Amino-Acids. Limnol. Oceanogr. 39, 743–761. doi:10.4319/lo.1994.39.4.0743

Heeb, M.B., Criquet, J., Zimmermann-Steffens, S.G., Von Gunten, U., 2014. Oxidative treatment of bromide-containing waters: Formation of bromine and its reactions with inorganic and organic compounds - A critical review. Water Res. 48, 15–42. doi:10.1016/j.watres.2013.08.030

Hooper, A.B., Vannelli, T., Bergmann, D.J., Arciero, D.M., 1997. Enzymology of the oxidation of ammonia to nitrite by bacteria, in: Antonie van Leeuwenhoek, International Journal of General and Molecular Microbiology. pp. 59–67. doi:10.1023/A:1000133919203

Hrudey, S.E., 2009. Chlorination disinfection by-products, public health risk tradeoffs and me.

Water Res. doi:10.1016/j.watres.2009.02.011

Huang, C.K., Shi, Y.J., El-Din, M.G., Liu, Y., 2015. Treatment of oil sands process-affected water (OSPW) using ozonation combined with integrated fixed-film activated sludge (IFAS). Water Res. 85, 167–176. doi:10.1016/j.watres.2015.08.019

Jacangelo, J.G., DeMarco, J., Owen, D.M., Randtke, S.J., 1995. Selected processes for removing NOM: An overview. J. / Am. Water Work. Assoc. 87, 64–77. doi:10.2307/41295153

Jafvert, C.T., Valentine, R.L., 1992. Reaction scheme for the chlorination of ammoniacal water. Environ. Sci. Technol. 26, 577–586. doi:10.1021/es00027a022

Jafvert, C.T., Valentine, R.L., 1987. Dichloramine decomposition in the presence of excess ammonia. Water Res. 21, 967–973. doi:10.1016/S0043-1354(87)80015-5

Jury, W.A., Elabd, H., Resketo, M., 1986. Field Study of Napropamide Movement Through Unsaturated Soil. Water Resour. Res. 22, 749–755. doi:10.1029/WR022i005p00749

Kaushal, S.S., Groffman, P.M., Band, L.E., Elliott, E.M., Shields, C.A., Kendall, C., 2011. Tracking nonpoint source nitrogen pollution in human-impacted watersheds. Environ. Sci. Technol. 45, 8225–8232. doi:10.1021/es200779e

Kiéné, L., Lu, W., Lévi, Y., 1998. Relative importance of the phenomena responsible for chlorine decay in drinking water distribution systems. Water Sci. Technol. 38, 219–227. doi:10.1016/S0273-1223(98)00583-6

Kim, J., Chung, Y., Shin, D., Kim, M., Lee, Y., Lim, Y., Lee, D., 2003. Chlorination by-products in surface water treatment process. Desalination 151, 1–9. doi:10.1016/S0011-9164(02)00967-0

Knocke, W.R., 1990. Alternative oxidants for the removal of soluble iron and manganese. AWWA Research Foundation and American Water Works Association.

Kool, J.L., Carpenter, J.C., Fields, B.S., 1999. Effect of monochloramine disinfection of municipal drinking water on risk of nosocomial Legionnaires' disease. Lancet 353, 272–277. doi:10.1016/S0140-6736(98)06394-6

Kuang, X., Sansalone, J., 2011. Cementitious porous pavement in stormwater quality control: pH and alkalinity elevation. Water Sci. Technol. 63, 2992–2998. doi:10.2166/wst.2011.505

Larson, R.A., Weber, E.J., 1994. Reaction mechanisms in environmental organic chemistry. CRC press.

Laspidou, C.S., Rittmann, B.E., 2002. A unified theory for extracellular polymeric substances, soluble microbial products, and active and inert bi omass. Water Res. 36, 2711–2720. doi:10.1016/S0043-1354(01)00413-4

Leao, N.I., 1981. Dissertation. University of California.

LeChevallier, M.W., Cawthon, C.D., Lee, R.G., 1988. Factors promoting survival of bacteria in chlorinated water supplies. Appl. Environ. Microbiol. 54, 649–654.

Liaw, a, Wiener, M., 2002. Classification and Regression by randomForest. R news 2, 18–22. doi:10.1177/154405910408300516

Liu, A., Egodawatta, P., Guan, Y., Goonetilleke, A., 2013. Influence of rainfall and catchment characteristics on urban stormwater quality. Sci. Total Environ. 444, 255–262. doi:10.1016/j.scitotenv.2012.11.053

Liu, H.M., Amy, G., 1993. Modeling Partitioning and Transport Interactions Between Natural Organic-Matter and Polynuclear Aromatic-Hydrocarbons in Groundwater. Environ. Sci. Technol. 27, 1553–1562.

Liu, S.G., Fan, C.F., Zhu, Z.L., 2011. Kinetics of Monochloramine Decay in Model and Distribution System Waters. Adv. Mater. Res. 183–185, 834–838.

doi:10.4028/www.scientific.net/AMR.183-185.834

Luh, J., Mariñas, B.J., 2014. Kinetics of bromochloramine formation and decomposition. Environ. Sci. Technol. 48, 2843–2852. doi:10.1021/es4036754

Lyman, R.A., 1992. Peak and off-peak residential water demand. Water Resour. Res. 28, 2159–2167. doi:10.1029/92WR01082

Ma, X., Bibby, K., 2017. Free chlorine and monochloramine inactivation kinetics of Aspergillus and Penicillium in drinking water. Water Res. 120, 265–271. doi:10.1016/j.watres.2017.04.064

Maestre, J.P., Wahman, D.G., Speitel, G.E., 2016. Monochloramine Cometabolism by Mixed-Culture Nitrifiers under Drinking Water Conditions. Environ. Sci. Technol. 50, 6240–6248. doi:10.1021/acs.est.5b05641

Maestre, J.P., Wahman, D.G., Speitel, G.E., 2013. Monochloramine cometabolism by Nitrosomonas europaea under drinking water conditions. Water Res. 47, 4701–4709. doi:10.1016/j.watres.2013.05.019

Makepeace, D.K., Smith, D.W., Stanley, S.J., 1995. Urban stormwater quality: Summary of contaminant data. Crit. Rev. Environ. Sci. Technol. 25, 93–139. doi:10.1080/10643389509388476

Margerum, D.W., Schurter, L.M., Hobson, J., Moore, E.E., 1994. Water chlorination chemistry: Nonmetal redox kinetics of chloramine and nitrite ion. Environ. Sci. Technol. 28, 331–337. doi:10.1021/es00051a021

Matilainen, A., Vepsäläinen, M., Sillanpää, M., 2010. Natural organic matter removal by coagulation during drinking water treatment: A review. Adv. Colloid Interface Sci. 159, 189–197. doi:10.1016/j.cis.2010.06.007

Mayer, P.W., Deoreo, W.B., Opitz, E.M., Kiefer, J.C., Davis, W.Y., Dziegielewski, B., Nelson, J.O., 1999. Residential End Uses of Water. Aquacraft, Inc. Water Eng. Manag. 310. doi:4309b

Mays, L.W., 2002. Water demand analysis, in: Urban Water Supply Handbook. McGRAW-HILL.

McElmurry, S.P., Long, D.T., Voice, T.C., 2014. Stormwater Dissolved Organic Matter: Influence of Land Cover and Environmental Factors. Environ. Sci. Technol. 48, 45–53. doi:10.1021/es402664t

McTavish, H., Fuchs, J.A., Hooper, A.B., 1993. Sequence of the gene coding for ammonia monooxygenase in Nitrosomonas europaea. J. Bacteriol. 175, 2436–2444.

Mitcham, R.P., Shelley, M.W., Wheadon, C.M., 1983. Free chlorine versus ammonia-chlorine: disinfection, trihalomethane formation, and zooplankton removal. J. Am. Water Works Assoc. 75, 196–198.

Moberg, L., Karlberg, B., 2000. An improved N,N'-diethyl-p-phenylenediamine (DPD) method for the determination of free chlorine based on multiple wavelength detection. Anal. Chim. Acta 407, 127–133. doi:10.1016/S0003-2670(99)00780-1

Morris, J. C. and Isaac, R.A., 1981. A critical review of kinetic and thermodynamic constants for the aqueous chlorine-ammonia system, in: R. L. Jolley, W. A. Brungs, J. A. Cotruvo, R. B. Cumming, J. S. Mattice, and V.A.J. (Ed.), Water Chlorination: Environmental Impact and Health Effects. Arbor Science, Ann Arbor, MI, pp. 49–62.

Morris, J.C., Christman, R.F., Glaze, W.H., Helz, G.R., Hoehn, R.C., Jolley, R.L., 1980. The chemistry of disinfectants in water: reactions and products, Drinking Water and Health. National Academy of Sciences, Washington, DC. doi:10.1016/0160-4120(91)90308-D

Muyzer, G., De Waal, E.C., Uitterlinden, A.G., 1993. Profiling of complex microbial populations by denaturing gradient gel electrophoresis analysis of polymerase chain reaction-amplified genes coding for 16S rRNA. Appl. Environ. Microbiol. 59, 695–700. doi:0099-2240/93/030695-06$02.00/0

Muyzer, G., Teske, A., Wirsen, C.O., Jannasch, H.W., 1995. Phylogenetic relationships of Thiomicrospira species and their identification in deep-sea hydrothermal vent samples by denaturing gradient gel electrophoresis of 16S rDNA fragments. Arch. Microbiol. 164, 165–172. doi:10.1007/BF02529967

Nakanishi, K., Solomon, P.H., 1977. Infrared Absorption Spectroscopy, Book section Analytical Techniques for Atmospheric Measurement.

Ni, B.J., Ruscalleda, M., Pellicer-Nàcher, C., Smets, B.F., 2011. Modeling nitrous oxide production during biological nitrogen removal via nitrification and denitrification: Extensions to the general ASM models. Environ. Sci. Technol. 45, 7768–7776. doi:10.1021/es201489n

Norman, T.S., Harms, L.L., Looyenga, R.W., 1980. The Use of Chloramines To Prevent Trihalomethane Formation. J. Am. Water Works Assoc. 72, 176–180.

Nouri, H., Beecham, S., Kazemi, F., Hassanli, A.M., 2013. A review of ET measurement techniques for estimating the water requirements of urban landscape vegetation. Urban Water J. 10, 247–259. doi:10.1080/1573062X.2012.726360

Okano, Y., Hristova, K.R., Leutenegger, C.M., Jackson, L.E., Denison, R.F., Gebreyesus, B., Lebauer, D., Scow, K.M., 2004. Application of Real-Time PCR to Study Effects of Ammonium on Population Size of Ammonia-Oxidizing Bacteria in Soil. Appl. Environ. Microbiol. 70, 1008–1016. doi:10.1128/AEM.70.2.1008-1016.2004

Pedersen, K., 1990. Biofilm development on stainless steel and pvc surfaces in drinking water. Water Res. 24, 239–243. doi:10.1016/0043-1354(90)90109-J

Peuravuori, J., Pihlaja, K., Välimäki, N., 1997. Isolation and characterization of natural organic matter from lake water: Two different adsorption chromatographic methods. Environ. Int. 23, 453–464. doi:10.1016/S0160-4120(97)00050-0

Piché, S., Larachi, F., 2006. Oxidation kinetics of Iron(II) complexes of trans-1,2-diaminocyclohexanetetraacetate (cdta) with dissolved oxygen: Reaction mechanism, parameters of activation and kinetic salt effects. Chem. Eng. Sci. 61, 3452–3462. doi:10.1016/j.ces.2005.12.015

Pitt, R., Maestre, A., Morquecho, R., 2004. The national stormwater quality database (NSQD, version 1.1), 1st Annual Stormwater Management Research Symposium Proceedings.

Postawa, A., Hayes, C., Criscuoli, A., Angelakis, F.M.A.N., Rose, J.B., Maier, A., McAvoy, D.C., 2013. Best practice guide on the control of iron and manganese in water supply. IWA publishing.

PricewaterhouseCoopers LLP, 2008. Alberta Pressure Vessel Manufacturing Sector Benchmarking Report 2008 Provincial Trends : Global Currents, PricewaterhouseCoopers LLP.

Qin, J.J., Oo, M.H., Kekre, K.A., Knops, F., Miller, P., 2006. Impact of coagulation pH on enhanced removal of natural organic matter in treatment of reservoir water. Sep. Purif. Technol. 49, 295–298. doi:10.1016/j.seppur.2005.09.016

R Development Core Team, R.F.F.S.C., 2008. R: A Language and Environment for Statistical Computing. Vienna Austria R Found. Stat. Comput. doi:10.1007/978-3-540-74686-7

Rittmann, B.E., Regan, J.M., Stahl, D.A., 1994. Nitrification as a source of soluble organic substrate in biological treatment. Water Sci. Technol. 30, 1–8.

Sablayrolles, C., Vialle, C., Vignoles, C., Montrejaud-Vignoles, M., 2010. Impact of carwash discharge on stormwater quality (Toulouse, France). Water Sci. Technol. 62, 2737–2746. doi:10.2166/wst.2010.929

Sarin, P., Snoeyink, V.L., Bebee, J., Jim, K.K., Beckett, M.A., Kriven, W.M., Clement, J.A., 2004. Iron release from corroded iron pipes in drinking water distribution systems: Effect of dissolved oxygen. Water Res. 38, 1259–1269. doi:10.1016/j.watres.2003.11.022

Sarin, P., Snoeyink, V.L., Bebee, J., Kriven, W.M., Clement, J.A., 2001. Physico-chemical characteristics of corrosion scales in old iron pipes. Water Res. 35, 2961–2969. doi:10.1016/S0043-1354(00)00591-1

Sathasivan, A., Chiang, J., Nolan, P., 2009. Temperature dependence of chemical and microbiological chloramine decay in bulk waters of distribution system. Water Sci. Technol. Water Supply 9, 493–499. doi:10.2166/ws.2009.387

Sathasivan, A., Fisher, J., Kastl, G., 2005. Simple method for quantifying microbiologically assisted chloramine decay in drinking water. Environ. Sci. Technol. 39, 5407–5413. doi:10.1021/es048300u

Sen-Kavurmaci, S., Birben, N.C., Tomruk, A., Bekbolet, M., 2016. Characterization of organic matter in natural waters by EEM fluorescence properties. Desalin. Water Treat. 57. doi:10.1080/19443994.2015.1022804

Sharp, E.L., Parsons, S.A., Jefferson, B., 2006a. Seasonal variations in natural organic matter and its impact on coagulation in water treatment. Sci. Total Environ. 363, 183–194. doi:10.1016/j.scitotenv.2005.05.032

Sharp, E.L., Parsons, S.A., Jefferson, B., 2006b. The impact of seasonal variations in DOC arising from a moorland peat catchment on coagulation with iron and aluminium salts. Environ. Pollut. 140, 436–443. doi:10.1016/j.envpol.2005.08.001

Shlens, J., 2014. A Tutorial on Principal Component Analysis. ArXiv 1–13. doi:10.1.1.115.3503

Siripong, S., Rittmann, B.E., 2007. Diversity study of nitrifying bacteria in full-scale municipal wastewater treatment plants. Water Res. 41, 1110–1120. doi:10.1016/j.watres.2006.11.050

Smith, E., Kamal, Y., 2009. Optimizing treatment for reduction of disinfection by-product (DBP) formation. Water Sci. Technol. Water Supply 9, 191–198. doi:10.2166/ws.2009.120

Snoeyink, V., Jenkins, D., 1980. Water chemistry. Wiley, New York.

Sollars, C.J., Peters, C.J., Perry, R., 1982. Bromide in urban runoff — water quality considerations, in: Efects of Waste Disposal on Groundwater and Surface Water (Proceedings of the Exeter Symposium). pp. 101–112.

Sontheimer, H., Kolle, W., Snoeyink, V.L., 1981. SIDERITE MODEL OF THE FORMATION OF CORROSION-RESISTANT SCALES. J. / Am. Water Work. Assoc.

Strassler, E., Pritts, J., Strellec, K., 1999. Preliminary data summary of urban storm water best management practices, US EPA.

Trote, T.W., Inman, G.W., Donald Johnson, J., 1980. Kinetics of Monochloramine Decomposition in the Presence of Bromide. Environ. Sci. Technol. 14, 544–549. doi:10.1021/es60165a008

United States Environmental Protection Agency, 1985. Ambient Aquatic Life Water Quality Creteria for Chlorine. Florida.

US EPA, OW, OGWDW, DWPD, 2005. Economic Analysis for the Final Stage 2 Disinfectants and Disinfection Byproducts Rule, Economic Analysis.

Valentine, R.L., 1986. Bromochloramine Oxidation of N , N-Diethyl-p -phenylenediamine in the Presence of Monochloramine. Environ. Sci. Technol. 20, 166–170. doi:0013-936X/86/0920-0166

Valentine, R.L., Jafvert, C.T., Leung, S.W., 1988. Evaluation of a chloramine decomposition model incorporating general acid catalysis. Water Res. 22, 1147–1153. doi:10.1016/0043-1354(88)90010-3

Valentine, R.L., Selleck, R.E., 1981. Effect of bromide and nitrite on the degradation of monochloramine, in: 4. Conference on Water Chlorination: Environmental Impact and Health Effects. Pacific Grove.

Vikesland, P.J., Ozekin, K., Valentine, R.L., 2001. Monochloramine decay in model and distribution system waters. Water Res. 35, 1766–1776. doi:10.1016/S0043-1354(00)00406-1

Vikesland, P.J., Ozekin, K., Valentine, R.L., 1998. Effect of natural organic matter on monochloramine decomposition: Pathway elucidation through the use of mass and redox balances. Environ. Sci. Technol. 32, 1409–1416. doi:10.1021/es970589a

Vikesland, P.J., Valentine, R.L., 2002. Modeling the kinetics of ferrous iron oxidation by monochloramine. Environ. Sci. Technol. 36, 662–668. doi:10.1021/es002058j

Vikesland, P.J., Valentine, R.L., 2000. Reaction pathways involved in the reduction of monochloramine by ferrous iron. Environ. Sci. Technol. 34, 83–90. doi:10.1021/es990511p

Wahman, A.D.G., Maestre, J.P., Jr, G.E.S., 2016. Title : Monochloramine cometabolism by drinking water relevant nitrifying biofilm 362–373. doi:10.5942/jawwa.2016.108.0092

Wahman, D.G., Katz, L.E., Speitel, G.E., 2006. Trihalomethane cometabolism by a mixed-culture nitrifying biofilter. J. / Am. Water Work. Assoc. 98.

Wahman, D.G., Katz, L.E., Speitel, G.E., 2005. Cometabolism of trihalomethanes by Nitrosomonas europaea. Appl. Environ. Microbiol. 71, 7980–7986. doi:10.1128/AEM.71.12.7980-7986.2005

Wahman, D.G., Speitel, G.E., 2012. Relative importance of nitrite oxidation by hypochlorous acid under chloramination conditions. Environ. Sci. Technol. 46, 6056–6064.

doi:10.1021/es300934x

Wahman, D.G., Wulfeck-Kleier, K. a, Pressman, J.G., 2009. Monochloramine disinfection kinetics of Nitrosomonas europaea using propidium monoazide quantitative PCR (PMA-qPCR) and LIVE/DEAD(R) BacLightTM. Appl Env. Microbiol 75, 5555–5562. doi:10.1128/AEM.00407-09

Wang, Y., Small, M.J., VanBriesen, J.M., 2017. Assessing the Risk Associated with Increasing Bromide in Drinking Water Sources in the Monongahela River, Pennsylvania. J. Environ. Eng. 143, 4016089. doi:10.1061/(ASCE)

Wegman, R.C.C., Hamaker, P., de Heer, H., 1983. Bromide-ion balance of a polder district with large-scale use of methyl bromide for soil fumigation. Food Chem. Toxicol. 21, 361–367. doi:10.1016/0278-6915(83)90089-3

Westerhoff, P., Chao, P., Mash, H., 2004. Reactivity of natural organic matter with aqueous chlorine and bromine. Water Res. 38, 1502–1513. doi:10.1016/j.watres.2003.12.014

White, R., Havalak, R., Nations, J., Thomas, J., Chalmers, D., Dewey, D., 2004. How much water is enough? Using pet to develop water budgets for residential landscapes.

Wilde, E.W., 1991. Comparison of three methods for measuring residual chlorine. Water Res. 25, 1303–1305. doi:10.1016/0043-1354(91)90071-W

Winid, B., 2015. Bromine and water quality - Selected aspects and future perspectives. Appl. Geochemistry. doi:10.1016/j.apgeochem.2015.10.004

Woolschlager, J., Rittmann, B., Piriou, P., Kiene, L., Schwartz, B., 2001. Using a comprehensive model to identify the major mechanisms of chloramine decay in distribution systems, in: Water Science and Technology: Water Supply. pp. 103–110. doi:10.1002/yd.430

Woolschlager, J.E., 2000. A Comprehensive Disinfection and Water Quality Model for Drinking

Water Distribution Systems. Northwestern University, Evanston.

Wu, W.W., Chadik, P. a, Delfino, J.J., 2003. The relationship between disinfection by-product formation and structural characteristics of humic substances in chloramination. Environ. Toxicol. Chem. 22, 2845–2852. doi:10.1897/02-542

Xue, Z., Lee, W.H., Coburn, K.M., Seo, Y., 2014. Selective reactivity of monochloramine with extracellular matrix components affects the disinfection of biofilm and detached clusters. Environ. Sci. Technol. 48, 3832–3839. doi:10.1021/es405353h

Yang, X., Shang, C., Lee, W., Westerhoff, P., Fan, C., 2008. Correlations between organic matter properties and DBP formation during chloramination. Water Res. 42, 2329–2339. doi:10.1016/j.watres.2007.12.021

Zaneti, R., Etchepare, R., Rubio, J., 2012. More environmentally friendly vehicle washes: Water reclamation. J. Clean. Prod. 37, 115–124. doi:10.1016/j.jclepro.2012.06.017

Zhang, Q., Davies, E.G.R., Bolton, J., Liu, Y., 2017. Monochloramine loss mechanisms in tap water. Water Environ. Res. doi:10.2175/106143017X14902968254421

Zhang, Q., Davies, E.G.R., Bolton, J.R., Liu, Y., 2018a. Monochloramine loss mechanisms and dissolved organic matter characterization in stormwater. Sci. Total Environ. 631–632, 745–754. doi:10.1016/j.scitotenv.2018.02.335

Zhang, Q., Gaafar, M., Davies, E.G.R., Bolton, J., Liu, Y., 2018b. Monochloramine dissipation study in storm sewer system. This paper has been submitted to Water Reseaerch in February 2018.

Zhang, Q., Gaafar, M., Yang, R.-C., Ding, C., Davies, E.G.R., Bolton, J., Liu, Y., 2018c. Field data analysis of active chlorine-containing stormwater samples. J. Environ. Manage. 206, 51–59.

Zhang, Y., Love, N., Edwards, M., 2009. Nitrification in drinking water systems. Crit. Rev. Environ. Sci. Technol. doi:10.1080/10643380701631739

Zhu, X., Zhang, X., 2016. Modeling the formation of TOCl, TOBr and TOI during chlor(am)ination of drinking water. Water Res. 96, 166–176. doi:10.1016/j.watres.2016.03.051

APPENDIX A. NOM and HA characteristics from different water sources

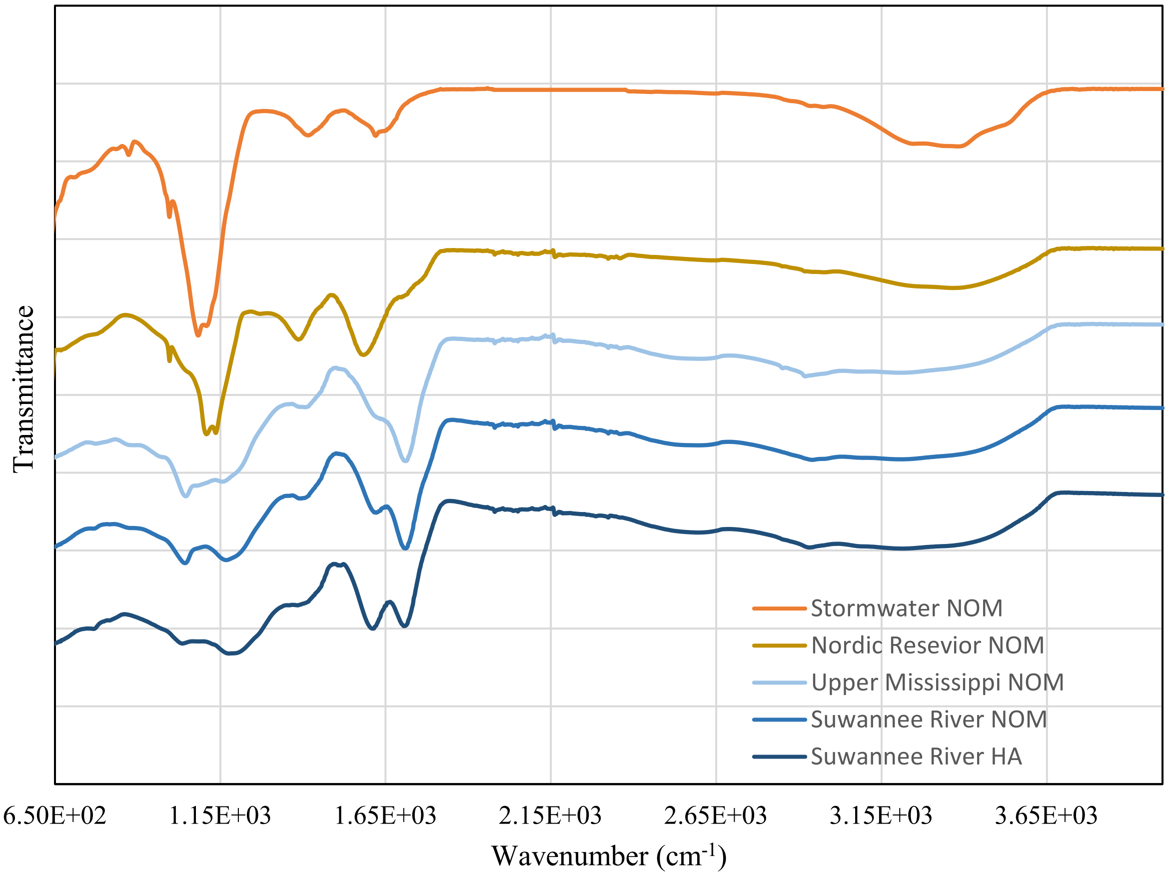

Fig. A1. FT-IR analysis of NOM and HA from different source waters

APPENDIX B. Additional stormwater characteristics from field sampling

Table B1. The ORP (mV) in stormwater samples collected during summer 2016

Date	Apr. 21	May 6	May 19	Jun. 1	Jun. 15	Jul. 7	Jul. 20	Aug. 8	Aug. 24	Sep. 8	Max.	Min.	Average
RES 1	193	201	181	194	250	202	166	198	169	213	250	166	196
RES 2	252	209	201	198	207	170	162	174	170	219	252	162	196
PRK 1	124	207	162	201	134	137	130	135	163	184	207	124	157
PRK 2	179	211	191	197	198	175	148	139	160	217	217	139	181
COM 1	209	195	203	175	221	168	178	165	229	161	229	161	190
COM 2	217	169	221	179	239	182	176	165	173	218	239	165	193
IND 1	233	209	242	178	208	189	147	212	185	245	245	147	204
IND 2	232	228	211	198	221	151	175	141	192	249	249	141	199

Table B2. The bacteria population (CFU/ml) in stormwater samples collected during summer 2016

Date	Apr. 21	May 6	May 19	Jun. 1	Jun. 15	Jul. 7	Jul. 20	Aug. 8	Aug. 24	Sep. 8	Max.	Min.	Average
RES 1	6×10^4	2.6×10^4	6×10^4	NA	4×10^4	1×10^4	3×10^4	8×10^3	NA	NA	6×10^4	8×10^3	3.3×10^4
RES 2	1×10^5	9×10^3	4×10^4	NA	1×10^5	1.2×10^4	1×10^5	7×10^3	NA	NA	1×10^5	7×10^3	5.2×10^4
PRK 1	7×10^5	8×10^4	9×10^4	NA	6×10^4	1.1×10^4	5×10^4	4×10^3	NA	NA	7×10^5	4×10^3	1.4×10^5
PRK 2	1×10^6	7×10^3	4×10^4	NA	3×10^4	1.1×10^4	4×10^4	1×10^4	NA	NA	1×10^5	7×10^3	3.4×10^4
COM 1	1.1×10^5	1.6×10^4	5×10^4	NA	NA	1.2×10^4	5×10^4	4×10^4	NA	NA	1.1×10^5	1.2×10^4	4.6×10^4
COM 2	9×10^4	1×10^4	3×10^5	NA	NA	3×10^4	4×10^4	3×10^4	NA	NA	3×10^5	1×10^4	8.3×10^4
IND 1	1.2×10^5	1.3×10^4	3×10^4	NA	1×10^4	9×10^3	2×10^4	4×10^3	NA	NA	1.2×10^5	4×10^3	2.9×10^4
IND 2	NA	1.4×10^3	4×10^4	NA	9×10^4	3×10^3	2×10^3	7×10^3	NA	NA	9×10^4	1.4×10^3	2.4×10^4

Table B3. The ORP (mV) in stormwater samples collected during summer 2015

Date	May 1	May 20	Jun. 3	Jun. 18	Jul. 8	Jul. 22	Aug. 5	Aug. 26	Sep. 10	Sep. 23	Max.	Min.	Average
RES 1	183	178	176	125	182	213	230	218	204	252	252	125	196
RES 2	232	157	190	229	187	264	254	174	238	247	264	157	217
PRK 1	242	173	169	186	164	159	142	117	166	248	248	117	176
PRK 2	252	185	191	218	160	223	192	215	227	258	258	160	212
COM 1	179	150	209	208	180	286	246	126	213	252	286	126	204
COM 2	150	147	189	193	166	266	223	160	223	243	266	147	196
IND 1	247	205	204	207	188	281	238	216	257	239	281	188	228
IND 2	220	215	168	80	155	237	218	237	255	185	255	80	197

Table B4. The bacteria population (CFU/ml) in stormwater samples collected during summer 2015

Date	May 1	May 20	Jun. 3	Jun. 18	Jul. 8	Jul. 22	Aug. 5	Aug. 26	Sep. 10	Sep. 23	Max.	Min.	Average
RES 1	NA	1.1×10^4	3.7×10^5	1.2×10^6	1.1×10^5	9.3×10^5	1.4×10^5	6.7×10^4	430000	4.3×10^5	1.2×10^6	1.1×10^4	4.1×10^5
RES 2	1×10^5	9×10^4	3.7×10^4	3.2×10^5	2.1×10^5	5.7×10^5	2.7×10^5	3.7×10^5	NA	1.2×10^6	1.2×10^6	3.7×10^4	3.5×10^5
PRK 1	4.3×10^4	1×10^4	6×10^4	3×10^3	5.5×10^4	1×10^5	1.6×10^4	NA	2.7×10^5	3.3×10^5	3.3×10^5	3×10^3	9.9×10^4
PRK 2	4×10^4	2.2×10^4	3.4×10^5	6×10^5	9.7×10^3	9.9×10^5	8.3×10^4	NA	8.3×10^5	7.7×10^5	9.9×10^5	9.7×10^3	4.1×10^5
COM 1	3.7×10^5	6×10^5	2.1×10^5	2.3×10^5	3×10^5	2.7×10^5	5.3×10^5	2.3×10^5	1.1×10^6	3.3×10^5	1.1×10^6	2.1×10^5	4.2×10^5
COM 2	1.7×10^5	5×10^5	1×10^6	2.3×10^6	3.5×10^5	5.3×10^4	2.7×10^5	1×10^6	1.6×10^4	2.3×10^5	2.3×10^6	1.6×10^4	5.9×10^5
IND 1	2.4×10^5	1.4×10^5	1.4×10^5	5.3×10^5	1.3×10^4	2×10^5	4.3×10^4	6.7×10^4	5.7×10^4	3.7×10^5	5.3×10^5	1.3×10^4	1.8×10^5
IND 2	9×10^4	3×10^4	1.7×10^5	5.3×10^5	2.5×10^5	5×10^5	5×10^5	2×10^5	6.3×10^5	3.3×10^5	6.3×10^5	3×10^4	3.2×10^5